

Preparation and Characterization of Microporous Activated Carbon from Biomass and its Application in the Removal of Chromium(VI) from Aqueous Phase

*Thesis submitted in partial fulfillment
of the requirement for the degree of*

Doctor of Philosophy

in

Chemical Engineering

by

Ramakrishna Gottipati

(Roll No – 507CH001)

Under the guidance of

Dr. Susmita Mishra



Department of Chemical Engineering
National Institute of Technology
Rourkela, Odisha – 769008
January 2012

**Department of Chemical Engineering
National Institute of Technology, Rourkela
Odisha, India – 769008**



Certificate

This is to certify that the thesis entitled '**Preparation and Characterization of Microporous Activated Carbon from Biomass and its Application in the Removal of Chromium(VI) from Aqueous Phase**' submitted by *Ramakrishna Gottipati* is a record of an original research work carried out by him under my supervision and guidance in partial fulfillment of the requirements for the award of the degree of *Doctor of Philosophy* in *Chemical Engineering* during the session July'2007 – January'2012 in the Department of Chemical Engineering, National Institute of Technology, Rourkela. Neither this thesis nor any part of it has been submitted for the degree or academic award elsewhere.

Dr. Susmita Mishra

Department of Chemical Engineering
National Institute of Technology, Rourkela

Acknowledgement

I would like to express my deep and sincere gratitude to Dr. Susmita Mishra for her invaluable supervision and esteemed guidance. As my supervisor, her insight, observations and suggestions helped me to establish the overall direction of the research and to achieve the objectives of the work. Her continuous encouragement and support have been always a source of inspiration and energy for me.

My sincere thanks are due to members of Doctoral Scrutiny Committee (DSC) and faculty members of Chemical Engineering Department for their suggestions and constructive criticism during the preparation of the thesis.

I acknowledge all my friends, research scholars, and staff of Chemical Engineering Department for their support during my research work.

I must acknowledge the academic resources provided by N.I.T., Rourkela and the research fellowship granted by Department of Science and Technology (DST) to carry out this work.

Finally, I am forever indebted to my parents, sister and brother-in-law for their understanding, endless patience and encouragement from the beginning.

Ramakrishna Gottipati

Dedicated to

My Family and Friends

Contents	Page No.
List of Figures	VII
List of Tables	XII
Nomenclature	XIV
Abstract	XVII
Chapter – 1: Introduction	1
1.1. Role of Activated Carbon	1
1.2. Hexavalent Chromium [Cr(VI)]	3
1.3. Motivation	3
1.3.1. The Problem	3
1.3.2. Health Impacts	4
1.3.3. Status of clean-up Activity	4
1.4. Objectives	5
1.5. Scope of the Study	5
1.6. Organization of Thesis	6
Chapter – 2: Literature Review	7
2.0. Summary	7
2.1. Types of Carbon materials	7
2.2. Activated Carbon	9
2.2.1. Historical Background	9
2.2.2. Preparation of Activated Carbon	11
2.2.2.1. <i>Physical Activation</i>	11
2.2.2.2. <i>Chemical Activation</i>	12
2.2.3. Structure of Activated Carbon	13
2.2.3.1. <i>Porous Structure</i>	13
2.2.3.2. <i>Crystalline Structure</i>	13
2.2.3.3. <i>Chemical Structure</i>	17

Chapter – 3: Materials and Methods	46
3.0. Summary	46
3.1. Materials	46
3.2. Methodology	46
3.2.1. Characterization of Precursor	46
3.2.1.1. <i>Estimation of Cellulose</i>	47
3.2.1.2. <i>Estimation of Lignin</i>	47
3.2.1.3. <i>Thermogravimetric Analysis</i>	47
3.2.1.4. <i>Proximate Analysis</i>	48
3.2.2. Preparation of Activated Carbon	48
3.2.2.1. <i>Effect of Impregnation</i>	49
3.2.2.2. <i>Effect of Carbonization Temperature</i>	49
3.2.2.3. <i>Effect of Holding Time</i>	50
3.2.3. Characterization of AC	50
3.2.3.1. <i>Proximate Analysis</i>	50
3.2.3.2. <i>Ultimate Analysis</i>	51
3.2.3.3. <i>Yield</i>	51
3.2.3.4. <i>Bulk Density</i>	51
3.2.3.5. <i>Porosity Characterization</i>	52
3.2.3.6. <i>Determination of Surface Chemistry</i>	53
3.2.3.7. <i>Microscopy</i>	53
3.2.3.8. <i>Other Analyses</i>	54
3.2.3.8.1. <i>X-ray diffraction spectroscopy</i>	54
3.2.3.8.2. <i>Iodine number</i>	54
3.2.3.8.3. <i>Methylene blue number</i>	55
3.2.4. Adsorption Experiments	55
3.2.5. Comparison and Regeneration	58
3.2.6. Modeling of Cr(VI) Adsorption	58

Chapter – 4: Preparation and Characterization of	
 Activated Carbon	59
4.0. Summary	59
4.1. Selection of Precursor	59
4.2. Preparation of AC	62
4.3. Effect of Process Parameters	62
4.3.1. Effect of Impregnation Ratio	62
4.3.1.1. <i>Effect of Impregnation on the Yield of AC</i>	63
4.3.1.2. <i>Nitrogen Gas Adsorption – Desorption Isotherms</i>	64
4.3.1.3. <i>Surface Area and Pore Volume</i>	68
4.3.1.4. <i>Micropore Surface Area and Micropore Volume</i>	71
4.3.2. Effect of Carbonization Temperature	74
4.3.2.1. <i>Effect of Carbonization Temperature on the Yield of AC</i>	74
4.3.2.2. <i>Nitrogen Gas Adsorption – Desorption Isotherms</i>	75
4.3.2.3. <i>Surface Area and Pore Volume</i>	78
4.3.2.4. <i>Micropore Surface Area and Micropore Volume</i>	81
4.3.3. Effect of Holding Time	84
4.3.3.1. <i>Effect of Holding Time on the Yield of AC</i>	
4.3.3.2. <i>Nitrogen Gas Adsorption – Desorption Isotherms</i>	84
4.3.3.3. <i>Surface Area and Pore Volume</i>	88
4.3.3.4. <i>Micropore Surface Area and Micropore Volume</i>	90
4.4. Optimum Conditions and Comparison	93
4.5. Pore Size Distribution (PSD)	94
4.6. Fourier Transform Infrared spectroscopy (FTIR)	96
4.7. Scanning Electron Microscope (SEM) and Transmission Electron Microscope (TEM) analysis	99
4.8. X – Ray Diffraction spectroscopy (XRD)	102

Chapter – 5:	Adsorption of Chromium(VI) on Activated Carbon	104
5.0.	Summary	104
5.1.	Effect of Process Parameters	105
5.1.1.	Effect of pH	105
5.1.2.	Effect of Adsorbent Dose	110
5.1.3.	Effect of Initial Chromium(VI) Concentration	115
5.1.4.	Effect of Temperature	121
5.2.	Adsorption Equilibrium Study	125
5.2.1.	Langmuir Isotherm	125
5.2.2.	Freundlich Isotherm	126
5.2.3.	Temkin Isotherm	128
5.2.4.	Dubinin – Radushkevich Isotherm	129
5.3.	Adsorption Kinetic Study	131
5.3.1.	Pseudo-First-Order Kinetic Model	132
5.3.2.	Pseudo-Second-Order Kinetic Model	134
5.4.	Adsorption Mechanism	138
5.4.1.	Intra-Particle Diffusion	138
5.4.2.	Boyd Model	141
5.5.	Adsorption Thermodynamic Study	144
5.6.	Role of Surface Chemistry	145
5.7.	Energy Dispersive X-ray spectroscopy (EDX)	147
5.8.	Comparison and Regeneration	149
5.8.1.	Porous Characteristics	149
5.8.1.1.	<i>N₂ Adsorption – Desorption Isotherms</i>	149
5.8.2.	Chromium(VI) Adsorption	152
5.8.3.	Regeneration of Spent AC	153
Chapter – 6:	Modeling of Chromium(VI) Adsorption	155
6.0.	Summary	155
6.1.	Full Factorial Design	155
6.2.	Designing of Experimental Matrix	156
6.3.	Modeling of Chromium(VI) Removal by AC-PA	159

6.3.1. Pareto Plot	160
6.3.2. Main Effects	161
6.3.3. Interaction Effects	162
6.3.4. Normal Probability Plot	164
6.3.5. Optimization	164
6.3.6. Validation Experiments	165
6.4. Modeling of Chromium(VI) Removal by AC-ZC	166
6.4.1. Pareto Plot	167
6.4.2. Main Effects	168
6.4.3. Interaction Effects	169
6.4.4. Normal Probability Plot	171
6.4.5. Optimization	172
6.4.6. Validation Experiments	173
6.5. Modeling of Chromium(VI) Removal by AC-PH	173
6.5.1. Pareto Plot	175
6.5.2. Main Effects	176
6.5.3. Interaction Effects	177
6.5.4. Normal Probability Plot	181
6.5.5. Optimization	181
6.5.6. Validation Experiments	182
Chapter – 7: Conclusions and Future Perspective	184
7.0. Summary	184
7.1. Conclusions	184
7.2. Scope of Research	185
References	187

List of Figures

Fig. No	Title	Page No
2.1.	Major allotropic forms of carbon and some of carbon structures derived from these forms.	8
2.2.	Graphical representation of pore structure in activated carbon.	15
2.3.	Layered structure of graphite.	16
2.4	Schematic illustration of structure of activated carbon: (a) graphitized carbon, and (b) non-graphitized carbon.	17
2.5	Type – I isotherm.	21
2.6	Type – II isotherm.	22
2.7	(a) Type – III isotherm and (b) Type – V isotherm.	22
2.8	Type – IV isotherm.	23
2.9	Type – VI isotherm.	23
2.10	Classification of adsorption-desorption hysteresis loops.	24
2.11	Distribution of Cr(VI) species as a function of pH.	32
2.12	Fraction of HCrO_4^- and $\text{Cr}_2\text{O}_7^{2-}$ at pH 4 as a function of total Cr(VI) concentration	32
2.13	The general model of a process or system.	44
3.1	Schematic diagram for preparation of activated carbon.	49
4.1	TGA analysis for (a) raw material and (b) raw material after impregnation with H_3PO_4 .	61
4.2	Effect of impregnation ratio on yield of ACs (a) AC-PA and (b) AC-ZC and AC-PH.	63
4.3	N_2 gas adsorption – desorption isotherms of AC-PA samples prepared at different impregnation concentrations.	65
4.4	N_2 gas adsorption – desorption isotherms of AC-ZC samples prepared at different impregnation ratios.	66
4.5	N_2 gas adsorption – desorption isotherms of AC-PH samples prepared at different impregnation ratios.	67
4.6	Effect of H_3PO_4 impregnation on surface area and pore volume of AC.	69
4.7	Effect of ZnCl_2 impregnation ratio on surface area and pore volume of AC.	70
4.8	Effect of KOH impregnation ratio on surface area and pore volume of AC.	71

4.9	Effect of H ₃ PO ₄ impregnation on micropore surface area and micropore volume.	72
4.10	Effect of ZnCl ₂ impregnation on micropore surface area and micropore volume.	73
4.11	Effect of KOH impregnation on micropore surface area and micropore volume.	74
4.12	Effect of carbonization temperature on the yield of prepared ACs.	75
4.13	N ₂ gas adsorption – desorption isotherms of AC-PA samples prepared at different carbonization temperatures.	76
4.14	N ₂ gas adsorption – desorption isotherms of AC-ZC samples prepared at different carbonization temperatures.	77
4.15	N ₂ gas adsorption – desorption isotherms of AC-PH samples prepared at different carbonization temperatures.	78
4.16	Effect of carbonization temperature on surface area and pore volume of AC-PA.	79
4.17	Effect of carbonization temperature on surface area and pore volume of AC-ZC.	80
4.18	Effect of carbonization temperature on surface area and pore volume of AC-PH.	81
4.19	Effect of carbonization temperature on micropore surface area and micropore volume of AC-PA.	82
4.20	Effect of carbonization temperature on micropore surface area and micropore volume of AC-ZC.	83
4.21	Effect of carbonization temperature on micropore surface area and micropore volume of AC-PA.	83
4.22	Effect of holding time on the yield of prepared ACs.	84
4.23	N ₂ gas adsorption – desorption isotherms of AC-PA samples prepared at different holding times.	85
4.24	N ₂ gas adsorption – desorption isotherms of AC-ZC samples prepared at different holding times.	86
4.25	N ₂ gas adsorption – desorption isotherms of AC-PH samples prepared at different holding times.	87
4.26	Effect of holding time on surface area and pore volume of AC-PA.	88
4.27	Effect of holding time on surface area and pore volume of AC-ZC.	89

4.28	Effect of holding time on surface area and pore volume of AC-PH.	90
4.29	Effect of holding time on micropore surface area and micropore volume of AC-PA.	91
4.30	Effect of holding time on micropore surface area and micropore volume of AC-ZC.	92
4.31	Effect of holding time on micropore surface area and micropore volume of AC-PH.	93
4.32	Pore size distribution of the prepared ACs (a) AC-PA (b) AC-ZC and (c) AC-PH.	96
4.33	FTIR analysis of (a) raw material and (b) AC-PA, AC-ZC and AC-PH.	98
4.34	SEM images of the prepared ACs (a) AC-PA (b) AC-ZC and (c) AC-PH.	100
4.35	TEM images of the prepared ACs (a) AC-PA (b) AC-ZC and (c) AC-PH.	101
4.36	XRD patterns of the prepared ACs.	103
5.1	Effect of pH on chromium(VI) removal by different ACs (a) AC-PA (b) AC-ZC and (c) AC-PH (Initial chromium concentration – 10 mg/L, adsorbent dose – 3.0 g/L, contact time – 3.0 h, and temperature – 30 °C).	107
5.2	Effect of pH on the percentage adsorption of Cr(VI) from aqueous solution by AC-PA (Initial chromium concentration – 10 mg/L, adsorbent dose – 3.0 g/L, contact time – 3.0 h, and temperature – 30 °C).	108
5.3	Effect of pH on the percentage adsorption of Cr(VI) from aqueous solution by AC-ZC (Initial chromium concentration – 10 mg/L, adsorbent dose – 3.0 g/L, contact time – 3.0 h, and temperature – 30 °C).	109
5.4	Effect of pH on the percentage adsorption of Cr(VI) from aqueous solution by AC-PH (Initial chromium concentration – 10 mg/L, adsorbent dose – 3.0 g/L, contact time – 3.0 h, and temperature – 30 °C).	109
5.5	Surface charge distribution for prepared ACs.	110
5.6	Effect of adsorbent dose on Cr(VI) adsorption by different ACs (a) AC-PA (b) AC-ZC and (c) AC-PH (pH–3.5 for AC-PA and 2.0 for AC-ZC and AC-PH, Cr(VI) concentration – 10.0 mg/L, contact time – 3.0 h, and temperature – 30 °C).	112
5.7	Effect of adsorbent dose on the percentage adsorption of Cr(VI) by AC-PA (pH–3.5, Cr(VI) concentration – 10.0 mg/L, contact time – 3.0 h, and temperature – 30 °C).	114

5.8	Effect of adsorbent dose on the percentage adsorption of Cr(VI) by AC-ZC (pH – 2.0, Cr(VI) concentration – 10.0 mg/L, contact time – 3.0 h, and temperature – 30 °C).	114
5.9	Effect of adsorbent dose on the percentage adsorption of Cr(VI) by AC-PH (pH – 2.0, Cr(VI) concentration – 10.0 mg/L, contact time – 3.0 h, and temperature – 30 °C).	115
5.10	Effect of initial metal concentration on Cr(VI) adsorption by different ACs (a) AC-PA (b) AC-ZC and (c) AC-PH (pH – 2.0, adsorbent dose – 3.0 g/l, contact time – 3.0 h and temperature – 30 °C).	117
5.11	Effect of initial metal concentration on the percentage adsorption of Cr(VI) by AC-PA (pH – 3.5, adsorbent dose – 3.0 g/l, contact time – 3.0 h and temperature – 30 °C).	118
5.12	Effect of initial metal concentration on the percentage adsorption of Cr(VI) by AC-ZC (pH – 2.0, adsorbent dose – 3.0 g/l, contact time – 3.0 h and temperature – 30 °C).	119
5.13	Effect of initial metal concentration on the percentage adsorption of Cr(VI) by AC-PH (pH – 2.0, adsorbent dose – 3.0 g/l, contact time – 3.0 h and temperature – 30 °C).	120
5.14	Adsorption trends of AC-PA at high initial Cr(VI) concentrations (pH – 3.5, adsorbent dose – 3.0 g/l, contact time – 3.0 h and temperature – 30 °C).	120
5.15	Effect of temperature on Cr(VI) adsorption by different ACs (a) AC-PA (b) AC-ZC and (c) AC-PH (pH–3.5 for AC-PA and 2.0 for AC-ZC and AC-PH, Cr(VI) concentration – 10.0 mg/L, adsorbent dose – 3.0 g/L, and contact time – 3.0 h).	122
5.16	Effect of temperature on percentage removal of Cr(VI) by AC-PA (pH – 3.5, Cr(VI) concentration – 10.0 mg/L, adsorbent dose – 3.0 g/L, and contact time – 3.0 h).	123
5.17	Effect of temperature on percentage removal of Cr(VI) by AC-ZC (pH – 2.0, Cr(VI) concentration – 10.0 mg/L, adsorbent dose – 3.0 g/L, and contact time – 3.0 h).	124
5.18	Effect of temperature on percentage removal of Cr(VI) by AC-ZC (pH – 2.0, Cr(VI) concentration – 10.0 mg/L, adsorbent dose – 3.0 g/L, and contact time – 3.0 h).	124

5.19	Langmuir isotherms of different ACs for the Cr(VI) adsorption data at 30 °C.	126
5.20	Freundlich isotherms of different ACs for the Cr(VI) adsorption data at 30 °C.	128
5.21	Temkin isotherms of different ACs for the Cr(VI) adsorption data at 30 °C.	129
5.22	Dubinin – Radushkevich isotherms of different ACs for the Cr(VI) adsorption data at 30 °C.	130
5.23	Pseudo first order plots for adsorption of Cr(VI) on AC-PA.	132
5.24	Pseudo first order plots for adsorption of Cr(VI) on AC-ZC.	133
5.25	Pseudo first order plots for adsorption of Cr(VI) on AC-PH.	133
5.26	Pseudo second order plots for adsorption of Cr(VI) on AC-PA.	135
5.27	Pseudo second order plots for adsorption of Cr(VI) on AC-ZC.	135
5.28	Pseudo second order plots for adsorption of Cr(VI) on AC-PH.	136
5.29	Intra-particle diffusion model for the adsorption of Cr(VI) on AC-PA.	139
5.30	Intra-particle diffusion model for the adsorption of Cr(VI) on AC-ZC.	140
5.31	Intra-particle diffusion model for the adsorption of Cr(VI) on AC-PH.	140
5.32	Boyd model for the adsorption of Cr(VI) on AC-PA.	142
5.33	Boyd model for the adsorption of Cr(VI) on AC-ZC.	143
5.34	Boyd model for the adsorption of Cr(VI) on AC-PH.	143
5.35	Plot of $\ln K_c$ vs. $1/T$ for adsorption of Cr(VI) on prepared AC samples.	145
5.36	Determination of surface functional groups of AC-PA by FTIR (a) before adsorption and (b) after adsorption.	147
5.37	EDX analysis of (a) AC-PA, (b) AC-ZC and (c) AC-PH (<i>a.1</i> is before adsorption and <i>a.2</i> is after adsorption).	148
5.38	N ₂ adsorption desorption isotherms of AC-PA and CAC.	150
5.39	Comparison of AC-PA and CAC for Cr(VI) removal efficiency.	152
6.1	Pareto plot for effects of individual factors and interactions for Cr(VI) removal by AC-PA.	161
6.2	Effect of main factors on response for AC-PA (a) pH, (b) concentration, (c) adsorbent dose and (d) temperature.	162
6.3	Contour plots of interactions for AC-PA (a) pH * Concentration and (b) Concentration * Adsorbent dose.	163
6.4	Normal probability plot of residuals for Cr(VI) removal by AC-PA.	164
6.5	Desirability fitted 3D surface plot for Cr(VI) removal by AC-PA (Adsorbent dose – 1 g/L and Temperature – 40 °C).	165

6.6	Pareto plot for effects of individual factors and interactions for Cr(VI) removal by AC-ZC.	168
6.7	Effect of main factors on response for AC-ZC (a) pH, (b) concentration, (c) adsorbent dose and (d) temperature.	169
6.8	Contour and cube plots of interactions for AC-ZC (a) pH * Concentration and (b) Concentration * Adsorbent dose (c) pH*Adsorbent dose*Temperature.	171
6.9	Normal probability plot of residuals for Cr(VI) removal by AC-ZC.	172
6.10	Desirability fitted 3D surface plot for Cr(VI) removal by AC-ZC (Adsorbent dose – 1 g/L and Temperature – 40 °C).	173
6.11	Pareto plot for effects of individual factors and interactions for Cr(VI) removal by AC-PH.	176
6.12	Effect of main factors on response for AC-PH (a) pH, (b) concentration, (c) adsorbent dose and (d) temperature.	177
6.13	Contour and cube plots of interactions for AC-ZC (a) pH * Adsorbent dose, (b) pH*Temperature (c) Concentration*Adsorbent dose (d) Adsorbent dose*Temperature (e) pH*Concentration*Temperature and (f) pH*Adsorbent dose*Temperature.	180
6.14	Normal probability plot of residuals for Cr(VI) removal by AC-PH.	181
6.15	Desirability fitted 3D surface plot for Cr(VI) removal by AC-PH (Adsorbent dose – 1.0 g/L and Temperature – 25 °C).	182

List of Tables

Table No	Title	Page No.
2.1	Various physical activating agents and precursors used for AC production.	12
2.2	Various chemical activating agents and precursors used for AC production.	13
2.3	Classification of pores according to their width.	14
2.4	Application of granular activated carbon in adsorption of various contaminants from gas and liquid phase.	29
2.5	Removal of heavy metals using activated carbon.	30
2.6	Hexavalent chromium compounds.	31

2.7	Chromium(VI) concentration in various industrial effluents.	31
2.8	Various techniques used for Cr(VI) removal and their drawbacks.	36
2.9	Comparison of activated carbons prepared from various feed stocks and the optimum conditions for Cr(VI) removal.	37
3.1	Different isotherm models used in the present study.	56
3.2	Different kinetic models used in the present study.	57
4.1	Comparison of chemical and physical properties of Bael fruit shell with other precursors.	60
4.2	AC preparation conditions and ranges of various parameters.	62
4.3	Optimum preparation conditions for ACs and their porous characteristics.	93
4.4	Comparison of porous characteristics of prepared ACs with ACs prepared from different precursors.	94
5.1	Langmuir, Freundlich, Temkin and D-R isotherm constants for the Cr(VI) adsorption on different prepared activated carbon samples.	131
5.2	Pseudo first order parameters for the adsorption of Cr(VI) on different prepared ACs.	137
5.3	Pseudo second order parameters for the adsorption of Cr(VI) on different prepared AC samples.	137
5.4	Intra-particle diffusion model parameters for adsorption of Cr(VI) on prepared AC samples.	141
5.5	Boyd model parameters for the adsorption of Cr(VI) on prepared AC samples.	144
5.6	Thermodynamic parameters for adsorption of Cr(VI) on AC samples.	145
5.7	Various functional groups found for AC-PA and their frequency ranges.	146
5.8	Comparison of surface characteristics of ACs.	151
5.9	Proximate and ultimate analyses of prepared ACs and CAC.	151
5.10	Comparison of other properties of prepared ACs with CAC.	151
5.11	Comparison of Cr(VI) adsorption capacities of activated carbons prepared from different precursors.	153
5.12	Regeneration of AC and efficiency of regenerated AC for Cr(VI) adsorption.	154
6.1	Experimental ranges and levels of the factors used in the factorial design.	157
6.2	Factorial design matrix with coded and real values.	157
6.3	Responses for the Cr(VI) removal by different ACs as per the designed	

	experimental matrix.	158
6.4	Estimated regression coefficients of model terms and their effects on the response for AC-PA.	159
6.5	ANOVA results for Cr(VI) removal by AC-PA.	160
6.6	Estimated regression coefficients of model terms and their effects on the response for AC-ZC.	166
6.7	ANOVA results for Cr(VI) removal data by AC-ZC.	167
6.8	Estimated regression coefficients of model terms and their effects on the response for AC-PH.	174
6.9	ANOVA results for Cr(VI) removal data by AC-PH.	175
6.10	Validation experiments conducted at conditions predicted by models.	183

Nomenclature

a_L	Affinity constant (L/mol)
A_T	Equilibrium binding constant (L/mg)
B_D	DR constant ($1/(J/mol)^2$)
B_T	Temkin constant related to heat of adsorption
C	BET constant
C_e	Equilibrium concentration of adsorbate in solution (mg/L)
C_i	Initial concentration of adsorbate in solution (mg/L)
D_i	Diffusion coefficient (m^2/g)
E	Apparent energy (J/mol)
F	Fraction of solute adsorbed at time t
ΔG°	Free energy change (kJ/mol)
ΔH°	Enthalpy change (kJ/mol)
h	Initial adsorption rate ($mg/g \text{ min}$)
K	DR constant
k_1	Pseudo-first-order constant ($1/min$)
k_2	Pseudo-second order rate constant ($g/mg \text{ min}$)
K_c	Equilibrium constant (L/g)
K_F	Freundlich constant ($(mol/g)(mol/L)^n$)

k_{id}	Rate constant for intra particle diffusion ($mg/g \text{ min}^{1/2}$)
K_L	Langmuir constant (L/g)
n	DA parameter
n^a	Amount of moles adsorbed ($mmol/g$)
n_m^a	Monolayer adsorption capacity ($mmol/g$)
$1/n$	Heterogeneity factor
p	Equilibrium pressure (Pa)
p^o	Saturation vapor pressure (Pa)
q_D	Adsorption capacity (mg/g)
q_e	Adsorption capacity (mg/g) (calculated)
Q_e	Adsorption capacity (mg/g) (experimental)
q_t	Adsorption capacity at time t (mg/g)
r	Radius (m)
R	Gas constant ($J/kmol$)
R_L	Separation factor
$\% R$	Percentage of R emoval or R esponse
ΔS^o	Entropy change (kJ/mol)
S_{mi}	Micropore surface area (m^2/g)
S_T	Total surface area (m^2/g)
t	Time (min)
$t^{1/2}$	Square root of time ($min^{1/2}$)
T	Temperature (K)
V	Volume adsorbed at STP (cm^3/g)
V_m	Volume of monolayer capacity (cm^3/g)
V_{mi}	Micropore volume (cm^3/g)
\tilde{V}_o	Micropore volume (cm^3/g)
V_T	Total pore volume (cm^3/g)
W	Volume of adsorbate (cm^3/g)

ρ	Density of liquid adsorbate (g/L)
β	Affinity coefficient

Abbreviations

AC	Activated Carbon
ACF	Activated Carbon Fibers
ANOVA	ANalysis Of Variance
AC-PA	Activated Carbon prepared by Phosphoric Acid activation
AC-PH	Activated Carbon prepared by Potassium Hydroxide activation
AC-ZC	Activated Carbon prepared by Zinc Chloride activation
BET	Brunauer Emmett Teller
df	degrees of freedom
DoE	Design of Experiments
DR	Dubinin Radushkevich
EDX	Energy Dispersive X-ray spectroscopy
FFA	Full Factorial Design
FTIR	Fourier Transform Infrared spectroscopy
GAC	Granular Activated Carbon
LPH	Low Pressure Hysteresis
NIT	National Institute of Technology
OVHA	Orissa Voluntary Health Organization
PAC	Powdered Activated Carbon
PID	Proportional Integral Derivative
PSD	Pore Size Distribution
SEM	Scanning Electron Microscope
TEM	Transmission Electron Microscope
TGA	Thermo-Gravimetric Analysis
WHO	World Health Organization
XRD	X-Ray Diffraction spectroscopy

Abstract

Water pollution has been a major challenge to environmental engineers today due to the release of toxic heavy metals from various industries. Among various heavy metals, hexavalent chromium [Cr(VI)] is considered as highly toxic due to its carcinogenicity and various health disorders. Different sources of Cr(VI) pollution include effluents from mining, electroplating, leather tanning and electroplating industries. Among various technologies, adsorptive removal of Cr(VI) by using different adsorbents is more promising and economical. Among various adsorbents used, activated carbon (AC) is well known for its high adsorption capacity due to large surface area and pore volume. In recent years, immense research has been focused towards converting the agricultural or lignocellulosic wastes into activated carbon, since this technology not only solves the problem of waste disposal but also converts a potential waste into a valuable product that can be used as an adsorbent for effluent treatment.

Bael fruit (*Aegle Marmelos*) shell, a lignocellulosic material was selected as the precursor for the preparation of microporous (< 2 nm) activated carbon in the present investigation. Activated carbon was prepared through chemical activation using phosphoric acid (AC-PA), zinc chloride (AC-ZC), and potassium hydroxide (AC-PH). The effect of various process parameters such as impregnation, carbonization temperature, and holding time on porous characteristics of the activated carbon was investigated.

Characterization of AC by N₂ adsorption-desorption isotherms at 77 K was carried out. Total surface area, micropore and mesopore surface area, total pore volume, micropore and mesopore volume, and pore size distribution of the samples were determined. The porous characteristics of prepared ACs were analyzed by applying various isotherm equations like Brunauer-Emmett-Teller (BET), Dubinin-Radushkevich (DR), and Dubinin-Astakhov (DA). The AC-PA prepared at optimum conditions (30% impregnation, 400°C carbonization temperature and 60 min holding time) constitutes highly microporous structure with micropore surface area (1625 m²/g) and micropore volume (0.56 cc/g). The pore size distribution of the prepared samples at optimized conditions shows that samples are comprised greatly with micropores (average pore diameter of 1.68 nm, 1.69 nm, and 1.54 nm for AC-PA, AC-ZC, and AC-PH,

respectively). The Scanning Electron Microscope (SEM) analysis revealed the heterogeneous surface structure of the samples and clearly depicts the presence of macropores which acts as channels to the microporous network while TEM analysis visualized the presence of micropores. The surface groups present on the AC surface were determined by the Fourier Transform Infrared Spectroscopy (FTIR) analysis. The proximate and ultimate analyses were carried out by using CHNS analyzer and by standard methods, respectively.

The batch adsorption studies of Cr(VI) on ACs were carried out at optimum conditions by H₃PO₄, ZnCl₂ and KOH activations. The effect of various process parameters like pH, initial metal concentration, adsorbent dose, contact time, and temperature on the efficiency of Cr(VI) removal was investigated. Maximum adsorption of Cr(VI) on AC-PA (98.74 %) was observed at pH 2. No significant change in efficiency was observed for AC-PA in pH range 2.0 – 5.0 and the 76 % removal was observed at neutral pH. The optimum conditions for adsorbent dose and temperature were determined as 3.0 g/L and 30 °C, respectively. Initial Cr(VI) concentration has no effect on AC-PA in the studied range (2 – 10 mg/L) and in case of AC-ZC and AC-PH, 8.0 mg/L and 2.0 mg/L were determined as optimum concentrations. The time required to reach equilibrium is different for different ACs (90, 150, and 240 min for AC-PA, AC-ZC and AC-PH, respectively). The adsorption equilibrium data was well explained by Freundlich isotherm and DR isotherm parameters suggested that the adsorption of Cr(VI) on prepared ACs is physical adsorption. The kinetic data were better followed the pseudo-second order kinetics and both film and pore diffusion mechanisms played important role. The exothermic nature and the randomness of the process were estimated from thermodynamic parameters. The porous characteristics and Cr(VI) removal efficiencies of prepared AC were very high compared to the commercial AC. The spent activated carbon was regenerated by using hot water (80 °C) and mild acid (0.1 M H₂SO₄) and the adsorption capacities and porous characteristics were compared with the mother sample.

Chromium(VI) adsorption process was modeled through Designing of Experiments (DoE) by using Full Factorial Design (FFD). Factorial design was used to reduce the number of experiments in order to achieve the best overall optimization of the process. Two-level and four-factor full factorial design was used to develop model equations for Cr(VI) removal by using Design Expert 7.1.6 software. The interpretation of effect of main factors and their interactions

was carried out and the developed models were validated by conducting experiments at the predicted conditions. For AC-PA, along with main factors interactions such as pH * concentration of Cr(VI), concentration of Cr(VI) * adsorbent dose, and pH * concentration of Cr(VI) * adsorbent dose * temperature were found to be significant on the response.

Key words: Adsorption; Activated carbon; Bael fruit shell; Chromium(VI); Micropores; Micropore surface area; Pore size distribution; Adsorption isotherm; Adsorption kinetics; Adsorption modeling; Full factorial design.

Introduction

1.1. Role of Activated Carbon

Over the last few decades, adsorption has gained importance as a purification, separation and recovery process on an industrial scale. Activated carbon (AC) is perhaps one of the most widely used adsorbents in industry for environmental applications. Activated carbons are carbons of highly microporous structure with both high internal surface area and porosity, and commercially the most common adsorbents used for the removal of organic and inorganic pollutants from air and water streams. Any cheap material with a high carbon content, low inorganics can be used as a raw material for the production of activated carbon (Bansal et al., 1988).

World demand for virgin activated carbon is forecast to expand by 9 % per annum through 2014 to 1.7 million metric tons (<http://www.marketresearch.com/Freedomia-Group-Inc-v1247/Activated-Carbon-2717702/>). Activated carbon demand will benefit from a continuing intensification of the global environmental movement as well as rapid industrialization. In most developing and developed countries, use of AC in pharmaceutical sector offers the strongest growth prospect. Additionally, environmental concerns in developing regions will spur new growth in water treatment applications, which is already the largest single market in developed countries. Besides the necessity of clean drinking water, government environmental regulations that vary by region also impact the demand for AC in this sector significantly.

The high adsorption capacities of activated carbons are related to the properties such as surface area, pore volume and pore size distribution (PSD). These unique characteristics depend on the type of raw materials employed for preparation of AC and the method of activation. Literature survey indicates that there have been many attempts to obtain low-cost activated carbons from agricultural wastes such as coconut shells (Azevedo et al., 2007; Hu and Srinivasan, 2001), wood (Gomez-Serrano et al., 2005; Klijanienko et al., 2008; Zuo et al., 2009), cotton stalk (Deng et al., 2010), almond shells (Bansode et al., 2003), rice husk (Fierro et al., 2010; Guo and Rockstraw, 2007), date pits (Girgis and EI-Hendawy, 2002), nut shells (Lua et

al., 2005; Yang and Lua, 2006), olive seeds (Stavropoulos and Zabaniotou, 2005), apricot stones (Youssef et al., 2005), and sugar cane bagasse (Cronje et al., 2011; Valix et al., 2004) etc.

Due to the increasing demand of AC, there is a strong need for the sorting out new precursors for the preparation of AC which should be cost effective at par with the commercially available AC. Although, a variety of raw materials were explored for the preparation of AC in earlier studies, scientists are still trying to explore new materials depending on their availability and suitability for AC production. However, the utilization of agricultural wastes as raw material for the preparation of activated carbon has increased notably in recent years.

Basically there are two different processes for the preparation of AC: physical activation and chemical activation. Physical activation involves carbonization of carbonaceous material followed by the activation of the resulting char at high temperatures (800 – 1100 °C) in presence of oxidizing agents such as CO₂ and steam. In chemical activation the precursor is mixed with a chemical agent and then pyrolyzed at low temperatures (400 – 600 °C) in absence of air. Chemical activation offers several advantages over physical activation as it is carried out in a single step combining carbonization and activation, performed at lower temperatures and therefore resulting in the development of a better porous structure. Moreover, the added chemicals for activation can be easily recovered (Ahmadpour and Do, 1996).

In the present study, Bael fruit (*Aegle marmelos Correa*) shell has been used as precursor for the preparation of activated carbon using chemical activation method. Bael, belongs to the family Rutaceae (Genus – *Aegle correa*; Species – *A. marmelos*), is a deciduous tree growing 12 – 15 m in height. It is widely distributed throughout the Indian peninsula along with Myanmar, Srilanka, Pakistan, Bangladesh, Nepal, Burma, Indonesia and Thailand (Fen and Rao, 2007). The Bael fruit also called as Indian quince and the fruit pulp is rich of various phytochemicals which have high medicinal importance. Normally, a Bael tree (of 10 years age) yields as many as 200 fruits in a season. Each Bael fruit on an average weighs about 0.5 kg, of which about 50 % is the weight of the shell (Janick and Paull, 2008). One tonne of bael shell can be obtained from about two tonnes of Bael fruits borne by about 10 trees. So, we aim to utilize the unused fruit shell as a raw material for the development of porous adsorbent.

1.2. Hexavalent Chromium [Cr(VI)]

The efficiency of activated carbons prepared by various chemical activations in the removal of hexavalent chromium [Cr(VI)] was investigated in this study. Chromium is usually found in industrial effluents such as electroplating, leather tanning and textile industries. Chromium, in wastewater can exist both as Cr(III) and Cr(VI). However, in potable waters, Cr(VI) appears as the most stable species due to the aerobic conditions in the environment. The trivalent form is not considered toxic. On the other hand, the detrimental effects of hexavalent chromium to biological systems and the environment have been well documented (Bagchi et al., 2002; Passow et al., 1961; Shanker et al., 2005). Exposure to Cr(VI) beyond the tolerance levels (0.05 mg/L) can have damaging effects on the human physiological, neurological and biological systems. Several methods have been adopted for the removal of Cr(VI) from aqueous phase (Agarwal et al., 2006; Baek et al., 2007; Dragan et al., 2004; Kyzas et al., 2009; Muthukrishnan and Guha, 2008; Yilmaz et al., 2008). These include chemical reduction and precipitation, ion exchange, evaporation and concentration, electrolysis and electroplating, ion flotation, activated sludge process and carbon adsorption. Adsorptive removal of pollutants by activated carbon is found to be the most effective, particularly for the removal of metal ions at low concentrations.

1.3. Motivation

Rapid industrialization has cumulatively increased the problem of drinking water scarcity and the demand for contaminated free water for daily consumption. A typical problem of chromium contamination in water is faced by the residents of Sukinda area in Jajpur district of Orissa, India. It has been included in the list of world's top ten polluted places (<http://www.blacksmithinstitute.org/wwpp2007/ten.php>), a survey carried out by Black Smith Institute, New York (Hindustan times, 16th September, 2007).

1.3.1. The Problem

Sukinda valley, in the state of Orissa, contains 97 % of India's chromite ore deposits and one of the largest open cast chromite ore mines in the world. Twelve mines continue to operate without any environmental management plans and over 30 million tons of waste rock is spread over the surrounding areas and the Brahmani riverbanks. Untreated water effluents are

discharged into the river from mines. This area is also flood-prone, resulting in further contamination of the water bodies. Approximately 70 % of the surface water and 60 % of the drinking water contains hexavalent chromium at more than double national and international standards (0.05 mg/L) and levels of over 20 times the standard have been recorded. The Brahmani river is the only water source for the residents and treatment facilities are extremely limited. The state pollution control board has conceded that the water quality at various locations suffers from very high levels of contamination.

1.3.2. Health Impacts

Nearly about 2,600,000 people at Sukinda area are potentially affected and are suffering from various ailments caused by Cr(VI) exposure mainly through drinking water. Gastrointestinal bleeding, tuberculosis and asthma are common ailments. Infertility, birth defects, and stillbirths and have also resulted. The Orissa Voluntary Health Association (OVHA), funded by the Norwegian government, reports acute health problems in the area. OVHA reported that 84.75 % of deaths in the mining areas and 86.42 % of deaths in the nearby industrial villages occurred due to chromite mine related diseases (<http://jigpu.wordpress.com/2007/09/16/>). The survey report claims that villages less than one kilometer from the sites were the worst affected, with 24.47% of the inhabitants found to be suffering from Cr(VI) pollution induced diseases.

1.3.3. Status of Clean-up Activity

The pollution problem from the chromite mines at Sukinda is well known and the mining industry has taken some steps to reduce the levels of contamination by installing treatment plants. However, according to state audits from Orissa, these have failed to meet agency regulations. The available methods could achieve the goal with very limited success. The Orissa government has said, “It is unique, it is gigantic and it is beyond the means and purview of the (Orissa Pollution Control) Board to solve the problem”.

1.4. Objectives

The overall objective of this work is to prepare a microporous activated carbon (AC) from Bael fruit shell for the efficient removal of hexavalent chromium from aqueous phase.

The specific objectives of this study are:

- To prepare a microporous activated carbon from Bael fruit shell by chemical activation and to investigate the effect of various chemical activating agents such as H_3PO_4 , $ZnCl_2$ and KOH on the porous characteristics of AC.
- To estimate the effect of various preparation parameters such as impregnation ratio, carbonization temperature and holding time on surface area, pore volume, micropore surface area and micropore volume of AC.
- To study and compare the surface characteristics of the developed AC with the commercially available AC.
- To remove hexavalent chromium from aqueous phase by ACs prepared at optimum conditions and to determine the effect of various process parameters such as pH, adsorbent dose, initial Cr(VI) concentration, contact time and temperature on the removal efficiency of ACs.
- To explore the viability of prepared AC for the removal of Cr(VI) and for regeneration by simple and feasible techniques as compared to commercial activated carbon.
- To model the Cr(VI) adsorption process on ACs by Design of Experiments (DoE) by using two-level and four-factor, Full Factorial Design (FFD).

1.5. Scope of the Study

This study shall provide a better solution to hexavalent chromium pollution in aqueous phase by developing an efficient microporous adsorbent. It will also provide an ideal technology to utilize and convert biomass waste into valuable product i.e. activated carbon which can be commercialized for the removal of contaminants from aqueous phase.

1.6. Organization of Thesis

The thesis has been organized in seven chapters. *Chapter-1* is an introductory chapter. *Chapter-2* contains the detailed literature review on various topics related to the present work. *Chapter-3* includes all the materials and methods involved in the work. *Chapter-4* contains the preparation of activated carbon from raw material at different operating conditions and its characterization. AC was prepared using different chemical activating agents such as H_3PO_4 , ZnCl_2 and KOH . Influence of impregnation ratio, carbonization temperature and holding time on the porous characteristics of AC was investigated. The samples prepared were characterized by N_2 adsorption-desorption isotherms. The evolution of various surface groups during the activation of AC was explored. *Chapter-5* portrays the potential of prepared activated carbon for Cr(VI) adsorption over a wide range of process parameters. Influence of operating parameters such as pH, adsorbent dose, contact time, initial metal concentration and temperature on rate of adsorption was explored. The prepared AC was compared with the commercial AC for Cr(VI) removal efficiency and the spent AC was regenerated by simple and feasible techniques. *Chapter-6* postulates various adsorption models developed for Cr(VI) adsorption on ACs by using Design of Experiments (DoE). A two-level and four-factor Full Factorial Design (FFD) was employed for the process modeling. Effects of main factors and their interactions on the response were estimated. *Chapter 7* contains conclusions and future perspective.

Literature Review

2.0. Summary

The objective of the study is to produce microporous activated carbon that can remove hexavalent chromium from aqueous solution. This chapter gives a detail review on the pertinent literature. It provides a thorough input on the history, types, characterization, and utilization etc. related to activated carbon. It also demonstrates about the overall parameters which influence Cr(VI) adsorption on activated carbon. Various surface properties that signifies the development of microporous structure and the methodology adopted is depicted.

2.1. Types of Carbon Materials

All the carbon materials composed of the carbon element has unique bonding with other elements and with itself. Depending on type of hybridization of the carbon atoms, the main allotropic forms of carbon (Delhaes, 1998) are classified as diamond, graphite and fullerenes.

Diamond forms a cubic 3D structure (sp^3 – based structure) in which each carbon atom bonds with four other carbon atoms through sp^3 σ bonds. The C-C bond length is 154 pm. Diamond has the highest atomic density of any solid and is the hardest material with the highest thermal conductivity and melting point. *Graphite* has a hexagonal layered structure (sp^2 – based structure) in which carbon atoms are bonded to neighboring carbon atoms by sp^2 σ and delocalized π bonds. Graphite has an even higher thermal conductivity than diamond and exhibits a good electrical conductivity. *Fullerenes* are three dimensional carbon structures where the bonds between the carbon atoms are bent to form an empty cage of sixty (C_{60}) or more carbon atoms. This is due to the re-hybridization, resulting in a $sp^{2+\epsilon}$ form, which is intermediate between sp^2 and sp^3 (Ebbesen and Takada, 1995).

The majority of carbons exhibit the allotropic forms, i.e. a sp^2 – based structure. Based on the degree of crystallographic order in third direction (c-direction), the allotropic form of graphite can be classified into graphitic carbons and non-graphitic carbons (Franklin, 1951).

Non-graphitic carbons in turn divided into graphitizable and non-graphitizable carbons. A graphitizable carbon is “a non-graphitic carbon which upon graphitization (heat treatment) is converted into graphitic carbon”, while a non-graphitizable carbon is “a non-graphitic carbon which cannot be transformed into graphitic carbon” by high-temperature treatment.

Carbons exhibit different structures depending on the size and such a wide variety of possible structures gives rise to a large amount of different types of carbons. Figure 2.1 shows a schematic representation of some of these carbon structures (Bandosz, 2006).

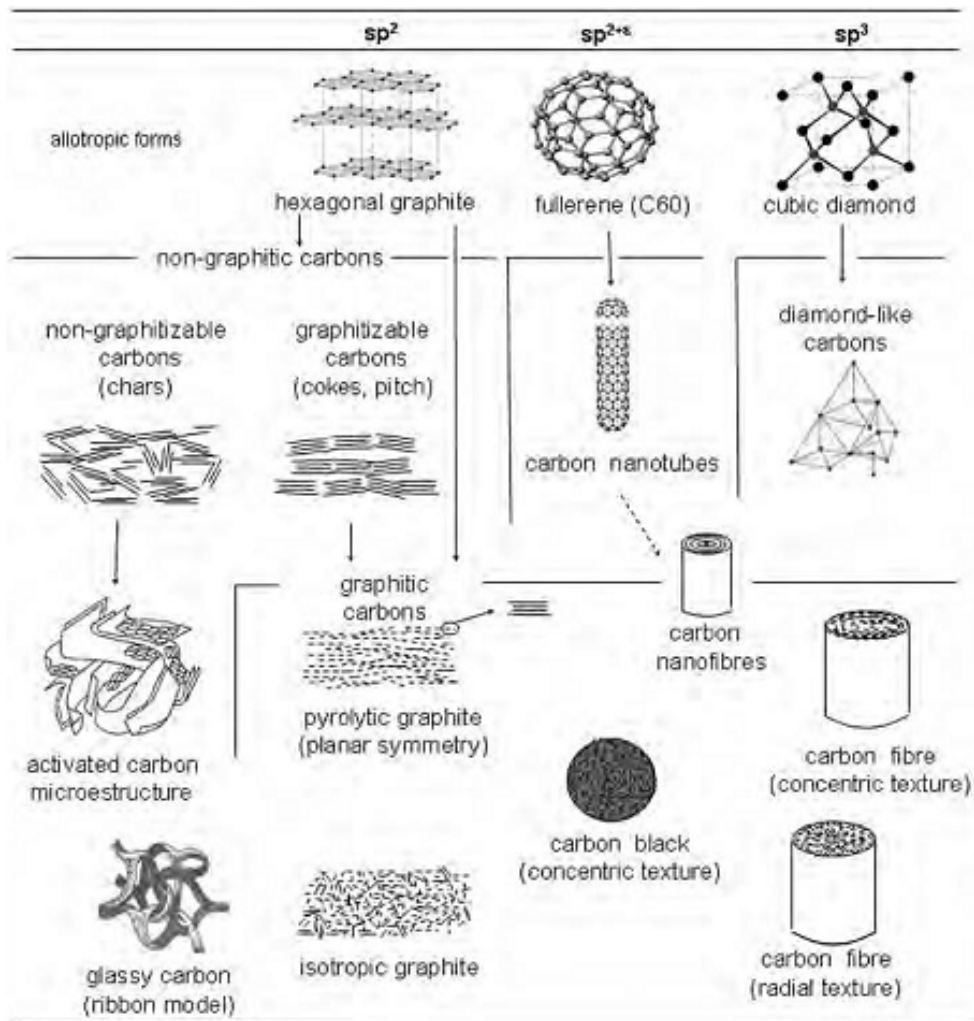


Fig. 2.1. Major allotropic forms of carbon and some of carbon structures derived from these forms (Bandosz, 2006)

2.2. Activated Carbon

Activated carbon (AC) is a non-graphitic, non-graphitizable carbon with a highly disordered microstructure. It is well known for high adsorption capacity due to its high surface area and porosity.

2.2.1. Historical Background

In ancient times (1500 B.C), activated carbon (AC) has been used for medicinal purposes. There after the adsorptive powers of AC were discovered in 1773 when Scheele (Dietz, 1944) conducted experiments with gases. However in 19th century, the industrial production of activated carbon was well established and gradually it replaced bone char in sugar refining processes (Bansal et al., 1988).

Historical production and use of activated carbon has been summarized below (1770 – 1931)

Year	Author	Significance
18th Century		
1773	Scheele	Recognized the adsorptive powers of the carbons (charcoal) by measuring the volumes of various gases adsorbed by carbons derived from different source materials.
1785	Lowitz	Studied the effectiveness of charcoal in decolorizing various aqueous solutions and this appears to be the first systematic account for application of char coal in liquid phase.
1793	Kehl	Discovered that carbon prepared from animal tissues could be used for color removal from solutions.
1794	–	An English sugar company used wood charcoal for the decolorizing sugar syrups but kept the method of preparing the carbon a secret.
19th Century		
1805	Delessert	Demonstrated the decolorizing power of charcoal for sugar-beet liquor.
1822	Bussy	Prepared activated carbon by heating blood with potash which has

20 – 50 times the decolorizing power of bone char. This was the first recorded example of producing an activated carbon by a combination of thermal and chemical processes.

1856	Stenhouse	Prepared the decolorizing chars by heating a mixture of flour, tar, and magnesium carbonate.
1862	Lipscombe	Prepared a carbon and applied to purify potable water
1865	Hunter	Recognized the gas adsorption properties of activated carbon prepared from coconut shells.
1868	Winser	Prepared activated carbon by heating paper mill waste with phosphates.
20th Century		
1900	Ostrejko	Set the basis for the development of commercial activated carbon through process involving (a) incorporation of metal chlorides before carbonization (b) selective oxidation with carbon dioxide at high temperatures.
1911	–	Using Ostrejko’s gasification approach activated carbon was prepared from wood by the Fanto Works, Austria with the trade name ‘Eponit’. It is the first activated carbon produced industrially and marketed as decolorizer for the sugar refining industry.
1913	Wunch	Recognized that the decolorizing capacity of Eponit was greatly increased by heating with zinc chloride.
1914–1918	–	With the introduction of poisonous gases in the First World War, the search for other precursors for the preparation of activated carbon with high adsorption capacity was boosted up to use in military respirators. Granular activated carbon with reliably controlled adsorptive and physical properties was developed by activating wood chips with zinc chloride. A group studying under Chaney, USA determined that carbon prepared from coconut shell has the combination of required characteristics.

1931 Kubelka Interpreted sorption phenomena on active carbon by the mechanism of capillary condensation.

Further research investigations and major breakthroughs were cited throughout the thesis.

2.2.2. Preparation of Activated Carbon

Generally activated carbon can be prepared from various raw materials including agricultural and forestry residues. Generally most of the precursors used for the preparation of activated carbon are rich in carbon (Prahas et al., 2008). Production of AC was achieved typically through two routes, physical activation and chemical activation (Bansal et al., 1988; Encinar et al., 1998).

Physical activation involves carbonization of raw material followed by the activation at high temperatures (between 800 and 1100 °C) in the presence of oxidizing gases like carbon dioxide or steam (Aworn et al., 2009; Bonelli et al., 2001; Cabal et al., 2009; Cagnon et al., 2009; Lopez de Letona Sanchez et al., 2006; Oh and Park, 2002; Petrov et al., 2008; Zabaniotou et al., 2008; Zhu et al., 2011), whereas chemical activation mixing of chemical agent with precursor and then followed by pyrolysis at moderate temperatures in the absence of air (Ahmadpour and Do, 1997; Budinova et al., 2006; Klijanienko et al., 2008; Munoz-Gonzalez et al., 2009; Rosas et al., 2009; Soleimani and Kaghazchi, 2008; Youssef et al., 2005; Zhang et al., 2005; Zuo et al., 2009).

Typical preparation of activated carbon involves carbonization of the raw material in the absence of oxygen, and activation of the carbonized product (Al-Duri, 1996; Ioannidou and Zabaniotou, 2007). Chemical activation, on the other hand enjoys the benefit of development of better porous structure in a single process route at low carbonization temperatures as compared to physical activation.

2.2.2.1. Physical Activation

Physical activation is a two-step process. It involves carbonization of raw material followed by activation at elevated temperatures in the presence of suitable oxidizing gases such as carbon dioxide, steam, air or their mixtures. Carbonization temperature ranges between 400 °C to 800 °C, and activation temperature ranges between 800 °C to 1100 °C. Physical activation of

various raw materials was shown in Table 2.1. Generally, CO₂ is used as activation gas, since it is clean, easy to handle, and it facilitates control of the activation process due to the slow reaction rate at high temperatures.

Table 2.1. Various physical activating agents and precursors used for AC production

Activating agent	Material	Source
Steam	Rice husk, corn cob, olive residues, sunflower shells, pinecone, rapeseed, cotton residues, olive-waste cakes, coal, rubberwood sawdust, fly ash, coffee endocarp	(Baçaoui, 2001; El-Hendawy et al., 2001; Haykiri-Acma et al., 2006; Lazaro et al., 2007; Lu et al., 2010; Malik, 2003; Nabais et al., 2008; Prakash Kumar et al., 2006; Zhang et al., 2011)
CO ₂	Oak, corn hulls, coconut shells, corn stover, rice straw, rice hulls, pecan shells, pistachio nutshells, coffee endocarp, sugarcane bagasse, corn cob, waste tyres, textile fibers, anthracite	(Ahmedna et al., 2000; Aworn et al., 2009; Betancur et al., 2009; Guo et al., 2009; Lua et al., 2004; Nabais et al., 2008; Salvador et al., 2009; Yang and Lua, 2003; Zhang et al., 2004; Zhu et al., 2011)
Air	Peanut hulls, almond shells, olive-tree wood, almond tree pruning, coal	(Ganan et al., 2006; Girgis et al., 2002; Liu et al., 2007; Marcilla et al., 2000; Ould-Idriss et al., 2011)

2.2.2.2. Chemical Activation

Preparation of activated carbon by chemical activation is a single step process in which carbonization and activation is carried out simultaneously. Initially the precursor is mixed with chemical activating agent, which acts as dehydrating agent and oxidant. Chemical activation offers several advantages over physical activation which mainly include (i) lower activation temperature (< 800 °C) compared to the physical activation temperature (800 – 1100 °C) (El-Hendawy et al., 2008), (ii) single activation step, (iii) higher yields, (iv) better porous characteristics, and (v) shorter activation times (Nowicki et al., 2006) The most commonly used chemical activating agents are H₃PO₄, ZnCl₂, and KOH. Table 2.2 shows various chemical agents used for the activation of AC prepared from different raw materials.

Table 2.2. Various chemical activating agents and precursors used for AC production

Activating agent	Material	Source
ZnCl ₂	Corn cob, coconut shells, macadamia nutshells, peanut hulls, almond shells, hazelnut shells, apricot stones, rice husk, tamarind wood, cattle-manure, pistachio-nut shells, bagasse, sunflower seed hulls.	(Acharya et al., 2009; Ahmadpour and Do 1997; Aygun et al., 2003; Azevedo et al., 2007; Cronje et al., 2011; Girgis et al., 2002; Liou, 2010; Lua and Yang, 2005; Qian et al., 2007; Sahu et al., 2010; Tsai et al., 1997, 1998; Yalcin and Sevinc 2000).
KOH	Rice straw, corn cob, macadamia nutshells, peanut hulls, olive seed, rice straw, cassava peel, petroleum coke, coal, cotton stalk, pine apple peel.	(Ahmadpour and Do 1997; Basta et al., 2009; Deng et al., 2010; Foo et al., 2011; Girgis et al., 2002; Oh and Park 2002; Kawano et al., 2008; Stavropoulos and Zabaniotou 2005; Sudaryanto et al., 2006; Tsai et al., 2001; Tseng et al., 2008; Wu et al., 2010, 2011).
H ₃ PO ₄	Hemp, Peanut hulls, almond shells, pecan shells, corn cob, bagasse, sunflower seed hulls, lignin, grain sorghum, rice straw, oak, birch, sewage sludge, chestnut wood, eucalyptus bark, rice hull, cotton stalk, jackfruit peel.	(Ahmedna et al., 2004; Deng et al., 2010; Diao et al., 2002; El-Hendawy et al., 2001; Fierro et al., 2010; Girgis et al., 2002; Gomez-Serrano et al., 2005; Guo and Rockstraw, 2007; Klijanienko et al., 2008; Liou, 2010; Montane et al., 2004; Patnukao and Pavasant, 2008; Prahas et al., 2008; Rosas et al., 2009; Wang et al., 2011; Zuo et al., 2009).
K ₂ CO ₃	Pine apple peel, corn cob, cotton stalk, almond shell, coconut shell, oil palm shell, pistachio shell, walnut shell, bamboo.	(Adinata et al., 2007; Deng et al., 2010; Foo et al., 2011a,b; Hayashi et al., 2002; Horikawa et al., 2010; Tsai et al., 2001).

2.2.3. Structure of Activated Carbon

The adsorption capacity of AC highly depends on the structure of activated carbon.

2.2.3.1. Porous Structure

The high adsorptive capacities of activated carbons are highly related to porous characteristics such as surface area, pore volume, and pore size distribution. All activated carbons have a porous structure, containing up to 15 % of mineral matter in the form of ash content (Bansal et al., 1988). The porous structure of AC formed during the carbonization

process and was developed further during activation, when the spaces between the elementary crystallites are cleared of tar and other carbonaceous material. The structure of pores and pore size distribution largely depends on the nature of the raw material and activation process route. The activation process removes disorganized carbon by exposing the crystallites to the action of activating agent which leads to the development of porous structure. The pore systems of activated carbon are of different kinds and the individual pores may vary greatly both in size and shape. Active carbons are associated with pores starting from less than a nanometer to several thousand nanometers. A conventional classification of pores according to their average width (w), which represents the distance between the walls of slit shaped pore or the radius of a cylindrical pore, proposed by [Dubinin et al., \(1960\)](#) and officially adopted by the International Union of Pure and Applied Chemistry (IUPAC) is summarized in [Table 2.3](#).

Table 2.3. Classification of pores according to their width ([IUPAC, 1972](#))

Type of pores	Width (w)
Micropores	< 2 nm (20 °A)
Mesopores	2 – 50 nm (20 – 500 °A)
Macropores	> 50 nm (> 500 °A)

The effective radii being less than 2 nm, the adsorption in micropores occurs through volume filling and there is no capillary condensation. Generally micropores have a pore volume of 0.15 to 0.70 cm³/g, and constitute about 95% of the total surface area of the AC. [Brunauer \(1970\)](#) and [Dubinin \(1979\)](#) further classified that the micropores can be subdivided into two overlapping microporous regions such as ultra-micropores (with effective pore radii less than 0.7 nm), and super-micropores (having radii of 0.7 to 2 nm). Generally the microporous structure of an adsorbent is characterized by adsorption of gases and vapors and, to a small extent, by small-angle x-ray technique ([Rosas et al., 2009](#); [Zuo et al., 2009](#); [Castro-Muniz et al., 2011](#); [Yang and Lua, 2006](#); [Liou, 2010](#)).

Mesopores, also termed as transitional pores, ranges from 2 to 50 nm of width. The surface area of mesopores does not constitute more than 5% of total surface area and their volume varies in between 0.1 and 0.2 cm³/g. However, by using special methods, it is possible to

enhance mesopores attaining a volume of 0.2 to 0.65 cm³/g and surface area of 200 m²/g. Capillary condensation and adsorption-desorption hysteresis are the characteristic features of mesopores (Aworn et al., 2008; Lei et al., 2006; Iang et al., 2010; Hao et al., 2011). Beside their contribution to the adsorption of adsorbate, mesopores act as conduits which lead the adsorbate molecule to the micropore network. The typical pore size distribution of activated carbon can be observed in Figure 2.2. Generally mesopores are characterized by adsorption-desorption isotherms of gases, by mercury porosimetry, and by electron microscopy (Liou, 2010; Zhu et al., 2007; Hu and Srinivasan, 2001; Kennedy et al., 2007).

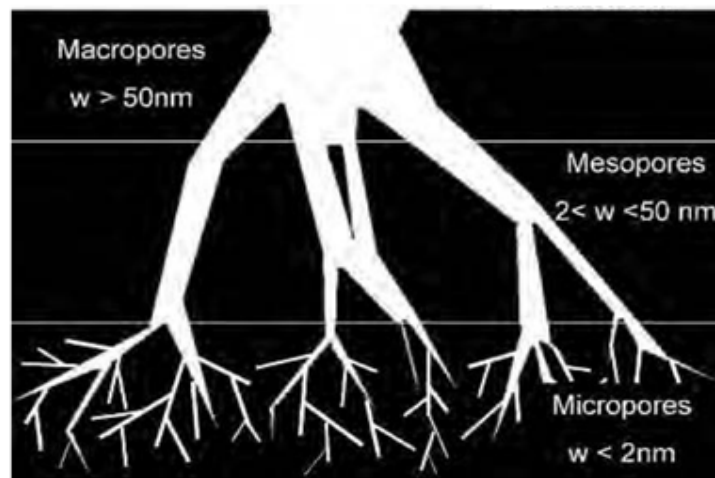


Figure 2.2. Graphical representation of pore structure in activated carbon

Pores having effective radii larger than 50 nm are considered as macropores, frequently in the range 500 to 2000 nm. The contribution of macropores to the total surface area and pore volume is very small and does not exceed 0.5 m²/g and 0.2 to 0.4 cm³/g, respectively. Hence, in adsorption process macropores are not of considerable importance but they act as transport channels for the adsorbate into the mesopores and micropores. Macropores can be characterized by mercury porosimetry and by electron microscopy (Jaramillo et al., 2010; Mittelmeijer-Hazeleger and Martin-martinez, 1992; Pastor-Villegas and Duran-Valle, 2002; Yao and Liu, 2012).

2.2.3.2. Crystalline Structure

Microcrystalline structure of activated carbons starts to develop during the carbonization process. The Crystalline structure of activated carbons differed from the graphite with respect to

the interlayer spacing. The interlayer spacing ranges between 0.34 and 0.35 in active carbons, which is 0.335 in case graphite. The basic structural unit of activated carbon is closely approximated by the structure of graphite. The graphite crystal is composed of layers of fused hexagons held by weak van der Waals forces shown in [Figure 2.3](#).

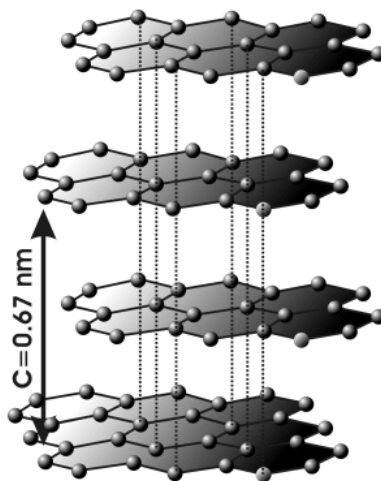


Figure 2.3. Layered structure of graphite

Much of the literature suggests a modified graphite structure for activated carbon. During the carbonization process free valences were created due to the regular bonding disruption of micro-crystallites. In addition, process conditions and presence of impurities influence the formation of vacancies (pores) in microcrystalline structure ([Skubiszewska-Zieba, 2010](#); [Yang and Lua, 2006](#); [Kennedy et al., 2004](#)).

Based on the graphitizing ability, active carbons are classified into two types, graphitizing and non-graphitizing carbons. Graphitizing carbon had a large number of graphite layers oriented parallel to each other. The carbon obtained was delicate due to the weak cross linking between the neighbor micro-crystallites and had a less-developed porous structure. The non-graphitizing carbons are hard due to strong cross-linking between crystallites and show a well developed microporous structure ([Franklin, 1951](#); [Jenkins and Kawamura, 1976](#)). The formation of non-graphitizing structure with strong cross-links is promoted by the presence of associated oxygen or by an insufficiency of hydrogen in the original raw material. The schematic representations of the structures of graphitizing and non-graphitizing carbons are shown in [Figure 2.4](#).

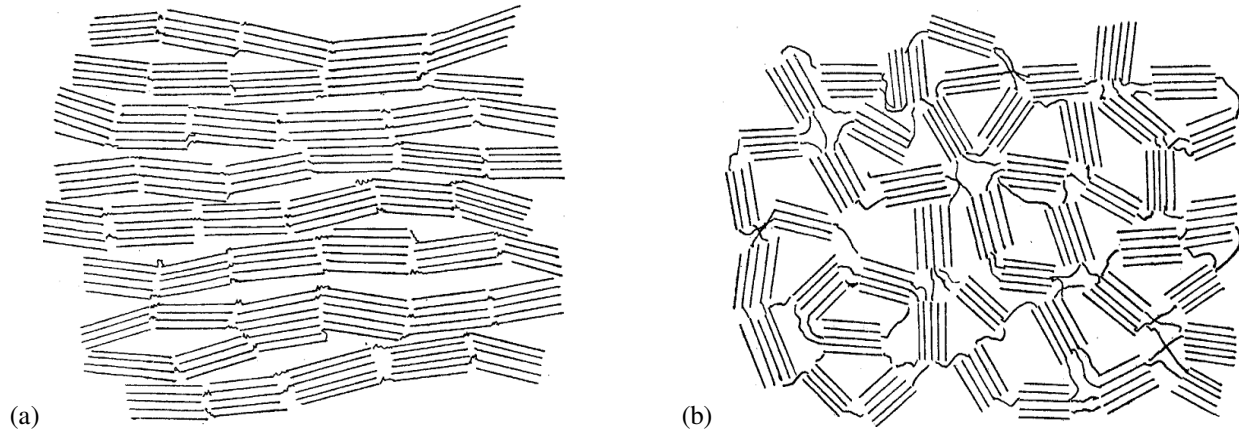


Figure 2.4. Schematic illustration of structure of activated carbon: (a) graphitized carbon, and (b) non-graphitized carbon (Franklin, 1951)

2.2.3.3. Chemical Structure

Besides the porous and crystalline structure, an active carbon surface has a chemical structure as well. Though the adsorption capacity of activated carbon is determined by its porous structure but is strongly influenced by a relatively small amount of chemically bonded heteroatoms (mainly oxygen and hydrogen) (Bansal et al., 1988). The variation in the arrangement of electron clouds in the carbon skeleton results in the creation of unpaired electrons and incompletely saturated valences which influences the adsorption properties of active carbons, mainly for polar compounds.

Activated carbons are invariably associated with significant amounts of oxygen, hydrogen (Rodriguez-Reinoso et al., 1992) and other heteroatoms like sulfur, nitrogen and halogens (Valix et al., 2006). These heteroatoms derived from the raw material involve in the structure of AC during carbonization process, or they may be chemically bonded to the surface during activation (Rodriguez-Reinoso, 1998). Much of the literature show that the heteroatoms are bonded to carbon atoms of the edges and corners of the aromatic sheets or to the carbon atoms at defect positions to form carbon-oxygen, carbon-hydrogen, carbon-sulfur, carbon-nitrogen, and carbon-halogen surface compounds, known as surface groups or surface complexes (Castro-Muniz et al., 2011; Valix et al., 2006).

A considerable effort has been directed to identify the role of surface chemistry of carbons on the adsorption of aromatics (Petrova et al., 2010; Valderrama et al., 2008; Tham et

al., 2011; Moreno-Castilla, 2004; Daifullah and Girgis, 2003; Adhoum and Monser, 2004; Garcia et al., 2004), dyes (Faria et al., 2004; Lie et al., 2006; Shi et al., 2010), heavy metals (Namasivayam et al., 2007; Duman and Ayranci, 2010; Mamcilovic, et al., 2011; Shen et al., 2010; Monser and Adhoum, 2002; Babel and Kurniawan, 2004; Chen et al., 2003; Zhang et al., 2011), etc from aqueous phase. In the field of catalysis, numerous works have focused on the role of surface chemistry with respect to the dispersion of catalyst, or the catalytic activity (Petkovic et al., 2009; Quintanilla et al., 2007; Calvo et al., 2010; Huang et al., 2003; Calafat et al., 1996; Fraga et al., 2002).

Oxygen is by far the most important heteroatom that influences the surface behavior, wettability, and electrical or catalytic properties of carbon. Boehm (Boehm, 1994) carried out research extensively on the presence of oxygen on the carbon surface in the form of functional groups. Generally, oxygen-containing functionalities are obtained by oxidation treatments of the carbon (Jaramillo et al., 2010; Daud and Houshamnd, 2010; Wang et al., 2004).

2.2.4. Classification of Activated Carbon

Activated carbons are complex products and the classification is difficult based on their preparation methods, physical properties, and surface characteristics. However, the general classification of activated carbons based on particle size divides them into Powered Activated Carbon (PAC), Granular Activated Carbon (GAC), and Activated Carbon Fibres (ACF) (Babel and Kurniawan, 2003).

2.2.4.1. Powered Activated Carbon

Powered Activated Carbon (PAC), has a typical particle size of less than 0.1 mm and the common size of the particle ranges from 0.015 to 0.025 mm. Typical applications of PAC are industrial and municipal waste water treatments, sugar decolorization, in food industry, pharmaceutical, and mercury and dioxin removal from a flue gas stream (Cook et al., 2001; Foo and Hameed, 2009; Ormad et al., 2008; Satyawali and balakrishnan, 2009; Zhang et al., 2006).

2.2.4.2. Granular Activated Carbon

Granular Activated Carbon (GAC), has mean particle size between 0.6 to 4 mm. It is usually used in continuous processes of both liquid and gas phase applications. GAC has an

advantage over PAC, of offering a lower pressure drop along with the fact that it can be regenerated and therefore reused more than once. In addition to the proper micropore size distribution, its high apparent density, high hardness, and a low abrasion index made GAC more suitable over PAC for various applications (Cerminara et al., 1995; Hai et al., 2011; Hijnen et al., 2010; Scharf et al., 2010; Zhang et al., 2008).

2.2.4.3. Activated Carbon Fibers

Activated carbon Fibers (ACFs) are carbonized carbons which are subsequently heat treated in an oxidizing atmosphere. ACF began to be developed in 1970 using the precursor viscose rayon which mainly consists of cellulose (Doying, 1966). Later thermoset polymer materials like saran and phenolic resins were used as precursors to produce ACF (Menendez-Diaz and Martin-Gullon, 2006). A good ACF precursor must be non-graphitic and non-graphitizable carbon fibre which was isotropic in nature. From the end of 1980s, interest is still centered on the production of ACFs from various inexpensive precursors (Derbyshire et al., 2001; Ko et al., 2002; Nahil and Williams, 2011; Oh and Jang, 2003; Oya et al., 1993; Rosas et al., 2009).

2.2.5. Characterization of Activated Carbon

Activated carbons are strongly heterogeneous due to the existence of different sizes of pores including micropores, mesopores and macropores. In addition, the surface heterogeneity of activated carbons is often significant because of various oxygen and other groups present on the surface. Surface and structural properties of the activated carbons can be studied directly by employing various techniques like electron microscopy, X-ray analysis and various spectroscopic methods. In addition, these properties can be investigated by indirect methods such as gas adsorption and thermal analyses. The data obtained from adsorption can be used mainly to extract information about surface heterogeneity and porosity of adsorbents.

The aim of this section is to provide an overview of the characterization of activated carbons by gas adsorption isotherms and by some other spectroscopic techniques.

2.2.5.1. Gas Adsorption Isotherms

Gas adsorption is one of the most extensively used techniques for characterization of porous materials. The adsorption isotherm gives lot of useful information regarding the adsorbate, the adsorbent, and the adsorbate – adsorbent interactions. For a given adsorbate adsorbed on a particular adsorbent one can write the adsorption isotherm (Kuzin, 1964) as:

$$x = f(p, T) \quad (2.1)$$

where, x is the amount of adsorbate adsorbed on unit mass of adsorbent, p is the pressure and T is the temperature of the adsorbate.

Gases such as N₂, Ar, Kr, CO₂ (Blanco-Lopez et al., 2000; Jagiello and Thommes, 2004; Lithoxoos et al., 2010; Ustinov et al., 2006) and vapors of low-boiling aliphatic hydrocarbons, alcohols, benzene, carbon tetrachloride, water etc (Cao et al., 2002; Bae and Do, 2002; Finqueneisel et al., 2005; Kim et al., 2006; Lodewyckx, 2010) are most widely used. Nitrogen and argon are most commonly used because of their nonpolarity in nature.

2.2.5.1.1. Qualitative Interpretation of Adsorption Isotherms

A visual inspection of isotherm shapes provides considerable information about the porous network present in the adsorbent. Experimental adsorption isotherms measured on a wide variety of gas-solid systems were grouped into six classes in the IUPAC classification. The first five types, i.e., type - I to type - V were originally proposed by Brunauer et al., (1940) and named as BDDT classification. The IUPAC 1985 classification included the type VI isotherm which was observed after the BDDT classification.

Type I or Langmuir isotherms are concave to the relative pressure (p/p^0) axis. The adsorption in Type I isotherms does not increase continuously but attains a limiting value shown by the plateau (Arami-Nitya et al., 2011) is due to the pores being so narrow that they cannot accommodate more than a single molecular layer. These isotherms are thus characterized by a plateau that is almost horizontal and parallel to the pressure axis. The adsorption at high relative pressures is small and tending to level off. This type of isotherms exhibited by microporous solids having relatively small external surfaces, for example, activated carbons and molecular

sieve zeolites. The shape of the isotherm can be well explained by Langmuir model. The typical type 1 isotherms of activated carbons were shown in Figure 2.5.

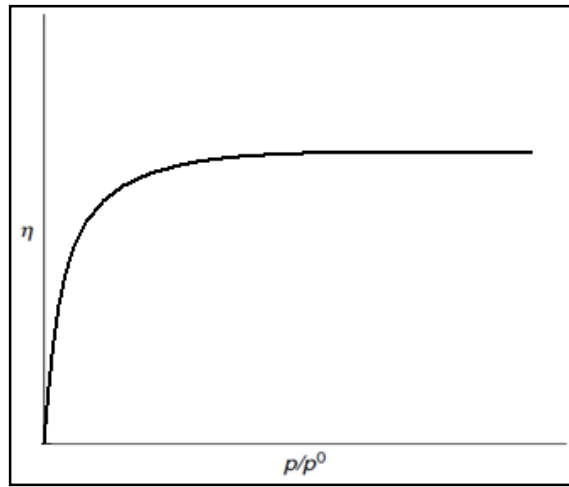


Figure 2.5. Type – I isotherm

Type II isotherms represents unrestricted monolayer-multilayer adsorption. The shape of isotherm, shown in Figure 2.6, is concave at low relative pressures, then almost linear and finally convex to the p/p^0 axis. The point at which the linear portion begins was termed as point *B* (Emmet and Brunauer, 1937) and this is considered as the point at which the monomolecular layer (monolayer) is completed and the beginning of the formation of the multimolecular layer (multilayer) thus the adsorption at this point should be equal to the monolayer capacity X_m . In their earlier work they suggested that the value at which the extrapolated linear branch cuts the adsorption axis termed as point *A*, might represent the monolayer capacity (Brunauer and Emmet, 1935). In calculating monolayer capacity point *B* was preferred than point *A*, because the value of monolayer capacity X_B calculated from point *B* agreed well with the value of monolayer capacity X_m , calculated using BET equation for a variety of systems (Drain and Morrison, 1952, 1953). Type II isotherms are obtained with non-porous or macroporous adsorbents.

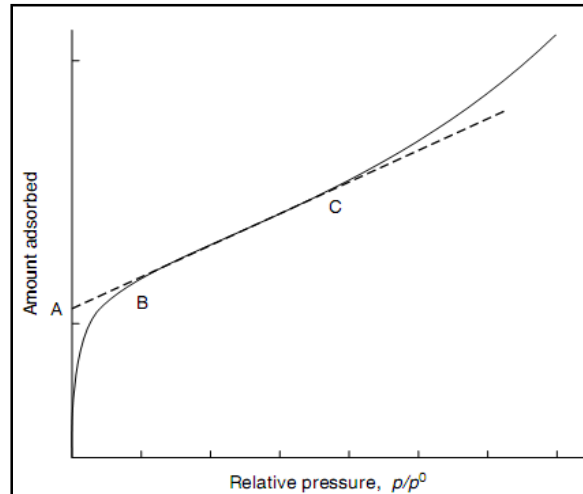


Figure 2.6. Type – II isotherm

Type III and type V isotherms are not common and are characterized by being convex to the pressure axis (Figure 2.7). Type III isotherms are convex to the p/p^0 axis over the complete range, whereas type V isotherm reaches a plateau at fairly high relative pressures, often at p/p^0 higher than 0.51, i.e., in the multilayer region. The convexity of isotherms is due to the cooperative adsorption, which means that the already adsorbed molecules enhance the further adsorption of other molecules. The adsorbate-adsorbent interactions are very weak and this results in small adsorption at lower relative pressures. After that the adsorbate-adsorbate interactions enhance the adsorption of other molecules and hence the isotherm becomes convex to the p/p^0 axis. Type III isotherms are generally obtained in case of nonporous adsorbents, and type V isotherms are uncommonly obtained on mesoporous or microporous adsorbents, provided that the adsorbent-adsorbate interactions are weak.

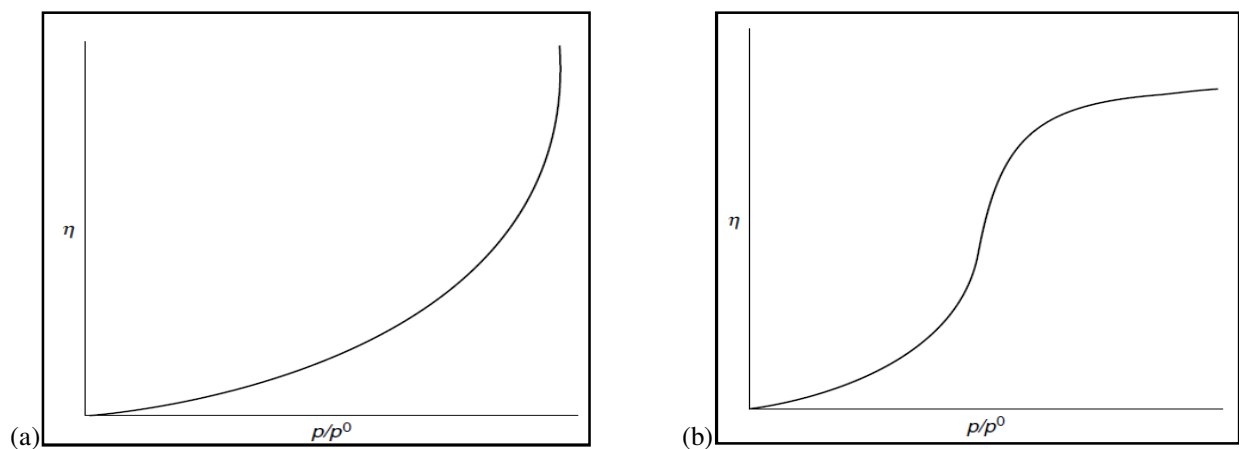


Figure 2.7. (a). Type – III isotherm and (b) Type – V isotherm

Type IV isotherms are associated with the capillary condensation in mesopores, indicated by the steep slope at higher relative pressures (Figure 2.8). The portion of isotherm which is parallel to the pressure axis is attributed to the filling of the larger pores by capillary condensation. The most significant characteristic of type IV isotherm is adsorption-desorption hysteresis. Type IV isotherms are obtained in the case of oxide gels and several porous carbon materials containing pores in the mesopore range.

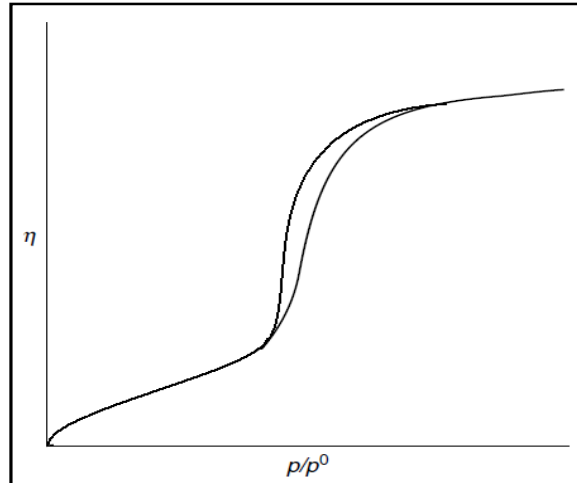


Figure 2.8. Type – IV isotherm

Type VI isotherm or stepped isotherm (Figure 2.9) is relatively rare and is associated with layer-by-layer adsorption on a highly uniform surface. The step height and sharpness depends on the system and temperature. Amongst the best examples of type VI isotherms are those obtained with Ar or Kr on graphitized carbon blacks at liquid nitrogen temperature.

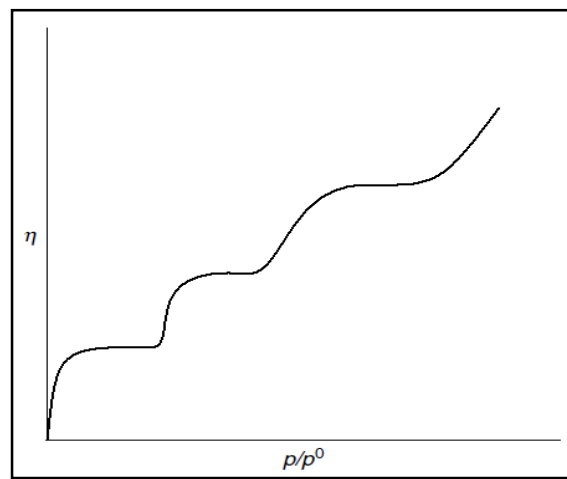


Figure 2.9. Type – VI isotherm

The adsorption process on mesoporous activated carbons is often accompanied by adsorption-desorption hysteresis (Hangstam et al., 1966; Burlakova and Naidich, 2005; Jia and Thomas, 2000; Jia et al., 2002). The hysteresis is usually attributed to the thermodynamic or network effects or the combination of these two effects (Burlakova and Naidich, 2005). According to the IUPAC classification, hysteresis loops are classified into four types as shown in Figure 2.10.

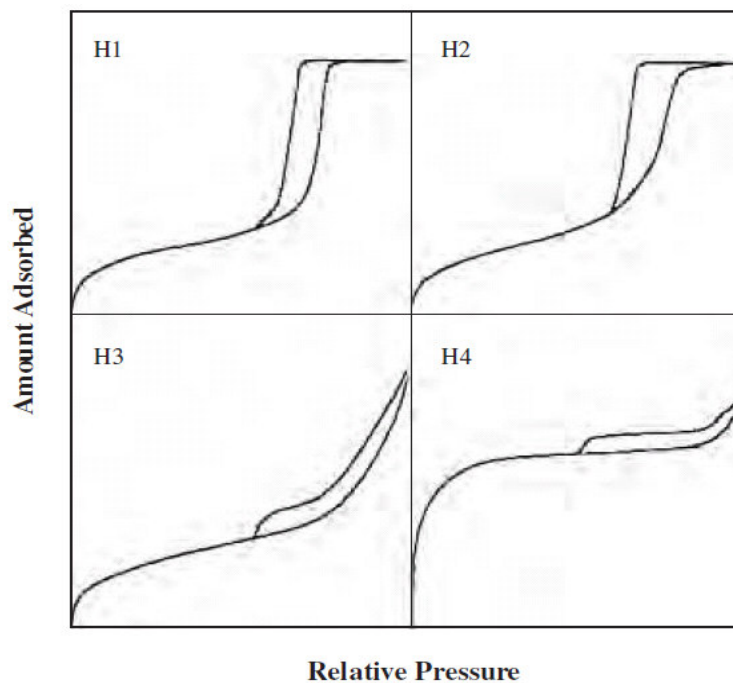


Figure 2.10. Classification of adsorption-desorption hysteresis loops

Type H1 loop exhibits parallel and nearly vertical branches. The H1 hysteresis loops are characteristic for materials containing cylindrical pore geometry and high degree of uniform pore size distribution (Polshina et al., 1996). The type H2 loop has a triangular shape and a steep desorption branch and it can be found in case of many porous inorganic oxides and was attributed to the pore connectivity effects (Jia and Thomas, 2000). Isotherms with type H3 loops that do not level off at relative pressures close to the saturation vapor pressure were reported for the materials containing slit-like pores. Type H4 loops feature parallel branches to the pressure axis and their occurrence have been mainly attributed to adsorption-desorption in narrow slit-like pores.

2.2.5.1.2. Quantitative Interpretation

The most commonly used equations to interpret adsorption isotherms are the Langmuir, the Brunauer-Emmet-Teller (BET), and the Dubinin-Radushkevich (DR) isotherm equations. Initially, the Langmuir and BET isotherms are used to interpret the adsorption isotherms of nonporous adsorbents, later they were applied for the isotherms obtained from microporous materials. On the other hand, the DR equation is a derivative of Rayleigh, Gaussian or Lorentzian distributions and is not based on a model of adsorption process.

The Langmuir Isotherm

The Langmuir isotherm equation is the first theoretically developed adsorption isotherm and based on this equation many equations are proposed later. Langmuir isotherm is more applicable to chemisorption, but is also often applied to physisorption isotherms of type I. A convenient form of Langmuir equation (Langmuir, 1918) is

$$\frac{p/p^o}{n^a} = \frac{1}{bn_m^a} + \frac{p/p^o}{n_m^a} \quad (2.2)$$

where, p is equilibrium vapor pressure (Pa), p^o is saturation vapor pressure (Pa). n^a is amount adsorbed (mmol/g), and n_m^a is monolayer adsorption capacity (mmol/g). The model is based on the following assumptions.

- i. Adsorbate molecules are attached to the surface of the adsorbent at definite localized sites.
- ii. Each site can hold only one adsorbate molecule.
- iii. All adsorption sites are energetically equivalent.
- iv. The interactions between the adsorbed molecules are negligible.

The BET (Brunauer-Emmet-Teller) Isotherm

An essential key parameter for characterization of porous solids is the specific surface area. Earlier studies reported the problem in measuring the high surface areas of microporous solids. Determination of specific surface area and saturation limit from an experimental isotherm is simple if the physical adsorption is limited to a close-packed monolayer. But, the main difficulty is physical adsorption generally involves multilayer adsorption and the formation of

second and subsequent molecular layers commences at pressures well below that required for completion of the monolayer. This problem was first solved by Brunauer, Emmet, and Teller (BET) by developing a simple isotherm model to estimate the monolayer capacity and hence the specific surface area. The simplified form of BET isotherm equation (Brunauer et al., 1938) is

$$\frac{p}{V(p^0-p)} = \frac{1}{V_m C} + \frac{(C-1)}{V_m C} \left(\frac{p}{p^0}\right) \quad (2.3)$$

where, V is the volume adsorbed at STP ($\text{cm}^3 \text{g}^{-1}$), V_m is the volume of monolayer capacity at STP ($\text{cm}^3 \text{g}^{-1}$), and the term C , the BET constant, is related to the energy of adsorption in the first adsorbed layer and its value is an indication of the magnitude of the adsorbent-adsorbate interactions. BET isotherm is based on following assumptions.

- i. Adsorption occurs only on well defined sites of adsorbent surface.
- ii. A molecule can act as a single adsorption site for a molecule of the upper layer.
- iii. The uppermost molecular layer is in equilibrium with the gas phase.
- iv. The molecular layer number tends to infinity at the saturation pressure.

The DR (Dubinin-Radushkevich) isotherm

Many microporous adsorbents including activated carbons contain pores over a wide range of pore sizes, including micro and mesopores. Hence, the isotherm obtained from such type of adsorbents reveals features from both type I and type IV isotherms. The filling of micropores occurs at very low relative pressures and is entirely governed by the enhanced gas-solid interactions. In addition to the strong adsorption potential a cooperative mechanism may play an important role in the micropore filling process. Dubinin and Radushkevich postulated an equation which allows the micropore volume to be calculated from the adsorption isotherm (Dubinin and Radushkevich, 1989):

$$\log W = \log(\tilde{V}_0 \rho) - \bar{K} \left[\log \left(\frac{p^0}{p} \right) \right]^2 \quad (2.4)$$

where, W is the volume of adsorbate filling micropores, ρ is the density of liquid adsorbate; \tilde{V}_0 is the micropore volume and k is defined as

$$k = 2.303K \left(\frac{RT}{\beta} \right)^2 \quad (2.5)$$

where, β is the affinity coefficient, and K is a constant, determined by the shape of the pore size distribution. A plot of $\log W$ versus $[\log(p^o/p)]^2$ should be a straight line with an intercept of $\log(\tilde{V}_o\rho)$, from which the micropore volume (\tilde{V}_o) can be calculated. The DR equation often fails to linearize when the adsorbent contains heterogeneous micropores. To overcome this, a more general equation, known as DA equation, was proposed by Dubinin and Astakhov. The linearized form of DA equation is

$$\ln W = \ln(\tilde{V}_o\rho) - \bar{K} \left[\ln \left(\frac{p^o}{p} \right) \right]^n \quad (2.6)$$

where, K is an empirical constant, and n is the Dubinin-Astakhov parameter. Depending on the type of micropore system, the value of n ranges from 2 to 5, and for adsorbents with homogeneous micropore structure, n is usually close to 2.

2.2.5.2. Spectroscopic Methods

The chemical structure of activated carbons can be investigated by using various spectroscopic techniques. Infrared (IR), Transmission and Absorption Infrared spectroscopy (T/A-IR), and Fourier Transform Infrared (FTIR) spectroscopy are the most commonly used spectroscopic techniques for the analysis of chemical structure of activated carbons.

Infrared spectroscopy (IR) is an important tool in various forms that can provide information about surface functional groups. Various studies have been cited on the IR studies of surface functional groups of carbon materials (Friedel and Hofer, 1970; Friedel and Carlson, 1972; Ishazaki and Marti, 1981). Furthermore, the sensitivity of IR measurements has been largely enhanced by Fourier-Transform (FT), Photoacoustic (PAS), and photothermal Beam Deflection (PDS) IR spectroscopy.

The transmission and absorption IR (T/A-IR) studies show low IR signal-to-noise ratio due to the preparation of pellets into thin layers (Ishazaki and Marti, 1981). The computerized Fourier-transform infrared spectroscopy (FTIR) has several advantages over conventional, dispersive spectroscopy. FTIR uses an interferometer in place of a grating or slits. This results in the availability of higher energy, of the order of 100 to 200 times over the dispersive system. This technique provides more precise information and also allows the measurement of lower concentrations of surface groups. The main advantages of FTIR over the conventional techniques

are the availability of higher energy throughout; the multiplex capability, and the greater accuracy of the frequency scale. This technique was used extensively for the analysis of surface functional groups of carbons materials (Chiang et al., 2002; Jaramillo et al., 2010; Kohl et al., 2010; Olivares-Marin et al., 2006; Shafeeyan et al., 2010; Shin et al., 1997).

2.3. Activated Carbon Applications

Activated carbon is an excellent and versatile adsorbent and its main applications include the adsorptive removal of color, odor, taste, and other undesirable organic and inorganic impurities from drinking waters; in the treatment of industrial waste water; air purification in food processing and chemical industries; in the purification of many chemical, food and pharmaceutical products; in respirators for work in hostile environments; and in a variety of other gas-phase applications. Nearly 80% of the total activated carbon is consumed for liquid-phase applications where, both granular and powdered activated carbons can be used (Moreno-Castilla and Rivera-Utrilla, 2001). For gas-phase applications, granular activated carbon is usually the choice. Table 2.4 documents various applications of granular activated carbon in removal of various contaminants.

The aqueous phase adsorption for the removal of both organic and inorganic compounds has been a very important application of activated carbon and researchers have reported potential applications of GAC to liquid phase. By using activated carbon, satisfactory results were obtained in the removal of organic chemicals from water (Gupta et al., 2006; Jarvie et al., 2005; Liyan et al., 2009; Namasivayam et al., 2007) and the adsorptive removal of organic compounds was compared with the inorganic ones (Moreno-Castilla, 2004).

Heavy metal ions stand out among the inorganic aquatic pollutants due to their persistence and toxicity. The heavy metal flux into groundwater and surface water has been increased randomly due to the unrestrained usage in industrial processes. Natural waters have been found to be contaminated with several heavy metals arising mostly from mining wastes and industrial discharges (Grousset et al., 1999; Schalscha and Ahumada 1998). According to World Health Organization (WHO, 2004; 2006), the most toxic heavy metals include cadmium, chromium, copper, lead, mercury, and nickel. A compilation of some studies for the removal of heavy metals by using activated carbon is presented in Table 2.5.

Table 2.4. Application of granular activated carbon in adsorption of various contaminants from gas and liquid phase

Contaminant	Source
Sulfur dioxide (SO ₂)	(Boudou et al., 2007; Gao et al., 2011; Gaur et al., 2006; Li et al., 2001a, b; Ling et al., 1999; Liu, 2008; Liu and Liu, 2011; Long et al., 2004; Lopez et al., 2007; Lopez et al., 2008; Mochida et al., 2000; Sumathi et al., 2010a,b,c; Wang et al., 2006).
Oxides of nitrogen (NO _x)	(Gao et al., 2011; Kante et al., 2009; Lee et al., 2002; Liu, 2008; Liu and Liu, 2011; Long et al., 2004; Miyawaki et al., 2011; Mochida et al., 2000; Sumathi et al., 2010a,b,c).
Hydrogen sulfide (H ₂ S)	(Bagreev et al., 2001a,b; Boudou et al., 2007; Chung et al., 2005; Huang et al., 2006; Masuda et al., 1999; Monteleone et al., 2011; Pipatmanomai et al., 2009; Sakanishi et al., 2005; Xiao et al., 2008; Yan et al., 2002; Yan et al., 2004).
VOCs	(Bansode et al., 2003; Cal et al., 1996; Das et al., 2004; Dwivedi et al., 2004; Huang et al., 2003; Li et al., 2011; Lu and Wey, 2007; Navarri et al., 2001; Sidheswaran et al., 2012; von Kienle et al., 1994; Yao et al., 2009).
Dyes	(Ahmad et al., 2011; Amin, 2009; Foo and Hameed, 2011; Gomez et al., 2007; Kadirvelu et al., 2003; Mohamed, 2004; Namasivayam et al., 2007; Rahman et al., 2005; Rozada et al., 2003; Sekaran et al., 1998; Stavropoulos and Zabaniotou, 2005; Valix et al., 2004; Wu and Tseng, 2006).
Phenolic compounds	(Aber et al., 2009; Ahmaruzzaman, 2008; Ariyadejwanich et al., 2003; Daifullah and Girgis, 1998; Gonzalez-Serrano et al., 2004; Laszlo, 2005; Laszlo and Szucs, 2001; Ren et al., 2011; Soto et al., 2011; Tancredi et al., 2004).
Heavy metals	(Table 2.5).
Pesticides	(Ayranci and Hoda, 2005; Gupta et al., 2011; Humbert et al., 2008; Ioannidou et al., 2010; Jusoh et al., 2011; Martin-Gullon and Font, 2001)

Table 2.5. Removal of heavy metals using activated carbon

Heavy metal	Source
Cadmium (Cd)	(Kadirvelu and Namasivayam, 2003; Madhava Rao et al., 2006; Monser et al., 2009; Tang et al., 2010; Tazar et al., 2009; Youssef et al., 2004).
Chromium (Cr)	(Di Natale et al., 2007; Hsu et al., 2009; Mohan et al., 2006; Muthukumaran and Beulah, 2011; Yue et al., 2009; Zhang et al., 2010).
Copper (Cu)	(Chen and Wu, 2004; Madhava Rao et al., 2006; Monser and Adhoum, 2002; Yang et al., 2009; Wang et al., 2011).
Lead (Pb)	(Dwivedi et al., 2008; Goel et al., 2005; Issabayeva et al., 2006; Mohammadi et al., 2010; Nadeem et al., 2006).
Nickel (Ni)	(Demirbas et al., 2002; Erdogan et al., 2005; Kadirvelu, et al., 2002; Kalavathy et al., 2010; Lu et al., 2008).
Mercury (Hg)	(Choi et al., 2009; Madhava Rao et al., 2009; Scala et al., 2011; Vitolo and Seggiani, 2002; Zhang et al., 2005).
Zinc (Zn)	(Kalavathy et al., 2010; Madhava Rao et al., 2008; Monser et al., 2002).

2.4. Chromium

2.4.1. Overview

Chromium is the 21st most abundant element in earth crust and its valance state ranges from -2 to +6, but it is generally found as trivalent [Cr(III)] and hexavalent chromium [Cr(VI)] in natural environments. Trivalent chromium occurs naturally in many vegetables, fruits, meat, grains and is often added to vitamins as a dietary supplement, whereas hexavalent chromium, most often produced by industrial processes and mining of chromium ore, is an indicator of environmental contamination. It occurs in combination with other elements as chromium salts, some of which are soluble in water.

Chromium is an extremely versatile element and finds a wide variety of uses. About 80% of the mined chromium is used for metallurgical applications, of which most is used in the stainless steel industry. It is used to manufacture ferrous and non-ferrous alloys, in chemical

industry for pigment production, electroplating, leather tanning, and as a catalyst in the synthesis of many organic chemicals (Palmer and Wittbrodt, 1991; Opperman and van Heerden, 2007).

2.4.2. Chemistry and Behavior

Elemental chromium is a transition group metal and the most commonly occurring states in chromium compounds are +2, +3, and +6 with the +2 being unstable and readily oxidizes to +3. Cr(III) compounds are most stable and the presence of Cr(VI) can generally be attributed to the industrial activity. Most of the Cr(III) compounds are sparingly soluble in water, whereas the majority of Cr(VI) compounds are highly soluble. Table 2.6 shows some of Cr(VI) compounds which are soluble in water.

Table 2.6. Hexavalent chromium compounds.

Compound	Form	Solubility in water
Sodium Chromate (Na ₂ CrO ₄)	Yellow Crystal	Soluble
Calcium Chromate (CaCrO ₄)	Yellow Crystal	Slightly soluble
Sodium Dichromate (Na ₂ Cr ₂ O ₇)	Orange red crystal	Soluble
Potassium Chromate (K ₂ CrO ₄)	Yellow Crystal	Soluble
Chromium Trioxide (CrO ₃)	Dark red/brown crystal	Soluble
Potassium Dichromate (K ₂ Cr ₂ O ₇)	Orange red crystal	Soluble
Strontium Chromate (SrCrO ₄)	Yellow crystal	Slightly soluble

Chromium(VI) generally exists in monomeric (HCrO₄⁻ and CrO₄⁻²) or bimeric state (Cr₂O₇⁻²). Presence of monomeric and bimeric species imparts yellow and orange colors to water, respectively (Palmer and Puls, 2004). The dependency of concentration of these species on the pH and concentration of Cr(VI) solution are depicted in Figures 2.11 and 2.12, respectively.

Table 2.7. Chromium(VI) concentration in various industrial effluents.

Type of effluent	Cr(VI) Conc. (mg/L)	Reference	Type of effluent	Cr(VI) Conc. (mg/L)	Reference
Sukinda effluent	4.3 – 8.5	Mishra, 2012	Leather industry effluent	10.3 – 345	Dhungana and Yadav, 2009
Electroplating discharge	3.0	Ganguli and Tripathi, 2002	Metal finishing industry	200	Sarin and Pant, 2006
Electropolishing plant	42.8	Davis et al., 1995	Chrome plating effluent	28.2	Selvaraj et al., 2003

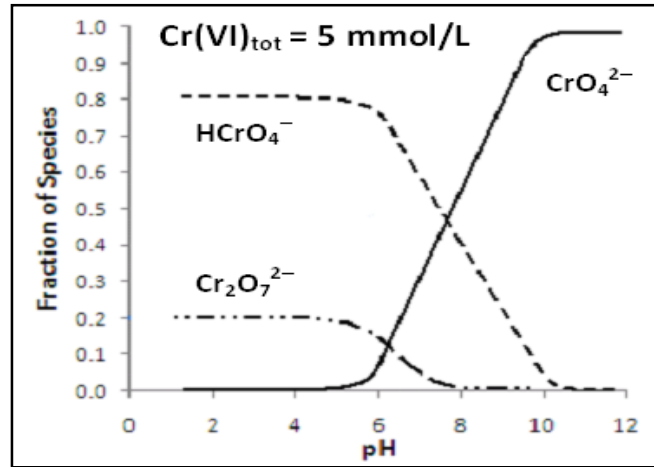


Figure 2.11. Distribution of Cr(VI) species as a function of pH (Palmer and Puls, 2004)

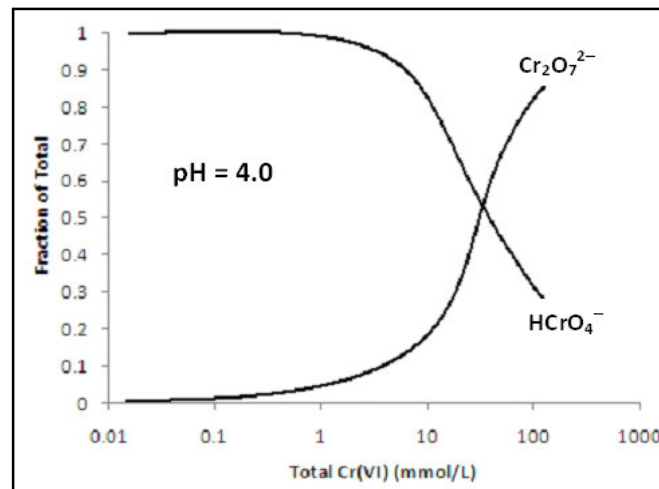


Figure 2.12. Fraction of HCrO_4^- and $\text{Cr}_2\text{O}_7^{2-}$ at pH 4 as a function of total Cr(VI) concentration (Palmer and Puls, 2004)

Under oxidizing conditions, chromium is present in the hexavalent state [Cr(VI)]. At concentrations less than 10 mM or at neutral pH, Cr(VI) exists in monomeric species H_2CrO_4 , HCrO_4^- , CrO_4^{2-} , and dimeric form $\text{Cr}_2\text{O}_7^{2-}$. It is evident (Figure 2.11) that CrO_4^{2-} predominates above pH 6.5 and HCrO_4^- dominates in the pH range of 1 to 6.5.

2.4.3. Environmental Occurrence

Almost all the sources of chromium in the earth's crust are in the trivalent state. The most important mineral deposit for chromium is in the form of chromite (FeCr_2O_4). Acid mine drainage can make the chromium available to the environment. Hexavalent chromium compounds are used in metal finishing and chrome plating, in stainless steel production, in the

manufacture of pigments, as corrosion inhibitors, and wood preservation. As the living matter does not produce energy required for the oxidation of Cr(III) to Cr(VI) in the organism, all the hexavalent chromium present in the environment is due to the human or industrial activities.

Hexavalent chromium is a strong oxidizing agent particularly in acidic media and tends to associate with oxygen, thereby forming chromate and dichromate (Lai and Lo, 2008). The mineral form of Cr(VI) rarely occurs naturally in the environment as the crocoite (PbCrO_4) and only a small amount of hexavalent chromium is formed by natural oxidation of Cr(III) in the soil, the rest is mostly introduced anthropogenically into the environment as a result of industrial processes (Barceloux, 1999).

2.4.5. Toxicology

Occupational exposure to hexavalent chromium generally occurs by inhalation and by skin (dermal) contact. Workers may be exposed by inhalation to fumes and mists containing Cr(VI) when hot-cutting or welding stainless steel, or other chromium-containing metal alloys. However, when a substance is inhaled, a small amount is inevitably ingested. The general public may be exposed to Cr(VI) by drinking water from contaminated sites. The tolerance limit for Cr (VI) for discharge into inland surface waters is 0.1 mg/l and in potable water is 0.05 mg/l (EPA 1990).

2.4.5.1. Effects of Short-term Exposure

Soluble trivalent chromium substances cause irritation to the eyes and skin, but this effect is usually related to their acidic nature. Chromium compounds can cause skin rashes in some people who are 'chromium-sensitive'. By contrast, hexavalent chromium is hazardous by all exposure routes:

- Inhalation may cause acute toxicity, irritation and ulceration of the nasal septum and respiratory sensitization (asthma).
- Ingestion may affect kidney and liver functions.
- Skin contact may result in systemic poisoning, damage or even severe burns.

2.4.5.2. Effects of Long-term Exposure

Exposure to hexavalent chromium, if prolonged or repeated, may lead to perforation of the nasal septum. The oral exposure of Cr(VI) can cause vomiting, oral ulcers, abdominal pain, indigestion, and diarrhea. Hematological effects such as leucocytosis and immature neutrophils were also noted. Both soluble and insoluble Cr(VI) compounds are able to cause structural damage to DNA, leading to genotoxicity. Studies indicate that Cr(VI) induced DNA damage may result in clastogenesis, altered gene expression, and the inhibition of DNA replication and transcription.

Chromium(VI) exists as highly soluble dichromate or chromate anions and is known to be toxic to all living organisms. It is proved to have a well-established carcinogen effect on human beings by the inhalation and oral route of exposure. The main concern about Cr(VI) compounds is associated with their mobility, which can easily lead to the contamination of both surface and ground waters (Bagchi et al., 2002; Cieslak-Golonka, 1996; Cohen et al., 1993; Costa, 1997). Cr(VI) can be toxic for biological systems (Shanker et al., 2005; Zhitkovich, 2005), and water-soluble Cr(VI) is extremely irritating and toxic to human body tissue owing to its oxidizing potential and easy permeating of biological membranes (Outridge and Scheuhammer, 1993). It leads to liver damage, pulmonary congestion, oedema, and skin irritation resulting in ulcer formation (Raji and Anirudhan, 1998). Chromium (VI) is toxic to numerous plants, animals, bacteria and as a confirmed human carcinogen, poses a great threat to human health and environment (Demirbas et al., 2004; Goswami and Ghosh, 2005). Trivalent chromium on the other hand, present mainly as relatively insoluble, immobile and non-toxic hydroxides and oxides (Palmer and Wittbrodt, 1991; Rai et al., 1987). The toxicity of trivalent chromium is 500 to 1000 times less to a living cell than hexavalent chromium (Costa, 2003). Hexavalent chromium has been recognized as more toxic among heavy metals and hence it receives much more attention.

2.5. Hexavalent Chromium Removal by Activated Carbons from Aqueous Phase

As discussed, the toxicity caused by hexavalent chromium is high and therefore priority is given to regulate this pollutant at the discharge level. Currently there are several methods available for the removal of Cr(VI) from industrial effluents. Chemical precipitation, coagulation, ion exchange, solvent extraction, and membrane filtration produce large amounts of sludge and waste that need to be disposed of and can consequently cause a lot of problems to the environment due to the presence of high content of chromium. Other techniques such as ultra-filtration, nano-filtration, and reverse osmosis are associated with high capital and operational costs. [Table 2.7](#) summarizes various technologies used for Cr(VI) removal and the difficulties of each process.

One of the technologies that can overcome these disadvantages is the adsorptive removal of hexavalent chromium by various adsorbents. In recent years, scientists focused on the preparation of adsorbents from various waste materials for the removal of contaminants from the environment as this technology not only solves the problem of waste disposal and also converts a potential waste to a valuable product. Adsorption by activated carbons for the removal of contaminants has various advantages over other processes. Activated carbons are very effective adsorbents due to their very high surface area and pore volume. Rate of adsorption by AC is very high and faster adsorption kinetics. High quality effluents can be obtained after treatment ([Mohan and Pittman Jr, 2006](#)).

2.5.1. Chromium(VI) Removal by Activated Carbons

Among the numerous adsorbents available, activated carbon has been undoubtedly the most popular and widely used for the removal of hexavalent chromium from aqueous phase. Activated carbon can be prepared from various precursors through different methods and operating conditions. The adsorption capacity of the prepared activated carbon depends mainly on the type of precursor used and method of preparation. List of different types of precursors, preparation conditions and their adsorption capacities for Cr(VI) were shown in [Table 2.8](#).

Table 2.8. Various techniques used for Cr(VI) removal and their drawbacks

Technique	Disadvantages	Source
Distillation	<ul style="list-style-type: none"> • Takes time for purification • Uses electricity all the time the unit is operating • Some contaminants can be carried into the condensate • Requires careful maintenance to ensure purity 	Owlad et al., 2008; Mohan and Pittman Jr, 2006
Ion exchange	<ul style="list-style-type: none"> • Resin fouling • Heating is required to maximize efficiency • Does not effectively remove particles, pyrogens or bacteria • High operating costs over long-term 	Pehlivan and Cetin, 2009; Tor et al., 2004
Filtration	<ul style="list-style-type: none"> • Low chemical and thermal stability • Membrane fouling • High capital cost • Requires tight operation and Maintenance 	Aroua, 2007; Dzyazko, 2007; Pugazhenth, 2005
Reverse osmosis	<ul style="list-style-type: none"> • Limited flow rates • Two to four gallons of water are flushed down the drain for each gallon of filtered water produced • Requires high pressure inflow • Damaged membranes are not easily detected • RO systems require maintenance 	Kang and Cao, 2012; Perez-Gonzalez et al., 2012; Radjenovic et al., 2008
Ultraviolet (UV) radiation	<ul style="list-style-type: none"> • Not suitable for water with high levels of suspended solids, turbidity, color, or soluble organic matter • Not effective against non-living contaminant, lead, asbestos, many organic chemicals, chlorine, etc • Requires electricity to operate 	Owlad et al., 2008

Table 2.9. Comparison of activated carbons prepared from various feed stocks and the optimum conditions for Cr(VI) removal

Precursor	Preparation conditions	Activating agent	C _o (mg/l)	pH	Temperature (°C)	Q _e (mg/g)	Source
Olive Stones	600 °C, 3 h	H ₂ SO ₄	5 – 50	1.5	30	71.0	(Attia et al., 2010)
Tamarind Seeds	110 °C, 5 h	H ₂ SO ₄	40 – 400	1 – 3	30	29.1	(Babu and Gupta 2008)
	110 °C, 5 h	H ₂ SO ₄	20 – 200	3.0	30	10.5	
AC(Filtrisorb–400)	–	–	100	2.5	25	75.6	(Sharma and Forster 1996a)
ACF–307	–	–	20 – 1000	5.5	–	60.0	(Aggarwal et al., 1999)
Coconut Fibers	600 °C	–	1 – 100	2.0	40	24.1	(Mohan et al., 2005)
	600 °C	H ₂ SO ₄	1 – 100	2.0	40	15.6	
Coconut Shell	600 °C	–	1 – 100	2.0	40	32.6	(Mohan et al., 2005)
	600 °C	H ₂ SO ₄	1 – 100	2.0	40	16.4	
ACF (Commercial)	–	–	1 – 100	2.0	10	116.9	
Fullerenes	–	–	34.2	4.5	25	5.5	(Lalvani et al., 1998)
	425 ± 25 °C	H ₂ SO ₄	20	2.5 – 3.0	30 ± 2	5.4	
Casurina equisetifolia leaves	425 ± 25 °C	Na ₂ HPO ₄	20	2.5 – 3.0	30 ± 2	5.0	(Ranganathan 2000)
	425 ± 25 °C, 1 h	ZnCl ₂	20	2.5 – 3.0	30 ± 2	18.6	

	850 ± 25 °C, 0.5 h	H ₂ SO ₄ + CO ₂	20	2.5 – 3.0	30 ± 2	11.6	
	850 ± 25 °C, 0.5 h	Na ₂ HPO ₄ + CO ₂	20	2.5 – 3.0	30 ± 2	17.2	
Hazelnut shell	150 °C, 24 h	H ₂ SO ₄	50 – 300	1.0	30	170.0	(Kobya 2004)
Cornelian cherry(CC),	200 °C, 24 h	H ₂ SO ₄	20 – 300	1.0	25	21.0	
Apricot stone (AS),	200 °C, 24 h	H ₂ SO ₄	20 – 300	1.0	25	21.0	(Demirbas et al., 2004)
Almond shells (ASC)	200 °C, 24 h	H ₂ SO ₄	20 - 300	1.0	25	20.0	
Waste tires	900 °C, N ₂ , 2 h	CO ₂ , 900 °C, 2 h	100 – 1000	2.0	22	30.0	
Saw dust	650 °C, N ₂ , 2 h	CO ₂ , 650 °C, 2 h	100 – 1000	2.0	22	24.65	(Hamadi et al., 2001)
<i>Hevea Brasilinesis</i> sawdust	400 °C, 1 h	H ₂ SO ₄ , 110 °C, 24 h	50 – 200	2.0	–	44.05	(Karthikeyan et al., 2005)
almond nutshells	170 °C, 0.5 h	N ₂ , 450 °C, 1 h	60 – 100	2.0	30	97.8	(Bhatti et al., 2007)
Tamarind wood	439 °C, 40 min	ZnCl ₂ (296 %)	10 – 50	1.0	30 ± 2	28.02	(Acharya et al., 2009)
Coconut Tree Sawdust	80 °C, 12 h	H ₂ SO ₄	5 – 20	3.0	–	3.46	(Selvi et al., 2001)
<i>Terminalia arjuna</i> nuts	500 °C, N ₂ , 1 h	ZnCl ₂ (300 %)	10 – 30	1.0	25	30.0	(Mohanty et al., 2005)
Activated carbon fibers (ACFs)	–	1) 1 M NaOH	51.9	3.0	25 ± 0.5	37.0	(Ko et al., 2004)
		2) 3 M H ₂ O ₂	51.9	3.0	25 ± 0.5	40.0	
		3) Non-treated ACFs	51.9	3.0	25 ± 0.5	42.0	

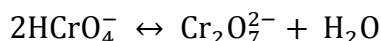
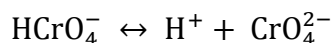
Fir Wood Slabs	700 °C, N ₂ , 2 h	KOH, N ₂ , 300 °C	5 – 200	3.0	25	180.3	(Khezami and Capart 2005)
Acticarbone	–	H ₃ PO ₄	5 – 200	3.0	25	124.6	
CAC (Merck–Germany)	–	–	25 – 100	5.5	20	66.8	(Barkat et al., 2009)
Tridax procumbens	160 ± 5 °C	H ₂ SO ₄	25 – 50	2.5	–	9.7	(Singanan et al., 2007)
Wood based AC			5 – 120	2.0	–	87.6	
Dust coal carbon	–	–	5 – 120	2.0	–	101.9	(Selomulya et al., 1999)
Coconut shell based AC			5 – 120	2.0	–	107.1	
Tuncbilek lignite							
1) AC 1	800 °C, N ₂ , 2 h	ZnCl ₂	250 – 1000	2.0	50	7.9	(Yavuz et al., 2006)
2) AC 2	800 °C, N ₂ , 1 h	CO ₂ , 950 °C, 3 h	250 – 1000	2.0	50	30.4	
Oil shale	270 °C, air	H ₂ SO ₄ + HNO ₃	25 – 300	4.0	22 ± 1	92.0	(Shawabkeh 2006)
Powdered AC (AC 1)	–	–	1 – 20	2.0	25	28.0	(Ram Mohan Rao and Basava Rao 2007)
Granular AC (AC 2)	–	–	1 – 20	2.0	25	16.0	
Aquacarb 207EA	–	–	25	5 – 8	20	7.0	(Natale et al., 2007)
Ground nut husk	150–155 °C, 24 h	H ₂ SO ₄	50	3.0	30	7.0	(Dubey and Gopal 2007)
	150–155 °C, 24 h	H ₂ + AgNO ₃	50	3.0	30	11.3	

2.5.2. Effect of Process Parameters

The effect of different process parameters such as pH, Initial metal concentration, contact time, adsorbent dose, and temperature were strongly studied and the optimum conditions determined in various studies can be found in [Table 2.8](#).

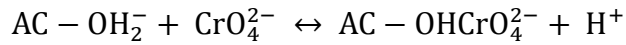
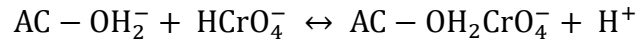
2.5.2.1. Effect of pH

The pH of the solution is an important factor for the removal of Cr(VI) by activated carbons. [Tang et al., \(2009\)](#) tested coconut shell based activated carbons for the removal of Cr(VI) at different pH values ranges from 2.0 to 8.0. They observed that the adsorption of Cr(VI) continuously decreased with the increase in pH and the maximum adsorption was observed at pH 2.0. Similar results were also obtained by [Goswami and Ghosh \(2005\)](#) and [Karthikeyan et al., \(2005\)](#). Chromium exists in different oxidation states and the stability of these forms depends on the pH of the system ([Sharma and Forster, 1994](#); [Hamadi et al., 2001](#)) and the equilibrium between different ionic species of chromium as follows ([Karthikeyan et al., 2005](#)):



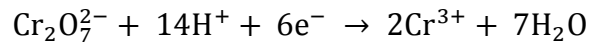
The rapid decrease in the removal of Cr(VI) with the increase of pH may be due to that low pH leads to an increase in H⁺ ions on the carbon surface, which results in significantly strong electrostatic attraction between HCrO₄⁻ and positively charged carbon surface ([Stumm and Morgan, 1996](#); [Benjamin, 2002](#), [Selomulya et al., 1999](#)). [Bhatti et al., \(2007\)](#) also found that the sorption capacity of AC prepared from almond shells was higher in acidic pH (<5) due to the negatively charged chromium species bind through electrostatic attraction to positively charged functional groups of the adsorbent surface. At pH >5, the decrease in sorption capacity is due to the increase of the negative charge on the adsorbent surface, thus the electrostatic force of attraction between the adsorbent surface and adsorbate ion decreased.

Based on the equilibrium constants of hydrolysis for Cr(VI), the two major species in the solution are HCrO_4^- (dominant in pH range of 1.0 to 6.0), and CrO_4^{2-} (dominant in pH range of 6.0 to 8.0). [Park et al., \(1999\)](#) and [Valdes et al., \(2002\)](#) explained the adsorption of Cr(VI) on activated carbon by the following reactions and they observed the pH of the final solution decrease due to the release of protons.

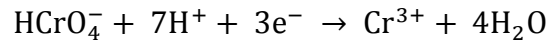


[Sharma and Forster \(1996\)](#) proposed totally different mechanism that the removal of Cr(VI) at low pH is governed by the active reduction reaction given by the following equations and they noticed the increase in pH of the final solution.

at low pH



at moderate pH



The effect of pH on the adsorption of Cr(VI) is attributed to the interactions between ions in solution and complexes formed at the adsorbent surface. The Cr(VI) can form different species at different pHs in aqueous solutions and the maximum adsorption of Cr(VI) on the various adsorbents was found at pH 2.0 and negligible at pH values over 8.0 ([Mohan et al., 2005](#)). The optimum pH values for different activated carbons for Cr(VI) removal were presented in [Table 2.8](#).

2.5.2.2. Effect of Contact Time and Initial Chromium(VI) Concentration

Activated carbons prepared using different precursors such as cornelian cherry, apricot stone, and almond shells were applied for the removal of Cr(VI) from aqueous solution ([Demirbas et al., 2004](#)). The removal of Cr(VI) for all the types of AC was shown to increase with time and initial Cr(VI) concentration. The amount adsorbed increased from 10.60 mg/g to

59.40 mg/g with the increase in initial Cr(VI) concentration from 20 to 300 mg/l in 72 h of contact time.

The adsorption of Cr(VI) on tamarind wood activated carbon was rapid initially within 20 min and with further increase of time the adsorption kinetics decreased, and finally reached equilibrium within 40 min. The adsorption capacities increased from 44 to 99% with the decrease of initial Cr(VI) concentration from 50 to 10 mg/l (Acharya et al., 2009). Similar type of results were also obtained by Attia et al., (2010), Selomulya et al., (1999), Khezami and Capart (2005).

Much slower rate of adsorption was reported for the removal of Cr(VI) by various commercially available ACs and the equilibrium was reached in about 5 days (Hu et al., 2003), whereas Cr(VI) removal by *Hevea Brasiliensis* sawdust activated carbon increases with time and attains equilibrium value at a time of about 300 min. The amount adsorbed was found to be dependent on the initial Cr(VI) concentration, and it increases with the increase in metal concentration. At low concentration of Cr(VI), the available surface for adsorption is very large, so that the removal becomes independent of the initial Cr(VI) concentration. However, at high concentrations this ratio is low concluding that the percentage removal depends on the initial concentration of Cr(VI) (Karthikeyan et al., 2005). Range of initial Cr(VI) concentrations used in various studies was presented in Table 2.8.

2.5.2.3. Effect of Adsorbent Dose

The Cr(VI) removal efficiency was found to increase with the increase of adsorbent dose in various studies and after reaching the optimum value, further increase in adsorbent dose does not shows any significant change (Lalvani et al., 1998; Dubey and Gopal, 2007; Barkat et al., 2007; Ranganathan, 2000). The trend of increase in removal capacity is due to the fact that the availability of more adsorption sites for the metal ions (Mohanty et al., 2005).

2.5.2.4. Effect of Temperature

Process temperature has a profound effect on heavy metal removal by using various adsorbents and the optimum temperature for better removal changes with the type of adsorbent and adsorbate. With the increase of temperature the uptake of Cr(VI) increases (Hu et al., 2003;

Barkat et al., 2007) continuously. The adsorption of Cr(VI) on activated carbon increases as the temperature increases and thus the adsorption reaction is endothermic in nature (Kartikeyan et al., 2005). The enhancement of adsorption capacity may be due to the chemical interaction between adsorbate ions and adsorbent, creation of some new adsorption sites or increase in the intraparticle diffusion of Cr(VI) into the pores of adsorbent at high temperatures (Namasivayam and Yamuna, 1995). Various adsorbents used for the removal of Cr(VI) and their respective optimum process temperatures were presented in Table 2.8.

The more increase in temperature, the higher the removal rate. This is explained by a combination of ‘activated diffusion’ and an increase in surface area caused by oxidation associated with the observed reduction of ions on the surface of carbonaceous material. Such activated adsorption would widen and deepen the very small micropores, i.e., causes ‘pore burrowing’ (Yavuz et al., 2006).

2.6. Design of Experiments (DOE)

2.6.1. Fundamentals of DOE

Design of Experiments (DOE) refers to the process of planning, designing, and analyzing the experiment so that valid and objective conclusions can be drawn effectively and efficiently.

A process is a transformation of inputs into outputs and sometimes, an output can also be referred as response. In performing a designed experiment, changes to the input variables (or factors) are to be made intentionally to observe the corresponding change in the response. Some of the inputs or factors can be controlled fairly easily and some of them are hard or expensive to control at standard conditions (Antony, 2003). The general model of a process or system was shown in Figure 2.13.

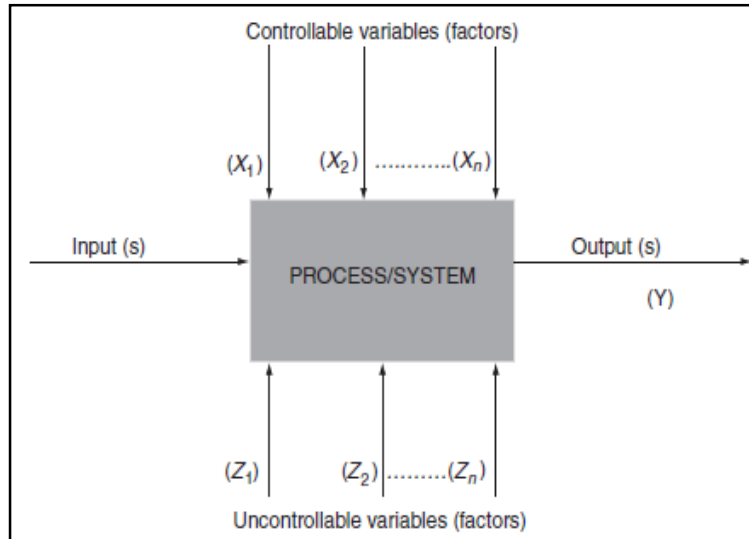


Figure 2.13. The general model of a process or system (Antony, 2003)

The easily controllable variables, represented by X_i (Figure 2.13), have a key role to play in the process characterization. The uncontrollable variables, represented by Z 's, are difficult to control during the experiment. These both controllable and uncontrollable factors are responsible for the variability in the response of the system. The fundamental strategy of DOE is to determine the optimal settings of controllable factors (X 's) to minimize the effects of uncontrollable factors (Z_i) on the response.

2.6.2. Factorial Designs

Many experiments involve the study of the effects of two or more factors. The general approach to determine the effect of parameters is the one-factor-at-a-time experimentation. This approach consists of selecting a starting point for each factor, then successively varying each factor over its range with the other factors held constant at the baseline level. The major disadvantage of this approach is that it fails to consider any possible interaction between the factors. The correct approach in dealing with several factors is to conduct a factorial experiment. This is an experimental strategy in which factors are varied together instead of one at a time (Elibol, 2002).

Full factorial and fractional factorial designs are widely used experimental designs at two-levels and three-levels. A full factorial design consists of all possible combinations of levels for all factors. A common experimental design is one with all input factors set at two-levels each.

These levels are called ‘high’ and ‘low’ or ‘+1’ and ‘-1’, respectively. The total number of experiments for studying k factors at 2-levels is 2^k . The 2^k full factorial design is particularly useful when the number of process parameters is less than or equal to 4. A fractional factorial design is a variation of the basic factorial design in which only a subset of the runs are used to provide good information about the main effects and some information about interaction effects (Montgomery, 1997; Brasil et al., 2005).

Factorial designs were used extensively in industrial research and development, and for process development (Ferreira et al., 2003; Carmona et al., 2005; Srinivasan and Viraraghavan, 2010; Zhao et al., 2009; Cestari et al., 2007; Baral et al., 2009). The application of factorial designs in process development can result in

- i. Improved process yields
- ii. Reduced variability and closer conformance to nominal or target requirements
- iii. Reduced development time
- iv. Reduced overall costs

2.7. Regeneration of Activated Carbon

One possible way to reduce the cost of adsorption process is to efficiently desorb the retained substances and by regenerating the adsorbent for repeated use. Thus, the regeneration of porous carbons is a crucial issue and requires a detailed investigation to ascertain if such procedures are economically attractive. Generally spent activated carbon can be regenerated by several methods such as chemical regeneration, thermal regeneration, and electro-chemical treatment so on. Among all the methods, thermal regeneration is by far the most commonly used because of its simplicity, high efficiency and solvent free property (Chiang and Wu, 1989; Suzuki, 1990; Torrents et al., 1997). Thermal regeneration includes pyrolysis in inert atmosphere or regeneration by steam. Hu et al (2003) successfully regenerated the spent activated carbon for Cr(VI) removal by treating with H_2SO_4 and reported high adsorption capacity and regeneration values. Ranganathan (2000) reported that treatment with NaOH and HCl can desorb about 65 % of Cr(VI) from the adsorbent prepared from *Casurina equisetifolia*.

Materials and Methods

3.0. Summary

This chapter describes in detail about various materials, chemical reagents and methodologies followed to achieve the objectives of the study. Methodology mainly includes characterization of precursor, preparation and characterization of activated carbon, application of AC in Cr(VI) removal and modeling of adsorption process.

3.1. Materials

The carbonaceous precursor used for preparation of activated carbon (AC) is Bael fruit shell and was collected from the premises of the N.I.T. campus. Prior to use, sample was washed gently with water to remove mud and other impurities present on the surface and then sundried for one week. Commercial activated carbon prepared from coconut shell was procured from Kalpaka chemicals, Tuticorin, India. All chemical reagents used in this work are procured from the Merck, India.

3.2. Methodology

3.2.1. Characterization of Precursor

Composition of the raw material is an important factor that dictates the selection of precursor for activated carbon production. The chemical composition of the precursor material, mainly the percentages of the cellulose and lignin present in Bael fruit shell were found by means of standard methods (Thimmaiah, 1999). Materials with high lignin content develops AC with high macropores (> 50 nm), whereas, materials with high cellulose yields AC with predominantly microporous structure (Daud and Ali, 2004; Gani and Naruse, 2007).

3.2.1.1. Estimation of Cellulose

About 3 ml of acetic : nitric reagent (150 ml of 80 % acetic acid + 15 ml of concentrated nitric acid) was mixed with the 0.5 – 1.0 g of sample in a vortex mixer and placed in water bath at 100 °C for 30 min. After centrifugation the collected residue was washed with water and added 1 ml of 67 % H₂SO₄ and left for 1 h. Then 1 ml of the solution was diluted to 100 ml and 10 ml of anthrone reagent was added to 1 ml of this solution and mixed well. The tubes were heated in water bath for 10 min and measured the absorbance at 630 nm after cooling (TAPPI, T 264). The amount of cellulose was determined from the standard graph (40 – 200 µg/L of cellulose).

3.2.1.2. Estimation of Lignin

The raw material is first oven dried and about 100 g of the sample was moistened with water in a mortar. Sample was grinded with ether until it is free from the chlorophyll pigment. The residue was collected by centrifuging at 5000 rpm. The sediment was washed with water and recentrifuged to collect the residue. 2 ml of NaOH was added to the residue and extracted at 70 – 80 °C for 12-16 h. 0.45 ml of 2.0 N HCl was added and pH was adjusted to 7 – 8 by using NaOH. Solution was centrifuged at 2000 rpm and supernatant was collected. To 0.8 ml of extract, 0.8 ml of 0.1 M sodium phosphate buffer was added at pH 7.0. To another aliquot of 0.8 ml of extract 0.8 ml of 0.1 M NaOH was added at pH 12.3. Absorbance (A) was measured at 245 nm and 350 nm (TAPPI T-222, TAPPI T-203). The amount of lignin is calculated by the difference between A₂₄₅ (pH – 7.0) and A₃₅₀ (pH – 12.3).

3.2.1.3. Thermogravimetric Analysis

The Thermogravimetric analysis (TGA) profile of the raw material clearly gives an approximation about the weight loss with respect to temperature due to the release of surface bounded water and volatile matter. TGA of the raw precursor (Bael fruit shell) was carried out by a thermogravimetric analyzer (Shimadzu, DTG – 60H). About 30 mg of the sample was taken in silica crucible and subjected to pyrolysis under N₂ flow (35 ml/min) to 900 °C with heating rate, 10 °C/min.

3.2.1.4. Proximate Analysis

Proximate analysis of the Bael fruit shell was carried out by using a thermogravimetric method (moisture and volatile matter) (Pastor-Villegas et al., 1993), ash content was determined by heating for about 8 h at 650 °C until mass constancy in muffle furnace, and the carbon content was estimated by difference (Duran-Valle et al., 2005).

3.2.2. Preparation of Activated Carbon

Bael fruit shell, collected after discarding the fruit pulp, was sun dried, crushed and grinded in a ball mill. The grinded sample was sieved to obtain the particles of uniform size, 1.0 – 1.5 mm. The precursor obtained was washed to remove surface bounded impurities and mud and dried at 100 °C for 12 h. Raw material of about 100 g was impregnated with different chemicals such as H₃PO₄, ZnCl₂ and KOH for 12 h in varying impregnations. For phosphoric acid impregnation 100 ml of different concentrations of H₃PO₄ (0, 10, 20, 30, 40 and 50 %) was used. For ZnCl₂ and KOH impregnations, different impregnation ratios (0.5, 1.0, 1.5, 2.0 and 2.5) were used. The impregnation was carried out at 70 °C in a hot air oven to achieve well penetration of chemical into the interior of the precursor.

About 10 g of the Bael fruit shell impregnated with different activating agents and different impregnations was transferred to a stain less steel reactor (150 mm length and 40 mm diameter) with narrow ports at both ends. The tube is placed inside an electric horizontal tubular furnace (Bysakh & Co) controlled by the proportional integral derivative (PID) controller. The furnace tube dimensions are 800 mm length and 50 mm in diameter. The temperature of the reaction zone was measured by the chromel – alumel (K-type) thermocouple. The pyrolysis of the samples was carried out under continuous flow of N₂ gas (200 ml/min). The carbonized samples were cooled to room temperature under inert atmosphere and washed with water followed by 0.1 M hydrochloric acid (HCl) to remove the residual chemical agents until the pH value of the rinsed water was neutral. The adsorbents prepared by H₃PO₄, ZnCl₂ and KOH activations were denoted as AC-PA, AC-ZC and AC-PH, respectively throughout the work. The schematic diagram for the preparation and activation of AC was shown in Figure 3.1.

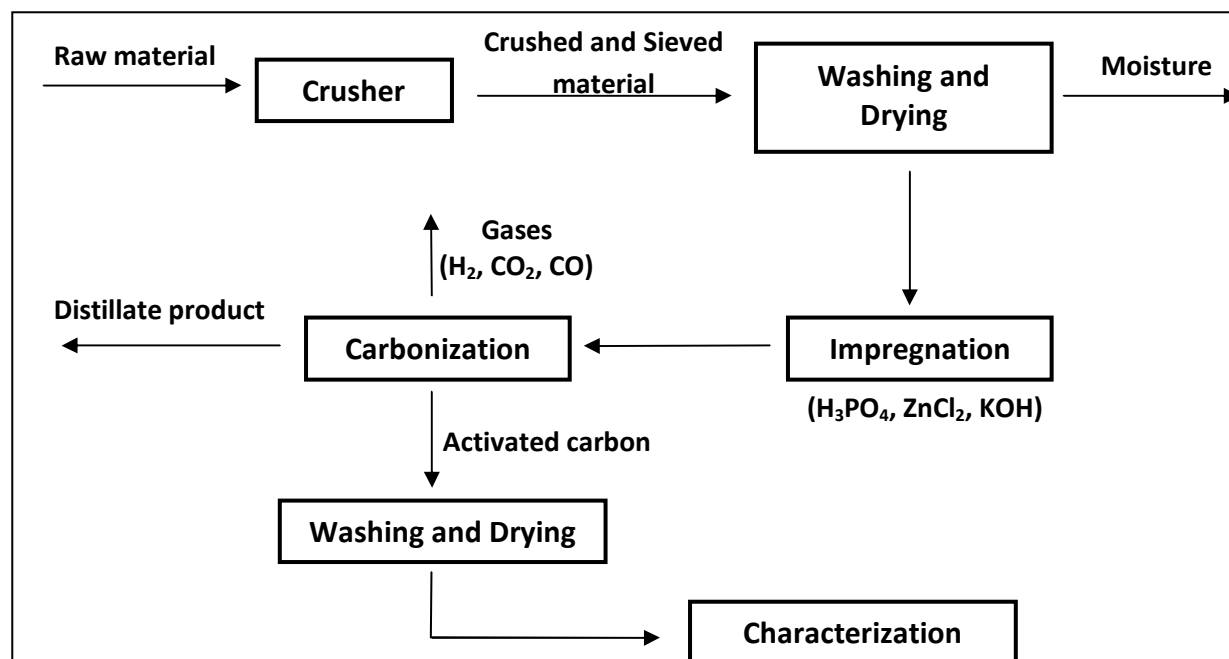


Figure 3.1. Schematic diagram for preparation of activated carbon

Different process parameters such as impregnation ratio, carbonization temperature and holding time were studied to estimate the effect on porous characteristics of ACs. Other factors such as N_2 gas flow rate (100, 200 and 300 ml/min) and the heating rate of the furnace (4, 8, 12 °C/min) are found to be not significantly affecting the porosity of the final carbon products.

3.2.2.1. Effect of Impregnation

The effect of impregnation of different chemical agents such as phosphoric acid (H_3PO_4), zinc chloride ($ZnCl_2$) and potassium hydroxide (KOH) on the porous characteristics was studied. Acid concentrations ranging from 0 – 50 % was used for impregnation in case of H_3PO_4 and impregnation ratios of 0.5 – 2.5 (0.5, 1.0, 1.5, 2.0, and 2.5) were used in case of $ZnCl_2$ and KOH. Impregnation ratio was determined as weight of precursor to weight of chemical agent. For H_3PO_4 activation, 100 mg of raw material was impregnated with 100 ml of different concentrations of acid.

3.2.2.2. Effect of Carbonization Temperature

Carbonization temperature is one of the most influencing factors for the development of porosity during activation process (Mohan et al., 2005; Ranganathan, 2000; Diao et al., 2002; Nabais et al., 2008). Effect of carbonization temperature on porous characteristics of developed

ACs was investigated in the range 400 – 700 °C (400, 500, 600, and 700 °C) for each chemical impregnation. The optimum carbonization temperature varies with the type of chemical used for impregnation.

3.2.2.3. Effect of Holding Time

Holding time is the duration of the sample kept at final carbonization temperature. The holding time at final temperature was varied in between 0 – 120 min (0, 30, 60, 90, and 120 min) to investigate its effect on porous characteristics.

3.2.3. Characterization of AC

Various properties of prepared activated carbons were characterized by following the standard procedures.

3.2.3.1. Proximate Analysis

The moisture content was found by oven-drying test method ([ASTM D2867 – 09](#)). A sample of carbon is put into a dry, closed capsule (of known weight) and weighed accurately. The capsule is opened and placed with the lid in a preheated oven (145 – 155 °C). The sample is dried to constant weight then removed from the oven and with the capsule closed, cooled to room temperature. The closed capsule is weighed again accurately. The percentage difference of weight is expressed as the moisture content of the sample.

The percentage of volatile matter of the AC samples was determined by the standard method ([ASTM D5832 – 98](#)). Approximately 1.0 g of the sample was taken in crucible with cover (of known weight). The covered crucible was placed in muffle furnace regulated at 950 °C for 7 min. Then the covered crucible was cooled to room temperature in a desiccator and recorded the weight. The percentage weight loss was regarded as the percentage of volatile matter.

To determine the ash content, dried sample of activated carbon weighed to the nearest 0.1 mg was taken into the crucible (of known weight). The crucible was placed in the muffle furnace at 650 °C and ashing was considered to be completed when constant weight is achieved. The crucible is cooled to room temperature in a desiccator and the percentage weight of the sample remained was considered as ash content ([ASTM D2866 – 94](#)). Fixed carbon is a calculated value

and it is the resultant of summation of percentage moisture, ash, and volatile matter subtracted from 100.

$$\text{Fixed carbon (\%)} = 100 - (\text{moisture, \%} + \text{ash, \%} + \text{volatile matter, \%}) \quad (3.1)$$

3.2.3.2. Ultimate Analysis

The ultimate analysis or elemental analysis was carried out by using CHNS analyzer (Elementar Vario EL CUBE). The percentage of oxygen was calculated by the difference as follows.

$$\text{Oxygen (\%)} = 100 - (C, \% + H, \% + N, \% + S, \%) \quad (3.2)$$

3.2.3.3. Yield

The yield of activated carbon (AC) was calculated on a chemical-free basis and can be regarded as an indicator of the process efficiency for the chemical activation process. The yield of AC is calculated as the percentage weight of the resultant activated carbon divided by weight of dried Bael fruit shell.

$$\text{Yield (\%)} = \frac{\text{Weight of AC after carbonization}}{\text{Weight of the raw material}} \times 100 \quad (3.3)$$

3.2.3.4. Bulk Density

The bulk density (ρ) of the AC was estimated by using pycnometer. Initially, the weight of pycnometer with inserted AC sample ($m_0 + m_{AC}$) was measured. Then the pycnometer filled up with water and the weight of water m'_{H_2O} (measured weight minus $m_0 + m_{AC}$) was noted. The volume of added water V'_{H_2O} obtained as

$$V'_{H_2O} = \frac{m'_{H_2O}}{\rho_{H_2O}} \quad (3.4)$$

The volume of AC (V_{AC}) is the difference between the volume of water that fills the empty pycnometer V and volume V'_{H_2O} .

$$V_{AC} = V - V'_{H_2O} = \frac{m_{H_2O} - m'_{H_2O}}{\rho_{H_2O}} \quad (3.5)$$

Density of AC was calculated as

$$\rho_{AC} = \frac{m_{AC}}{V_{AC}} \quad (3.6)$$

3.2.3.5. Porosity Characterization

Nitrogen (N₂) gas adsorption-desorption isotherms on prepared ACs at liquid nitrogen temperature (−195.6 °C) were carried out using an automatic adsorption unit, Autosorb – 1 (Quantachrome). The samples were degassed at 200 °C for 5 h prior to analysis so as to remove any adsorbed moisture or other impurities bounded to the surface of the sample.

Surface area (S_T) values were calculated from the experimental adsorption isotherm over a relative pressure range of 0.01 to 0.3 using the standard BET (Brunauer, Emmett and Teller) method. The BET equation is given as (Brunauer et al., 1938)

$$\frac{p}{V(p^0-p)} = \frac{1}{V_m C} + \frac{(C-1)}{V_m C} \left(\frac{p}{p^0} \right) \quad (3.7)$$

where, V is the volume adsorbed at STP (cm³g^{−1}), V_m is the volume of monolayer capacity at STP (cm³g^{−1}), and the term C , the BET constant, is related to the energy of adsorption in the first adsorbed layer and its value is an indication of the magnitude of the adsorbent-adsorbate interactions.

The total pore volume (V_T) of the samples was determined as the total volume of N₂ gas adsorbed at high relative pressure (0.995) (Sricharoenchaikul et al., 2008).

The micropore surface area (S_{mi}) and micropore volume (V_{mi}) were determined by applying Dubinin – Radushkevich (DR) equation commonly used in its linear form for analysis of activated carbons (McEnaney, 1987). The DR equation was applied to the experimental N₂ isotherm data at 77 K to determine the micropore characteristics of ACs and the DR equation can be written as

$$\log W = \log(\tilde{V}_0 \rho) - \bar{K} \left[\log \left(\frac{p^0}{p} \right) \right]^2 \quad (3.8)$$

where, W is the volume of adsorbate filling micropores, ρ is the density of liquid adsorbate; \tilde{V}_0 is the micropore volume and k is defined as

$$k = 2.303K \left(\frac{RT}{\beta} \right)^2 \quad (3.9)$$

where, β is the affinity coefficient, and K is a constant, determined by the shape of the pore size distribution. A plot of $\log W$ versus $[\log(p^o/p)]^2$ should be a straight line with an intercept of $\log(\tilde{V}_o\rho)$, from which the micropore volume (\tilde{V}_o) can be calculated. The DR equation often fails to linearize when the adsorbent contains heterogeneous micropores. To overcome this drawback a more general equation known as DA equation, proposed by Dubinin and Astakhov was used. The linearized form of DA equation is

$$\ln W = \ln(\tilde{V}_o\rho) - \bar{K} \left[\ln \left(\frac{p^o}{p} \right) \right]^n \quad (3.10)$$

where, K is an empirical constant, and n is the Dubinin-Astakhov parameter. Depending on the type of micropore system, the value of n ranges from 2 to 5, and for adsorbents with homogeneous micropore structure, n is usually close to 2.

3.2.3.6. Determination of Surface Chemistry

The surface functional groups of the ACs were estimated by Fourier Transform Infrared (FTIR) spectroscopy (FTIR-2000, Perkin Elmer) analysis. FTIR spectra of different samples were recorded within 400 – 4000 cm^{-1} . The transmission spectra of the samples were recorded using the KBr pellet. About 1.0 – 2.0 % of the sample was mixed with dry KBr and grinded in mortar. Then the sample was transferred to hydraulic press. The pressure in hydraulic pump was increased until it reaches 20,000 prf and then the pressure was slowly released. The pellet which is homogeneous and transparent in appearance was inserted into the IR sample holder for the analysis. The pellets were dried overnight at 100 °C before the spectra were recorded.

3.2.3.7. Microscopy

The surface morphology of the AC samples was analyzed by the Scanning Electron microscope (SEM) (JEOL, JSM-T330) which was coupled with Energy dispersive X-ray spectrometer (EDS) to carryout elemental analysis. Samples were analyzed by Transmission Electron Microscope (TEM) (JEOL, 2010 UHR) to visualize the porous nature of the adsorbents. Alcohol (40 %) was used as solvent to spread the sample on the grid for TEM analysis. The sample preparation for TEM was described elsewhere (Ishizaki et al., 1988).

3.2.3.8. Other Analyses

3.2.3.8.1. X-ray diffraction spectroscopy

The extent of graphitization in prepared ACs was determined by X-ray diffractometer (Philips X'PERT). Scans were run with a step size of 0.02°/s of 2θ , typically in the angle range between 10° and 70°.

3.2.3.8.2. Iodine number

The iodine number (IN) is a relative indicator of porosity in an activated carbon. It is a measure of micropore content of the AC (up to 2 nm). The iodine number is determined according to the [ASTM D4607-94](#) method. The iodine number is defined as the milligrams of iodine adsorbed by 1.0 g of carbon when the iodine concentration of the filtrate is 0.02 N (0.02 mol/L). It is based upon a three-point isotherm. A standard iodine solution is treated with three different weights of activated carbon under specified conditions. The activated carbon sample is treated with 10.0 mL of 5% HCl and boiled for 30 s and subsequently cooled. About 100 mL of 0.1 N (0.1 mol/L) iodine solution is added to the mixture and stirred for 30 s. The resulting solution is filtered and 50 mL of the filtrate is titrated with 0.1 N (0.1 mol/L) sodium thiosulfate and using starch as indicator. The iodine amount adsorbed per gram of carbon (X/M) is plotted against the iodine concentration in the filtrate (C), using logarithmic axes. Until the residual iodine concentration (C) is within the range of 0.008 to 0.04 N (0.008 to 0.04 mol/l), the whole procedure is repeated using different carbon masses for each isotherm point. A least squares fitting regression is applied for the three points. The amount of iodine adsorbed in milligrams per gram of carbon at a residual iodine concentration of 0.02 N is represented as the iodine number. The X/M and C values are calculated by the equations 3.11 and 3.12 respectively.

$$\frac{X}{M} (mg/g) = \left\{ (N_I \times 126.93 \times V_I) - \left[\frac{(V_I + V_{HCl})}{V_F} \right] \right\} / M_C \quad (3.11)$$

$$C = (N_{Na_2S_2O_3} \times V_{Na_2S_2O_3}) \quad (3.12)$$

where N_I is the iodine solution normality, V_I is the added volume of iodine solution, V_{HCl} is the added volume of 5% HCl, V_F is the filtrate volume used in titration, $N_{Na_2S_2O_3}$ is the sodium

thiosulfate solution normality, $V_{\text{Na}_2\text{S}_2\text{O}_3}$ is the consumed volume of sodium thiosulfate solution and M_C is the mass of activated carbon.

3.2.3.8.3. Methylene blue number

The methylene blue number (MBN) is a measure of mesoporosity (2 – 5 nm) present in AC. The methylene blue number is defined as the maximum amount of dye adsorbed on 1.0 g of adsorbent. In this assay, 10.0 mg of activated carbon are placed in contact with 10.0 mL of a methylene blue solution at different concentrations (10, 25, 50, 100, 250, 500 and 1000 mg/L) for 24 h at room temperature (approximately 25 °C). The remaining concentration of methylene blue is analyzed using a UV/Vis spectrophotometer (Jasco, V-530) (Nunes and Guerreiro, 2011).

The amount of methylene blue adsorbed from each solution is calculated by the equation 3.13

$$MBN (mg/g) = \frac{(C_o - C_e) \times V}{M} \quad (3.13)$$

3.2.4. Adsorption Experiments

Batch adsorption experiments for adsorption of Cr(VI) on prepared activated carbons were conducted using aqueous solutions of the metal. A stock solution of 100 mg/L of Cr(VI) was prepared by dissolving 282.9 mg of potassium dichromate in 1.0 L of distilled water. The stock solution was diluted as required to obtain different concentrations of Cr(VI) solutions. For each run, a definite amount of AC was added to 100 ml of Cr(VI) solution taken in 250 ml Erlenmeyer flasks. All the adsorption experiments were carried out at constant temperature of 30 °C in an environmental incubator shaker (DENEb Instruments) at constant shaking speed of 120 rpm. Concentration of hexavalent chromium in solution was determined by UV/Vis absorption spectrophotometer at 540 nm by complexing Cr(VI) with 1,5-diphenylcarbazide (Clesceri et al., 1998; Hosseini-Bandegharai et al., 2010). The indicator was prepared by dissolving 250 mg of diphenylcarbazide in 50 ml of acetone which develops a pink color by reacting with Cr(VI).

Adsorption of Cr(VI) on developed ACs was conducted with 100 ml of solution taken into 250 ml Erlenmeyer flasks by varying different parameters such as pH (2.0 – 11.0), initial Cr(VI) concentration (2.0 – 10.0 mg/L), adsorbent dose (0.5 – 4.0 g/L) and temperature (20.0 – 50.0 °C). Batch adsorption experiments were performed by contacting 3.0 g/L of the selected

carbon sample with 100 ml of the aqueous solution of different initial concentrations and pH values. Simultaneously, a control sample without adsorbent at the same experimental conditions was studied. All the experiments were carried out in triplicate and the mean values were considered.

Adsorption equilibrium isotherms on the three prepared ACs were determined using sample dosage of 3.0 g/L, initial Cr(VI) concentration of 10.0 mg/L and at different pH values. For these experiments the flasks were incubated at constant temperature (30 °C) and agitation speed (120 rpm) for 3h of contact time to attain equilibrium. The pH values were adjusted with dilute sulfuric acid and sodium hydroxide solutions by using pH meter (Systronics 361 – micro). Different types of isotherms studied were tabulated in [Table 3.1](#).

Langmuir isotherm is based on the assumptions that adsorption cannot proceed beyond monolayer coverage, all surface sites are equivalent and can accommodate only one adsorbate molecule, and the ability of a molecule to adsorb at a given site is independent of the occupation of neighboring sites. The Freundlich isotherm model assumes that the adsorption takes place on heterogeneous surfaces which have different adsorption energies. The Temkin isotherm model assumes that the heat of adsorption of all molecules decreases linearly with coverage due to adsorbate-adsorbate interactions and adsorption is characterized by a uniform distribution of binding energies. The Dubinin-Radushkevich (DR) isotherm model gives an idea about the type of adsorption depending on the activation energies.

Table 3.1. Different isotherm models used in the present study

Isotherm model	Equation
Langmuir	$\frac{C_e}{q_e} = \frac{1}{K_L} + \frac{a_L}{K_L} C_e$
Freundlich	$\ln q_e = \ln K_F + (1/n) \ln C_e$
Temkin	$q_e = B_T \ln A_T + B_T \ln C_e$
Dubinin-Radushkevich (DR)	$\ln q_e = \ln q_D - 2B_D RT \ln(1 + 1/C_e)$

The adsorption percentage and adsorption capacity (Q_e) of prepared AC for Cr(VI) were calculated according to following equations

$$\text{Adsorption (\%)} = \frac{(C_o - C_e)}{C_o} \times 100 \quad (3.14)$$

$$Q_e = \frac{(C_o - C_e)V}{W} \quad (3.15)$$

where, C_o and C_e are the initial and equilibrium concentrations (mg/L), respectively of Cr(VI) in solution, V is the volume of the solution (L), and W is the weight (g) of the adsorbent.

Adsorption kinetic studies were carried out by using the pseudo-first order and pseudo-second order models, and particle diffusion and film diffusion models.

Table 3.2. Different kinetic models used in present study

Kinetic model	Equation
Pseudo-first order model	$\log(q_e - q_t) = \log q_e - \frac{k_1}{2.303} t$
Pseudo-second order model	$\frac{t}{q_t} = \frac{1}{k_2 q_e^2} + \frac{1}{q_e} t$
Intra-particle diffusion	$q = k_{id} t^{1/2}$
Boyd model	$F = \frac{6}{\pi^2} \exp(-Bt)$ $Bt = -0.4977 - \ln(1 - F)$ $B = \frac{\pi^2 D_i}{r^2}$

The nature of the adsorption of Cr(VI) on prepared ACs was determined by estimating the thermodynamic parameters of the process such as free energy (ΔG°), enthalpy (ΔH°) and entropy (ΔS°).

3.2.5. Comparison and Regeneration

The porous characteristics and Cr(VI) adsorption capacities of activated carbons prepared from Bael fruit shell by different chemical activations were compared with commercially available AC prepared from coconut shell.

Regeneration of spent AC was carried out by simple method by using hot water and mild acid (0.1 M H₂SO₄). The spent AC (3 g) was taken in 100 ml distilled water and heated up to 80 °C for 10 to 15 min for 2 times to remove physically adsorbed Cr(VI). Then the sample was washed with 100 ml of 0.1 M H₂SO₄ to remove Cr(VI) which is retained on the surface of the adsorbent due to some interactions. Finally again the sample was washed with distilled water until the pH of the water reaches near to neutral.

3.2.6. Modeling of Cr(VI) Adsorption

Modeling of the adsorption of Cr(VI) on prepared ACs was carried out by using Full Factorial Design (FFD) by Designing of Experiments (DoE) using the software Design Expert – 7.1.6 (Stat-Ease, Inc). Factorial design is employed to reduce the total number of experiments in order to achieve the best overall optimization conditions of the process. Effect of various factors such as pH, Cr(VI) concentration, adsorbent dose and temperature on the percentage removal of Cr(VI) by each type of AC was studied. The effect of main factors as well as the effect of their interactions on the response was determined.

In the present study, a two-level and four-factor full factorial design (2⁴ runs) was used for the modeling of adsorption process. The general mathematical model developed by using factorial design is as follows

$$R = X_0 + X_1A + X_2B + X_3C + X_4D + X_5AB + X_6AC + X_7AD + X_8BC + X_9BD + X_{10}CD + X_{11}ABC + X_{12}ABD + X_{13}ACD + X_{14}BCD + X_{15}ABCD \quad (3.16)$$

where, R is the response, X₀ is the global mean, X_i represents the other regression coefficients and A, B, C and D are the coded symbols for the factors under study.

Preparation and Characterization of Activated Carbon

4.0. Summary

The raw material, Bael fruit shell, was characterized to estimate its suitability for the preparation of activated carbon. AC was prepared by chemical activation by impregnating the precursor with different chemical agents such as H_3PO_4 , $ZnCl_2$, and KOH. Effect of various preparation parameters like impregnation, carbonization temperature and holding time on porous characteristics of ACs was determined by N_2 gas adsorption-desorption isotherms. Optimum conditions for the preparation of AC were estimated by estimating the micropore surface area, and micropore volume and their respective contribution to total surface area and total pore volume. Various other characterizations such as pore size distribution (PSD), SEM and TEM analysis, EDX and XRD were carried out to be acquainted with other properties of ACs.

4.1. Selection of Precursor

Activated carbons (ACs) can be produced from any carbonaceous materials, both naturally occurring and synthetic. Process economics however dictates the selection of readily available and cheaper feed stocks. Most commonly used precursors for the production of commercial ACs are coconut shell, wood, fruit stones, etc. Biomass precursors offer most economical service because they are renewable with low mineral content and appreciable hardness.

Literature pertaining to use of lignocellulosic materials such as nutshells, coconut shells, apricot stones, plum stones is very extensive. On the contrary, Bael fruit (*Aegle Marmelos*) shell received much less attention as a precursor for the preparation of AC. The chemical composition and various physical properties of bael fruit shell were presented in [Table 4.1](#). Proximate and ultimate analyses were performed for the raw material. The proximate analysis was conducted following the procedure described elsewhere ([UNE 32001-81, 1981](#); [UNE 32019-84, 1984](#)). The ultimate analysis was performed using a CHNS analyzer. The results reported in [Table 4.1](#) indicate that the bael fruit shell has a high cellulose content (24.35 %) and low lignin content

(19.9 %) than that of coconut shell, which is an important factor for preparation of AC. However, ultimate analysis highlights that the precursor has negligible sulfur and low nitrogen content with high carbon and oxygen contents.

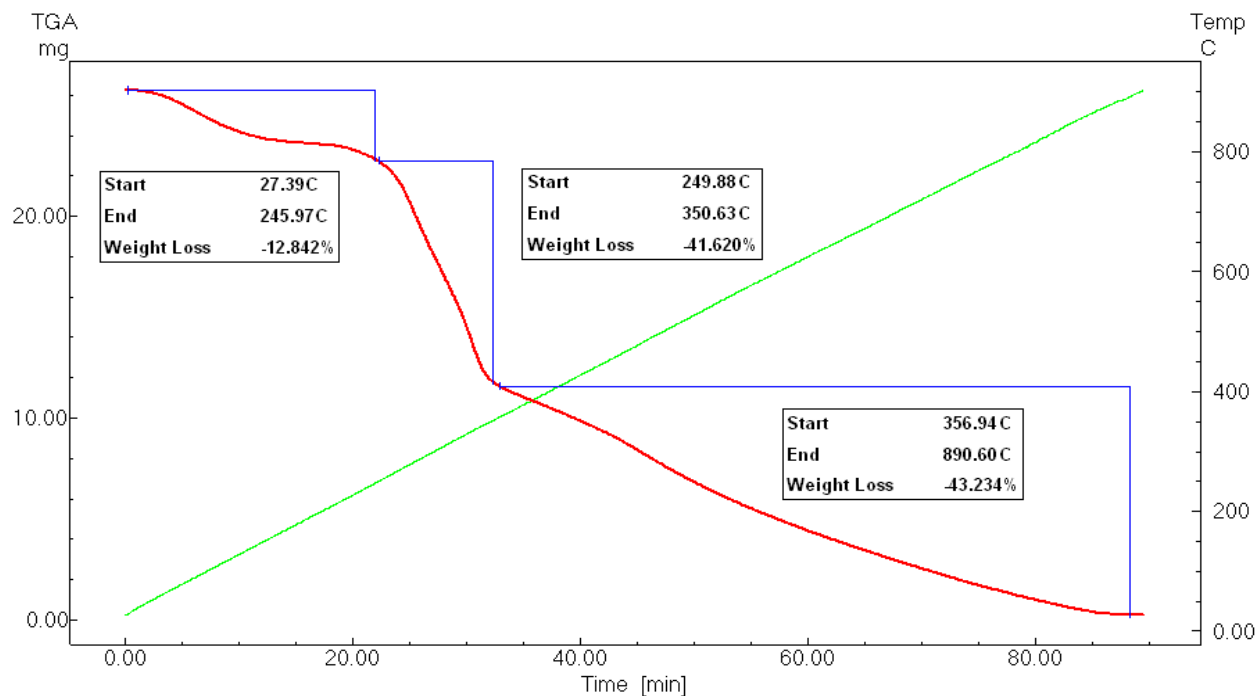
Table 4.1. Comparison of chemical and physical properties of Bael fruit shell with other precursors

Property	Coconut shell	Bael fruit shell
Chemical composition		
Cellulose	19.82	24.35
Lignin	30.11	19.90
Hemicellulose + Others ^a	50.07	55.75
Proximate analysis (Mozammel et al., 2002)		
Moisture	10.46	8.27
Volatile Matter	67.67	72.12
Fixed Carbon	18.29	16.72
Ash	3.58	2.89
Ultimate analysis (Yusup et al., 2010)		
C	40.12	46.91
H	2.56	6.22
N	0.61	0.79
S	0.23	0.07
O ^b	56.48	46.01

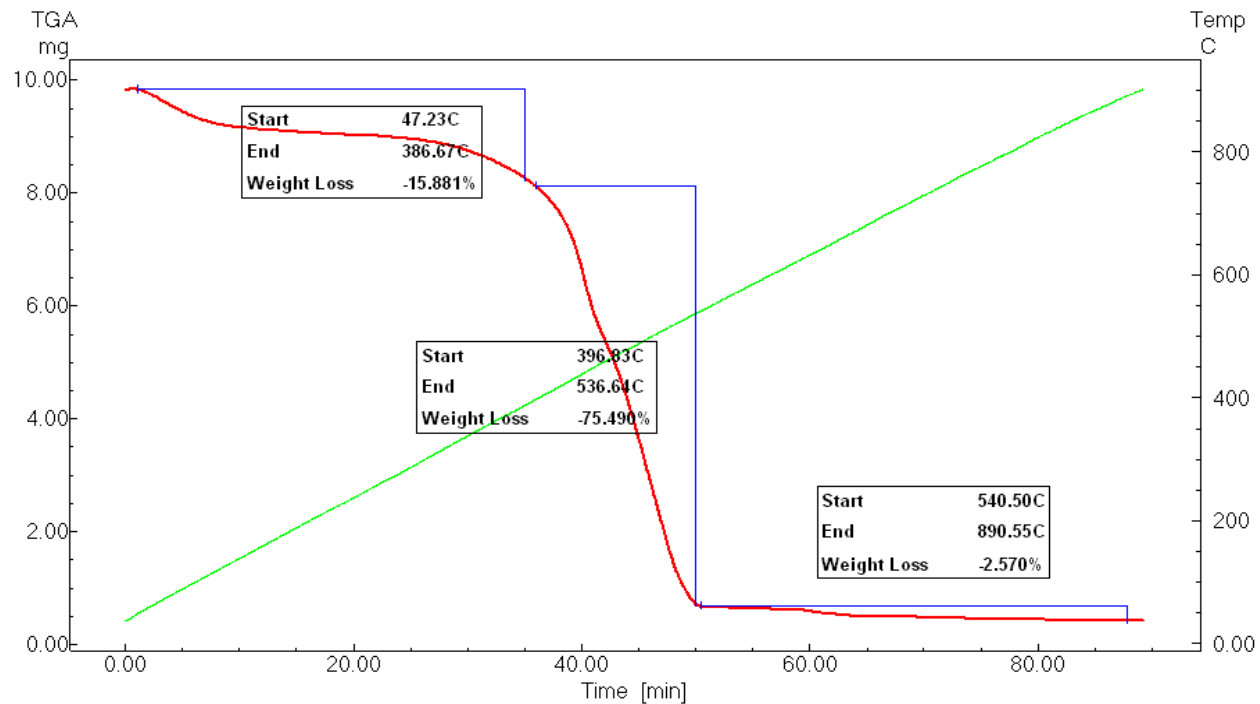
^{a, b} by difference

Figure 4.1 illustrates the thermogravimetric profile of the raw material (Bael fruit shell) and H₃PO₄ impregnated sample. The TGA was conducted in N₂ atmosphere with temperature range 25 to 900 °C. The heating rate of 10 °C/min was maintained. In case of raw material, the first step represents 12.84 % of weight loss in the temperature range 27 °C to 246 °C due to the surface bound water and moisture release. The steep weight loss (42 %) was evidenced in the temperature range from 250 °C to 351 °C. This weight loss is attributed mainly to the decomposition of cellulose and other low molecular weight furan derivatives. Above 350 °C, the weight loss is gradual and continuous up to 850 °C but to the decomposition of hemicellulose and lignin. Hence, the range 400 °C to 700 °C is considered as the carbonization temperature in this study. For H₃PO₄ impregnated sample the shift in temperature for weight loss is clearly

observed and the major weight loss (about 76 %) occurred in the temperature range 397 °C to 537 °C.



(a)



(b)

Figure 4.1. TGA analysis for (a) raw material and (b) raw material after impregnation with H₃PO₄

4.2. Preparation of AC

Washed and cleaned Bael fruit shells (after discarding the plum) were sundried for a week, which facilitated easy crushing and grinding. 100 g of the sample obtained after sieving (0.5 – 1.0 mm) was impregnated with 100 ml of diluted H_3PO_4 (85 wt %) to varying concentration in the range (0 – 50 %). Similarly, each 100 g of sieved sample was mixed with 100 ml solution of dissolved chemicals such as ZnCl_2 and KOH in varying concentrations (0.5 – 2.5 w/w). All the samples were soaked for overnight at room temperature and then transferred to a stain less steel reactor with narrow ports of 6 mm dia at both the ends. Gases and liquid vapors were vented through these narrow ends. The tube is admitted into an electric tubular furnace and heated to final temperature ranges between 400 – 700 °C, at a rate of 4 °C/min and under continuous N_2 flow of 200 ml/min. Holding time at final temperature was varied in between 0 – 120 min and the cooled samples were subjected to thorough washing with hot water (80 °C), mild acid (0.1 M HCl) and base (0.1 M NaOH) till the effluent water shows the neutral pH. The samples were dried at 110 °C for overnight and stored in air tight containers. The ranges of various preparation parameters were tabulated in [Table 4.2](#).

Table 4.2. AC preparation conditions and ranges of various parameters

Parameter	H_3PO_4	ZnCl_2	KOH
Impregnation Ratio	0 – 50 %	0.25 – 2.5 (w/w)	0.5 – 2.5 (w/w)
Carbonization Temperature (°C)	400 – 700	400 – 700	400 – 700
Holding Time (Min)	0 – 120	0 – 120	0 – 120

4.3. Effect of Process Parameters

In the preparation of activated carbon (AC) by chemical activation, the development of porosity depends on various process parameters such as impregnation ratio, carbonization temperature and holding time.

4.3.1. Effect of Impregnation Ratio

Impregnation ratio is defined as the ratio of chemical activating agent to the precursor. Impregnation ratio is a key parameter for the preparation of AC by chemical activation. Type of

the chemical used and effect of impregnation ratio on various properties of prepared samples were explored in this section.

4.3.1.1. Effect of Impregnation on the Yield of AC

The yield of activated carbon was calculated from the weight of the resultant activated carbon divided by weight of dried Bael fruit shell. The yield of AC increased with increase of impregnation up to certain value and then decreased. As generally recognized, the transformation from lignocellulosic materials into carbon involved releasing of O and H atoms as H_2O , CO , CO_2 , CH_4 , aldehydes or distillation of tar. The carbonization yield depends on the amount of carbon removed by binding with O and H atoms (Caturla et al., 1991). The effect of impregnation ratio and the chemical used for activation on the yield of AC was shown in Figure 4.2. In case of H_3PO_4 impregnation, maximum yield (74.47 %) was obtained at 20 % impregnation, whereas in case of $ZnCl_2$ and KOH the maximum yields were obtained at 2.0 (69.33 % and 85.33 %, respectively). Increasing impregnation ratio increases the release of volatiles from the sample and therefore the decrease in yield can be observed. The lower yield with the higher impregnation might be caused by the enhancement of carbon burn-off by extra activating agent (Qian et al., 2007).

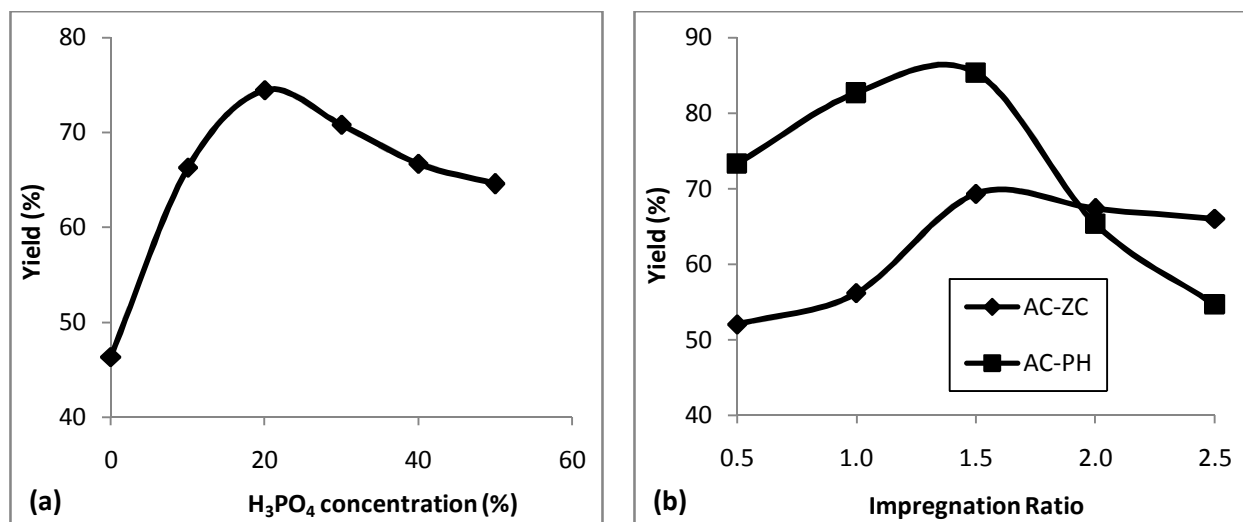


Figure 4.2. Effect of impregnation ratio on yield of ACs (a) AC-PA and (b) AC-ZC and AC-PH

4.3.1.2. Nitrogen Gas Adsorption – Desorption Isotherms

Nitrogen (N_2) gas adsorption-desorption isotherms of the activated carbons prepared with different chemical activating agents such as H_3PO_4 , $ZnCl_2$, and KOH at different impregnation ratios were carried out to investigate the porous characteristics.

Figure 4.3 illustrates the volume of N_2 adsorbed on AC prepared at various concentrations of H_3PO_4 used for impregnation. The figure depicts that the volume of N_2 adsorbed increases with the increase in concentration of H_3PO_4 . The high acid concentration would enhance the porosity development (Diao et al., 2002; Girgis and El-Hendawy, 2002) and hence the increase in adsorption of N_2 . The adsorption capacity increased with increase in H_3PO_4 concentration and reached maximum (392.61 cc/g) for AC prepared at 40 % impregnation. Further increase in acid concentration resulted in negative trend due to the damage of porous structure or may be due to the formation of polyphosphate layer which acts as a skin covering the porous structure. These results are in agreement with the findings of Girgis and Hendawy (2002). It is proposed that H_3PO_4 impregnation not only promotes the pyrolytic decomposition of raw material but also leads to the formation of cross linked structure (Jagtoyen and Derbishire, 1998).

The broad hysteresis loops found at low acid concentrations (10 % and 20 %) confirmed the existence of mesoporosity which narrowed at higher acid concentrations due to the absence of mesopores. The isotherms obtained at higher impregnations resemble typical Langmuir isotherms (type – I), being extremely microporous (Sing et al., 1985). Samples prepared at low impregnation ratios (10 % and 20 %) exhibited low pressure hysteresis (LPH) ($P/P_0 < 0.3$) which occurs due to the swelling of non-rigid walls in pores with trapping of adsorbate molecules (Gregg and Sing, 1982), and/or retention of molecules in pores similar in size to them (Freeman et al., 1993).

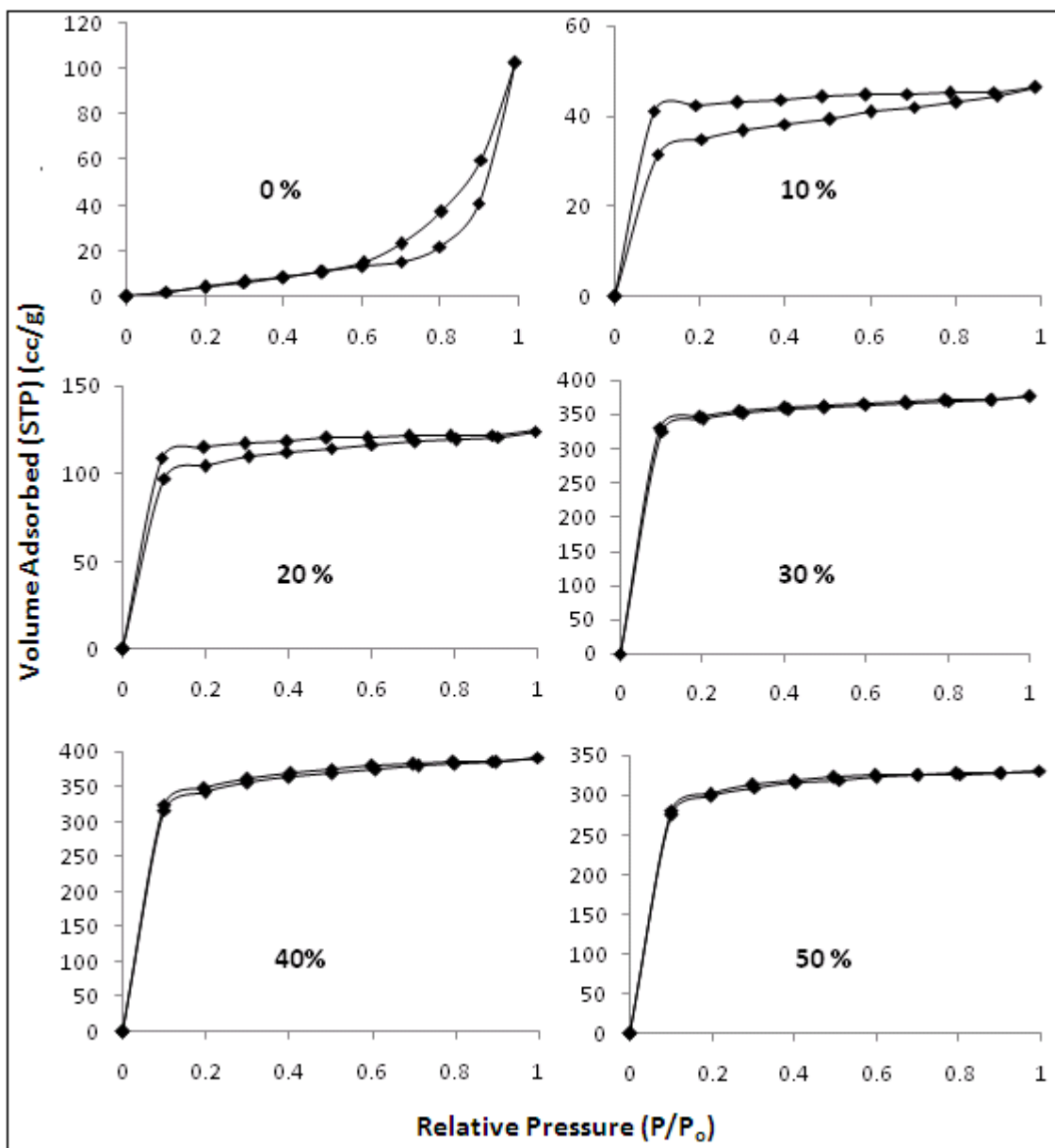


Figure 4.3. N₂ gas adsorption – desorption isotherms of AC-PA samples prepared at different impregnation concentrations

Figure 4.4 shows the N₂ adsorption-desorption isotherms of the ACs samples prepared by different ZnCl₂ impregnations and carbonized at 500 °C for 1 h. The carbons exhibited steep type – I isotherms which indicate high content of microporosity with a narrow pore size distribution. With the increase of impregnation ratio from 0.25 to 2.0, the volume of N₂ adsorbed gradually increased (65.92 cc/g to 342.04 cc/g), which suggests the evolution of new pores. The decrement in the volume of N₂ adsorbed (214.8 cc/g) with further increase in impregnation ratio to 2.5 is

due to the destruction of pore walls caused by high impregnation of ZnCl_2 to the precursor. However, development of mesoporosity as indicated by the pronounced desorption hysteresis loops is observed at low impregnation ratios. Small hysteresis loops, steeper branches, and widening of the knee at low pressures are the indications for the development of mesopores. It confirms to the findings reported by the authors [Rosas et al \(2009\)](#) and [Diao et al \(2002\)](#).

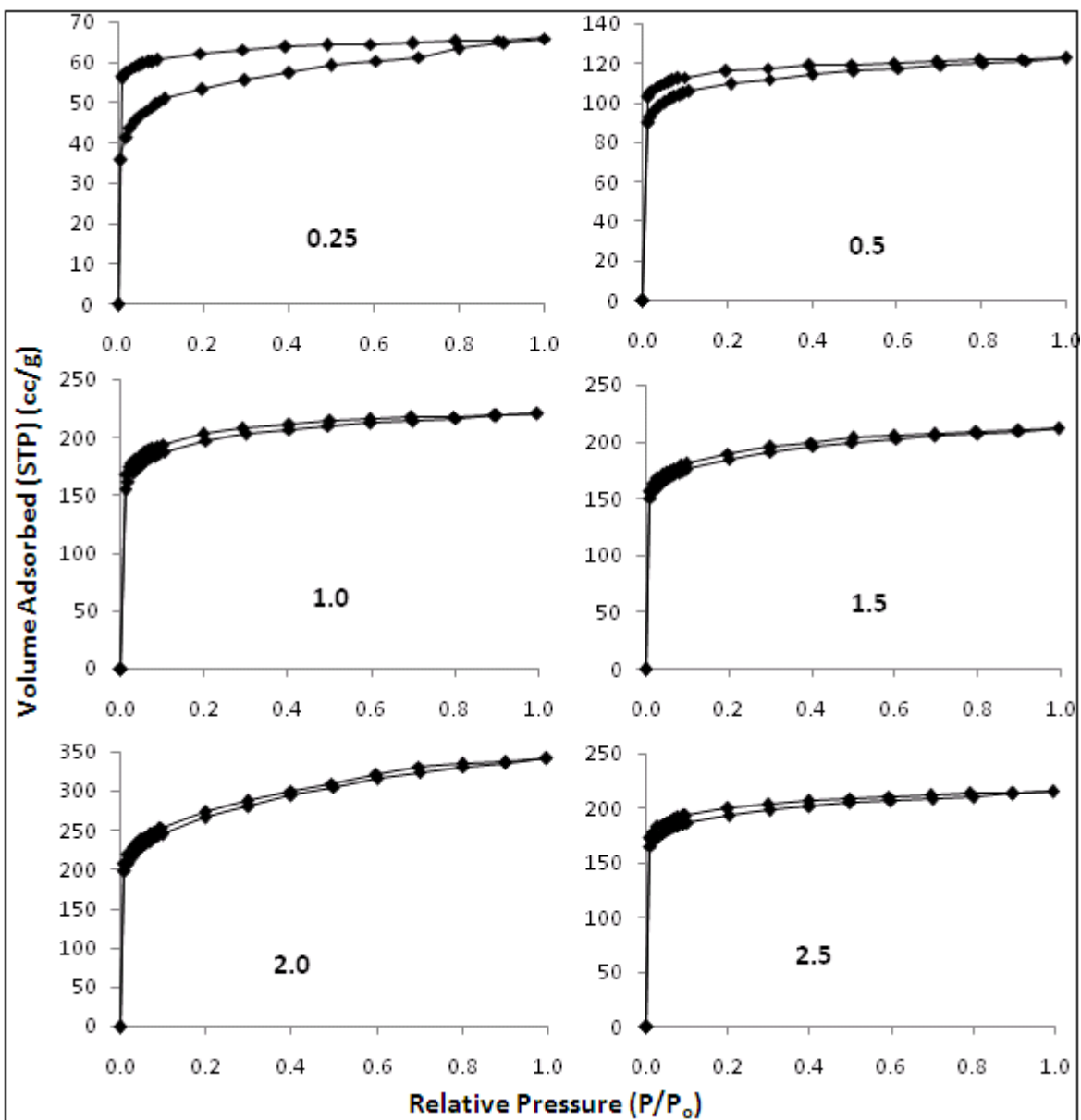


Figure 4.4. N_2 gas adsorption – desorption isotherms of AC-ZC samples prepared at different impregnation ratios

N_2 adsorption-desorption isotherms of KOH activated carbon prepared at different impregnation ratios (0.5 to 2.5), and carbonized at $600\text{ }^\circ\text{C}$ for 1 h were presented in [Figure 4.5](#).

The N_2 adsorption capacity of the samples increased from 37.31 cc/g to 215.12 cc/g with the increase of impregnation ratio from 0.5 to 2.0 and then decreased to 122.68 cc/g with the further increase of impregnation ratio to 2.5. The low pressure hysteresis (LPH) tends to decrease with the increase of impregnation ratio denoting the distribution of micropores with uniform pore width. Preparation of activated carbons from a variety of precursors by KOH activation was reported by various authors (Deng et al., 2010; Kawano et al., 2008; Tseng et al., 2008).

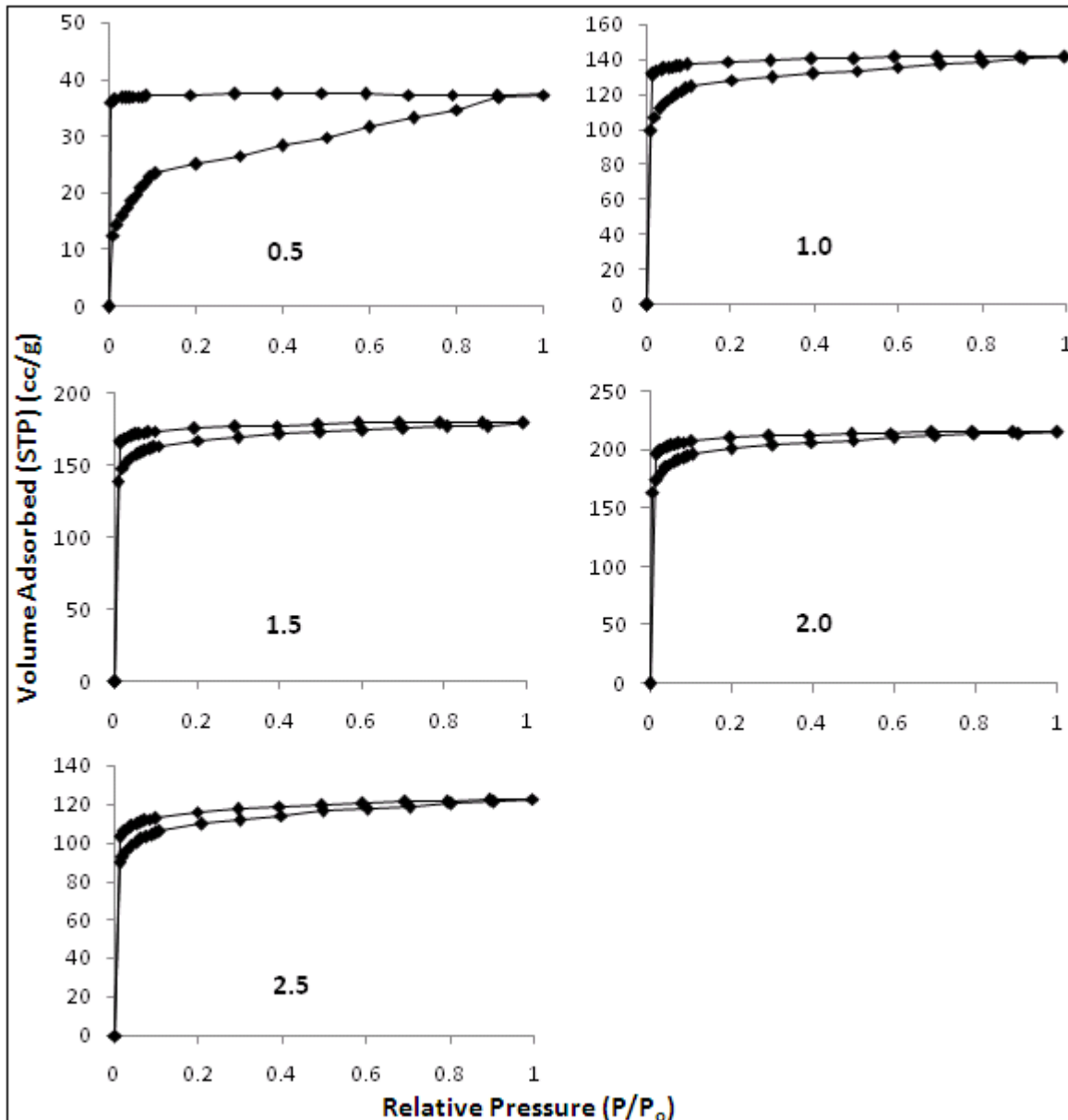
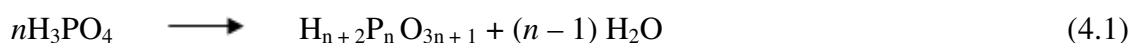


Figure 4.5. N_2 gas adsorption – desorption isotherms of AC-PH samples prepared at different impregnation ratios

4.3.1.3. Surface Area and Pore Volume

Activating agents play a critical role in surface area and porosity development. The typical effect of H_3PO_4 concentration on the surface area and pore volume of the ACs was shown in Figure 4.6. H_3PO_4 impregnated samples at varying concentrations were carbonized at $400\text{ }^\circ\text{C}$ for 1 h holding time. As acid concentration increased from 10 % to 40 % the surface area and pore volume of ACs were enhanced from $205\text{ m}^2/\text{g}$ to $1739\text{ m}^2/\text{g}$ and 0.07 cc/g to 0.60 cc/g , respectively. A 12 h impregnation of the raw material promoted the penetration of acid into the interior and depolymerization of the constituents into smaller units (Jagtoyen and Derbyshire, 1998; Lopez et al., 1996). Increase in H_3PO_4 impregnation ratio promotes degradation of the carbon structure with subsequent carbonization which causes charring and aromatization of the carbon skeleton and creation of the porous structure (El-Hendawy et al., 2001; Molina-Sabio, 2004; Olivares-Marin, 2006). Girgis et al (1998) prepared activated carbon from apricot stones by H_3PO_4 activation (20 – 50 %) and observed a progressive increase in BET surface area $700\text{ m}^2/\text{g}$ to $1400\text{ m}^2/\text{g}$. Phosphoric acid impregnation produces phosphate and polyphosphate bridges for connecting and crosslinking the biopolymer fragments. These reactions become pronounced with dehydration of the samples that creates an expanded state of highly porous surface. This porosity is accessible after removal of residuals by thorough washing (Rosas et al., 2009; Diao et al., 2002, Patnukao and Pavasant, 2008). Reaction occurs during H_3PO_4 activation can be represented as



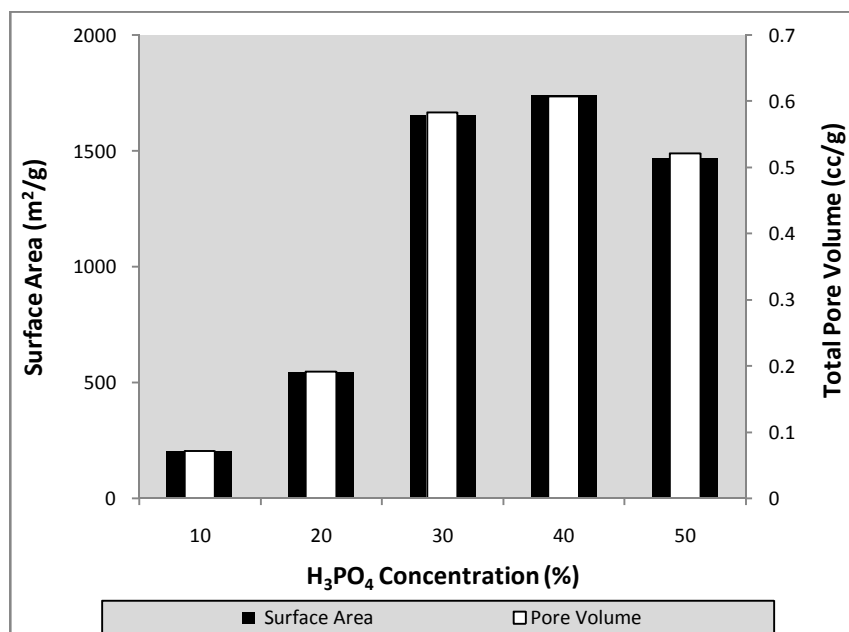


Figure 4.6. Effect of H₃PO₄ impregnation on surface area and pore volume of AC

Influence of ZnCl₂ impregnation ratio on surface characteristics of AC was depicted in Figure 4.7. With the increase of impregnation ratio, surface area and pore volume gradually increased and achieved its peak value at 2.0 whereas the trend reversed at higher impregnation. Similar results were obtained in various studies with different types of precursors with ZnCl₂ activation (Khalili et al., 2000; Qian et al., 2007). It is evident that as the ZnCl₂ impregnation ratio increases both pore volume and surface area improved. At impregnation ratio 2.0, carbonization temperature 500 °C with 1 h holding time maximum surface properties such as surface area (1488 m²/g) and pore volume (0.529 cc/g) were attained. ZnCl₂ acts as a dehydration agent during activation that inhibits tar formation and any other liquids that can clog up the pores of the sample (Rodriguez-Reinoso and Molina-Sabio, 1992; Guo and Lua, 2000). With ZnCl₂ impregnation, the movement of the volatiles through the pore passages was not hindered and volatiles were released from the carbon surface with activation. The mechanism of pore formation in AC prepared from Bael fruit shell by ZnCl₂ activation is not well known. However, Smisek and Cerney (1970) explained that ZnCl₂ mainly degrades cellulose by dehydration during pyrolysis. This causes aromatization of the carbonaceous skeleton. The fundamental difference resides in the activation which is a decisive stage in the creation of pores.

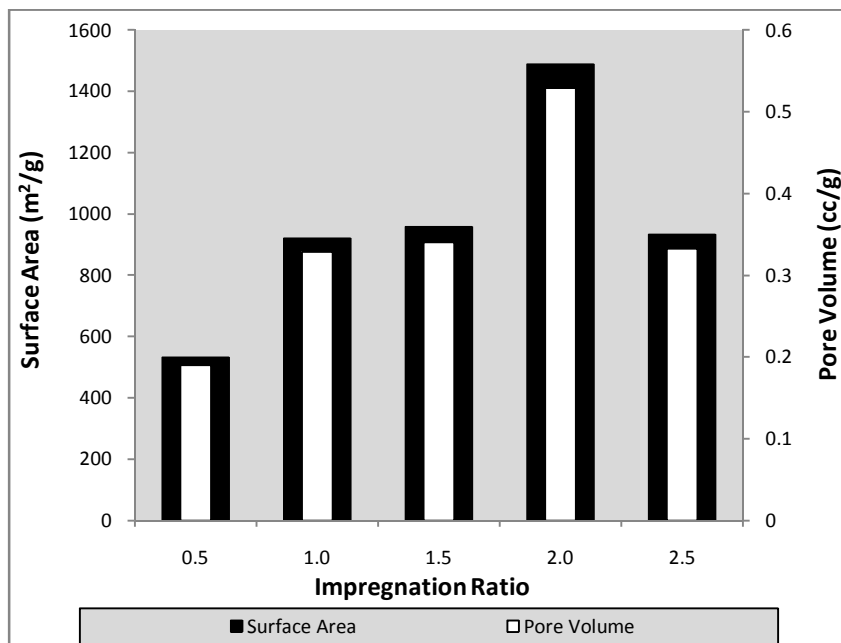
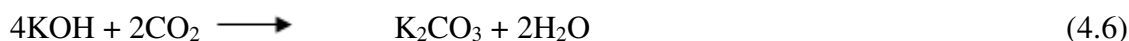
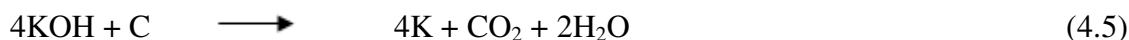
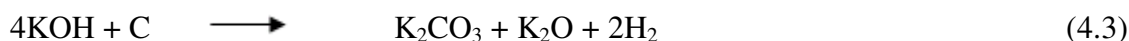


Figure 4.7. Effect of ZnCl₂ impregnation ratio on surface area and pore volume of AC

Figure 4.8 illustrates the effect of KOH impregnation on surface area and porosity. Surface area of the samples increased from 161.0 to 936.7 m²/g and pore volume increased from 0.06 to 0.33 cc/g with the increase of impregnation ratio from 0.5 to 2.0. However, further increase in impregnation ratio beyond 2.0 resulted in decrement of surface area and pore volume. The generally accepted chemistry of KOH activation involves redox reactions in which carbon is oxidized to carbonate and the hydroxide reduction induces the evolution of potassium and hydrogen (Hsu and Teng, 2000; Lillo-Rodenas et al., 2004; Okada et al., 2003). Reactions taking place during KOH activation are:



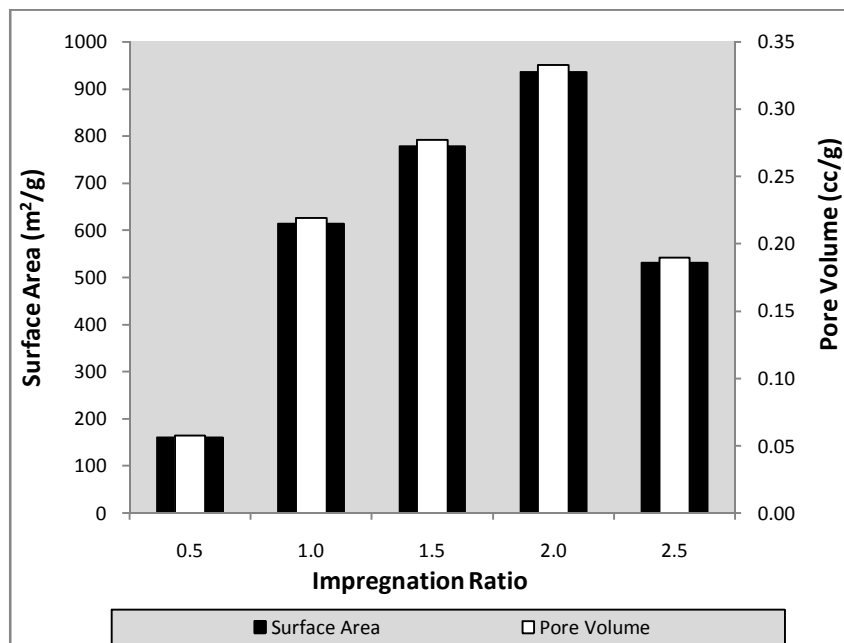


Figure 4.8. Effect of KOH impregnation ratio on surface area and pore volume of AC

4.3.1.4. Micropore Surface Area and Micropore Volume

Nitrogen adsorption-desorption isotherms confirm that all the samples prepared by chemical activation with various chemical agents were rich in micropores. The contribution of micropores to the porous characteristics was investigated by applying DR isotherm. The role of micropores in attaining high surface area and pore volume is appreciable and the evolution of micropores was affected greatly by the type and concentration of the chemical used for impregnation.

Figure 4.9 depicts the micropore surface area and micropore volume of ACs prepared by H₃PO₄ activation. Micropore surface area (S_{mi}) and micropore volume (V_{mi}) showed increasing trend with the increase of H₃PO₄ impregnation up to 30 % and then followed the reverse trend with further increment in acid concentration. ACs prepared by H₃PO₄ activation liberates tar at lower temperature that is more pronounced at higher impregnation of H₃PO₄. Tar acts as a binder that fills the inter space within the precursor. Increase in carbonization activates the release of tar that provides mechanical rigidity and well developed microporous structure (Rosas et al., 2009). Maximum values of micropore surface area (1625 m²/g) and micropore volume (0.56 cc/g) were obtained for the sample prepared at 30 % H₃PO₄ impregnation and carbonized at 400 °C for 1 h holding time. Micropore volume (0.56 cc/g) contributes 93.33 % of the total

pore volume (0.60 cc/g). The hysteresis loops (Figure 4.3) of N₂ adsorption – desorption isotherms observed at higher concentrations (40 % and 50 %) and slight decrease in the volume of N₂ adsorbed confirmed the transformation of micropores to mesopores (Ip et al., 2008; El-Hendawy, 2003). Therefore, impregnation of precursor with 30 % of H₃PO₄ was considered as the optimum concentration for the development of microporosity.

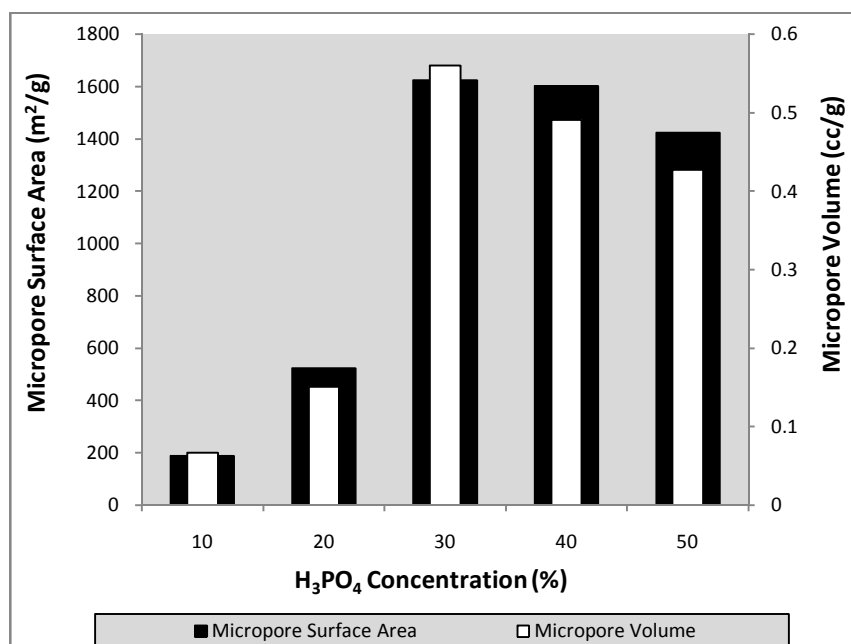


Figure 4.9. Effect of H₃PO₄ impregnation on micropore surface area and micropore volume

The change in the micropore surface area (S_{mi}), and micropore volume (V_{mi}) by varying impregnation ratio of ZnCl₂ to precursor was presented in Figure 4.10. Micropore characteristics of the samples prepared with different impregnation ratios ranging from 0.5 to 2.5 with carbonization at 500 °C for 1 h holding time were analyzed by applying DR isotherm. A gradual change in the shape of the isotherm and N₂ adsorption capacity with the increase of impregnation ratio indicates highly microporous distribution (Figure 4.2). With the increase of impregnation ratio, the evolution of micropores increased gradually up to 2.0 and then declined. Micropore surface area increased from 513.8 m²/g to 1339 m²/g and micropore volume increased from 0.18 cc/g to 0.48 cc/g with the increase of impregnation ratio from 0.5 to 2.0. Further increase in impregnation ratio to 2.5 did not show appreciable change in microporosity. The absence of broad hysteresis loop and decrement in total pore volume at 2.5 impregnation ratio again confirmed the destruction of microporous network without any widening of micropores. The

obtained results were different from that of [Hu et al. \(2001\)](#), who proposed an activation method for production of microporous and mesoporous ACs by ZnCl_2 activation from coconut and palm shells.

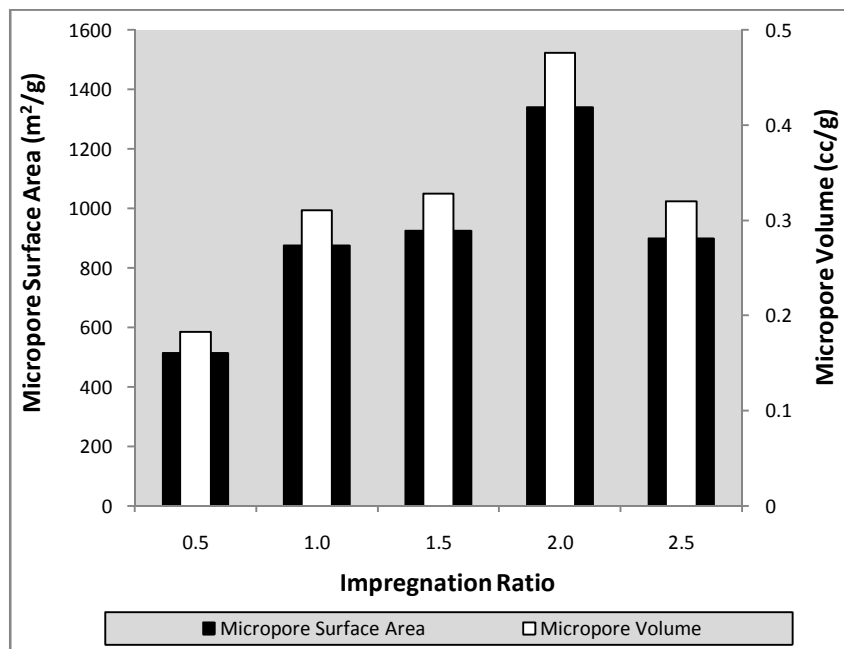


Figure 4.10. Effect of ZnCl_2 impregnation on micropore surface area and micropore volume

Effect of KOH impregnation on the evolution of micropores was depicted in [Figure 4.11](#). Samples were prepared at carbonization temperature of $600\text{ }^\circ\text{C}$ for 1 h of holding time and with different impregnation ratios (0.5 – 2.5). The micropore surface area (S_{mi}) and micropore volume (V_{mi}) increased gradually with increase of impregnation ratio from 0.5 to 2.0 and then decreased with further increase. The maximum values of S_{mi} and V_{mi} obtained for AC prepared at 2.0 impregnation ratio by applying DR isotherm are $924\text{ m}^2/\text{g}$ and $0.32\text{ cc}/\text{g}$, respectively. The major uptake of N_2 occurred at low relative pressure (less than 0.1) indicates the availability of high volume of micropores with narrow pore size distribution ([Figure 4.5](#)). Creation of microporosity is attributed to the removal of K metal that intercalated between the graphene layers at higher temperatures of activation ([Marsh and Rodriguez-Reinoso, 2006](#)).

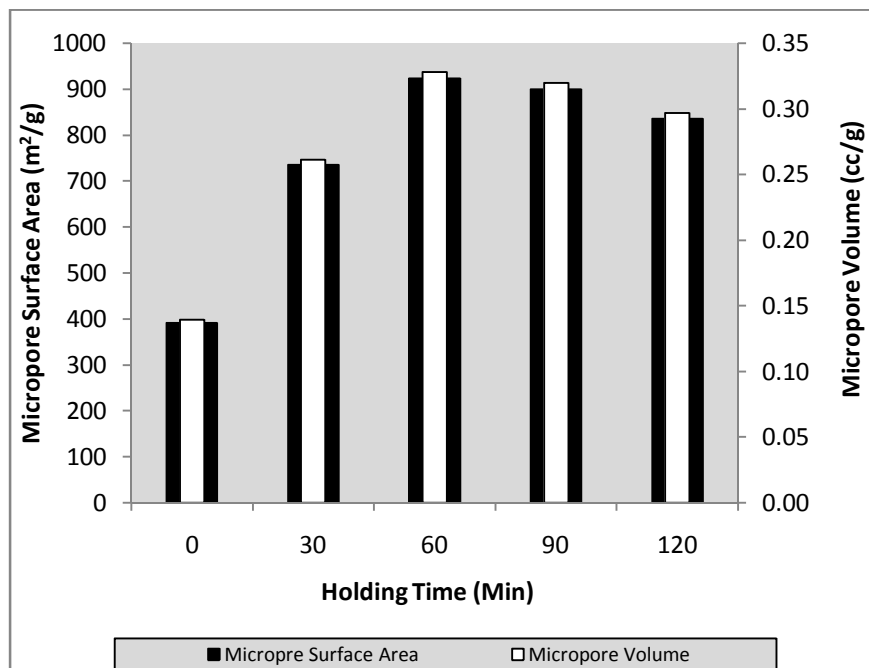


Figure 4.11. Effect of KOH impregnation on micropore surface area and micropore volume

4.3.2. Effect of Carbonization Temperature

The final carbonization temperature is a key parameter in the preparation of AC which has a significant effect on the yield and porous characteristics. The effect of carbonization temperature on the preparation AC using different precursors was investigated by several authors (Acharya et al., 2009; Basta et al., 2009; Deng et al., 2010; Foo et al., 2011; Girgis et al., 2002; Lua and Yang, 2005; Tsai et al., 2001; Tseng et al., 2008; Wu et al., 2010, 2011).

4.3.2.1. Effect of Carbonization Temperature on the Yield of AC

Figure 4.12 represents the effect of carbonization temperature on yield of ACs prepared by different chemical activations. In all three cases, the percentage yield obtained decreased with the increase of temperature. This is mainly due to the promotion of carbon burn-off and tar volatilization at higher temperatures (Adinata et al., 2007). With the increase of carbonization temperature from 400 °C to 700 °C, the yield of prepared ACs decreased from 70.82 to 55.77 %, 72.0 to 40.86 % and 84.0 to 56.0 % for AC-PA, AC-ZC and AC-PH, respectively.

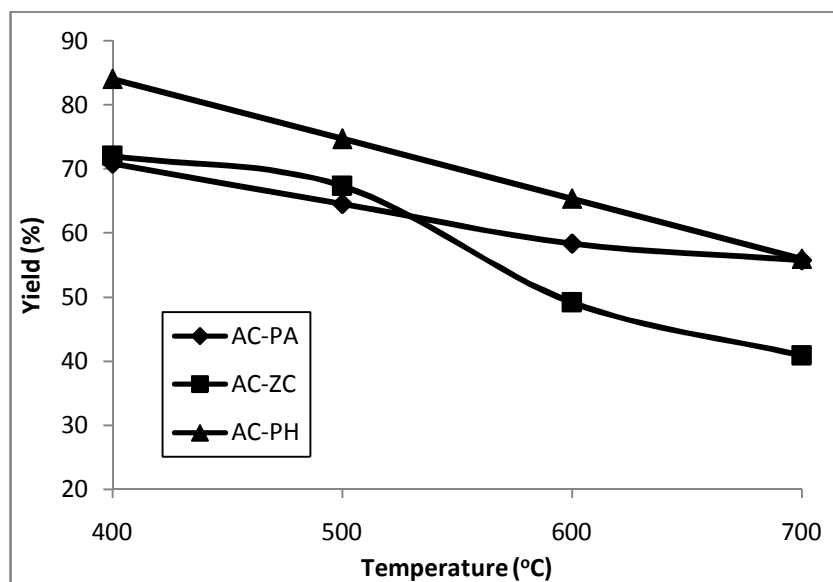


Figure 4.12. Effect of carbonization temperature on the yield of prepared ACs

4.3.2.2. Nitrogen Gas Adsorption – Desorption Isotherms

The N_2 adsorption-desorption isotherms of the ACs prepared at different temperatures ranging from 400 to 700 °C were carried out to investigate the porous characteristics. The acid concentration used for impregnation was kept constant at 30 % in case of H_3PO_4 and an impregnation ratio of 2.0 in the case of both $ZnCl_2$ and KOH . The holding time of 1 h at final carbonization temperature was maintained in all cases.

Figure 4.13 depicts the adsorption-desorption isotherms of activated carbon samples prepared by H_3PO_4 activation at different carbonization temperatures. It has been established by several researchers that carbonization temperature around 450 °C is optimum for AC preparation from agricultural waste residues by H_3PO_4 activation (Girgis and Hendawy, 2002). For the present study, carbonization at 300 °C of Bael fruit shell impregnated with H_3PO_4 has insignificant role in formation of porous structure. Rising of carbonization temperature to 400 °C resulted in well developed porosity at optimum impregnation (30 % H_3PO_4). It is observed that with increasing of carbonization temperature from 400 °C to 700 °C, the N_2 adsorption capacity of the ACs decreased from 377.21 cc/g to 214.43 cc/g. Earlier studies (Liou, 2010; Diao et al., 2002) reported porosity reduction with rise in temperature which was ascribed to the breakdown of micropore structure resulting in low internal surface area. The activation proceeds relatively at low temperature (400 °C) with a significant development of microporous network. The

widening of the ‘knee’ of the isotherms at low relative pressures is typical for the materials with wide micropores suggesting pore widening with the increase of temperature (Jagtøyen and Derbyshire, 1998; Solum et al., 1995). A noticeable transition from microporosity to mesoporosity occurs at activation temperatures between 500 °C and 700 °C which is confirmed by the presence of hysteresis loops at higher temperatures.

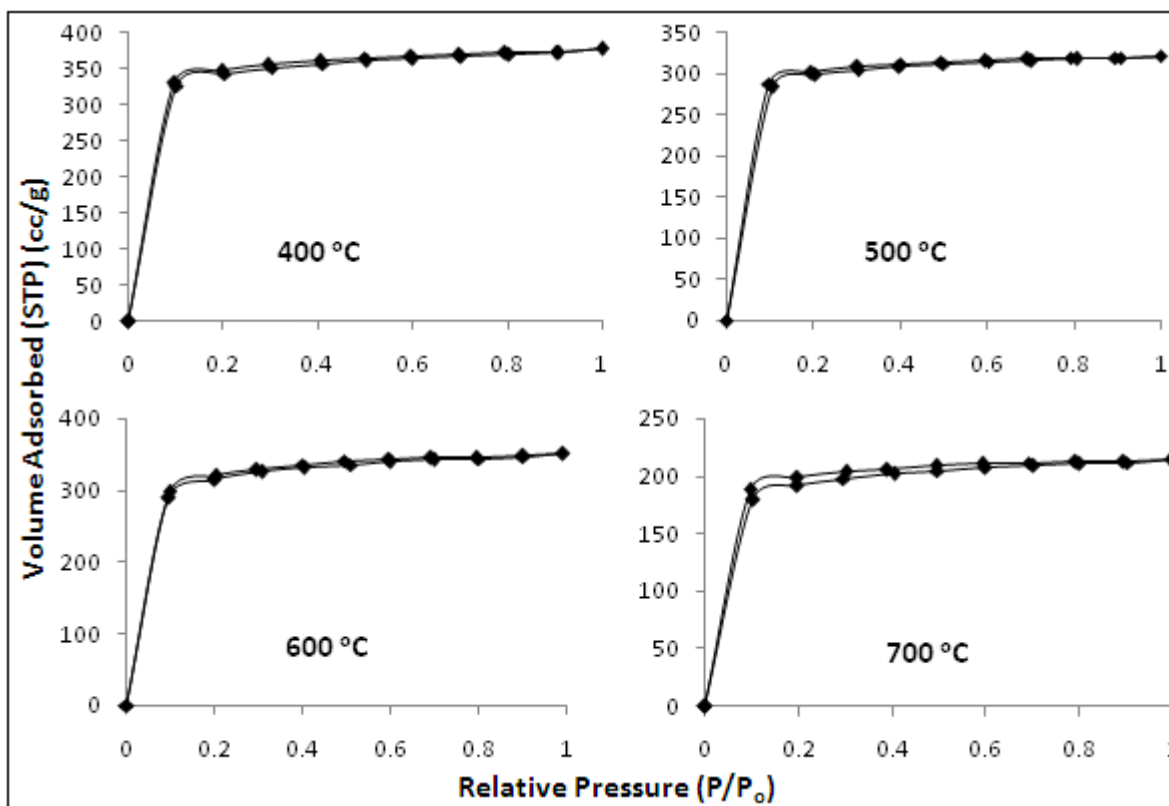


Figure 4.13. N₂ gas adsorption – desorption isotherms of AC-PA samples prepared at different carbonization temperatures

Figure 4.14 shows N₂ gas adsorption-desorption isotherms for ZnCl₂ activated samples prepared at different carbonization temperatures by keeping impregnation ratio and holding time constant at 2.0 and 1 h, respectively. From the figure, it was observed that at 500 °C the volume of N₂ adsorbed is high as compared to the samples prepared at other temperatures. All the isotherms obtained represent typical microporous adsorbents and the narrow hysteresis loops observed are due to the evolution of narrow mesopores at higher temperatures. The steep branches of isotherms obtained at 400 °C and 500 °C represent the presence of mesopores along with micropores. Isotherms obtained for the samples prepared at higher temperatures (600 °C and 700 °C) are parallel to the P/P₀ axis which reveals the presence of narrow micropores. The more

open knees at low relative pressures of isotherms at 400 °C and 500 °C represent the presence of mesopores (Diao et al., 2002).

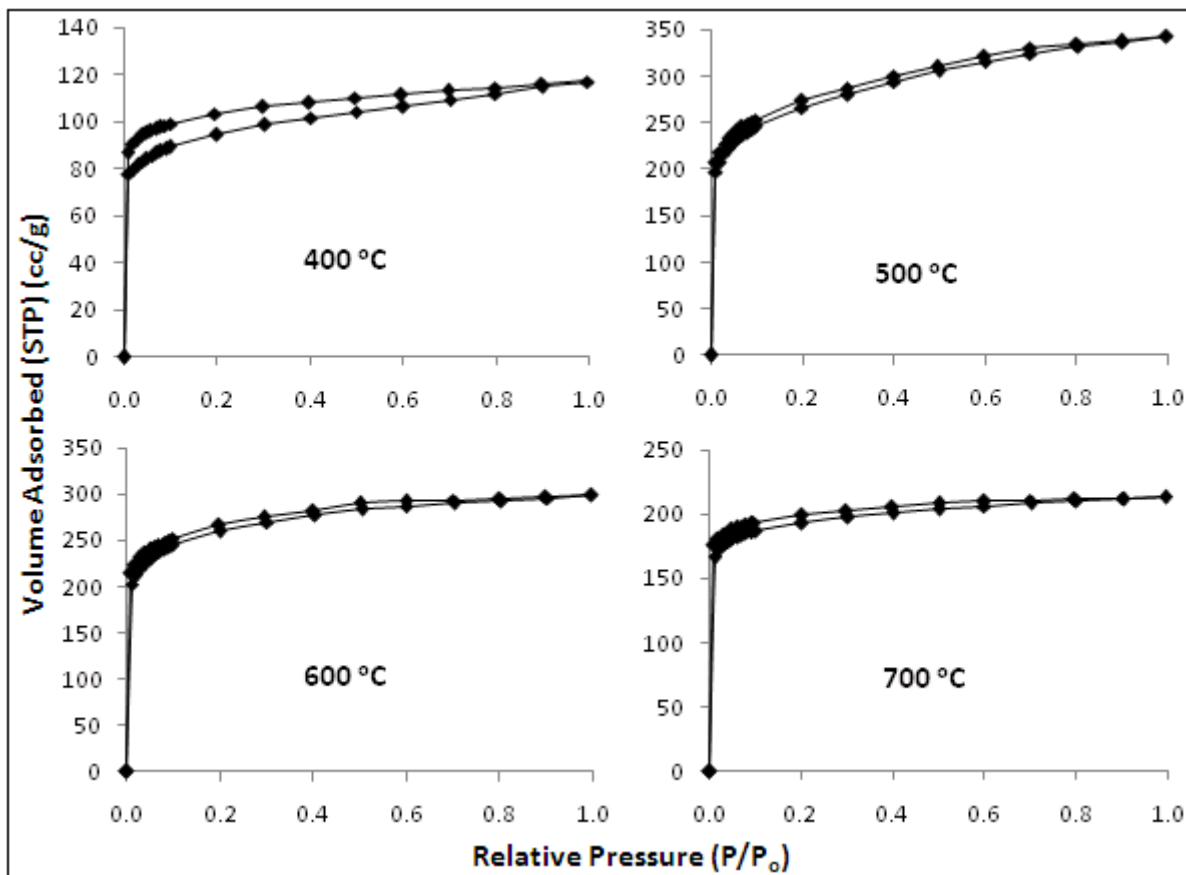


Figure 4.14. N₂ gas adsorption – desorption isotherms of AC-ZC samples prepared at different carbonization temperatures

Nitrogen adsorption-desorption isotherms of KOH activated AC samples prepared at varying carbonization temperatures at 2.0 impregnation ratio and 1 h holding time were shown in Figure 4.15. The N₂ adsorption capacity of the prepared ACs increases with the increase of carbonization temperature from 400 °C to 600 °C and then declined with the increase in temperature. Maximum adsorption capacity (215.12 cc/g) was achieved at 600 °C. Despite the narrow hysteresis loop, the adsorption isotherm obtained at 600 °C resembles a typical type – I isotherm which consists of micropores at a great extent.

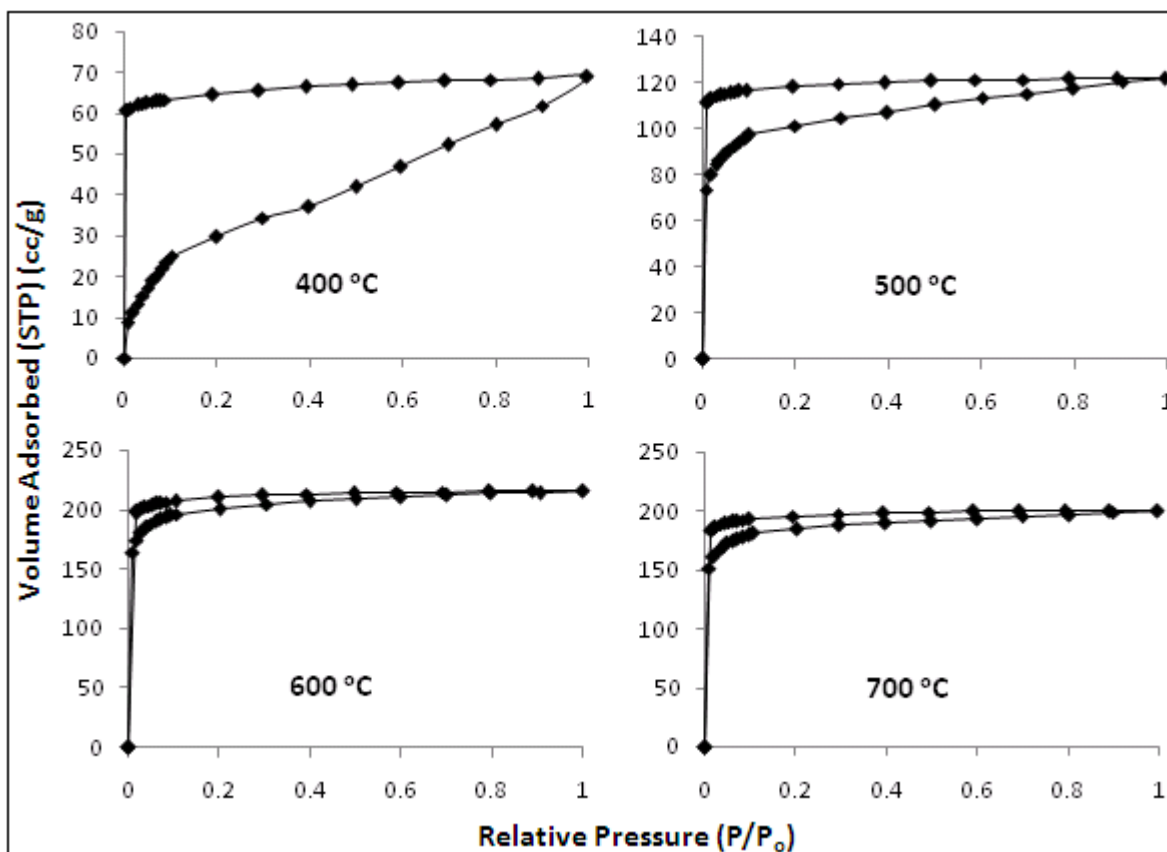


Figure 4.15. N₂ gas adsorption – desorption isotherms of AC-PH samples prepared at different carbonization temperatures

4.3.2.3. Surface Area and Pore Volume

The effect of carbonization temperature on surface area and pore volume within the range 400 to 700 °C was investigated for the samples activated at different chemical conditions. Although, the precursor used for AC preparation is same, the optimum temperature was found to be different for different chemical activating agents.

The influence of the carbonization temperature on specific surface area (S) and pore volume (V) of H₃PO₄ ACs were shown in Figure 4.16 by keeping other factors constant (H₃PO₄ impregnation – 30 % and holding time – 1 h). Surface area and pore volume decreased with the increase in temperature from 400 °C to 700 °C. The higher values obtained for surface area and pore volume are 1657 m²/g and 0.58 cc/g, respectively for AC prepared at 400 °C. Beyond 500 °C, surface area and pore volume decreases which may be due to the collapse of micropores formed at low temperature (400 °C) and due to the extensive carbon burn off. It leads to

widening of pores and destruction of pore walls resulting in reduction in pore volume. Similar results have been reported by other researchers (Haimour and Emeish, 2006; Hu and Srinivasan, 1999; Srinivasakannan and Abu Bakar, 2004). At low temperatures (around 400 °C) phosphoric acid catalyzes the hydrolysis of the glycosidic linkages in hemicellulose and cellulose and it cleaves aryl ether bonds in lignin, obtaining many transformations that include dehydration, degradation and condensation. These reactions promoted the release of H₂O, CO, CO₂, and CH₄ at low temperatures and consequently evolution of more porosity (Jagtoyen and Derbyshire, 1998). Therefore, the optimum value of carbonization temperature was considered as 400 °C for H₃PO₄ activation.

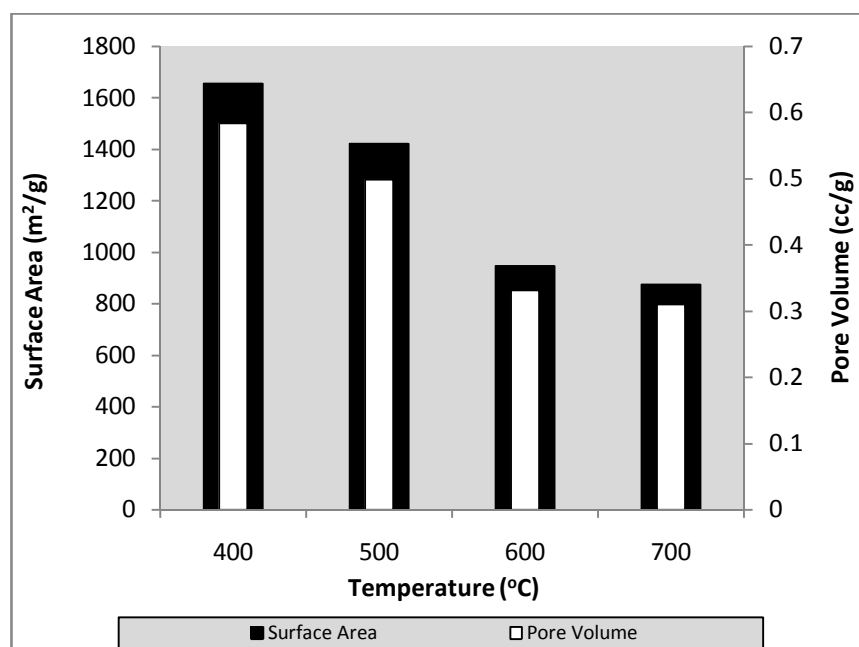


Figure 4.16. Effect of carbonization temperature on surface area and pore volume of AC-PA

Surface area and pore volume of ACs altered to a great extent with the change in carbonization temperature for ZnCl₂ activated samples. Role of final carbonization temperature in the development of porous characteristics of ZnCl₂ activated samples was shown in Figure 4.17. To determine the effect of carbonization temperature (400 – 700 °C) on porous characteristics, other parameters like impregnation ratio and holding time were maintained constant at 2.0 and 1.0 h, respectively. From the figure it is evident that 500 °C is the optimum carbonization temperature that showed high surface area (1488 m²/g) and pore volume (0.53 cc/g) and further increase in pyrolysis temperature resulted in gradual decrease in S_T and V_T .

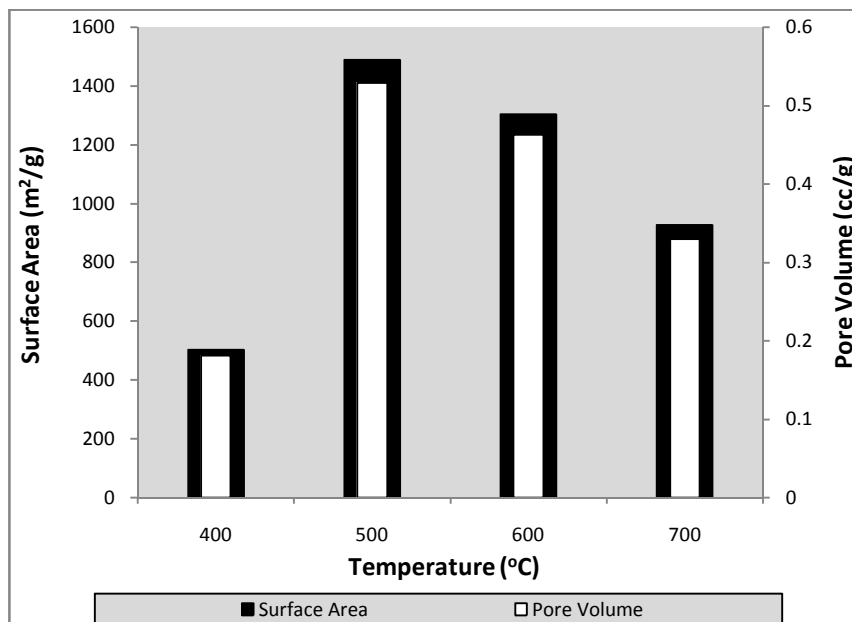


Figure 4.17. Effect of carbonization temperature on surface area and pore volume of AC-ZC

Variation in surface area (S_T) and pore volume (V_T) with the change in carbonization temperature of KOH activated AC samples were revealed in [Figure 4.18](#). Samples analyzed were prepared at different carbonization temperatures with 2.0 impregnation ratio of KOH to precursor and 1 h holding time at final temperature. With the increase of temperature from 400 °C to 600 °C, both surface area and pore volume were increased and showed decreasing trend with further increase of temperature to 700 °C. The maximum values of S_T and V_T obtained for the sample prepared at 600 °C (impregnation ratio, 2.0 and holding time, 1 h) were 937 m²/g and 0.33 cc/g, respectively.

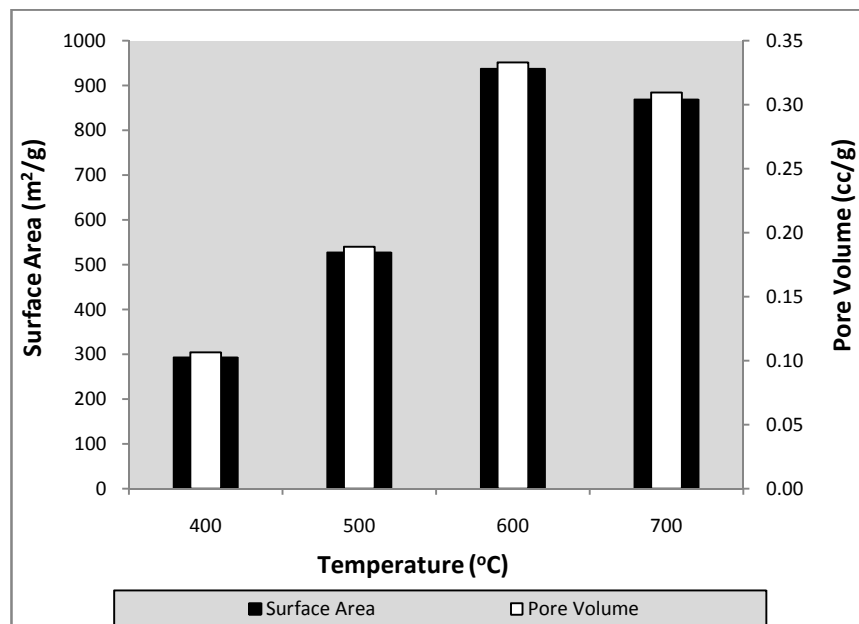


Figure 4.18. Effect of carbonization temperature on surface area and pore volume of AC-PH

4.3.2.4. Micropore Surface Area and Micropore Volume

As discussed previously, the contribution of micropores to achieve high surface area and pore volume is highly appreciable for the prepared samples with various chemical activations. Besides the impregnation ratio, the carbonization temperature also influences the evolution of micropores to a greater extent.

The adsorbents prepared by H_3PO_4 activation at different carbonization temperatures were rich in micropores and hence micropore surface area (S_{mi}) and micropore volume (V_{mi}) contributed greatly to the total surface area (S_T) and total pore volume (V_T) of the samples. Maximum values of S_{mi} (1625 m²/g) and V_{mi} (0.57 cc/g) were achieved for the sample carbonized at 400 °C with 30 % H_3PO_4 impregnation concentration and 1 h holding time. The trend of changes in microporous characteristics of H_3PO_4 activated carbons with different carbonization temperatures were presented in Figure 4.19. The results obtained at 400 °C were appreciable and confirmed that the porous network formed was not due to the evaporation of phosphorus-containing constituents, but due to the exposure of pores on thorough washing.

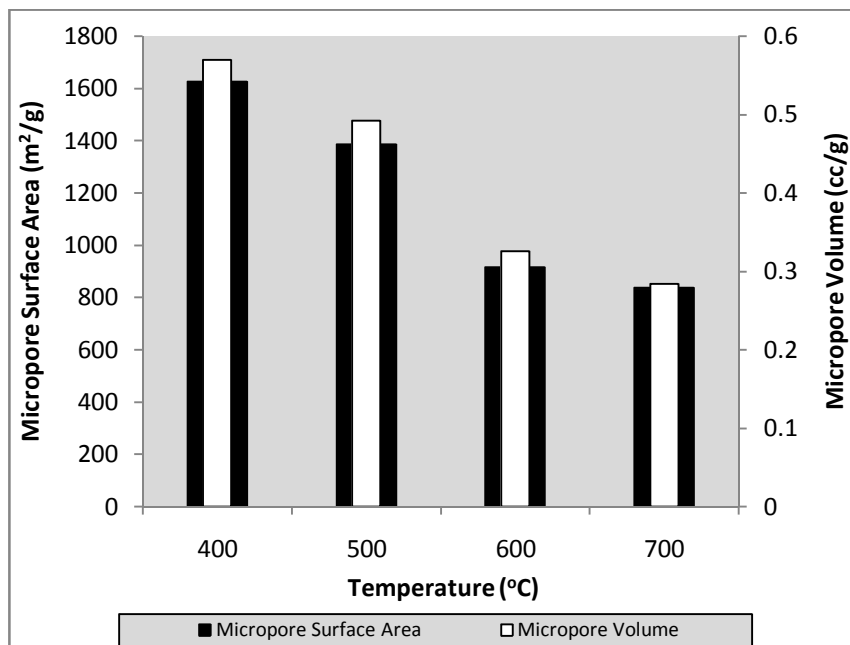


Figure 4.19. Effect of carbonization temperature on micropore surface area and micropore volume of AC-PA

Effect of carbonization temperature on the micropore properties of ZnCl₂ activated carbon samples was shown in Figure 4.20. With the increase of temperature from 400 to 500 °C, micropore surface area (S_{mi}) and micropore volume (V_{mi}) increased randomly and then decreased gradually with the rise in temperature. Higher values of S_{mi} (1339 m²/g) and V_{mi} (0.48 cc/g) were obtained at carbonization temperature of 500 °C (impregnation ratio, 2.0 and holding time, 1 h). The gradual decrease in S_{mi} and V_{mi} beyond 500 °C may be due to the collapse of the porous structure which resulted in decrease of S_T and V_T . The preferable results obtained at 500 °C revealed that the most of porosity could be developed from the spaces left by ZnCl₂ after acid wash rather than volatilization of ZnCl₂ which has boiling point at above 732 °C (Qian et al., 2007).

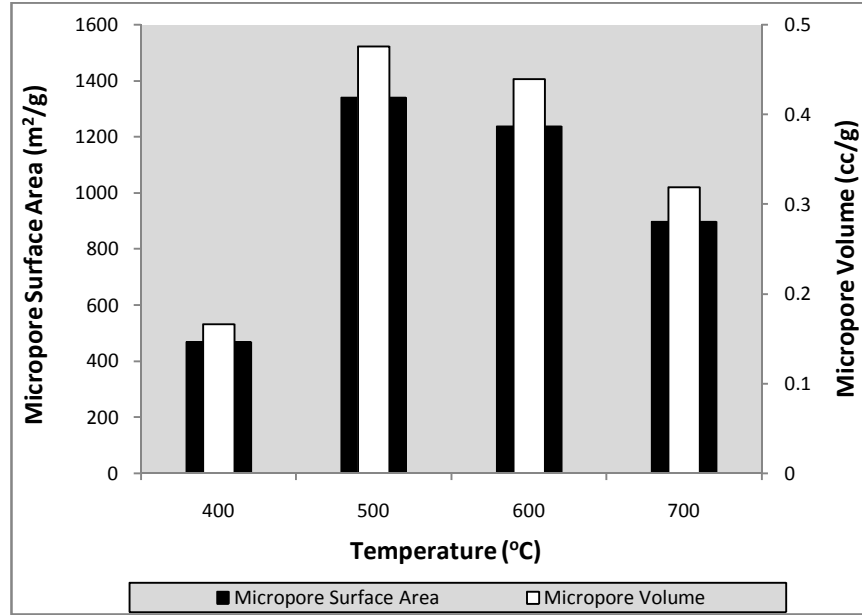


Figure 4.20. Effect of carbonization temperature on micropore surface area and micropore volume of AC-ZC

The evolution of micropores and changes in micropore surface (S_{mi}) area and micropore volume (V_{mi}) with the change in carbonization temperature of KOH activated samples at 2.0 impregnation ratio and 1 h holding time were illustrated in Figure 4.21. With the increase of temperature from 400 °C to 600 °C, S_{mi} and V_{mi} increased from 218 m²/g to 924 m²/g and 0.08 to 0.33 cc/g, respectively. As compared to micropores, the contribution of mesopores and macropores to the total surface area and pore volume was negligible.

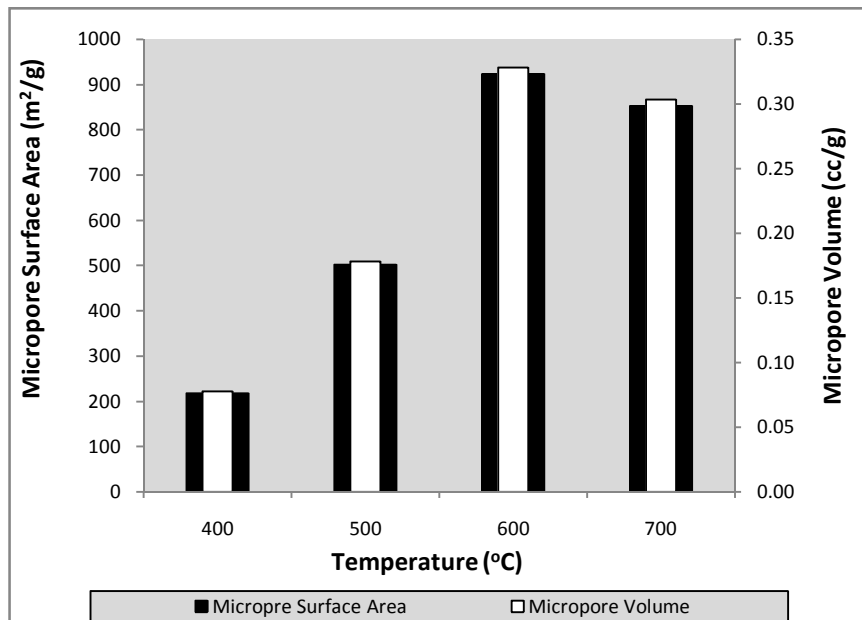


Figure 4.21. Effect of carbonization temperature on micropore surface area and micropore volume of AC-PA

4.3.3. Effect of Holding Time

Along with impregnation ratio and final carbonization temperature, holding time at final carbonization temperature played an important role in the development of porous structure. The AC samples were prepared at optimum conditions of impregnation ratio and carbonization temperature with different holding times (0 – 120 min).

4.3.3.1. Effect of Holding Time on the Yield of AC

Figure 4.22 represents the effect of holding time at final carbonization temperature on yield of ACs prepared. In all three cases, the percentage of yield obtained was decreased with the increase of holding time (0 – 120 min). The yield was decreased at longer holding times because of the higher carbon burn-off (Qian et al., 2007). With the increase of holding time from 0 to 120 min, the yield of prepared ACs was decreased from 73.86 to 62.81 %, 83.33 to 54.00 % and 84.66 to 52.00 % for AC-PA, AC-ZC and AC-PH, respectively. It could be attributed to the release of more volatiles by keeping the sample for longer duration at final carbonization temperature.

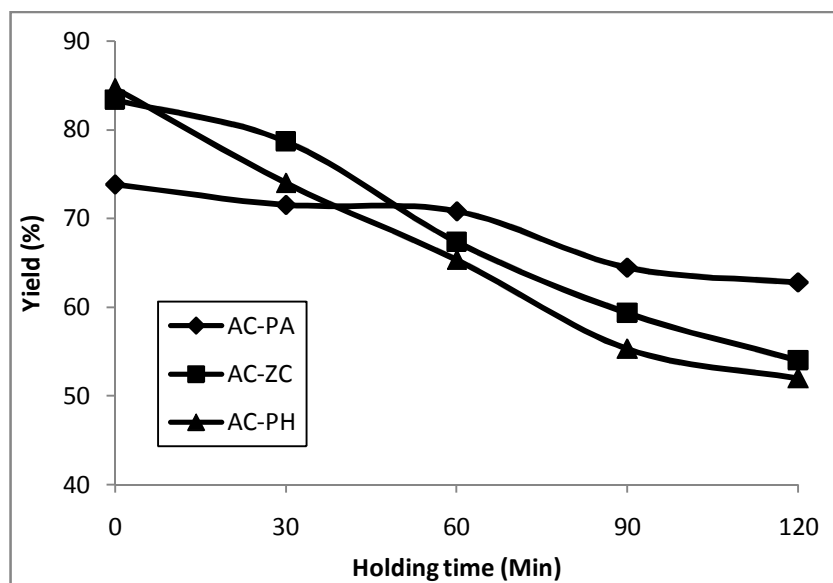


Figure 4.22. Effect of holding time on the yield of prepared ACs

4.3.3.2. Nitrogen Gas Adsorption – Desorption Isotherms

The nitrogen gas adsorption-desorption isotherms were carried out to reveal the effect of holding time on porous characteristics of ACs prepared by H_3PO_4 , $ZnCl_2$, and KOH activations.

The influence of holding time on the N₂ adsorption capacity of ACs prepared by H₃PO₄ activation can be observed in Figure 4.23. The N₂ adsorption capacity increased greatly with the increase of holding time from 0 to 60 min and then decreased. It clearly indicates that 60 min of holding time is the optimum value and the shape of the isotherm and the absence of hysteresis loop strongly confirmed the presence of immense micropores. The hysteresis loop observed at low relative pressures for 0 min holding time indicates the presence of mesopores. With the increase of holding time, the isotherm became more parallel to the P/P₀ axis at high relative pressures which is a typical characteristic of microporous solids (Youssef et al., 2005).

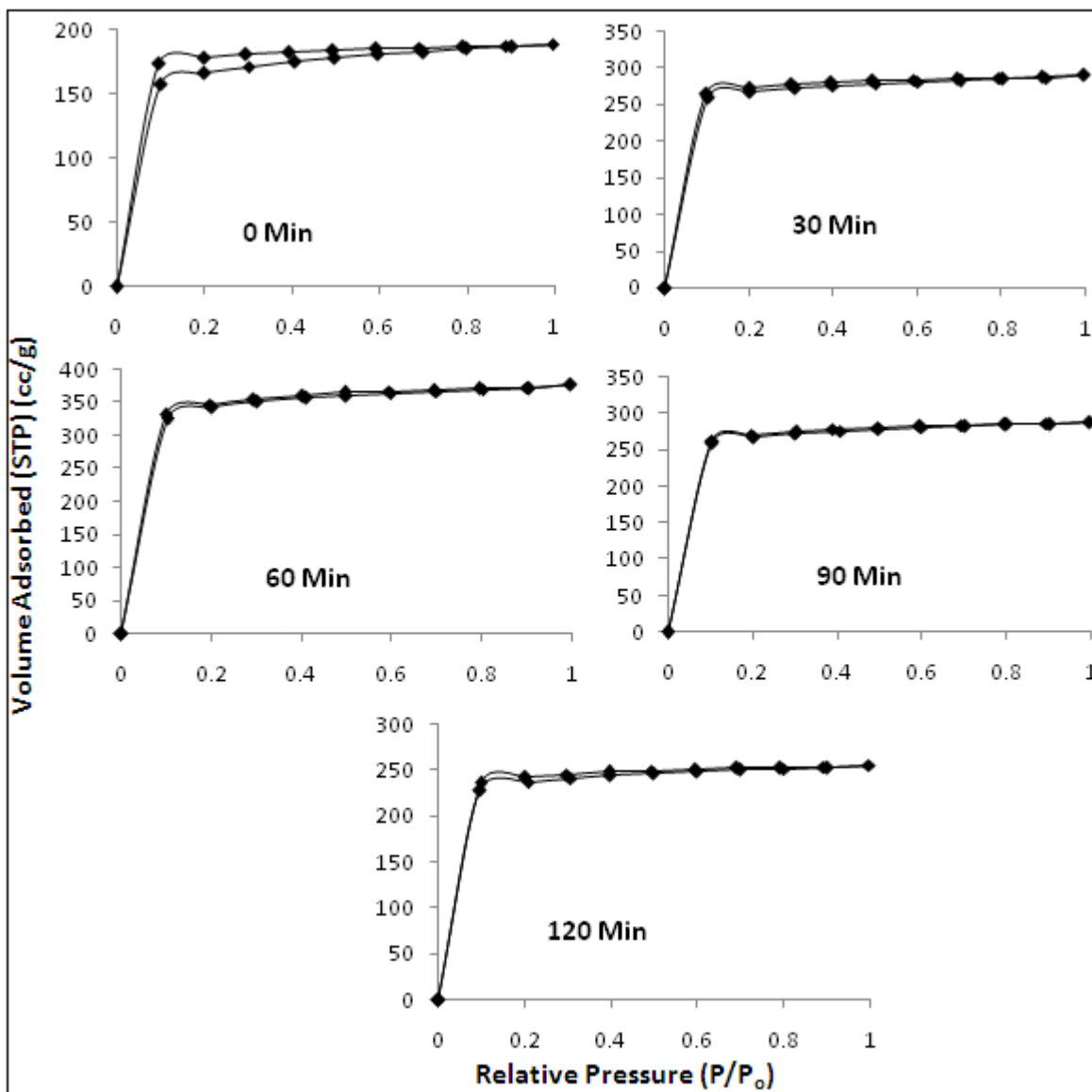


Figure 4.23. N₂ gas adsorption – desorption isotherms of AC-PA samples prepared at different holding times

The N₂ adsorption isotherms of samples prepared at different holding times by ZnCl₂ activation at optimum operating conditions were shown in Figure 4.24. The N₂ gas adsorption capacity increased as the holding time increases and extended till 60 min and then decreased. All the carbons obtained are of typically microporous (type – I) with little amount of mesopores which was confirmed by the narrow hysteresis loops. The volume of N₂ adsorbed continuously increased with the pressure exhibiting a steep branch of isotherm at 60 min due to the availability of narrow mesopores.

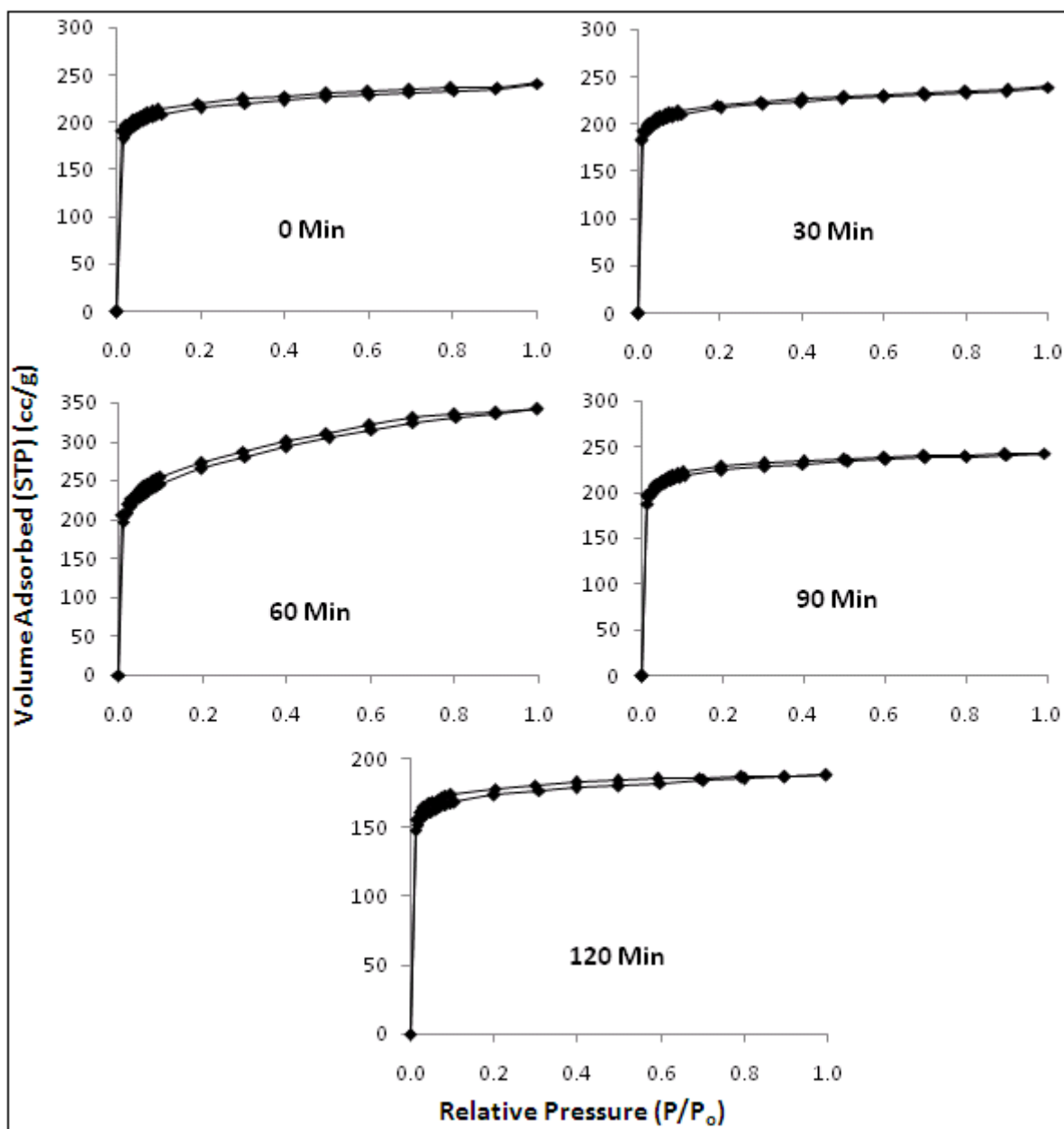


Figure 4.24. N₂ gas adsorption – desorption isotherms of AC-ZC samples prepared at different holding times

The porous characteristics of the prepared KOH activated samples at different holding times were studied using N_2 adsorption-desorption isotherms. Holding time duration at final temperature showed significant effect on the N_2 adsorption capacity of the samples prepared by KOH activation. From Figure 4.25, with the increase of holding time, the N_2 adsorption capacity of the samples increased and reaches maximum at 60 min and then decreased. Though the decrement in the width of the hysteresis loop beyond 60 min showed the presence of immense micropores, the decrement in the volume of N_2 shows the availability of reduced pore volume.

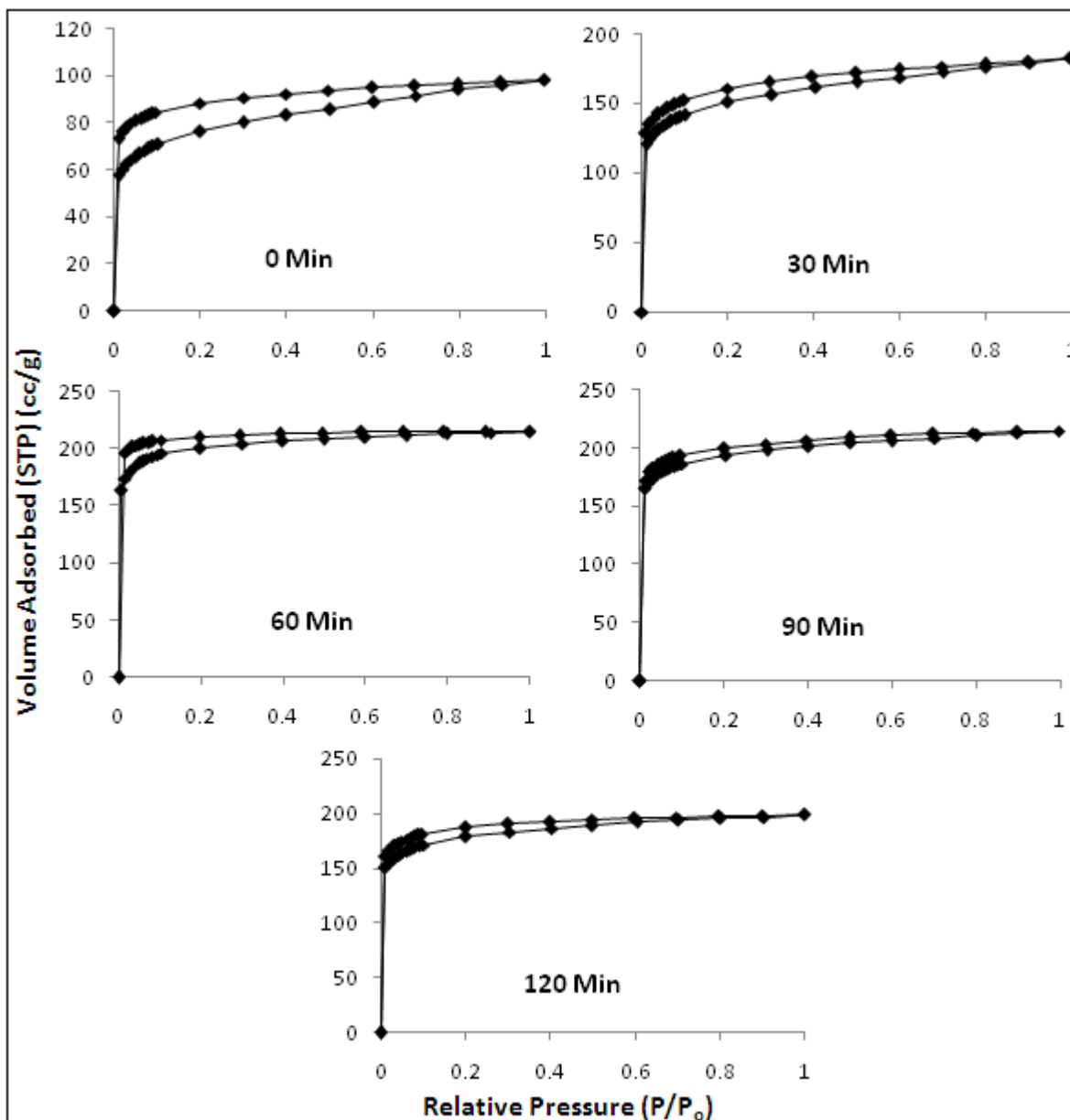


Figure 4.25. N_2 gas adsorption – desorption isotherms of AC-PH samples prepared at different holding times

4.3.3.3. Surface Area and Pore Volume

Surface area and pore volume of the prepared activated carbons by KOH activation are highly dependent on the duration of holding time at final carbonization temperature. The optimum values of holding time changes with the type of precursor and type of chemical used for activation.

Figure 4.26 illustrates the change in surface area (S_T) and pore volume (V_T) of the ACs prepared by H_3PO_4 activation with different holding times at final carbonization temperature ranging from 0 to 60 min. The S_T and V_T values were increased from 833 m^2/g to 1657 m^2/g and 0.3 cc/g to 0.58 cc/g , respectively with the increase of holding time from 0 to 60 min at 400 °C. Samples were prepared at optimum conditions (H_3PO_4 concentration, 30 % and carbonization temperature, 400 °C) and different holding times (0 to 120 min). Further increase in the holding time beyond 60 min resulted in the decrement of surface area and pore volume. This indicates that longer duration of holding time caused some of the pores to enlarge or even collapse, thus reducing the surface area and pore volume (Diao, et al., 2002).

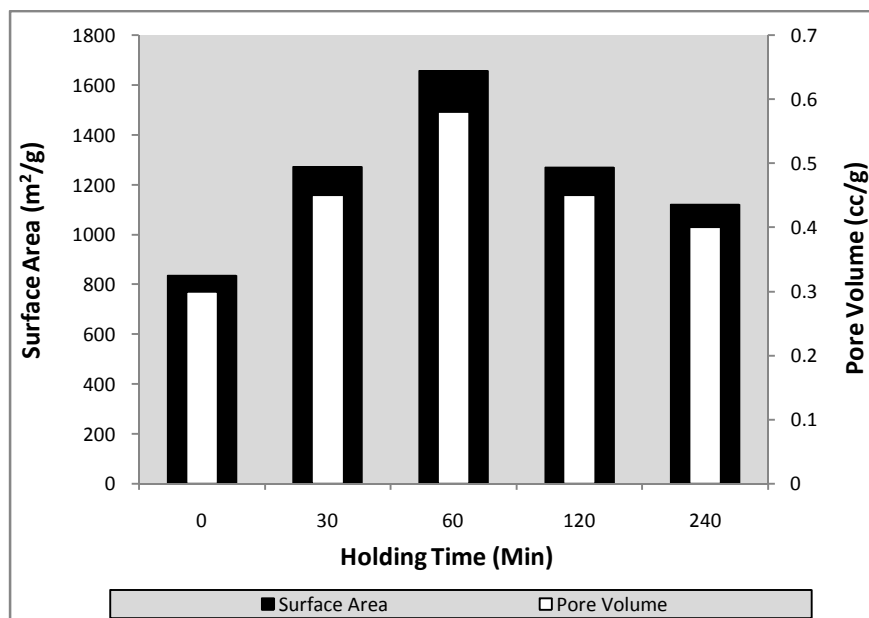


Figure 4.26. Effect of holding time on surface area and pore volume of AC-PA

Surface area (S_T) and pore volume (V_T) of $ZnCl_2$ activated samples with different holding times were characterized and shown in Figure 4.27. ACs were prepared at optimum conditions of carbonization temperature (500 °C), impregnation ratio (2.0) and at different holding times

ranging from 0 to 120 min. Initially at 0 min of holding time, greater values of S_T and V_T were observed and then gradually increased with the increase of holding time and reached maximum at 60 min. Further increase of holding time resulted in weakening of pore walls due to more evaporation of volatiles which caused the destruction of pores.

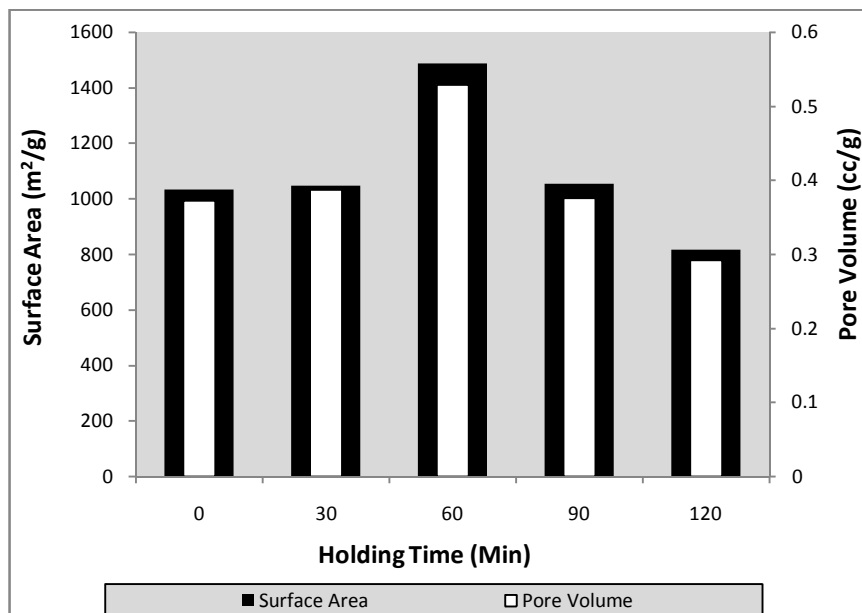


Figure 4.27. Effect of holding time on surface area and pore volume of AC-ZC

Surface area and pore volume of the KOH activated samples pyrolyzed at 600 °C for different holding times ranging from 0 to 120 min and with an impregnation ratio of 2.0, were presented in [Figure 4.28](#). With the increase of holding time, surface area and pore volume are increased gradually up to 60 min and then decreased slowly with further increase. There is not much change in the both properties for the samples prepared at 60 and 90 min of holding time. But, the values are slightly decreased with the increase of holding time beyond 60 min.

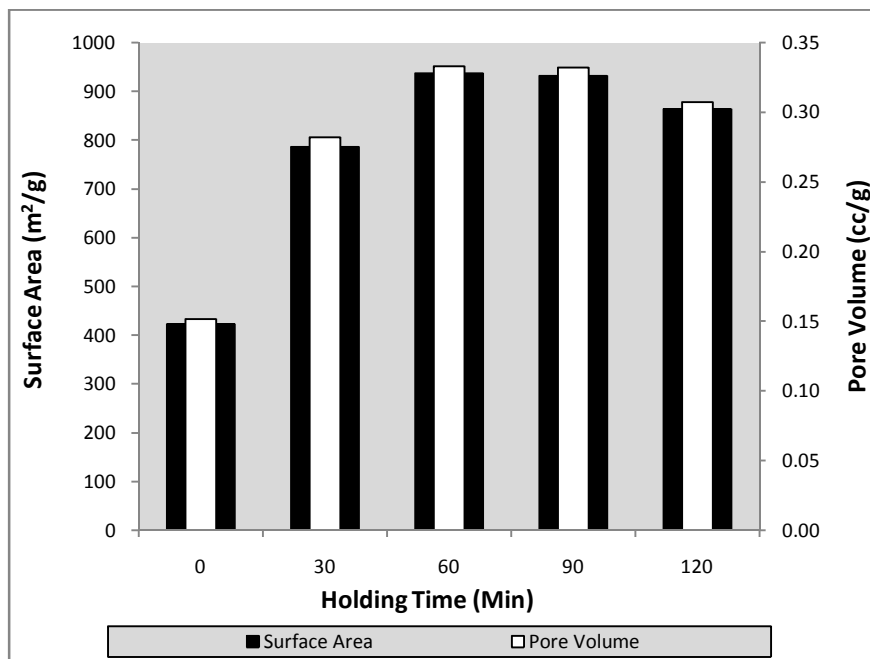


Figure 4.28. Effect of holding time on surface area and pore volume of AC-PH

4.3.3.4. Micropore Surface Area and Micropore Volume

The evolution of micropores also greatly depends on the holding time at final carbonization temperature along with impregnation ratio and carbonization temperature. The contribution of micropores is highly appreciable for achieving high surface area and pore volume of the prepared samples in all the three cases of chemical activation.

The effect of holding time on the micropore evolution of H_3PO_4 activated carbon samples were shown in Figure 4.29. Since the contribution of micropores is very high to the total surface area and pore volume, the trends of micropore surface area and micropore volume are also followed the same fashion of total surface area and pore volume. Preferable results of micropore surface area – $1625 \text{ m}^2/\text{g}$ and micropore volume – 0.56 cc/g were obtained at 60 min holding time. Micropores contributed majorly in attaining high surface area and pore volume of ACs prepared at optimum conditions i.e., H_3PO_4 concentration – 30 %, carbonization temperature – $400 \text{ }^\circ\text{C}$, and holding time – 1 h.

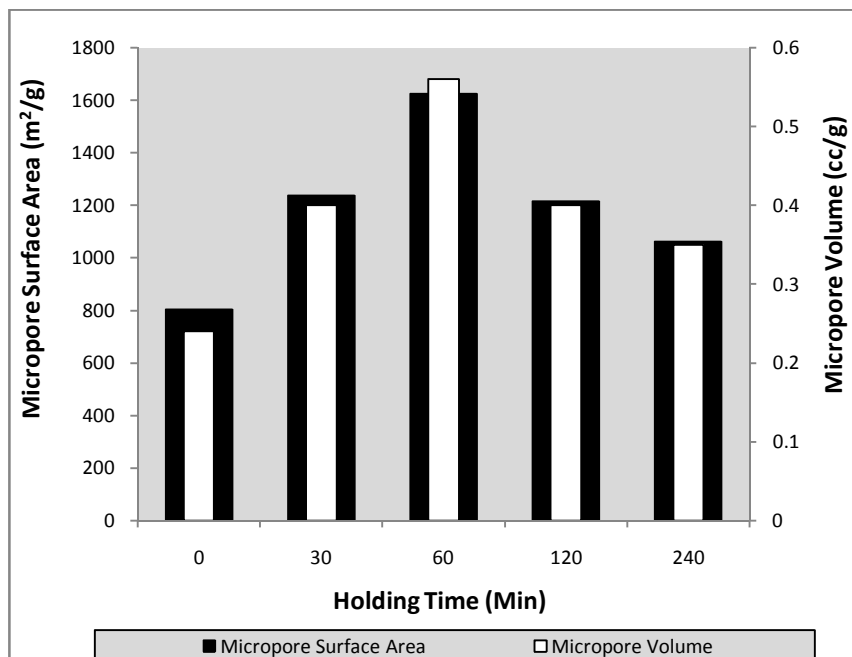


Figure 4.29. Effect of holding time on micropore surface area and micropore volume of AC-PA

Figure 4.30 shows micropore surface area and micropore volume changes in ZnCl_2 activated samples with the change in holding time at final temperature. Activated carbons prepared majorly consist of micropores and their contribution to the total surface area and pore volume is appreciable. Optimum values of micropore surface area and micropore volume obtained for the sample prepared at 60 min of holding time by keeping other parameters at optimal conditions were $1339 \text{ m}^2/\text{g}$ and 0.48 cc/g , respectively. However, by prolonged heating of samples at final temperature the micropore surface area and micropore volume decreased significantly due to the weakening and destruction of porous network.

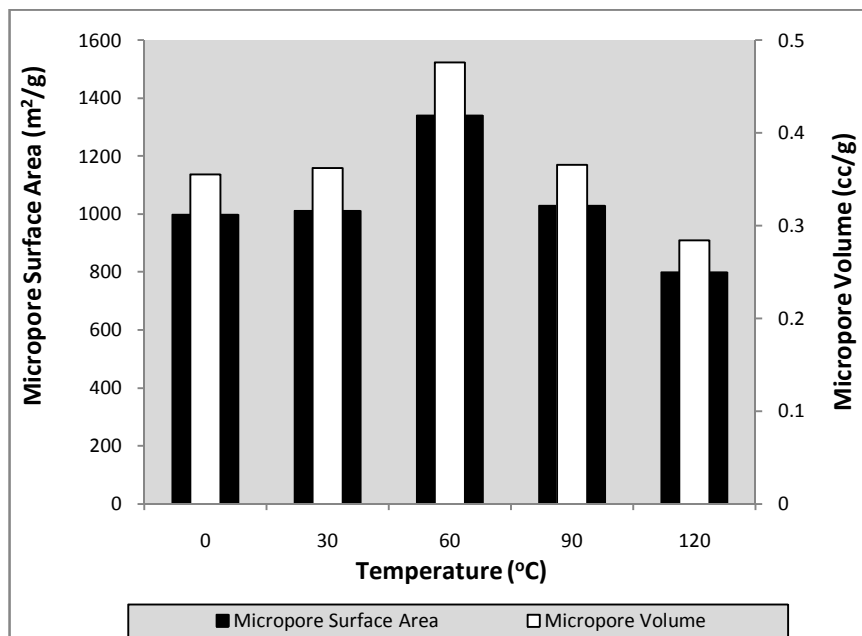


Figure 4.30. Effect of holding time on micropore surface area and micropore volume of AC-ZC

Micropore analysis was carried out by applying DR isotherm. Micropore surface area (S_{mi}) and micropore volume (V_{mi}) of the samples prepared by KOH activation with different holding times were shown in Figure 4.31. Micropores comprise 97 % of the total surface area and pore volume of the samples. The maximum values of S_{mi} and V_{mi} obtained are 924 m²/g and 0.32 cc/g, respectively at 60 min of holding time. It is also observed that prolonged heating caused the micropores to widen and thus resulted in decrement in micropore surface area and micropore volume.

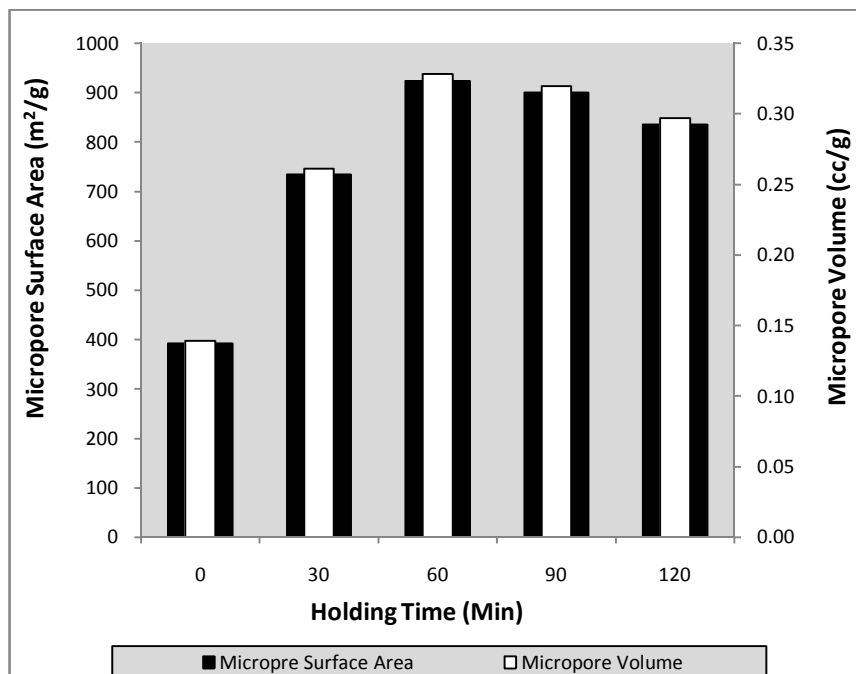


Figure 4.31. Effect of holding time on micropore surface area and micropore volume of AC-PH

4.4. Optimum Conditions and Comparison

The optimum preparation conditions investigated for various parameters and the porous characteristics of ACs prepared at these conditions were presented in [Table 4.3](#).

Table 4.3. Optimum preparation conditions for ACs and their porous characteristics

AC type	Impregnation	Carbonization temperature (°C)	Holding time (min)	S_T	V_T	S_{mi}	V_{mi}	$(V_{mi}/V_T) \times 100$	D_{avg} (nm)
AC-PA	30 %	400	60	1657	0.58	1625	0.56	98	1.68
AC-ZC	2.0	500	60	1488	0.53	1339	0.48	91	1.69
AC-PH	2.0	600	60	937	0.33	924	0.32	97	1.54

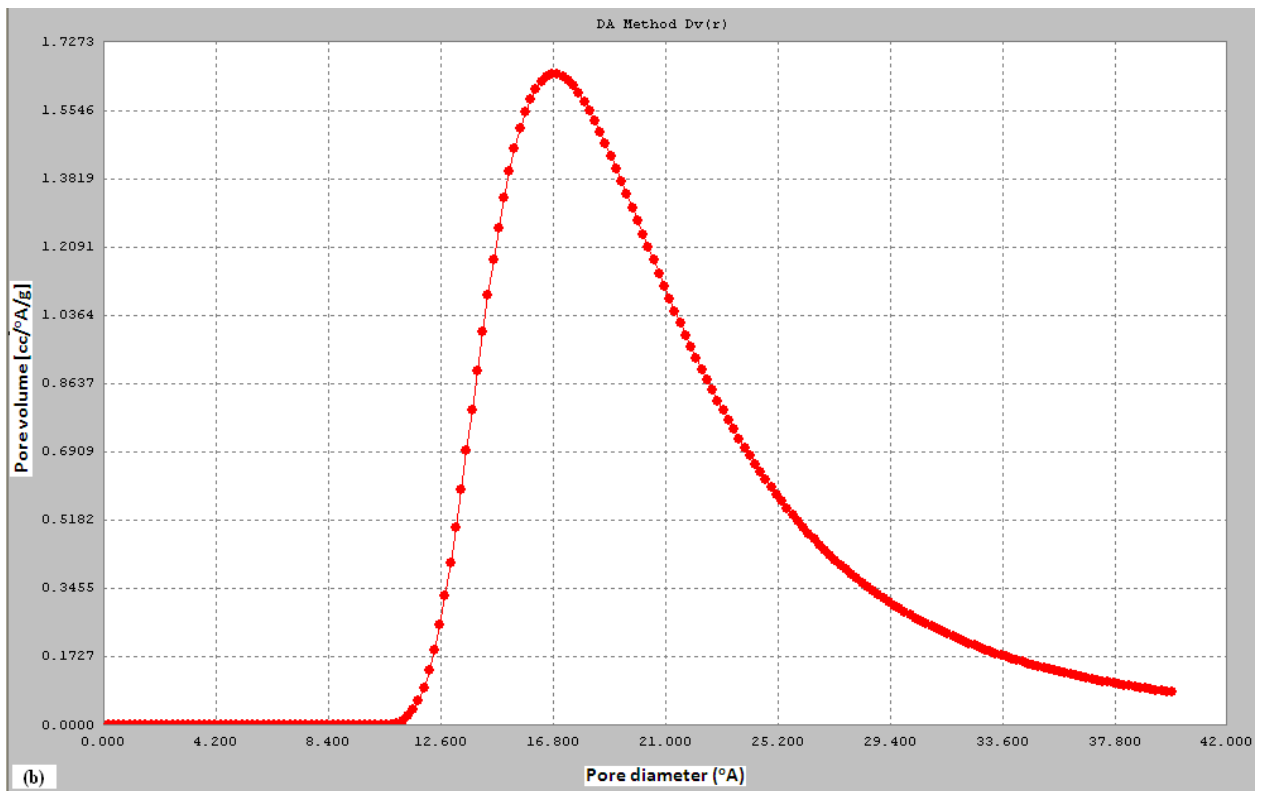
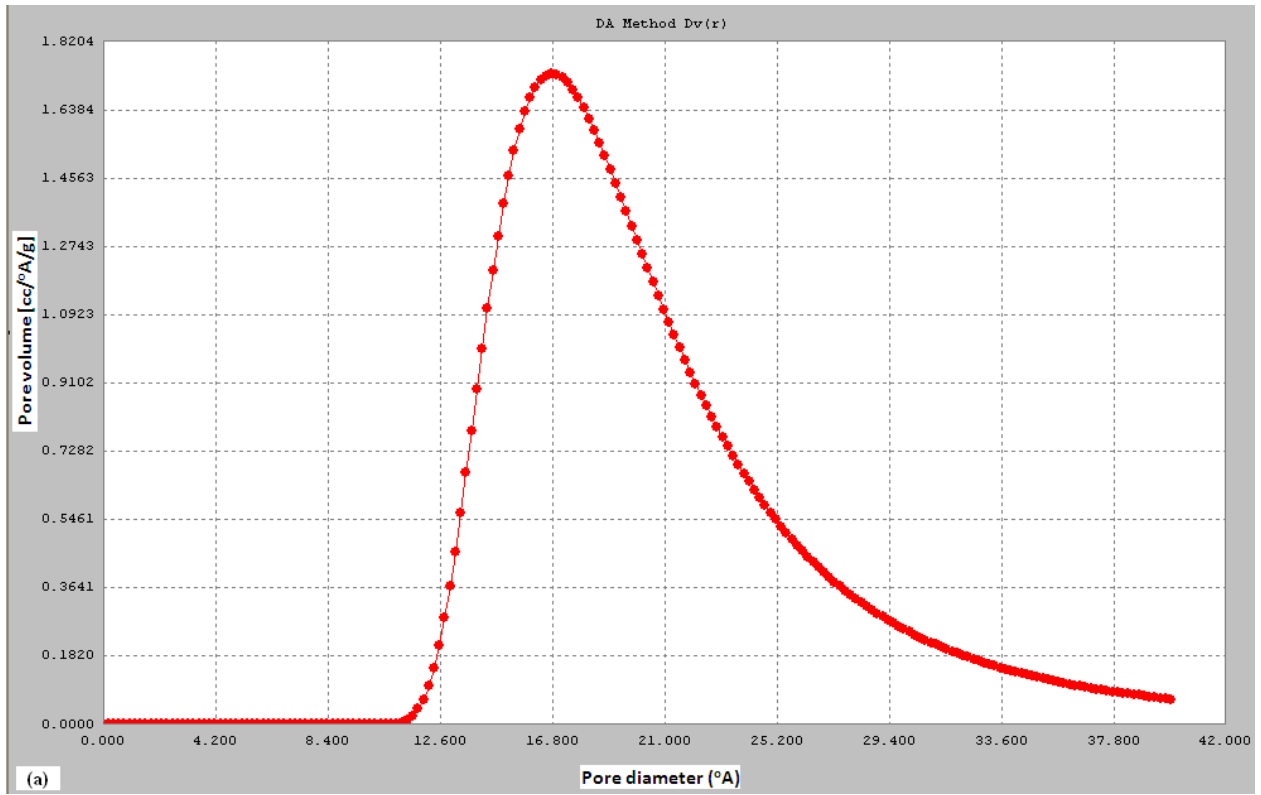
The porous characteristics of various activated carbons prepared from different precursors by activating with H_3PO_4 , $ZnCl_2$, and KOH were compared in the [Table 4.4](#).

Table 4.4. Comparison of porous characteristics of prepared ACs with ACs prepared from different precursors

Chemical agent	Precursor	Surface Area (m ² /g)	Pore volume (cc/g)	Source
H ₃ PO ₄	Hemp fibers	1355	1.250	Rosas et al., 2009
	Ploy(p-phenylene terephthalamide)	1774	0.830	Castro-Muniz et al., 2011
	Grain sorghum	528	0.197	Diao et al., 2002
	Rice straw	786	1.050	Fierro et al., 2010
	Birch wood	1165	1.296	Klijanienko et al., 2008
	Sewage sludge	377	0.243	Wang et al., 2011
	Chestnut wood	783	0.288	Gomez-Serrano et al., 2005
	Eucalyptus bark	1239	1.109	Patnukao and Pavasant, 2008
	Bael fruit shell	1657	0.580	Present study
ZnCl ₂	Apricot stones	728	0.327	Youssef et al., 2005
	Tamarind wood	1322	1.042	Achrya et al., 2009
	Hazelnut bagasse	1489	0.932	Demiral et al., 2008
	Pistachio nut shell	1635	0.832	Lua and Yang, 2005
	Rice husk	750	0.380	Kalderis et al., 2008
	Enteromorpha prolifera	1416	0.90	Li et al., 2010
	Bael fruit shell	1488	0.53	Present study
KOH	Corn cob hulls	1516	1.082	Wu et al., 2011
	Olive stones	1090	0.38	Ubago-Perez et al., 2006
	Cotton stalks	621	0.38	Deng et al., 2010
	Rice straw	866	0.57	Basta et al., 2009
	Pineapple peel	1006	0.59	Foo and Hameed, 2011
Bael fruit shell	937	0.33	Present study	

4.5. Pore Size Distribution (PSD)

The pore size distribution (PSD) of the ACs prepared at optimum conditions was determined by the Dubinin-Astakhov (DA) equation and presented in Figure 4.32. From the figure it was confirmed that the adsorbents contain micropores (< 2 nm) with the average diameter of 1.68, 1.69 and 1.54 nm for AC-PA, AC-ZC and AC-PH, respectively.



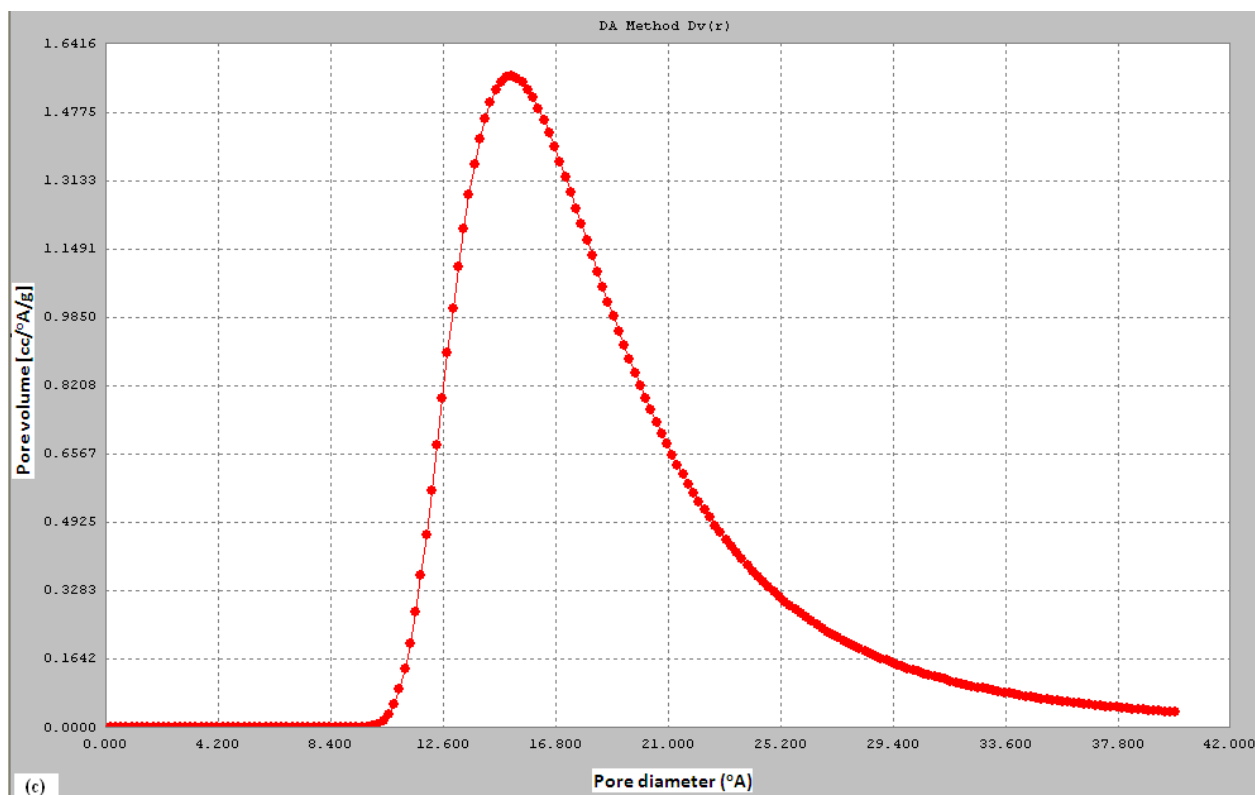


Figure 4.32. Pore size distribution of the prepared ACs (a) AC-PA (b) AC-ZC and (c) AC-PH

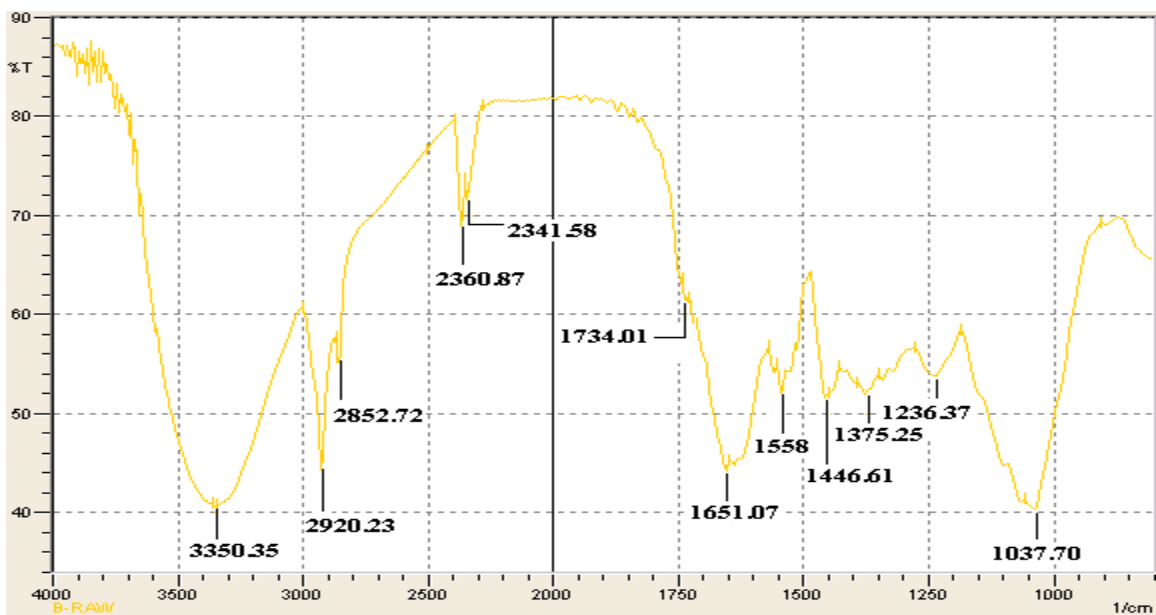
4.6. Fourier Transform Infrared spectroscopy (FTIR)

The surface chemistry of the raw bael fruit shell was compared with the H_3PO_4 activated sample in Figure 4.33. Raw material consists of several functional groups which include amines, hydroxyl groups, aldehydes, various unsaturated hydrocarbons, carbonyl compounds, phosphates and sulfonates (Olivares-Marin et al., 2006; Phan et al., 2006; Nabais et al., 2008). Whereas, the spectrum of prepared AC is very simple consisting of considerable number of peaks or functional groups. The various functional groups of IR spectrum of AC-PA were described in Chapter 5. The complete interpretation of IR spectra was carried out by Coates (2000).

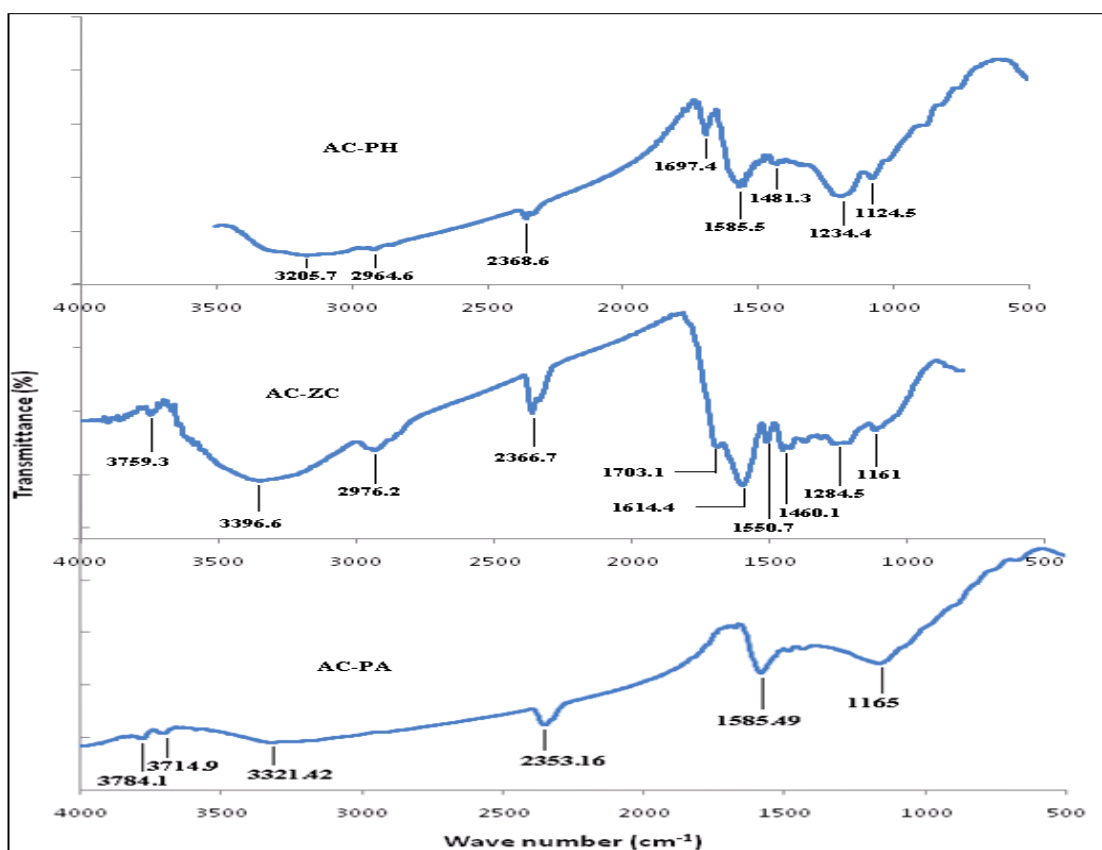
In case of raw material, the broad peak observed at 3350.35 cm^{-1} is due to the presence of hydroxyl groups (O – H stretch) on the surface. The sharp peaks observed at 2920.23 cm^{-1} and 2852.72 cm^{-1} are due to the asymmetric and symmetric stretchings of methylene (C – H) group, respectively. Bands due to the presence of silane (Si – H) groups can be observed in the range $2100 - 2360\text{ cm}^{-1}$. The weak bands observed between $1350 - 1260\text{ cm}^{-1}$ might be due to the existence of in-plane bending of primary or secondary OH groups or due to the presence C – N

stretch of aromatic amines. The existence of phenol (C – O stretch) was confirmed by the peak obtained at 1236.37 cm^{-1} . Peaks found at 1651.07 cm^{-1} and 1037.70 cm^{-1} were due to primary amine groups. Band at 1651.07 cm^{-1} is due to the N – H bend and at 1037.70 cm^{-1} is due to the C – N stretch of phenols. The N – H bend of the secondary amines was observed at 1558 cm^{-1} . The sharp peaks at 1375.25 and 1446.61 were attributed to the C – H bending vibrations in methane and methylene groups, respectively. Various weak bands observed throughout the spectrum consist of various functional groups such as nitrogen-oxy compounds ($1560 - 1540\text{ cm}^{-1}/ 1380 - 1350\text{ cm}^{-1}$), phosphorus-oxy compounds ($1350 - 1250\text{ cm}^{-1}$ and $1050 - 990\text{ cm}^{-1}$), sulfur-oxy compounds ($1335 - 1300\text{ cm}^{-1}$ and $1200 - 1100\text{ cm}^{-1}$) and silicon-oxy compounds ($1055 - 1020\text{ cm}^{-1}$).

The FTIR analysis of prepared ACs reveals a simple spectrum in case of AC-PA compared to AC-ZC and AC-PH. The broad peaks at around 3321 , 3396 and 3205 cm^{-1} are assigned to presence of OH groups (adsorbed moisture) on surface. The C – H stretchings observed in the raw material were disappeared in case of AC-PA whereas, in case of AC-ZC and AC-PH these stretchings are shifted to higher wave number. Silane (Si – H) groups in the raw material as well as prepared ACs were confirmed by the peak at around 2360 cm^{-1} . A little shift of the bands corresponding to silane groups was observed in prepared ACs. The presence of amine groups are confirmed by the peaks observed in the range $1650 - 1550\text{ cm}^{-1}$ and $1190 - 1130\text{ cm}^{-1}$ and are due to the N – H and C – N stretchings, respectively.



(a)

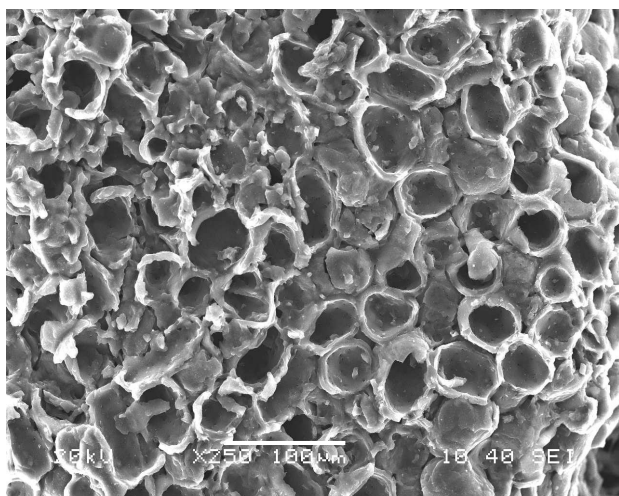


(b)

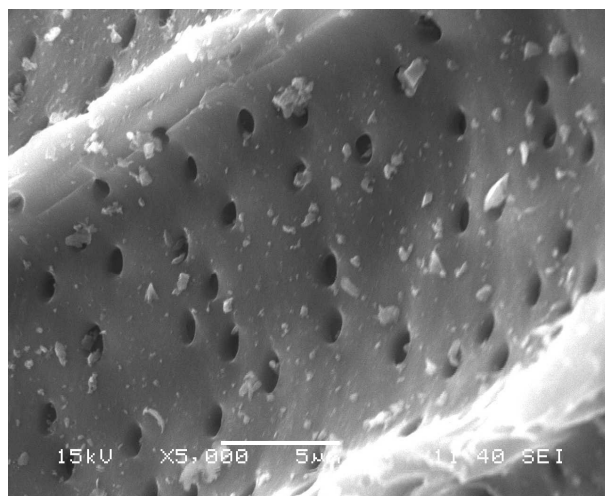
Figure 4.33. FTIR analysis of (a) raw material and (b) AC-PA, AC-ZC and AC-PH

4.7. Scanning Electron Microscope (SEM) and Transmission Electron Microscope (TEM) analysis

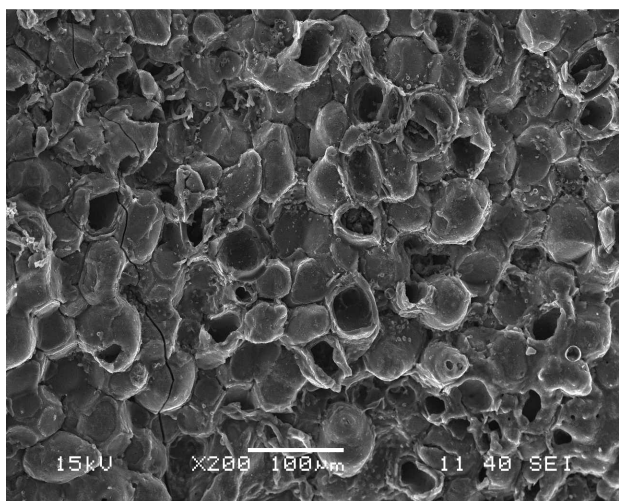
The prepared activated carbons were examined by Scanning Electron Microscope (SEM) to analyze the surface of the adsorbents. SEM micrographs of the chemically activated carbons by H_3PO_4 , $ZnCl_2$, and KOH were presented in Figure 4.34. In all three cases, well-developed porous surface was observed at higher magnification. The pores observed from SEM images are having diameter in micrometer (μm) range. These pores are considered as channels to the microporous network. From the figure, it can be observed that all the adsorbents have rough texture with heterogeneous surface and a variety of randomly distributed pore size.



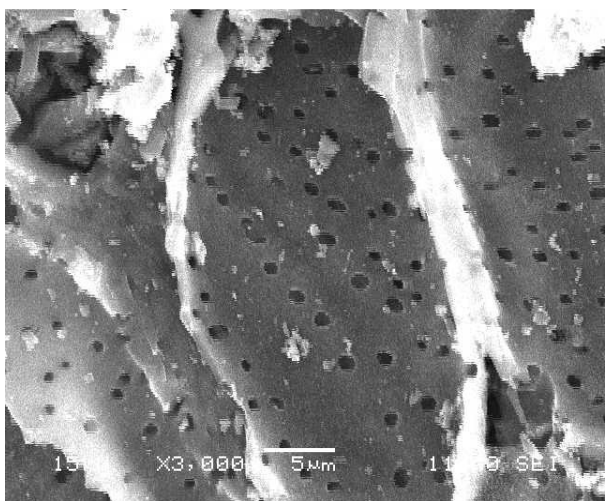
(a.1)



(a.2)



(b.1)



(b.2)

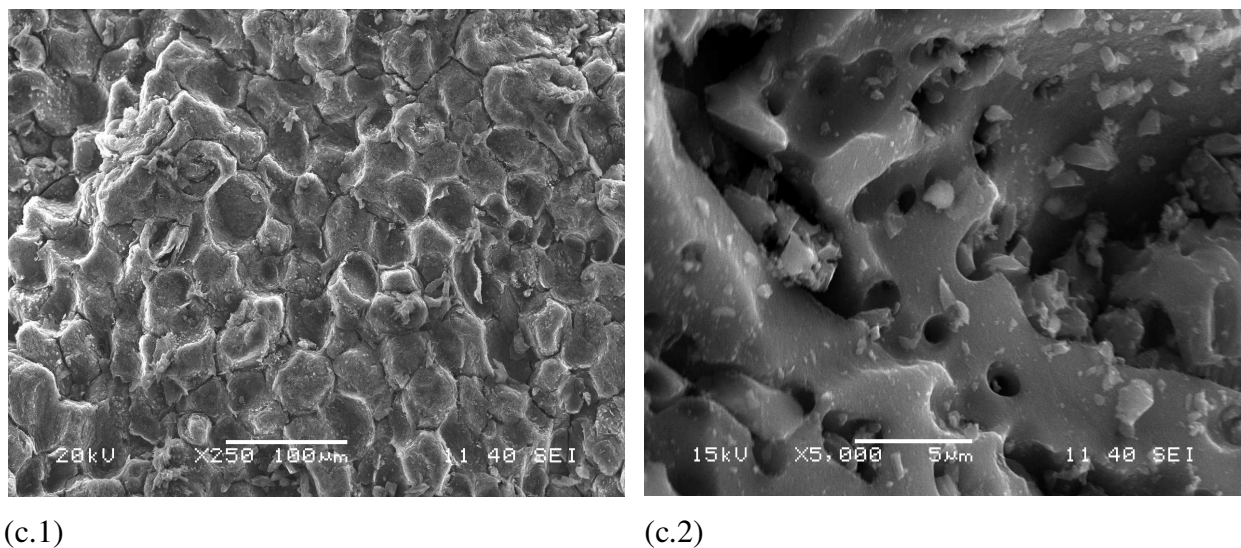
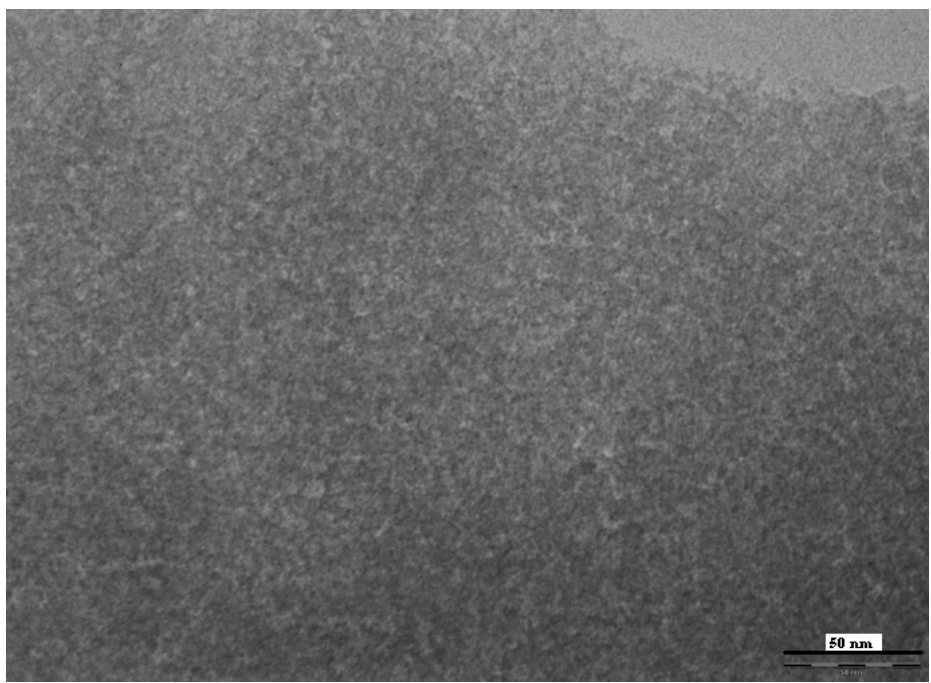
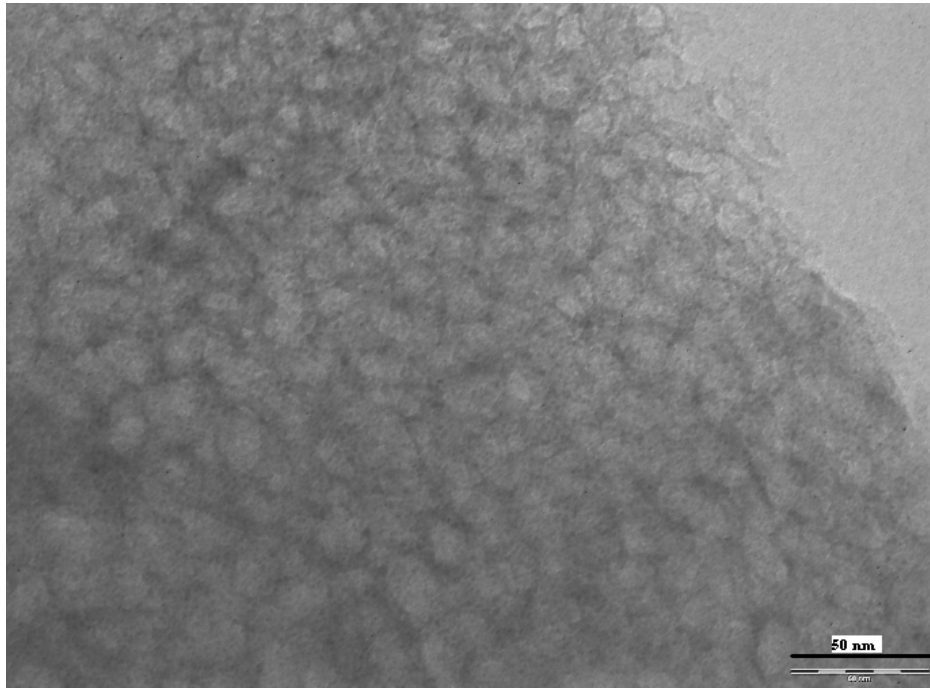


Figure 4.34. SEM images of the prepared ACs (a) AC-PA (b) AC-ZC and (c) AC-PH

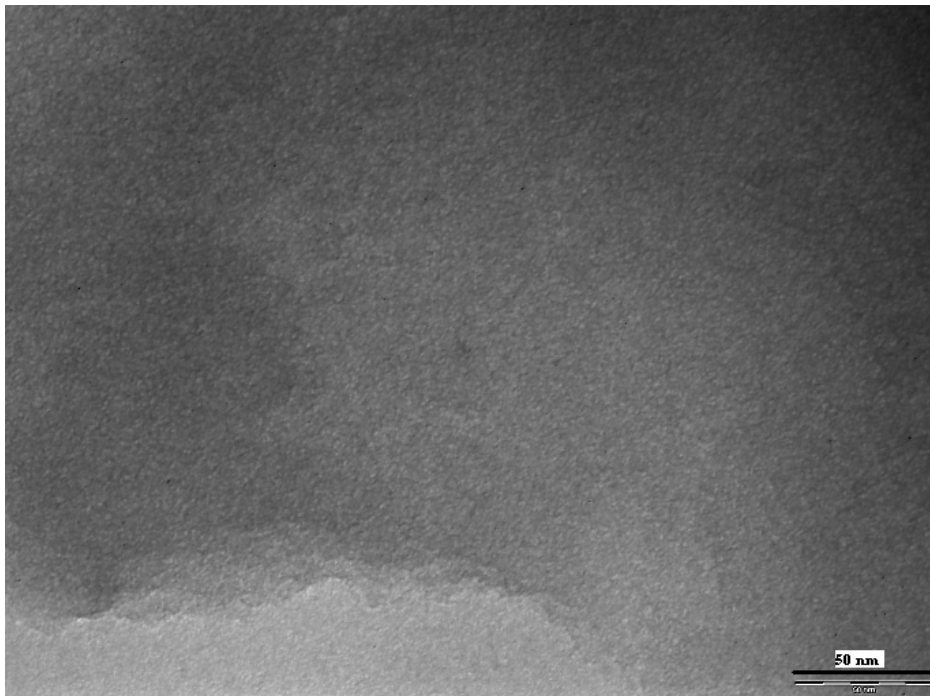
As the prepared carbons are of highly microporous (pores having width in nanometers) in nature, ACs prepared at optimum conditions by different chemical activations were characterized by Transmission Electron Microscope (TEM) to observe the internal microporous network. Figure 4.35 shows the TEM images of the chemically activated ACs. Analytical electron microscopy studies of activated carbons were reported by various authors (Ishizaki et al., 1988; Williams and Reed, 2006). From the figure, micropores of uniform pore size were observed clearly in all the cases.



(a)



(b)



(c)

Figure 4.35. TEM images of the prepared ACs (a) AC-PA (b) AC-ZC and (c) AC-PH

4.8. X – Ray Diffraction spectroscopy (XRD)

Franklin, on the basis of XRD studies, classified activated carbons into two types, based on their graphitizing ability (Franklin, 1951). The non-graphitizing carbons are hard and show a well-developed microporous structure due to the formation of strong cross-linking between the neighboring randomly oriented elementary crystallites. Whereas, graphitizing carbons has weak cross-linking and had a less developed porous structure (Bansal et al., 1988).

Figure 4.36 shows the X-ray diffraction profiles of the ACs prepared at optimum conditions. The AC samples with broad peaks and absence of sharp peak that revealed predominantly amorphous structure, which is an advantageous property for well-defined porous adsorbents (Tongpoothorn et al., 2011). Broad peaks found at around 24° for all the samples confirm that the samples are non-graphitized and can have high microporous structure (Zhao et al., 2009) which was confirmed by the gas adsorption isotherms. The other sharp peaks observed in case of AC-ZC confirmed the presence of Zn metal by interacting with other functional groups. The sharp peaks observed at 31.71° , 34.29° , 36.15° and 47.39° are may be due to the presence of zinc p – benzoquinone dioxime (32-1985 from JCPDS PDF number) and the peaks found at 56.49, 62.79, 67.85 and 68.97 are due to the presence of zinc guanidinium sulfate (76-0798 from JCPDS PDF number).

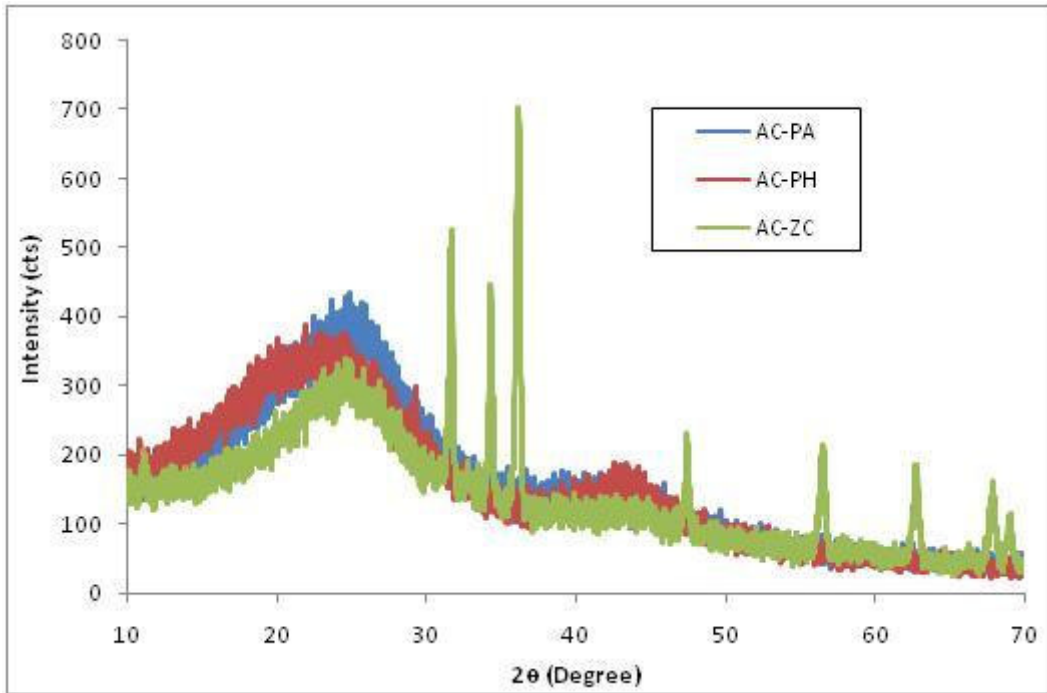


Figure 4.36. XRD patterns of the prepared ACs

Adsorption of Chromium(VI) on Activated Carbon

The demand for activated carbon (AC) depends on its suitability in various applications. This chapter emphasizes on proper utilization of AC to remove heavy metals, typically for Cr(VI).

5.0. Summary

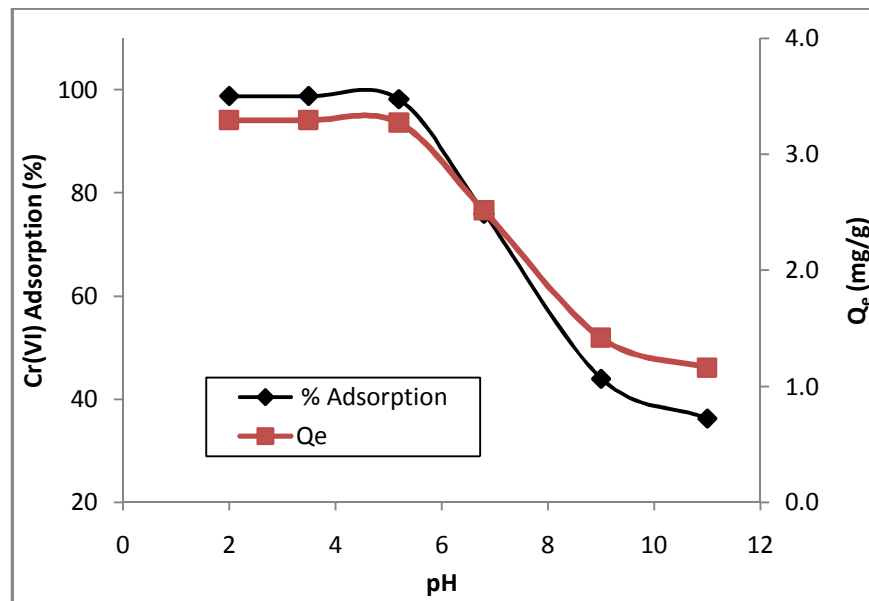
Application of activated carbon in Cr(VI) adsorption is significantly influenced by its method of preparation. Chemical activation method using different chemical activating agents such as H_3PO_4 , ZnCl_2 and KOH was employed for the preparation of AC. The adsorbents prepared by H_3PO_4 , ZnCl_2 and KOH activations are denoted as AC-PA, AC-ZC and AC-PH, respectively. The influence of various process parameters such as contact time, initial metal concentration, pH, adsorbent dose, and temperature on adsorption of Cr(VI) on prepared activated carbons were investigated. Distribution of Cr(VI) adsorption data between solid and liquid phase was expressed through different isotherm models such as Freundlich, Langmuir, Temkin and DR isotherms. The experimental kinetic data were fitted to pseudo-first order and pseudo-second order models. Intra particle diffusion and Boyd models were used to evaluate the rate controlling step in the process of Cr(VI) adsorption. Thermodynamic parameters were estimated to determine the nature and spontaneity of adsorption process.

The porous characteristics and Cr(VI) removal efficiencies of prepared AC by H_3PO_4 activation and commercial AC were compared and the spent AC-PA was regenerated by simple and feasible techniques.

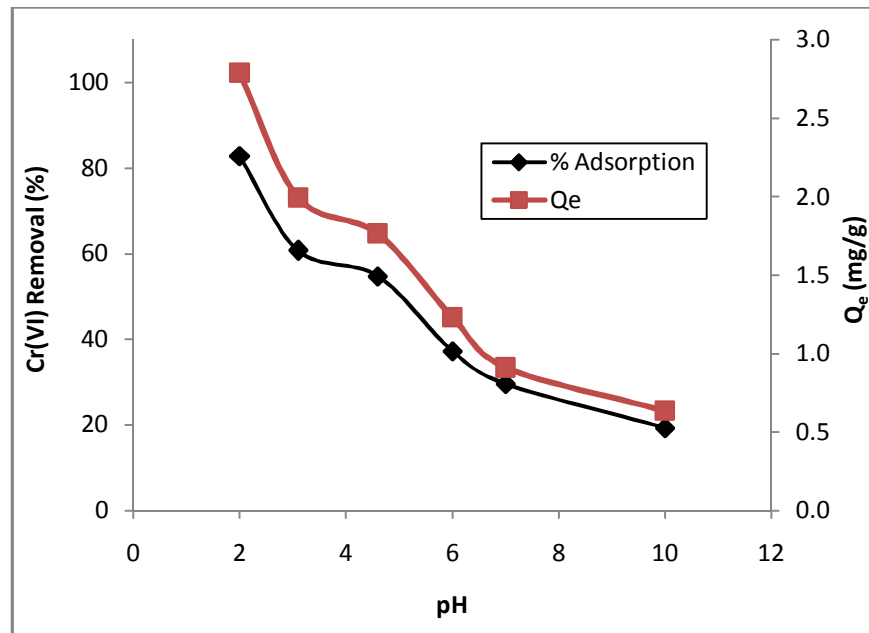
5.1. Effect of Process Parameters

5.1.1. Effect of pH

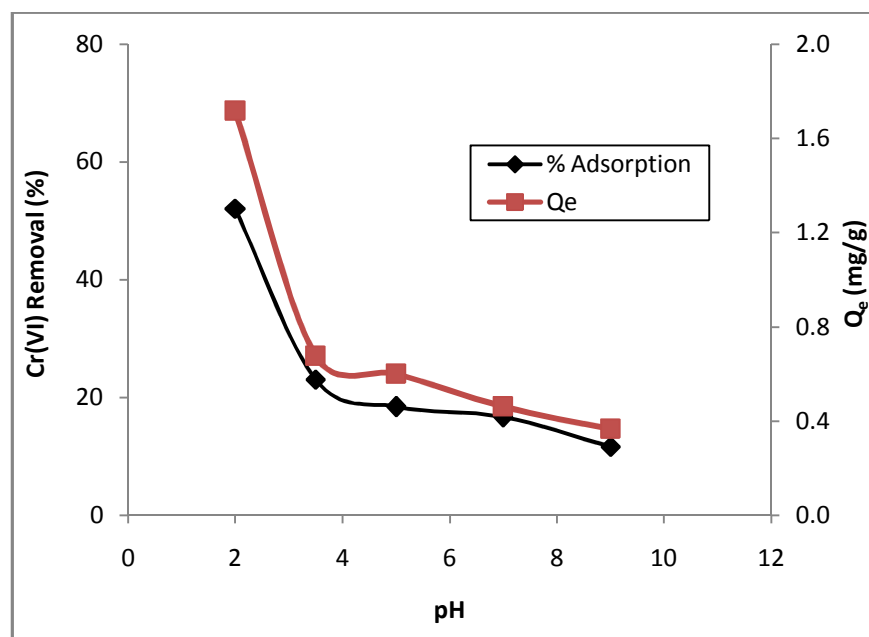
Significance of various process parameters on adsorption of pollutants from aqueous phase has been well established. Solution pH is one of the important process parameters that significantly influences the adsorption of Cr(VI) on adsorbent (Acharya et al., 2009; Tang et al., 2009; Karthikeyan et al., 2005; Zhang et al., 2010). ACs prepared by various chemical activations were employed for Cr(VI) removal at different pH values (2.0 – 11.0). The preliminary experiments were performed at definite experimental conditions (initial chromium concentration – 10.0 mg/L, adsorbent dose – 3.0 g/L, contact time – 3.0 h, and temperature – 30 °C). Figure 5.1 shows the higher removal of Cr(VI) at acidic pH. It is true for ACs prepared from Bael fruit shell at different conditions and AC-PA showed high Cr(VI) removal capacity as compared to the other two ACs. It is evident from the figure that the percentage adsorption is higher at acidic pH (2.0 – 5.0), reaching maximum of about 99 %. But it decreased gradually with the increase in pH. The adsorption capacity of AC-PA for Cr(VI) at pH 2.0 was 3.30 mg/g, which was reduced to 1.15 mg/g with increase of pH to 11.0. Similarly, for AC-ZC and AC-PH the maximum adsorption capacities observed at pH 2.0 (2.79 mg/g and 1.72 mg/g, respectively), which were decreased randomly with increase of pH. The results obtained are in close agreement with previously reported studies (Aggarwal et al., 1999; Barkat et al., 2009; Natale et al., 2007). Similarly AC-ZC witnessed maximum Cr(VI) reduction (82.73 %) at pH 2.0. Significant change in Cr(VI) removal was observed in pH range 3.0 to 6.0 using AC-ZC. However, this change was negligible at higher pH. At pH 2.0, AC-PH showed maximum (52.02 %) adsorption for Cr(VI). Significant decrease in percentage adsorption occurred with change of pH from 2.0 to 3.5.



(a)



(b)



(c)

Figure 5.1. Effect of pH on chromium(VI) removal by different ACs (a) AC-PA (b) AC-ZC and (c) AC-PH (Initial chromium concentration – 10 mg/L, adsorbent dose – 3.0 g/L, contact time – 3.0 h, and temperature – 30 °C)

The dependence of Cr(VI) adsorption on pH can largely be related to type and ionic state of the functional groups present on the surface of adsorbent and as well as the metal chemistry in the solution. High adsorption of Cr(VI) at low pH can be attributed to availability of Cr(VI) in different forms and the surface groups of the adsorbent. At acidic pH the predominant Cr(VI) species are HCrO_4^- and $\text{Cr}_2\text{O}_7^{2-}$ and above neutral pH only CrO_4^{2-} is stable (Palmer and Puls, 2004). When the pH of the solution decreases to the range 2.0 – 6.0, the equilibrium shifts to dichromate according to the overall equilibrium as follows:



Under acidic conditions, the surface of the adsorbent becomes highly protonated and favors the adsorption of Cr(VI) in the anionic form (Palmer and Puls, 2004; Selomulya et al., 1999). With the increase of pH, the degree of protonation of the surface decreases gradually and that results in low adsorption of Cr(VI). Moreover, as pH increases there is competition between OH^- and CrO_4^{2-} ions, the former being the dominant species at higher pH. The reduction in net positive surface potential of adsorbent results in the weakening of electrostatic forces between Cr(VI) species and adsorbent, which ultimately leads to reduced adsorption capacity.

Adsorption trends of Cr(VI) on activated carbons such as AC-PA, AC-ZC and AC-PH were shown in Figures 5.2, 5.3 and 5.4, respectively. ACs prepared using different activating agents attained equilibrium at different contact times. AC-PA, AC-ZC, and AC-PH were attained equilibrium at 120, 180 and 240 min, respectively. Variation in Cr(VI) adsorption on AC-PA was observed from 98.74 to 75.93 % with increase in pH from 2.0 to 6.8. Adsorption of Cr(VI) on AC-ZC and AC-PH decreased from 82.30 to 30.53 % and 38.16 to 16.65 % when pH rises from 2.0 to 6.8. Other adsorbents such as activated neem (*Azadirachta Indica*) leaf, coconut shell activated carbon, activated char coal and beech saw dust witnessed maximum uptake of Cr(VI) at lower pH (Babu and Gupta, 2007; Choudhari et al., 2011; Mor et al., 2007; Owlad et al., 2010).

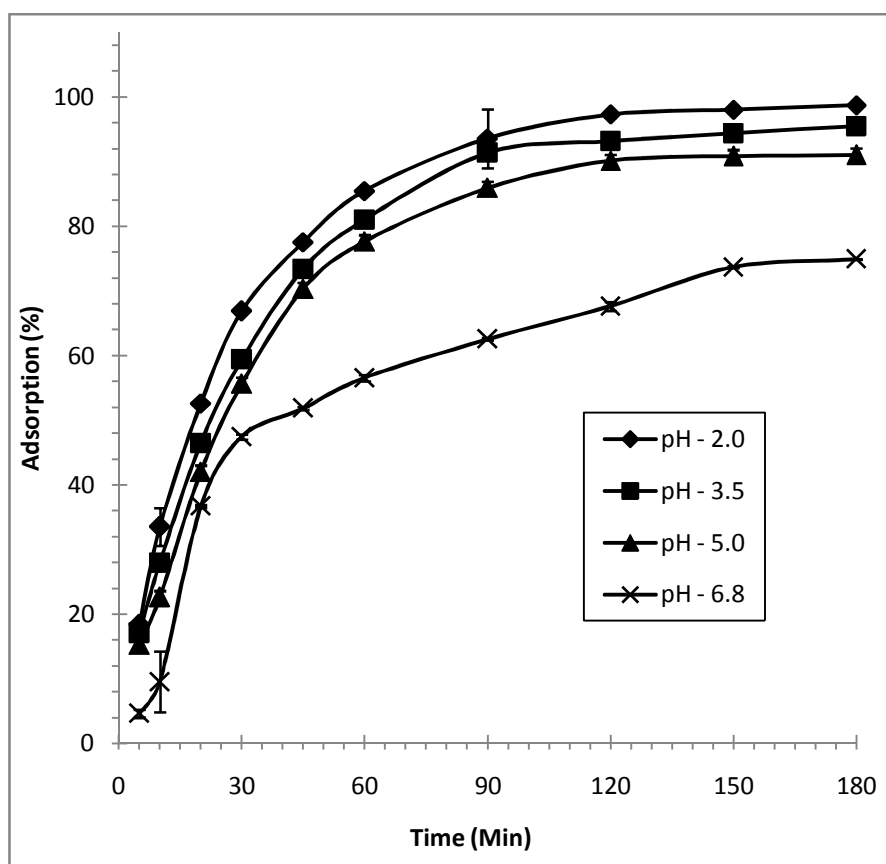


Figure 5.2. Effect of pH on the percentage adsorption of Cr(VI) from aqueous solution by AC-PA (Initial chromium concentration – 10 mg/L, adsorbent dose – 3.0 g/L, contact time – 3.0 h, and temperature – 30 °C)

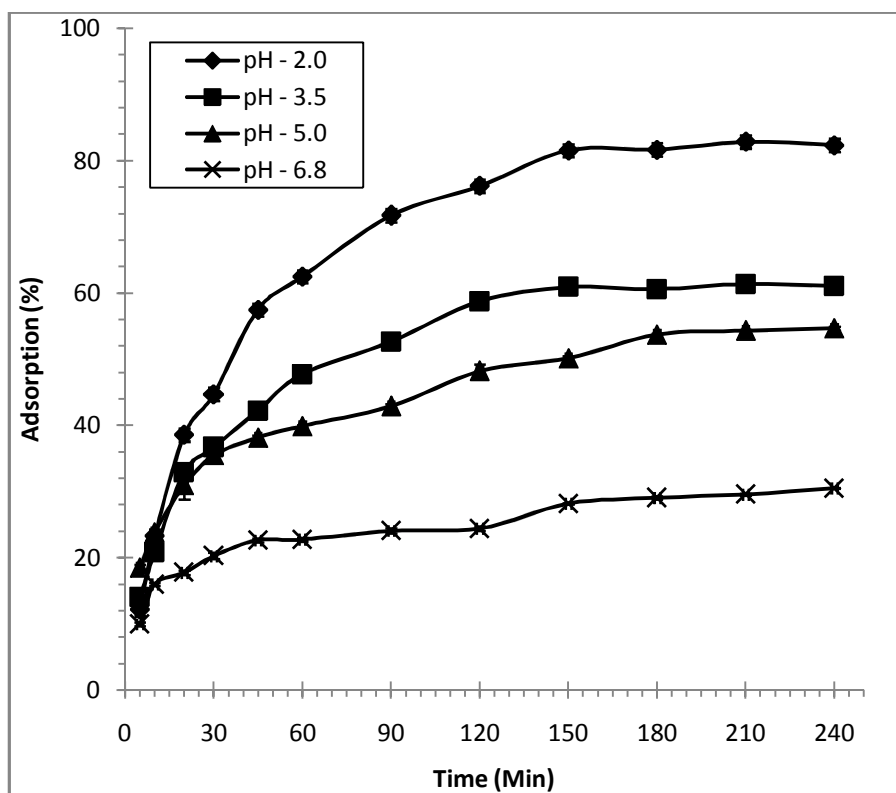


Figure 5.3. Effect of pH on the percentage adsorption of Cr(VI) from aqueous solution by AC-ZC (Initial chromium concentration – 10 mg/L, adsorbent dose – 3.0 g/L, contact time – 3.0 h, and temperature – 30 °C)

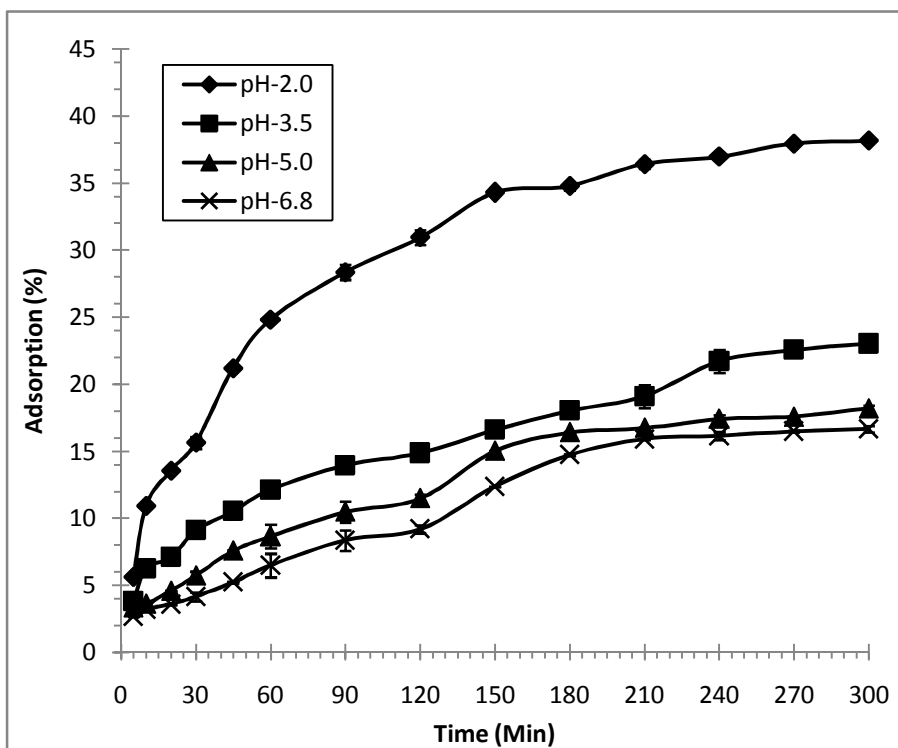


Figure 5.4. Effect of pH on the percentage adsorption of Cr(VI) from aqueous solution by AC-PH (Initial chromium concentration – 10 mg/L, adsorbent dose – 3.0 g/L, contact time – 3.0 h, and temperature – 30 °C)

Activated carbons are considered as amphoteric solids due to the existence of variety of surface functional groups (Song et al., 2010). Therefore, the isoelectric point (IEP) of the ACs can be evaluated at pH value where the zeta potential is zero. IEP is used to qualitatively assess the polarity of the adsorbent surface charge (Li et al., 2001). At $\text{pH} < \text{IEP}$, the adsorbent has positive surface charge and can act as anion exchanger. While at $\text{pH} > \text{IEP}$, the surface charge of the adsorbent is negative, which benefits for cations adsorption. The IEP of AC-PA is 4.2, while it is less than 2.0 in case of AC-ZC ($\text{pH} = 1.9$) and AC-PH ($\text{pH} = 1.3$). Aggarwal et al (1999) reported the formation of oxyanions such as $\text{Cr}_2\text{O}_7^{2-}$ and CrO_4^{2-} in aqueous solution at pH 2.0 and 7.5, respectively. With the increase of solution pH, the repulsion between negatively charged adsorbent surface and Cr(VI) oxyanions increases. The trends of zeta potential for various prepared ACs (Figure 5.5) suggested that AC-PA might have more tendency for Cr(VI) cations as compared to other ACs even at high pH. The high zeta potential values with increasing pH are attributed to the presence of oxygen surface functional groups on AC surface. This is in agreement with the experimental observations showing better adsorption of AC-PA.

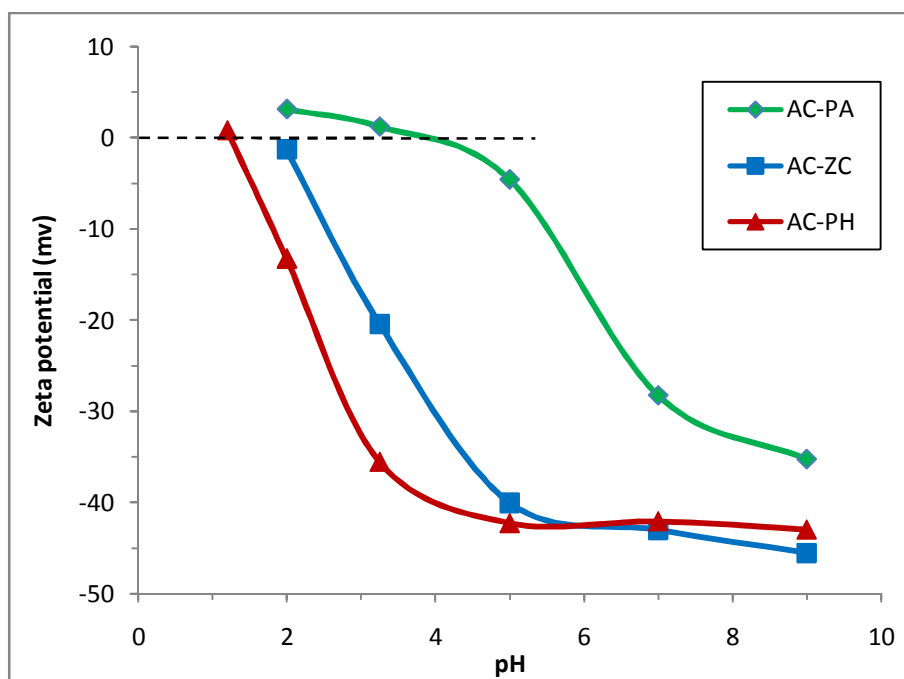
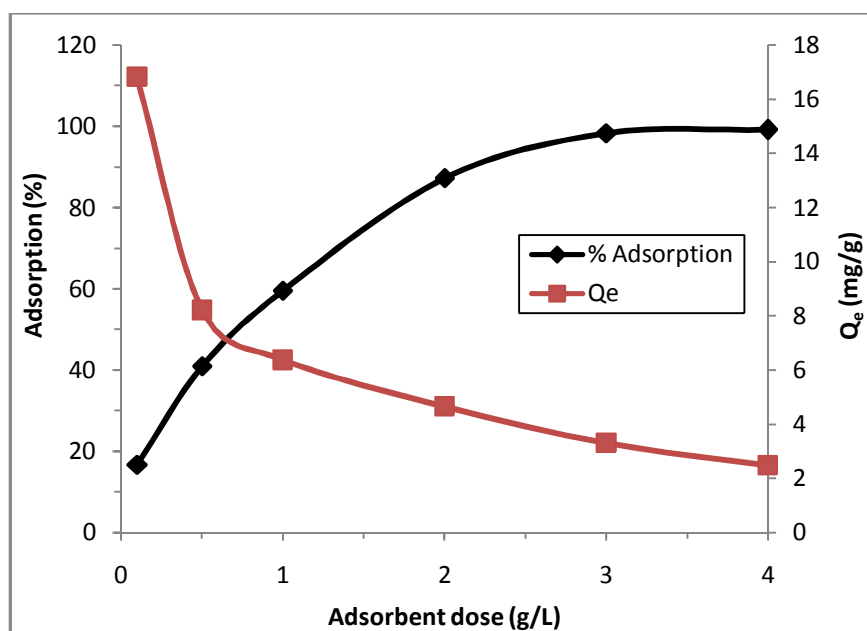


Figure 5.5. Surface charge distribution for prepared ACs

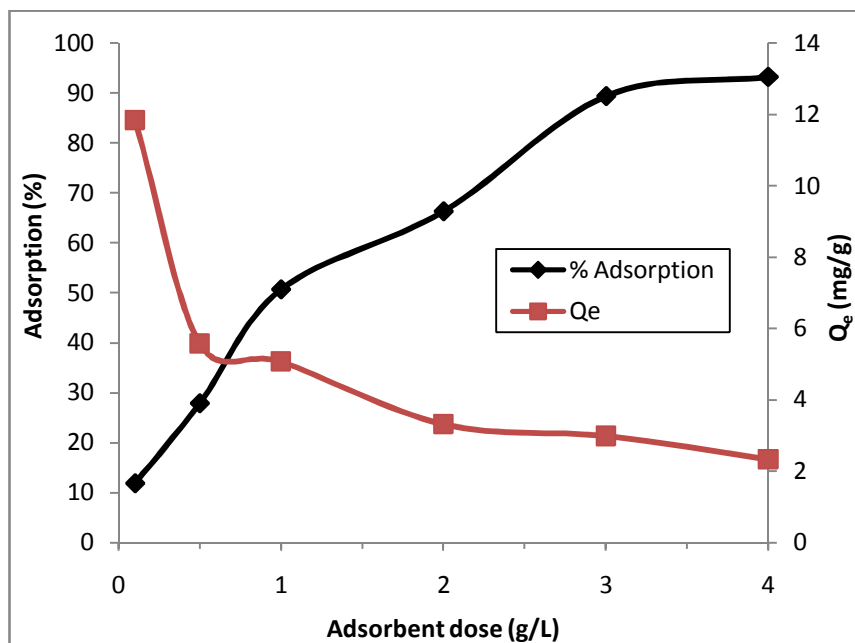
5.1.2. Effect of Adsorbent Dose

The effect of adsorbent dose on adsorption of Cr(VI) using AC-PA, AC-ZC and AC-PH was illustrated in Figure 5.6. Different doses of adsorbents ranging from 1.0 – 4.0 g/L were considered and other process parameters were maintained constant ($\text{pH} = 3.5$ for AC-PA and 2.0

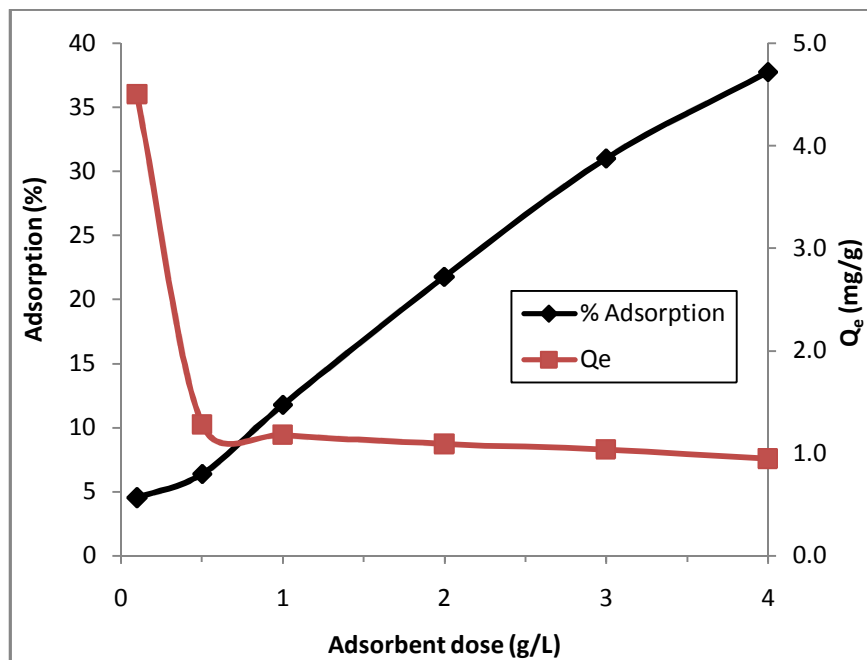
for AC-ZC and AC-PH, Cr(VI) concentration – 10.0 mg/L, contact time – 3.0 h, and temperature – 30 °C). The maximum percentage removal of Cr(VI) was observed for AC-PA as compared to the other two types of ACs. Maximum Cr(VI) adsorption was achieved using 3.0 g/L of adsorbent dose for both AC-PA and AC-ZC within 180 min. AC-PH evidenced less adsorption of Cr(VI) within the studied range (1.0 – 4.0 g/L) of adsorbent dose comparing to other ACs. The adsorption capacities rapidly decreased with increase of adsorbent dose from 0.25 to 0.5 in all the cases and then the decrement is gradual with further increase of adsorbent dose to 4.0 g/L. For AC-PA, the adsorption capacity (Q_e) decreased from 16.8 mg/g to 2.5 mg/g with the increase of adsorbent dose from 0.25 g/L to 4.0 g/L. In case of AC-ZC and AC-PA, Q_e values decreased from 11.8 mg/g to 2.3 mg/g and 4.5 mg/g to 0.9 mg/g, respectively with increase of adsorbent dose. The low adsorption percentage can be ascribed to the fact that all the adsorbents have a limited number of active sites that would have achieved saturation above a certain adsorbate concentration.



(a)



(b)



(c)

Figure 5.6. Effect of adsorbent dose on Cr(VI) adsorption by different ACs (a) AC-PA (b) AC-ZC and (c) AC-PH (pH-3.5 for AC-PA and 2.0 for AC-ZC and AC-PH, Cr(VI) concentration – 10.0 mg/L, contact time – 3.0 h, and temperature – 30 °C)

Figures 5.7, 5.8, and 5.9 show Cr(VI) adsorption on AC-PA, AC-ZC, and AC-PH, respectively at varying adsorbent doses. A gradual increase in Cr(VI) adsorption percentage is observed for all the samples with increasing adsorbent dose. AC-PA exhibits high adsorption rate

and achieved maximum adsorption of 98.33 % at 4.0 g/L of adsorbent dose. The gradual increase in Cr(VI) removal with increase in adsorbent dose is due to available adsorption sites. A negligible change was observed in percentage adsorption of Cr(VI) with increase in adsorbent dose beyond 3.0 g/L for AC-PA and AC-ZC. However, AC-PH continues to show increasing trend and the maximum adsorption (37.77 %) can be observed at 4.0 g/L. This trend is expected because as the adsorbent dose increases the number of adsorbent particles increases and hence more Cr(VI) ions attach to the adsorption sites (Barkat et al., 2007; Dubey and Gopal, 2007; Mohanty et al., 2005; Ranganathan, 2000). At a particular adsorbent dose the percentage adsorption reaches equilibrium by maintaining constant initial Cr(VI) concentration. The adsorbent dose of 3.0 g/L was considered as optimum.

AC-PA demonstrated Cr(VI) adsorption in two stages. In the first stage, instantaneous adsorption can be observed within 60 min which can be clearly observed at high adsorbent dose (3.0 g/L). The rate of Cr(VI) adsorption gradually changed beyond 80 min with negligible changes. The intensity of adsorption is gradual at low adsorbent dose (1.0 g/L).

Similarly, the intensity of adsorption became more pronounced at high adsorbent dose of AC-ZC. At 1.0 g/L, the rate of adsorption was very slow and achieved equilibrium in 180 min showing minor changes to percentage adsorption observed at 60 min. It is due to the fact that at 10 mg/L of initial Cr(VI) concentration, the available active sites on 1.0 g/L of adsorbent were insufficient. Thus, the sites are filled up as early in 60 min with less competition at prolonged time. Cr(VI) adsorption on AC-PH evidences gradual increase at higher adsorbent doses.

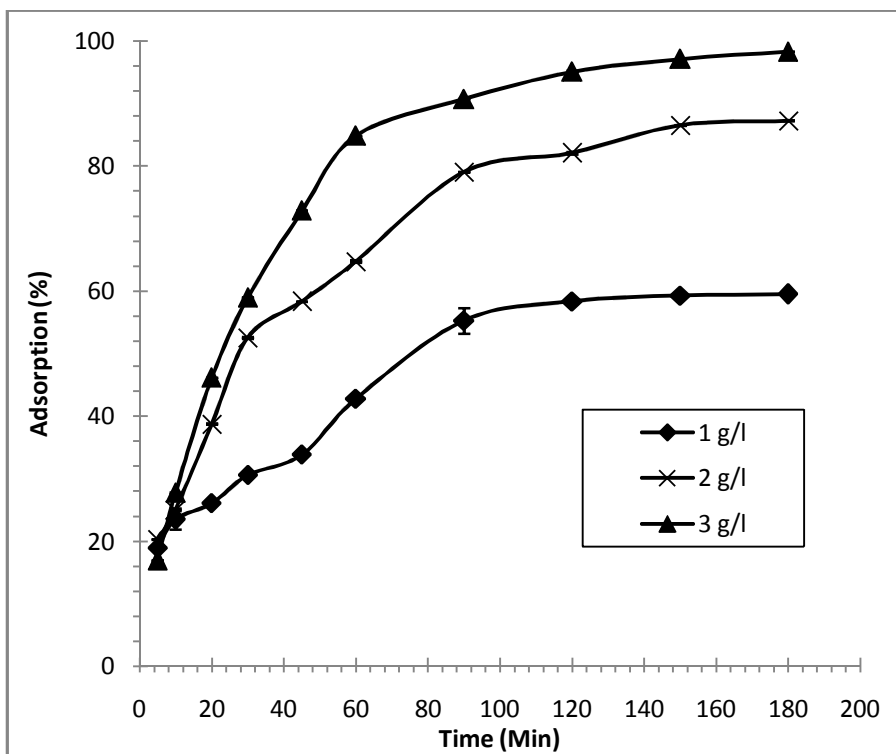


Figure 5.7. Effect of adsorbent dose on the percentage adsorption of Cr(VI) by AC-PA (pH-3.5, Cr(VI) concentration – 10.0 mg/L, contact time – 3.0 h, and temperature – 30 °C)

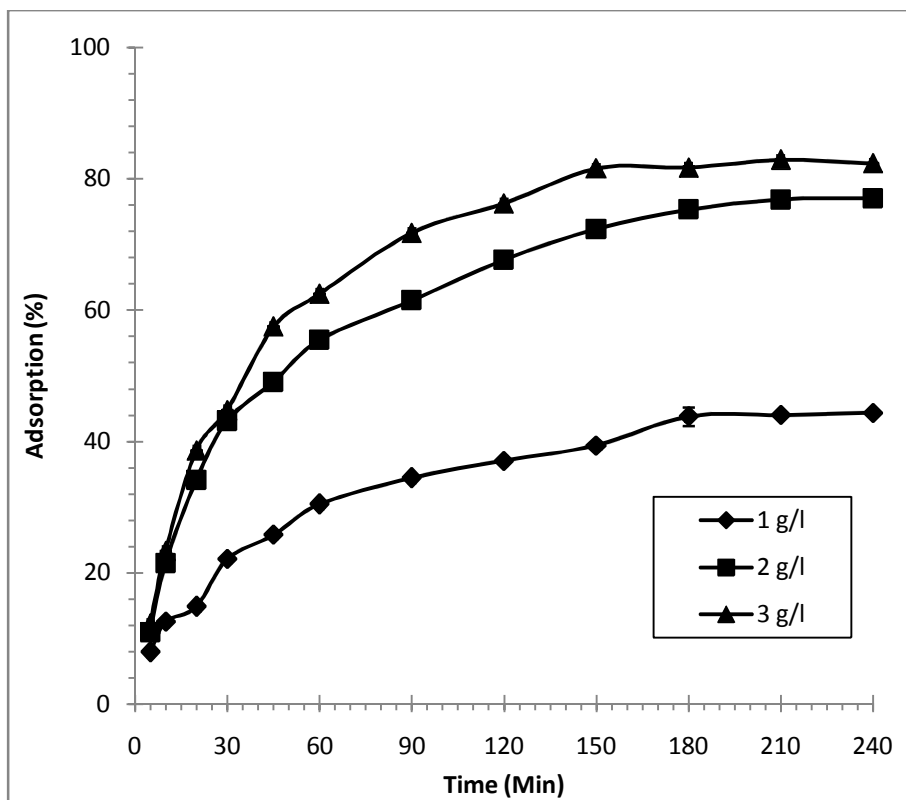


Figure 5.8. Effect of adsorbent dose on the percentage adsorption of Cr(VI) by AC-ZC (pH – 2.0, Cr(VI) concentration – 10.0 mg/L, contact time – 3.0 h, and temperature – 30 °C)

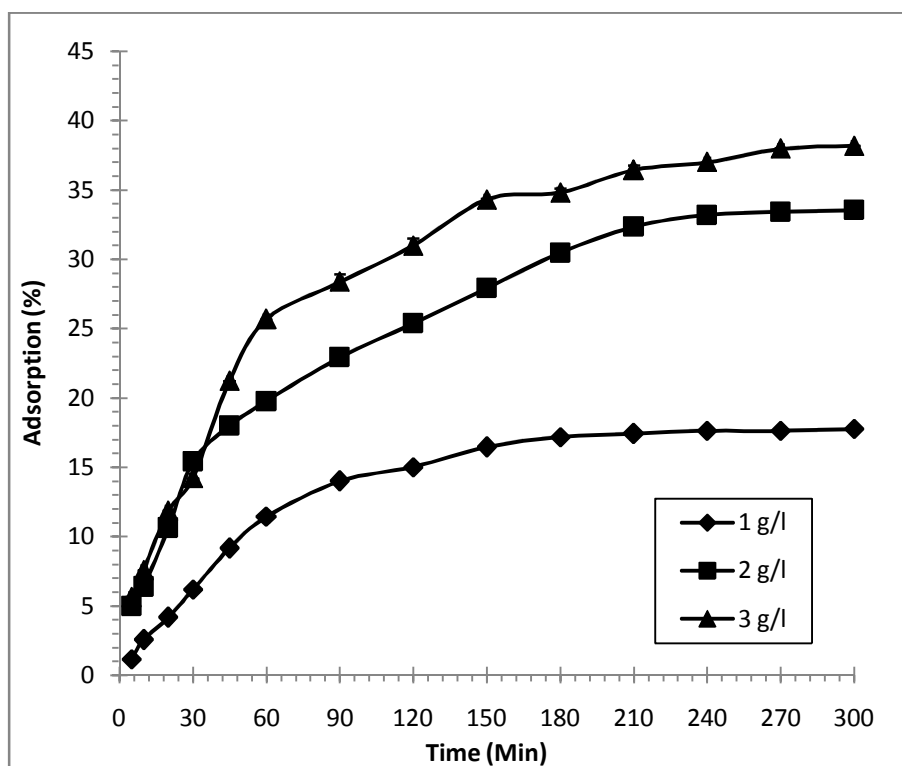
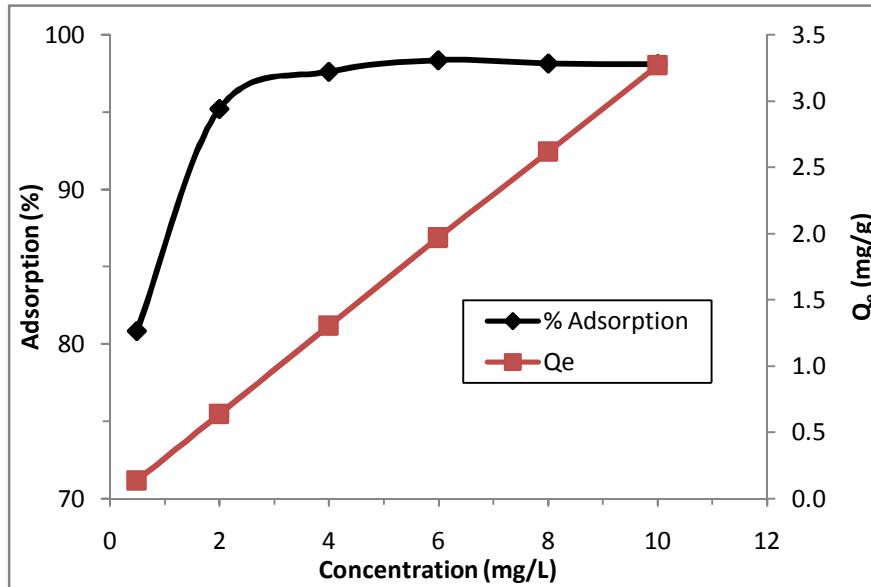


Figure 5.9. Effect of adsorbent dose on the percentage adsorption of Cr(VI) by AC-PH (pH – 2.0, Cr(VI) concentration – 10.0 mg/L, contact time – 3.0 h, and temperature – 30 °C)

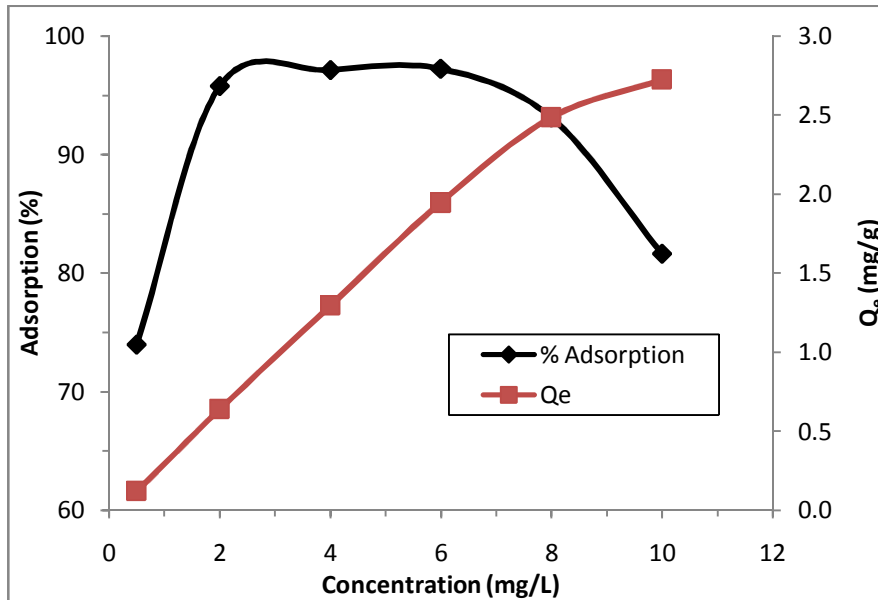
5.1.3. Effect of Initial Chromium(VI) Concentration

The initial concentration of metal ions in the solution is an important parameter as the metal concentration changes over a broad range in industrial effluents. Figure 5.10 depicts the changes in adsorption trends of ACs with variation in initial concentration of adsorbate in the solution and at definite experimental conditions (pH – 2.0, adsorbent dose – 2.0 g/l, contact time – 3.0 h and temperature – 30 °C). The adsorption behavior in figure clearly indicates the increasing trend of Cr(VI) adsorption on AC-PA (80.84 % to 98.38 %) as the initial Cr(VI) concentration increased from 0.5 to 10.0 mg/L. Similar trend was also observed for AC-ZC, that depicts increasing trend from 74 % to 97.23 % with the increase of metal concentration from 0.5 mg/L to 6 mg/L. However, further increase in metal concentration to 10 mg/L resulted decrease in adsorption to 81.66 %. For AC-PH, gradual improvement in metal adsorption was observed from 75 % to 92.67 % with the increase in Cr(VI) concentration from 0.5 mg/L to 2.0 mg/L and then exhibited an opposite trend and finally reduced to 52.51 % with increase in Cr(VI) concentration to 10 mg/L. Esmaeili et al (2010) reported about 91 % of Cr(Vi) removal from aqueous solution by activated carbon prepared from marine algae. The Q_e values were increased

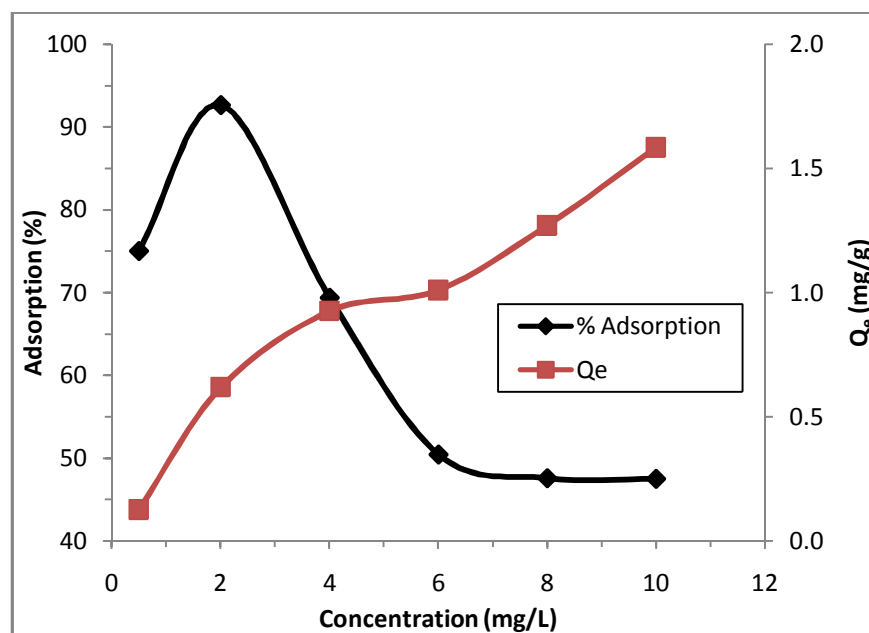
continuously with the increase of initial metal concentration from 2.0 mg/L to 10.0 mg/L and reached 3.3 mg/g, 2.7 mg/g and 1.6 mg/g for AC-PA, AC-ZC and AC-PH, respectively.



(a)



(b)



(c)

Figure 5.10. Effect of initial metal concentration on Cr(VI) adsorption by different ACs (a) AC-PA (b) AC-ZC and (c) AC-PH (pH – 2.0, adsorbent dose – 3.0 g/l, contact time – 3.0 h and temperature – 30 °C)

Plots for percentage of Cr(VI) adsorption versus adsorption time by ACs prepared by H_3PO_4 , $ZnCl_2$, and KOH activations were shown in Figures 5.11, 5.12 and 5.13, respectively. It is evident from the figures that the equilibrium time is dependent on the adsorbate concentration and it varied from 60 min to 210 min by varying initial metal concentration and type of adsorbent.

AC prepared by H_3PO_4 activation (AC-PA) showed instantaneous adsorption of Cr(VI) within first 30 min and then increased gradually till it became constant after 120 min. At 2 mg/L and 10 mg/L initial metal concentrations, the percentages of Cr(VI) adsorbed were 98.6 % and 98.38 %, respectively over 180 min of contact time. No significant changes were evidenced in percentage adsorption with the change in Cr(VI) concentration in the studied range (2.0 – 10.0 mg/L) using AC-PA. It can be attributed to the presence of even more unoccupied adsorption sites on the surface of AC-PA. On the other hand, adsorption of Cr(VI) on AC-ZC and AC-PH clearly followed the decreasing trend with the increase of metal concentration. The Cr(VI) adsorption on AC-ZC and AC-PH reduced by 14.13 % and 40.16 % with the increase of metal concentration from 2 mg/L to 10 mg/L, respectively. At lower initial metal concentrations, sufficient adsorption sites are available for adsorption of Cr(VI) ions. At higher concentrations, relatively less available sites induced reduction in adsorption of Cr(VI) on the AC surface.

Similar results were reported by many authors using different types of adsorbents (Acharya et al., 2009; Khezami and Capart, 2005). Hence Cr(VI) adsorption studies at higher concentrations (25 – 100 mg/L) were carried out by using AC-PA (Figure 5.14).

Adsorption is very fast at initial stages due to the high concentration gradient of adsorbate in solution and in adsorbent and also due to the availability of more vacant adsorption sites on the surface of adsorbent at the beginning. The adsorptive removal progressively increased with time due to the limited mass transfer of the adsorbate molecules from liquid to the external surface of AC, and reached equilibrium due to slower internal mass transfer within the adsorbent particles (Acharya et al., 2009).

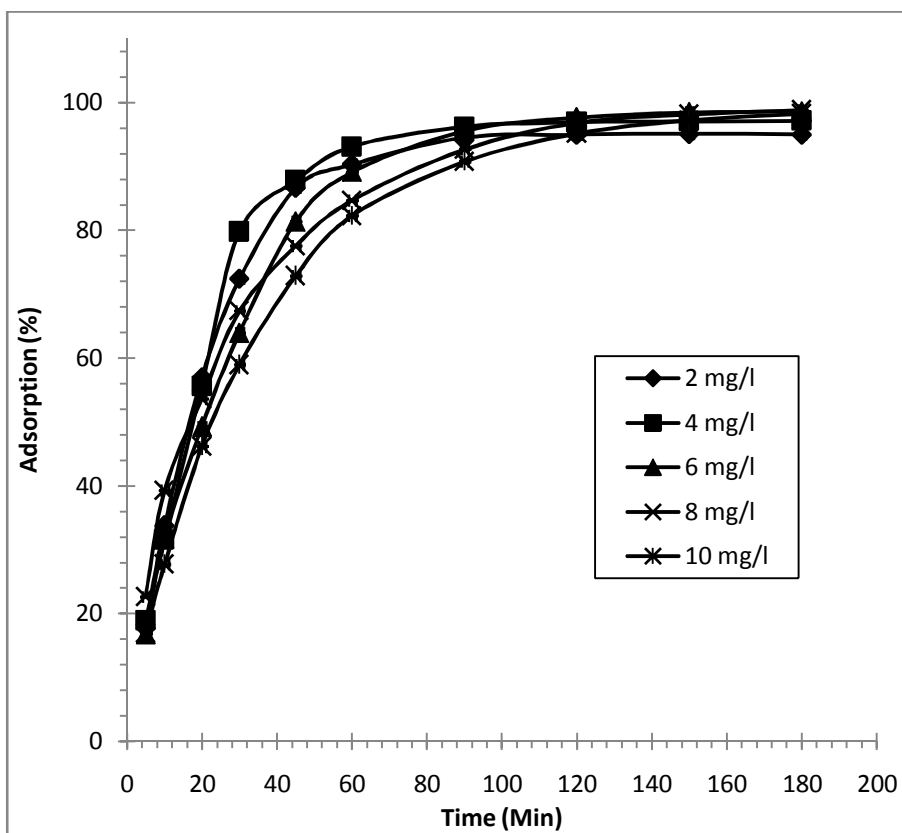


Figure 5.11. Effect of initial metal concentration on the percentage adsorption of Cr(VI) by AC-PA (pH – 3.5, adsorbent dose – 3.0 g/l, contact time – 3.0 h and temperature – 30 °C)

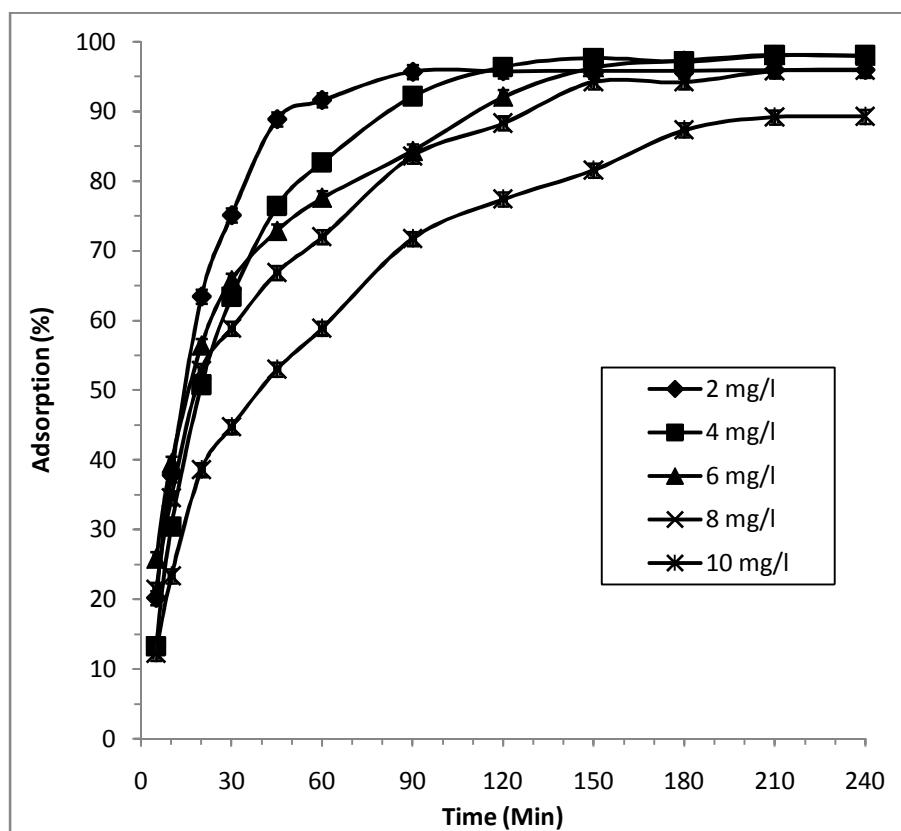


Figure 5.12. Effect of initial metal concentration on the percentage adsorption of Cr(VI) by AC-ZC (pH – 2.0, adsorbent dose – 3.0 g/l, contact time – 3.0 h and temperature – 30 °C)

The nature of adsorbent and available adsorption sites affect the rate of Cr(VI) adsorption. The mechanism of solute transfer to the solid surface involves diffusion through the fluid film around the adsorbent particle and diffusion through the pores to the internal adsorption sites. In the initial stage the concentration gradient between the film and available pores being large, the rate of Cr(VI) adsorption is faster. This rate decreases in the later stage primarily due to the slow pore diffusion of the solute into the bulk of the adsorbent.

It is also observed that the rate of adsorption of Cr(VI) reduced gradually as initial metal concentration rises from 2 mg/L to 10 mg/L. This can be clearly observed within 20 to 40 min time interval in case of AC-PA.

In case of AC-ZC, much difference in rate of adsorption was observed within first 120 min and gradually reached its maximum (95.98 %) in 240 min whereas, significant difference was observed in the Cr(VI) adsorption percentage in case of AC-PH throughout the studied range of contact time.

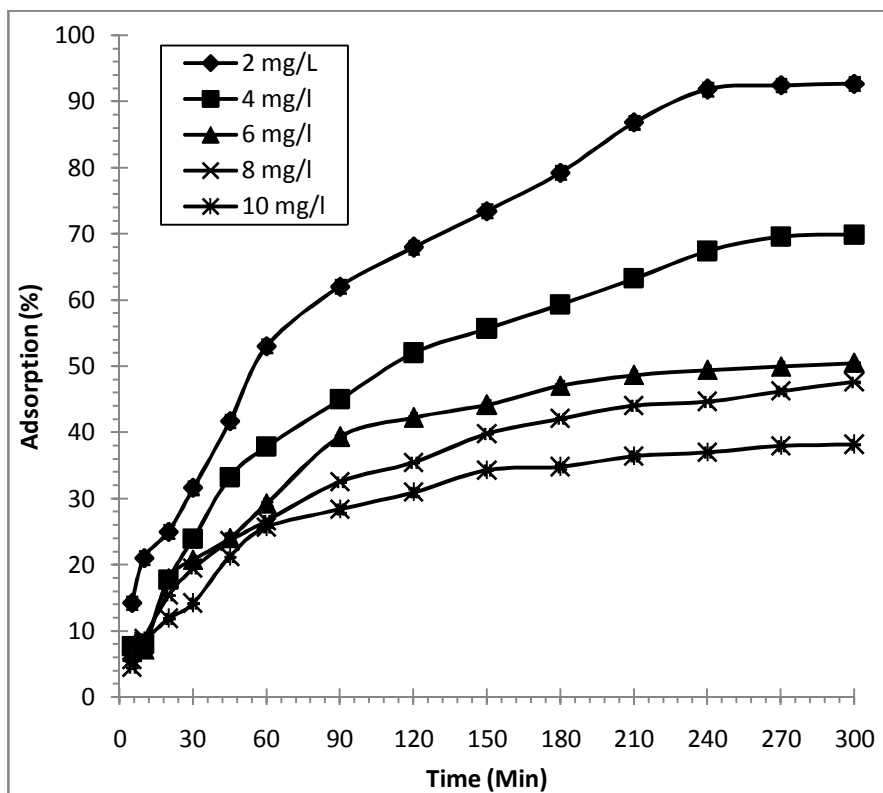


Figure 5.13. Effect of initial metal concentration on the percentage adsorption of Cr(VI) by AC-PH (pH – 2.0, adsorbent dose – 3.0 g/l, contact time – 3.0 h and temperature – 30 °C)

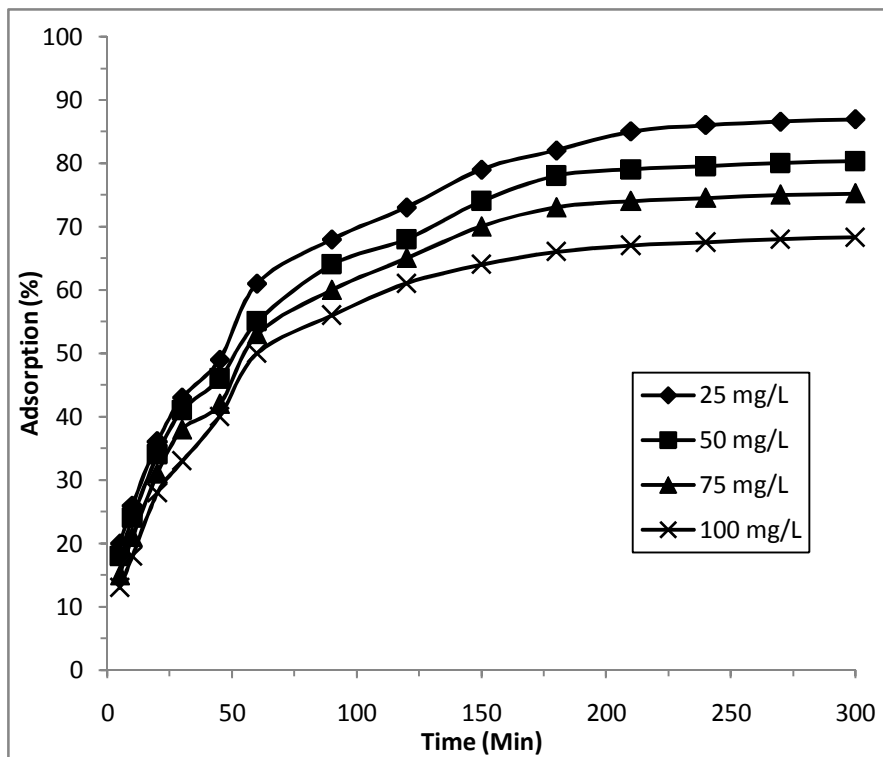
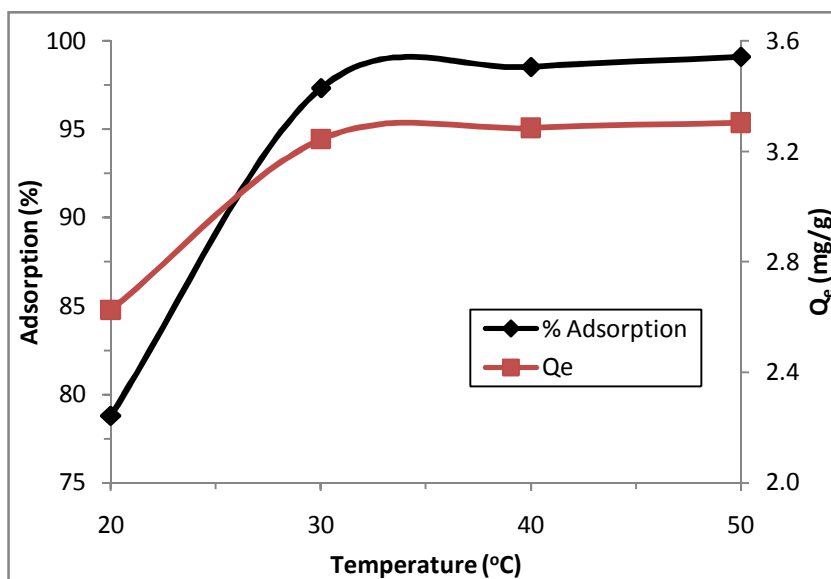


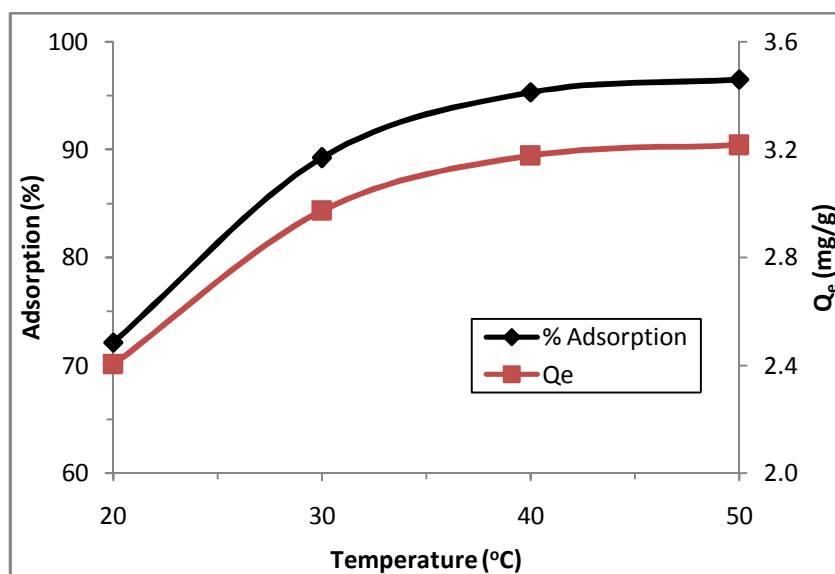
Figure 5.14. Adsorption trends of AC-PA at high initial Cr(VI) concentrations (pH – 3.5, adsorbent dose – 3.0 g/l, contact time – 3.0 h and temperature – 30 °C)

5.1.4. Effect of Temperature

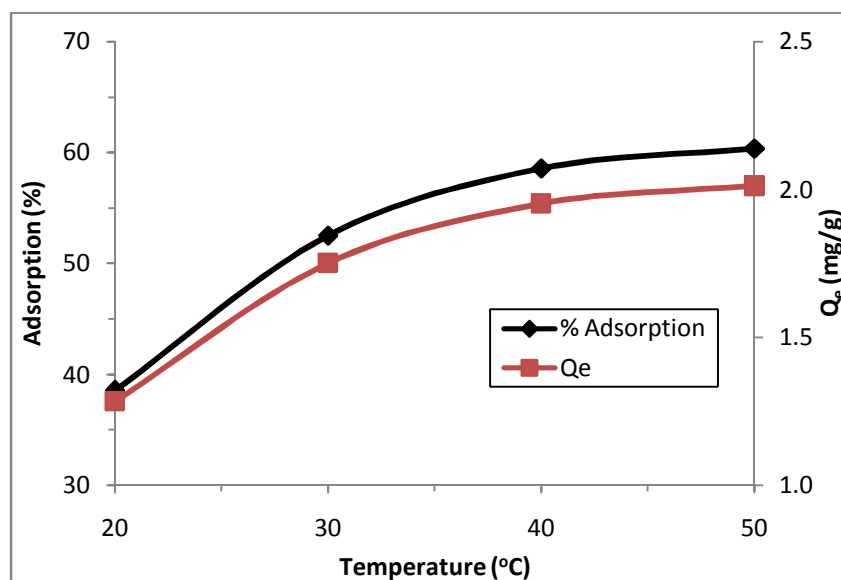
Effect of temperature on Cr(VI) adsorption on AC-PA, AC-ZC, and AC-PH was shown in Figure 5.15. Experiments were performed in the temperature range 20 – 50 °C at constant Cr(VI) concentration (10.0 mg/L), adsorbent dose (3.0 g/L), contact time (3.0 h) and pH (3.5 for AC- PA and 2.0 for AC-ZC and AC-PH). Adsorption of Cr(VI) on all the adsorbents witnessed the increase in adsorption percentage and adsorption capacity (Q_e) from 20 °C to 30 °C and no significant change with further increase of temperature.



(a)



(b)



(c)

Figure 5.15. Effect of temperature on Cr(VI) adsorption by different ACs (a) AC-PA (b) AC-ZC and (c) AC-PH (pH–3.5 for AC-PA and 2.0 for AC-ZC and AC-PH, Cr(VI) concentration – 10.0 mg/L, adsorbent dose – 3.0 g/L, and contact time – 3.0 h)

The rate of adsorption on AC-PA at different temperatures is illustrated in Figure 5.16. The figure represents high rate of adsorption at 50 °C. However low rate of Cr(VI) adsorption was observed at 20 °C within studied range of time. A rapid increase in adsorption was observed initially (within 60 min) at different temperatures and then a gradual increase was observed. The adsorption of Cr(VI) on AC-PA, AC-ZC, and AC-PH increased from 78.78 to 98.54 %, 75.55 to 98.36 %, and 38.53 to 58.26 %, respectively with the rise in temperature from 20 to 50 °C (Figures 5.16, 5.17 and 5.18, respectively).

The increase in percentage adsorption of Cr(VI) by prepared ACs indicates an endothermic process. At higher temperatures the rate of diffusion of solute within the pores of the adsorbent increases since diffusion is an endothermic process. Thus, the percentage adsorption of Cr(VI) increases as the rate of diffusion of Cr(VI) ions in the external mass transport process increases with temperature (Meena et al., 2008). The high percentage adsorption of Cr(VI) in case of AC-PA may be due to the high diffusion rate of Cr(VI) ions into the pores as the surface area and pore volume of the adsorbent were large compared to the other two types (Ref. Table in chapter 4). Moreover, at low temperatures the kinetic energy of Cr(VI) species is low and hence contact between the metal ions and the active sites of AC is insufficient, resulting in reduced adsorption efficiency. Increased adsorption with temperature may also be

due to the increase in number of adsorption sites generated as a result of breaking of some internal bonds near edge of active surface sites of adsorbent (Pandey et al., 1986). In case of AC-PA and AC-ZC, the change in percentage adsorption is negligible at higher temperatures (> 30 °C) whereas, AC-PH displayed different adsorption percentages at different temperatures.

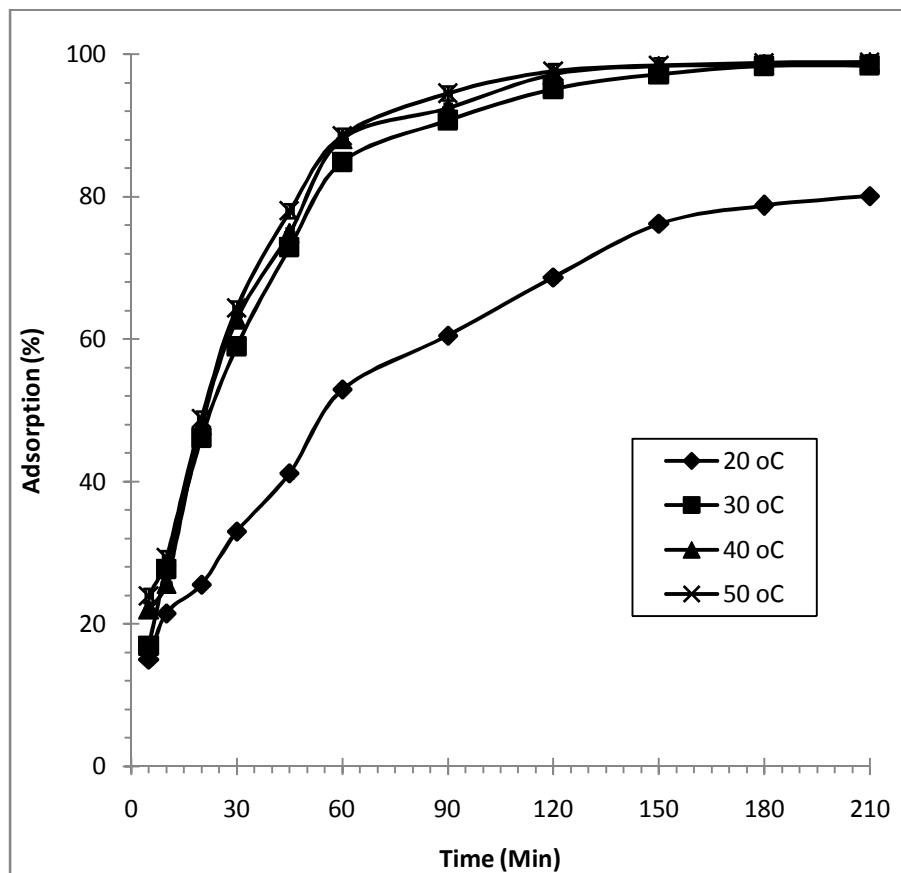


Figure 5.16. Effect of temperature on percentage removal of Cr(VI) by AC-PA (pH – 3.5, Cr(VI) concentration – 10.0 mg/L, adsorbent dose – 3.0 g/L, and contact time – 3.0 h)

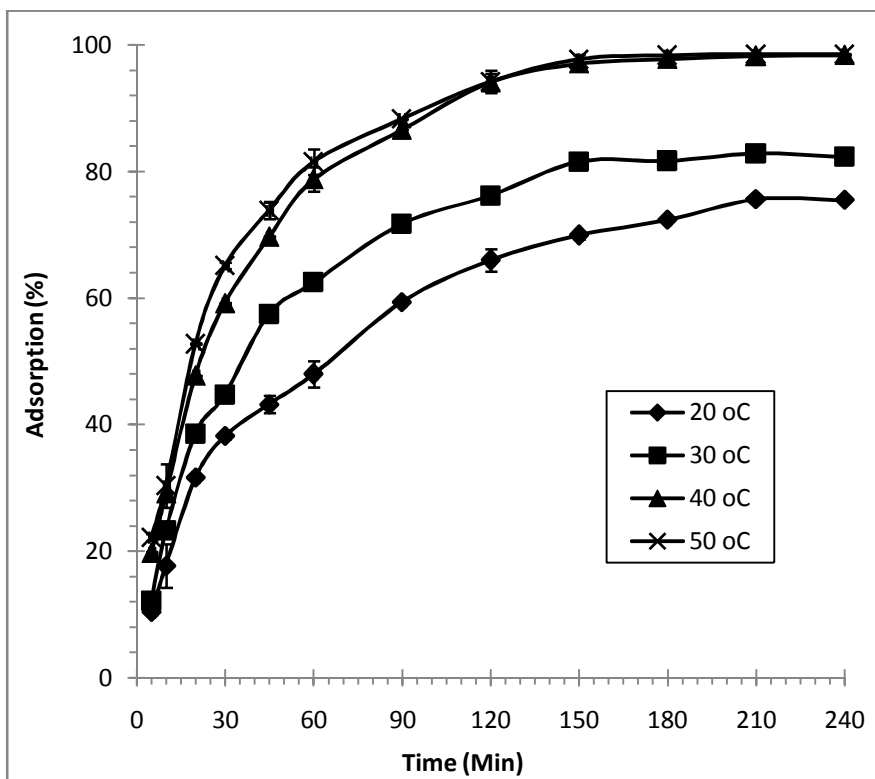


Figure 5.17. Effect of temperature on percentage removal of Cr(VI) by AC-ZC (pH – 2.0, Cr(VI) concentration – 10.0 mg/L, adsorbent dose – 3.0 g/L, and contact time – 3.0 h)

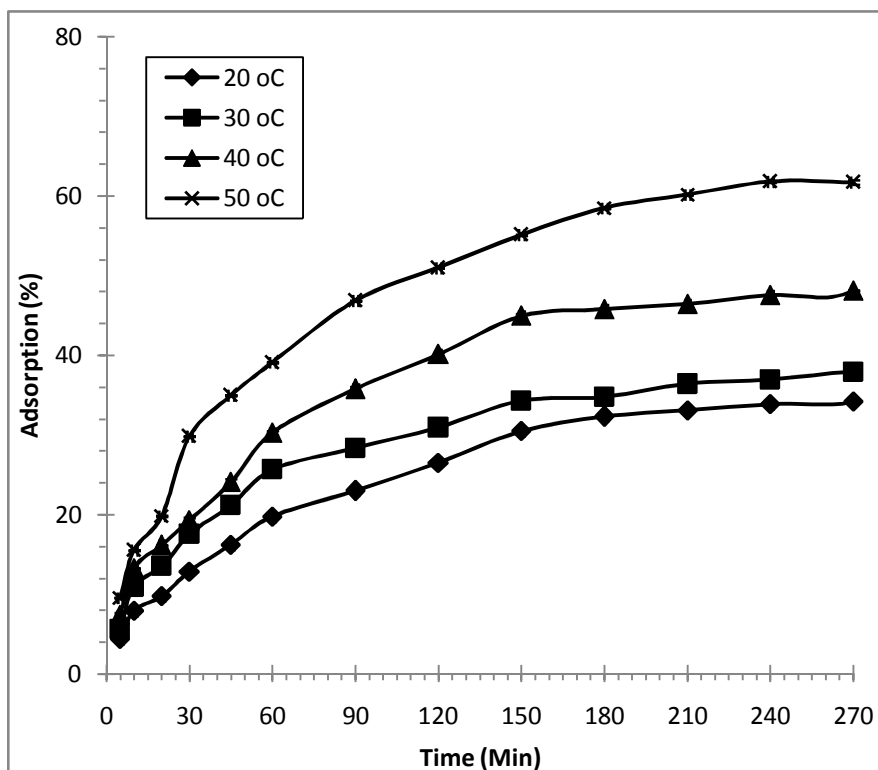


Figure 5.18. Effect of temperature on percentage removal of Cr(VI) by AC-ZC (pH – 2.0, Cr(VI) concentration – 10.0 mg/L, adsorbent dose – 3.0 g/L, and contact time – 3.0 h)

5.2. Adsorption Equilibrium Study

The successful representation of the dynamic adsorptive separation of solute from solution by an adsorbent depends upon a good description of the equilibrium between the two phases. Adsorption equilibrium is established when the amount of solute being adsorbed onto the adsorbent is equal to the amount being desorbed (Allen et al., 2003). The equilibrium adsorption isotherms were depicted by plotting solid phase concentration (q_e) against liquid phase concentration (C_e) of solute.

5.2.1. Langmuir Isotherm

Adsorption isotherm explains the interaction between adsorbate and adsorbent and is critical for design of adsorption process. The Langmuir, Freundlich, Temkin, and D-R isotherms are the most frequently used models to describe the experimental data of adsorption. In the present work these four isotherms were applied to investigate the adsorption process of Cr(VI) on prepared ACs at different conditions of process parameters.

The Langmuir isotherm is applicable to homogeneous sorption where the sorption of each sorbate molecule on to the surface has equal sorption activation energy and is represented as follows (Dubinin and Radushkevich, 1947; Choy et al., 2000):

$$q_e = \frac{K_L C_e}{1 + a_L C_e} \quad (5.1)$$

where q_e is the solid phase sorbate concentration at equilibrium, K_L and a_L are the Langmuir isotherm constants.

The linear form of Langmuir equation is given as

$$\frac{C_e}{q_e} = \frac{1}{K_L} + \frac{a_L}{K_L} C_e \quad (5.2)$$

The adsorption data were analyzed according to the linear form of equation (equation 5.2). The plots of C_e/q_e versus C_e are linear which indicate that the adsorption data fitted reasonably to the Langmuir isotherm (Figure 5.19). The constants were evaluated from the slope a_L/K_L and intercept $1/K_L$, where K_L/a_L gives the theoretical monolayer saturation capacity Q_0 . The Langmuir constants obtained for all the three adsorbents are summarized in Table 5.1. The negative value of a_L obtained for AC-PA indicates the inefficiency of Langmuir model to explain

the adsorption process. The adsorption data of other two adsorbents (AC-ZC and AC-PH) were well fitted to the Langmuir equation with reasonably high regression coefficients. The essential characteristics of Langmuir isotherm can be explained in terms of a dimensionless constant, separation factor (R_L), which is represented as

$$R_L = \frac{1}{1+a_L C_i} \quad (5.3)$$

where, C_i and a_L are the initial concentration and constant related to the affinity of binding sites with the metal ions, respectively. The value of R_L , a positive number ($0 < R_L < 1$), signifies the feasibility of the adsorption process for all developed ACs.

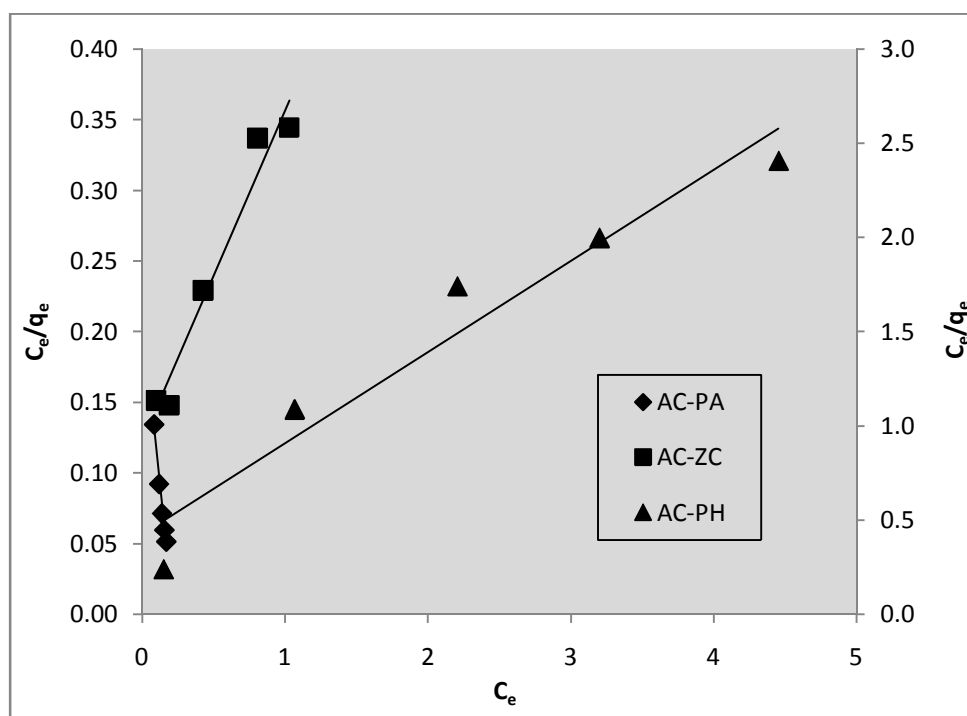


Figure 5.19. Langmuir isotherms of different ACs for the Cr(VI) adsorption data at 30 °C

5.2.2. Freundlich Isotherm

The most important multisite or multilayer adsorption isotherm for heterogeneous surfaces is the Freundlich isotherm which is characterized by the heterogeneity factor $1/n$, and is represented by the equation:

$$q_e = K_F C_e^{1/n} \quad (5.3)$$

where, q_e is the solid phase concentration in equilibrium, C_e is the liquid phase sorbent concentration at equilibrium, K_F is the Freundlich constant and $1/n$ is the heterogeneity factor. The magnitude of n gives an indication on the favorability of adsorption. It is generally stated that the values of n in the range 2 – 10 represent good, 1 – 2 moderately good, and less than 1 poor adsorption characteristics (Aksu and Kutsal, 1991). The Freundlich isotherm is an empirical equation based on an exponential distribution of adsorption sites and energies. The linear form of Freundlich equation is:

$$\ln q_e = \ln K_F + \frac{1}{n} \ln C_e \quad (5.4)$$

where, the intercept $\ln K_F$ is a measure of adsorption capacity, and the slope $1/n$ is the adsorption intensity.

The values of K_F and n were calculated from the intercept and slope of the plots $\ln q_e$ against $\ln C_e$ (Figure 5.20). The Freundlich isotherm describes reversible adsorption and was not restricted to the formation of monolayer. The isotherms were found to be linear as evidenced from correlation coefficients obtained in the range of 0.963 – 0.996. The Freundlich isotherm showed a better fit to the adsorption data than Langmuir isotherm suggesting heterogeneous nature of the ACs. Freundlich sorption isotherm constants were determined for all the ACs and are summarized in Table 5.1. The steepness and curvature of isotherms were obtained from the values of K_F and n (Akgerman and Zardkoohi, 1996). The value of K_F signifies the adsorption intensity and higher K_F value of AC-PA confirmed the higher adsorption capacity for Cr(VI) as compared to other ACs i.e. AC-ZC and AC-PH. The obtained K_F and n values of AC-PA are 4.07 and 5.1, respectively.

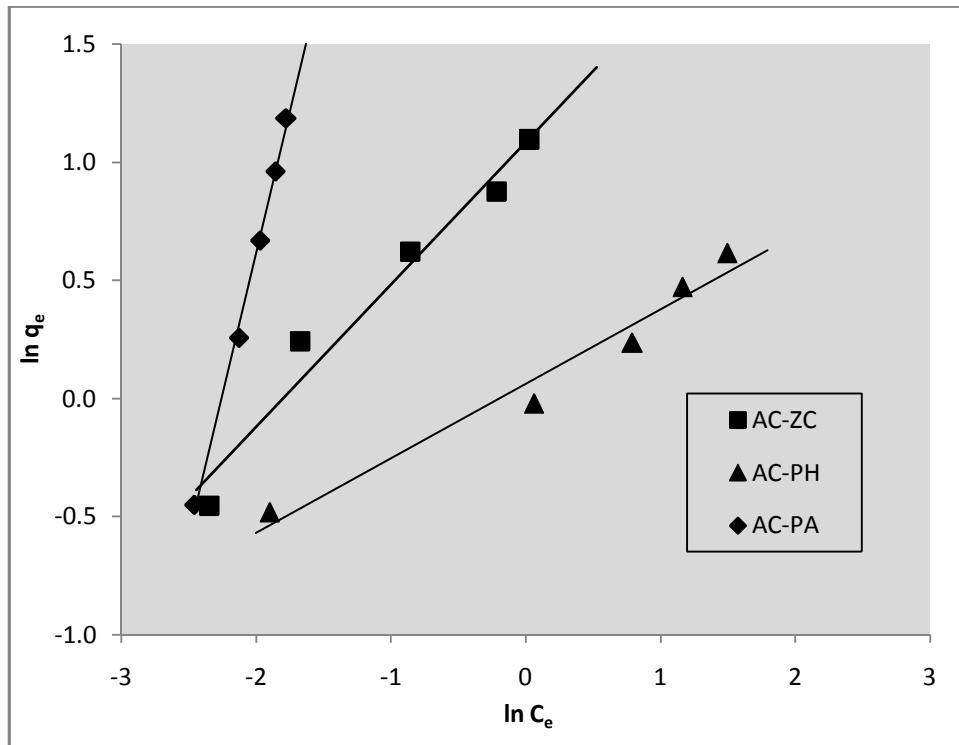


Figure 5.20. Freundlich isotherms of different ACs for the Cr(VI) adsorption data at 30 °C

5.2.3. Temkin Isotherm

Temkin isotherm model contains a parameter that explicitly accounts for the interaction of adsorbent and adsorbate species. It is based on the assumption that the heat of adsorption of all the molecules in the layer diminishes linearly with coverage which is attributed to adsorbate – adsorbate repulsions. It also assumes that adsorption is due to uniform distribution of binding energy. Contrary to Freundlich model, it assumes that fall in heat of adsorption is linear rather than logarithmic. The Temkin equation can be given as (Temkin and Pyzhev, 1940):

$$q_e = B_T \ln A_T + B_T \ln C_e \quad (5.5)$$

where, $B_T = RT/b$, T (K) is the absolute temperature; R is the universal gas constant (8.314 J/K mol); A_T (L/mg) is the equilibrium binding constant that corresponds to the maximum binding energy; B_T is related to the heat of adsorption; and q_e and C_e are the amount of adsorbate adsorbed per unit weight of adsorbent and equilibrium concentration of adsorbate remained in solution, respectively. The Temkin isotherm parameters were obtained by plotting q_e versus $\ln C_e$ shown in Figure 5.21. The positive values (Table 5.1) of adsorption energy (B_T) obtained indicate that the process is exothermic, which is contrary to the obtained results. The low R^2

values obtained (0.916, 0.974 and 0.881 for AC-PA, AC-ZC and AC-PH, respectively) suggest that the adsorption data does not follow the Temkin isotherm.

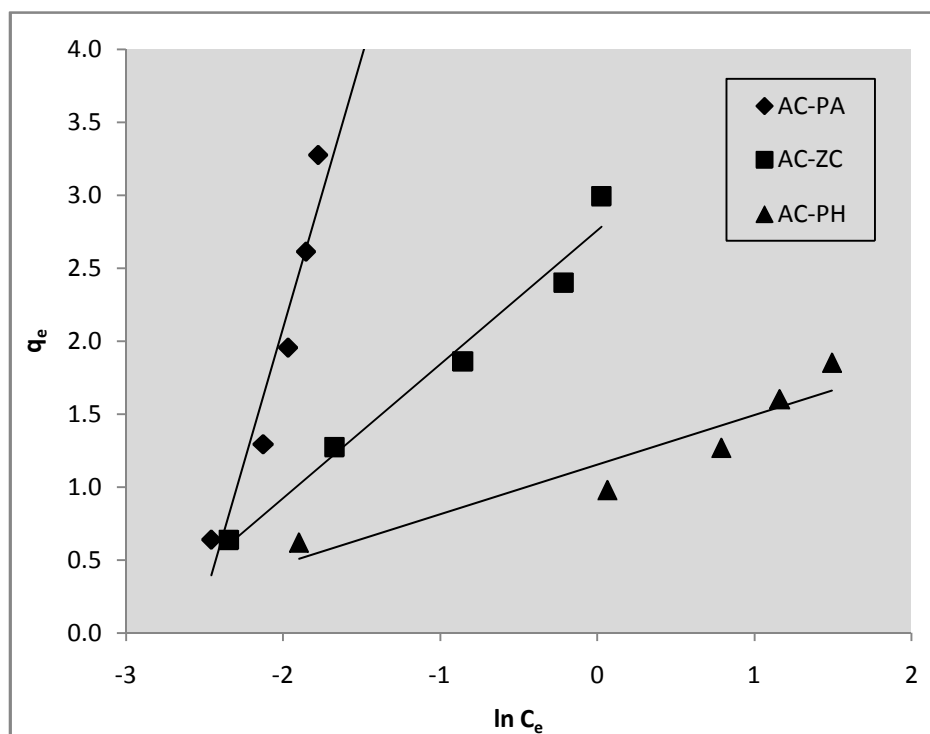


Figure 5.21. Temkin isotherms of different ACs for the Cr(VI) adsorption data at 30 °C

5.2.4. Dubinin – Radushkevich Isotherm

The linear form of Dubinin – Radushkevich (DR) isotherm equation is presented as (Igwe and Abia, 2007):

$$\ln q_e = \ln q_D - 2B_D RT \ln(1 + 1/C_e) \quad (5.6)$$

A plot of $\ln q_e$ against $RT \ln(1 + 1/C_e)$ shown in Figure 5.22 yielded straight lines and indicates a good fit of the isotherm to the experimental data. The apparent energy (E) of adsorption from DR isotherm model can be estimated using the equation given below.

$$E = \frac{1}{\sqrt{2B_D}} \quad (5.7)$$

The DR isotherm constants and mean free energy were presented in Table 5.1. It was found that the DR isotherm model gives a satisfactory fit for Cr(VI) adsorption data irrespective of type of AC with high regression coefficients (0.999 for AC-PA, 0.994 for AC-ZC, and 0.969 for AC-PH). The magnitude of the activation energy can be used to determine the type of

adsorption process. Although it is not well supported to determine the rate controlling step from activation energy, the simplicity makes it easy to have a general insight into the undergoing process. If the value of $E < 8$ kJ/mol, the adsorption type can be explained by physisorption, and if E is in the range of 8 – 18 kJ/mol then the adsorption type is ion exchange (Maji et al., 2007). And also the process is classified as film-diffusion-controlled when $E < 16$ kJ/mol, particle-diffusion-controlled when E is 21 – 38 kJ/mol, and chemical-reaction-controlled when $E > 50$ kJ/mol (Boyd and Soldano, 1953; Helfferich, 1962; Swami and Dreisinger, 1995). The low values of apparent energies obtained for all the samples ranging from 0.037 – 0.05 kJ/mol confirms that the adsorption of Cr(VI) on prepared ACs is physical adsorption (Horsfall Jnr et al., 2004).

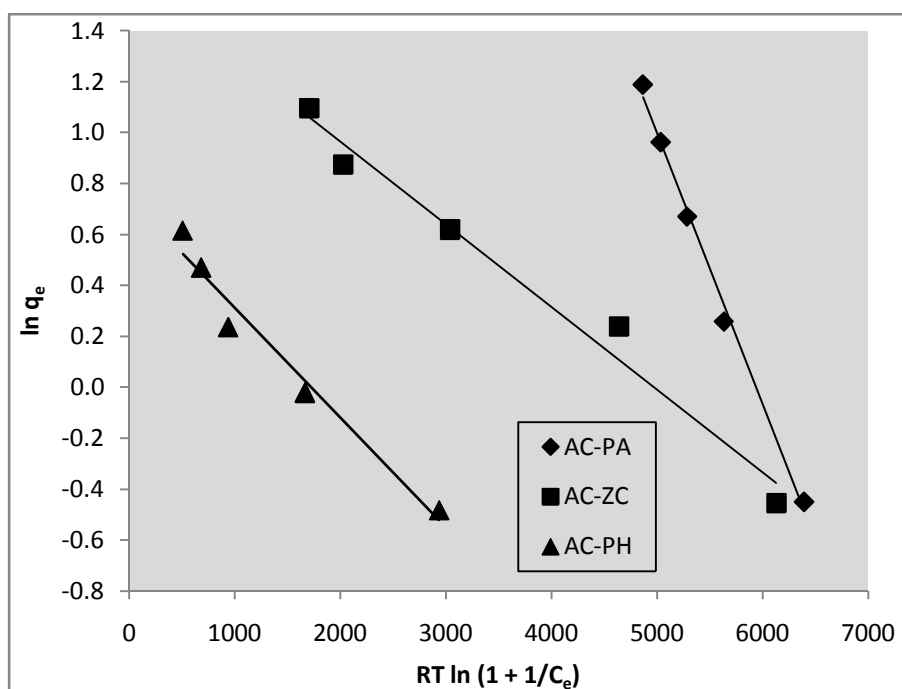


Figure 5.22. Dubinin – Radushkevich isotherms of different ACs for the Cr(VI) adsorption data at 30 °C

Table 5.1. Langmuir, Freundlich, Temkin and D-R isotherm constants for the Cr(VI) adsorption on different prepared activated carbon samples

Isotherm parameters	AC - PA	AC - ZC	AC - PH
Langmuir			
K_L (L/g)	4.65	8.20	2.35
a_L (L/mol)	-4.63	1.92	1.13
Q_o (mg/g)	1.01	4.27	2.07
R_L	0.02	0.05	0.08
R^2	0.981	0.960	0.937
Freundlich			
K_f [(mol/g)(mol/L) ⁿ]	4.07	2.95	1.06
$1/n$	0.196	0.602	0.315
R^2	0.996	0.965	0.963
Temkin			
B_T	3.71	0.92	0.34
A_T (L/mg)	12.96	20.20	29.91
R^2	0.916	0.974	0.881
Dubinin - Radushkevich			
$B \times 10^{-4}$ (1/(J/mol) ²)	2.0	2.5	3.5
q_D (mg/g)	1.47	2.37	4.75
E (J/mol)	30.15	57.74	70.71
R^2	0.995	0.979	0.969

5.3. Adsorption Kinetic Study

Adsorption kinetic study is important in determining the efficiency of adsorption. Kinetic models have been exploited to test the experimental data and to determine the mechanism of adsorption and its potential rate-controlling step that include mass transfer and chemical reaction. Adsorption kinetics expressed as the solute removal rate that controls the residence time of the sorbate in solid-solution interface. These models include pseudo-first order and pseudo-second order models, and particle diffusion and film diffusion models.

5.3.1. Pseudo-First-Order Kinetic Model

Lagergren proposed a pseudo-first-order kinetic model. This model was successfully applied to describe the kinetics of many adsorption systems. The integral form of the model equation expressed as follows (Ho, 2004):

$$\log(q_e - q_t) = \log q_e - \frac{k_1}{2.303} t \quad (5.8)$$

where, q_e and q_t (mg/g) are the amount of Cr(VI) that was adsorbed at the equilibrium and at time t (min), respectively and k_1 (1/min) is the rate constant. The values of k_1 and q_e were calculated from the slopes and intercepts of $\log(q_e - q_t)$ against the t plots and were presented in Table 5.2. The pseudo first order plots of Cr(VI) adsorption on AC-PA, AC-ZC and AC-PH are shown in Figures 5.23, 5.24 and 5.25, respectively. The lower correlation coefficients obtained suggest that the adsorption of Cr(VI) on prepared activated carbons does not follow the pseudo first order kinetics. Pseudo-first order kinetic model does not comply with the kinetic data which can be attributed to the control of boundary layer over Cr(VI) adsorption at the initial stages (Boudrahem et al., 2009).

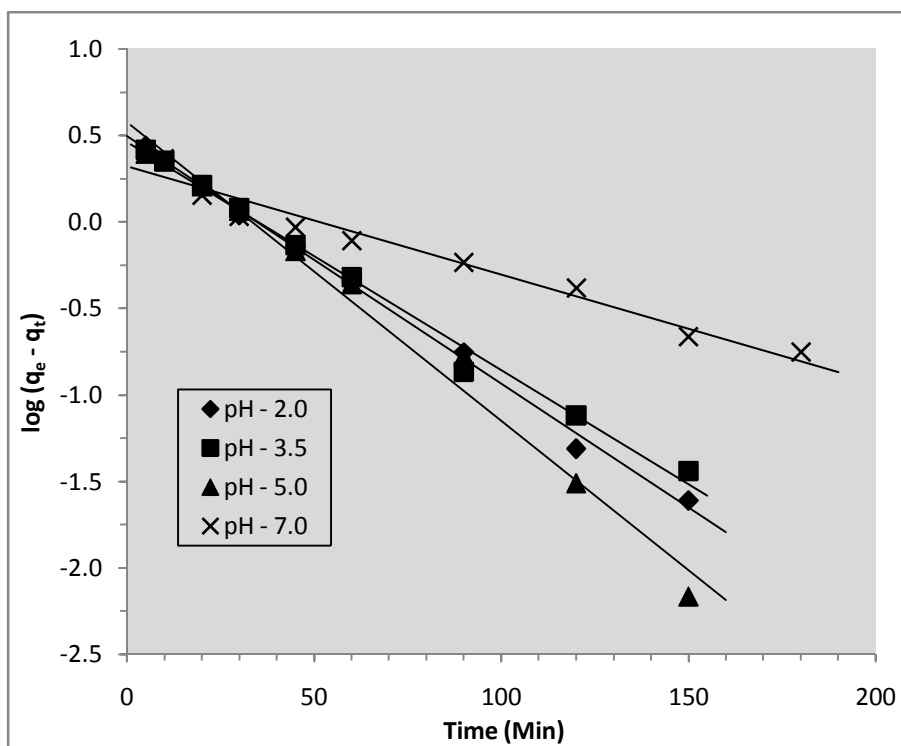


Figure 5.23. Pseudo first order plots for adsorption of Cr(VI) on AC-PA

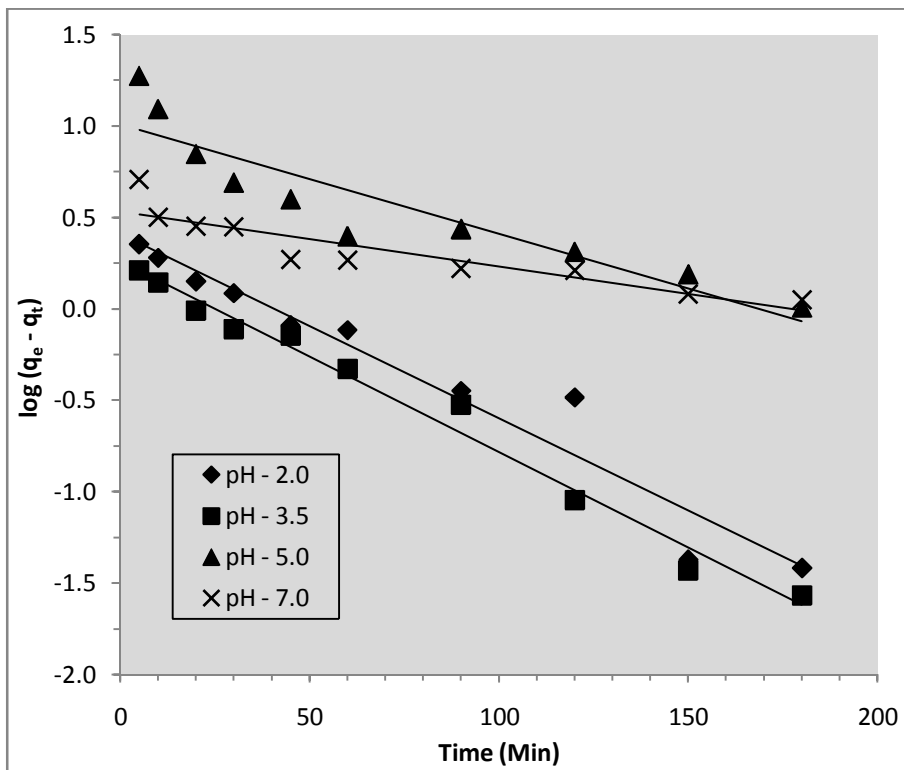


Figure 5.24. Pseudo first order plots for adsorption of Cr(VI) on AC-ZC

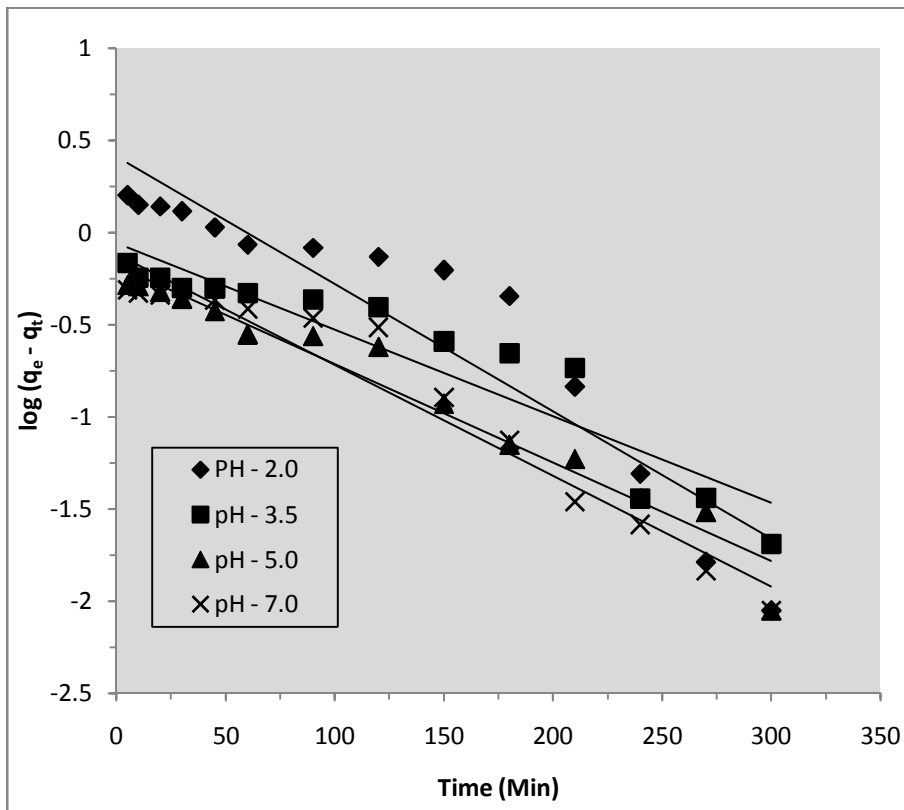


Figure 5.25. Pseudo first order plots for adsorption of Cr(VI) on AC-PH

5.3.2. Pseudo-Second-Order Kinetic Model

The adsorption kinetics may also be described by a pseudo-second-order kinetic model (Ho, 2006 a, b). The linearized integral form of the model is represented as

$$\frac{t}{q_t} = \frac{1}{k_2 q_e^2} + \frac{1}{q_e} t \quad (5.9)$$

where, q_e and q_t (mg/g) are the amount of Cr(VI) that was adsorbed at the equilibrium and at time t (min), respectively and k_2 is the pseudo-second-order rate constant of adsorption (g/mg min). The initial adsorption rate, h ($k_2 q_e^2$), has been widely used for evaluation of the adsorption rates (Ho and McKay, 1998, 1999; Ho, 2000). This model is based on the assumption that the rate of occupation of adsorption sites is proportional to the square of number of unoccupied sites (Karthikeyan et al., 2007; Sag and Aktay, 2002).

From the slopes and intercepts of the linear plots obtained by plotting t/q_t versus t , the values of the pseudo-second-order rate constants q_e and k_2 were calculated and given in Table 5.3. The pseudo second order plots of AC-PA, AC-ZC and AC-PH were shown in Figures 5.26, 5.27 and 5.28, respectively. For all the three types of ACs the results showed a very good compliance with the pseudo-second-order equation with high regression coefficients. The regression (R^2) values obtained are very close to unity and the adequate fitting of the plots confirmed that the adsorption of Cr(VI) by the prepared ACs followed pseudo second order kinetics. The values of h followed the trend AC-PA > AC-ZC > AC-PH indicating that AC-PA adsorbs Cr(VI) more rapidly than AC-ZC and AC-PH.

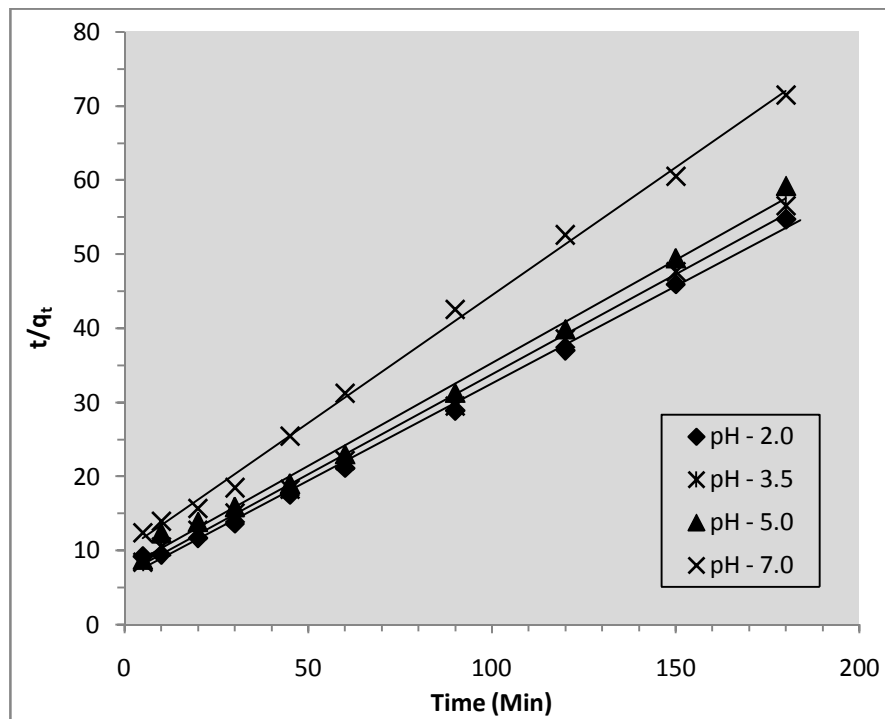


Figure 5.26. Pseudo second order plots for adsorption of Cr(VI) on AC-PA

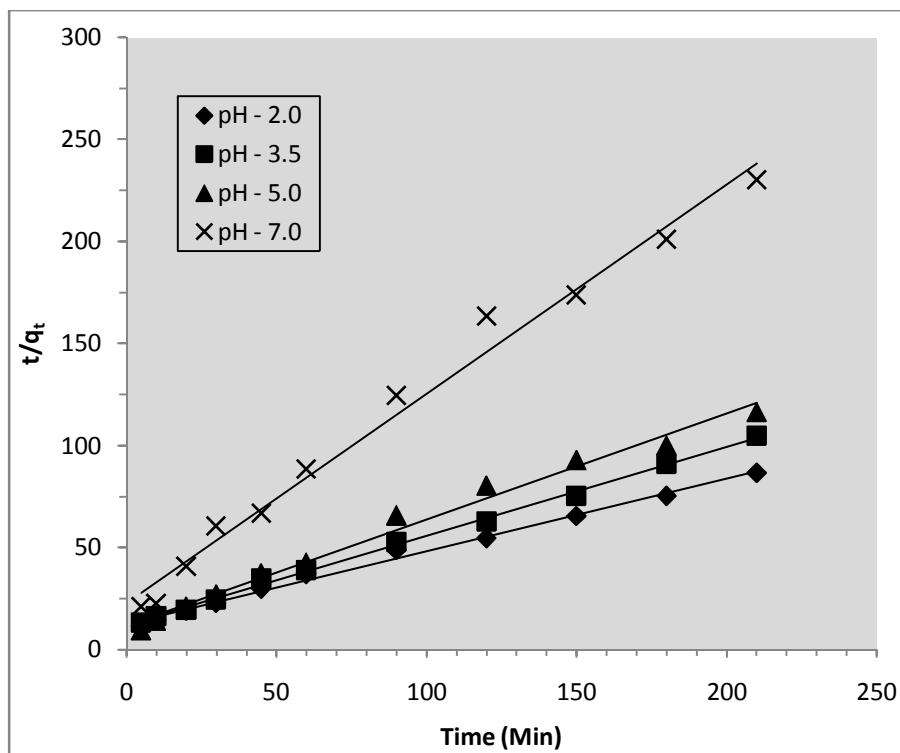


Figure 5.27. Pseudo second order plots for adsorption of Cr(VI) on AC-ZC

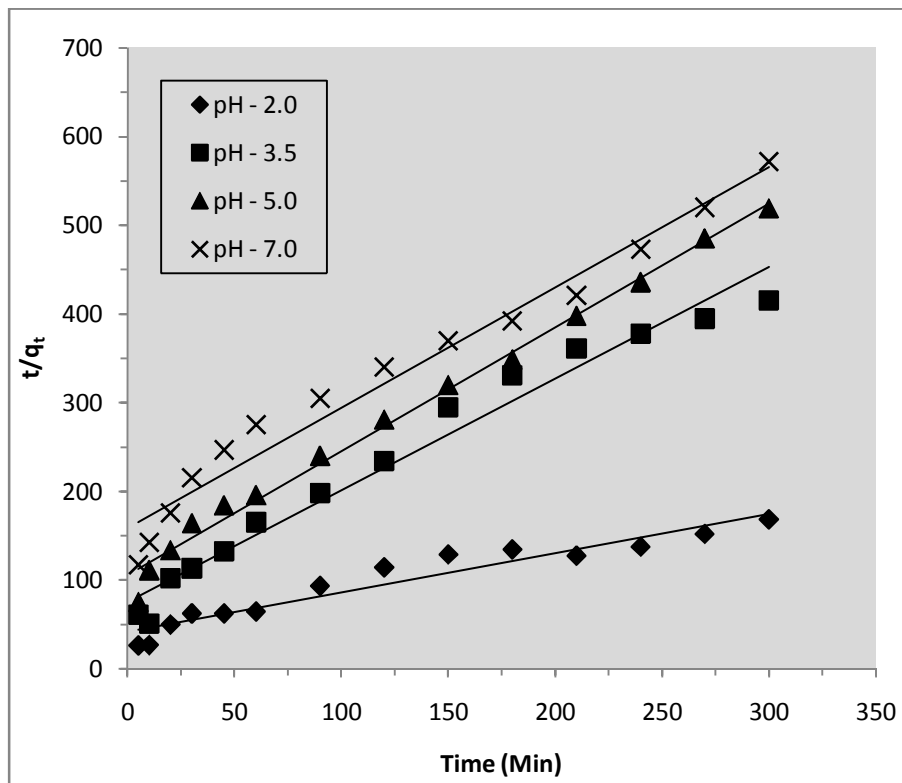


Figure 5.28. Pseudo second order plots for adsorption of Cr(VI) on AC-PH

Table 5.2. Pseudo first order parameters for the adsorption of Cr(VI) on different prepared ACs

pH	AC-PA			AC-ZC			AC-PH		
	K_1 (1/min)	q_e (mg/g)	R^2	K_1 (1/min)	q_e (mg/g)	R^2	K_1 (1/min)	q_e (mg/g)	R^2
2.0	0.032	3.119	0.997	0.023	2.559	0.948	0.014	2.600	0.875
3.5	0.029	2.897	0.992	0.023	1.820	0.984	0.009	0.879	0.875
5.0	0.039	3.758	0.986	0.014	10.162	0.843	0.012	0.668	0.961
6.8	0.014	2.084	0.964	0.007	3.412	0.823	0.014	0.767	0.948

Table 5.3. Pseudo second order parameters for the adsorption of Cr(VI) on different prepared AC samples

pH	AC – PA					AC – ZC					AC – PH				
	K_2 (g/mg min)	q_e (mg/g)	h (mg/g min)	R^2	$Q_e(\text{exp})$	K_2 (g/mg min)	q_e (mg/g)	h (mg/g min)	R^2	$Q_e(\text{exp})$	K_2 (g/mg min)	q_e (mg/g)	h (mg/g min)	R^2	$Q_e(\text{exp})$
2.0	0.011	3.817	0.16	0.996	3.3	0.010	2.801	0.08	0.993	2.8	0.005	2.257	0.025	0.925	1.8
3.5	0.011	3.717	0.15	0.997	3.2	0.016	2.288	0.08	0.997	2.0	0.021	0.795	0.013	0.971	0.7
5.0	0.010	3.610	0.13	0.995	3.1	0.023	1.923	0.08	0.986	1.8	0.019	0.716	0.009	0.991	0.6
6.8	0.012	2.907	0.10	0.997	2.5	0.046	0.976	0.04	0.986	1.1	0.012	0.737	0.006	0.971	0.5

5.4. Adsorption Mechanism

It is always important to predict the rate limiting step in an adsorption process to understand the mechanism associated with the phenomena. For a solid-liquid adsorption process, the solute transfer is usually characterized by either external mass transfer or intraparticle diffusion or both. Generally three types of mechanisms are involved in the adsorption process, mentioned as follows (Chingombe et al., 2006).

1. Metal ion from the bulk liquid to the liquid film or boundary layer surrounding the adsorbent.
2. Transport of solute ions from the boundary film to the external surface of the adsorbent (film diffusion).
3. Transfer of ions from the surface to the intra-particle active sites (particle diffusion).
4. Adsorption of ions by the active sites of adsorbent.

Because the first step is not involved with adsorbent and the fourth step is a very rapid process, they do not belong to the rate controlling steps. Therefore, the rate controlling steps mainly depend on either film diffusion or particle diffusion.

5.4.1. Intra-Particle Diffusion

Weber and Morris model is a widely used intra-particle diffusion model to predict the rate controlling step (Weber and Morris, 1963; Wang et al., 2010). When mass transfer is the controlling step, it is important to identify the diffusion mechanism. According to intra-particle diffusion model, the initial rate of diffusion is given by the following equation:

$$q = k_{id}t^{1/2} \quad (5.10)$$

where, q (mg/g) is the amount adsorbed at time t , k_{id} is the rate constant of intra-particle diffusion and $t^{1/2}$ ($\text{min}^{1/2}$) is the square root of time. The values of k_{id} ($\text{mg/g min}^{1/2}$) were determined from the slopes of respective plots of q versus $t^{1/2}$.

The plots of q_t against $t^{1/2}$ at different pH values showed multi-linearity characterizations with two steps occurred in the adsorption process (Wu et al., 2005) and are shown in Figures 5.29, 5.30 and 5.31 for AC-PA, AC-ZC and AC-PH, respectively. The initial steep portion is due to the instantaneous adsorption on the external surface and the second step is the gradual

adsorption stage, where intra-particle diffusion is rate controlling (Cheung et al., 2007). The larger slopes of the initial steep sections indicate that the rate of Cr(VI) adsorption is higher in the beginning due to the instantaneous availability of larger surface area and adsorption sites. The lower slopes of the second subdued portions are due to the decreased concentration gradient which make the diffusion of Cr(VI) ions into the micropores of the adsorbent. The obvious two steps of the process suggested that the intra-particle diffusion is not only the rate controlling step for the adsorption of Cr(VI) (Ho and Ofomaja, 2005). As the pH shifts to more acidic, the slopes of the plots increased confirming the higher Cr(VI) adsorption at acidic pH. The calculated values of rate constants (k_{id}) and regression coefficients (R^2) were presented in Table 5.4. It was observed that the k_{id} values continuously decreased with the increase in pH and the maximum values were obtained for AC-PA at pH 2.0. The higher values of k_{id} (Table 5.4) for all ACs corresponded to the lower values of k_2 (Table 5.3), indicating that the intra-particle diffusion retards the adsorption process. This also indicates that in all cases, the adsorption of Cr(VI) is rather complex and involves more than one diffusive mechanism.

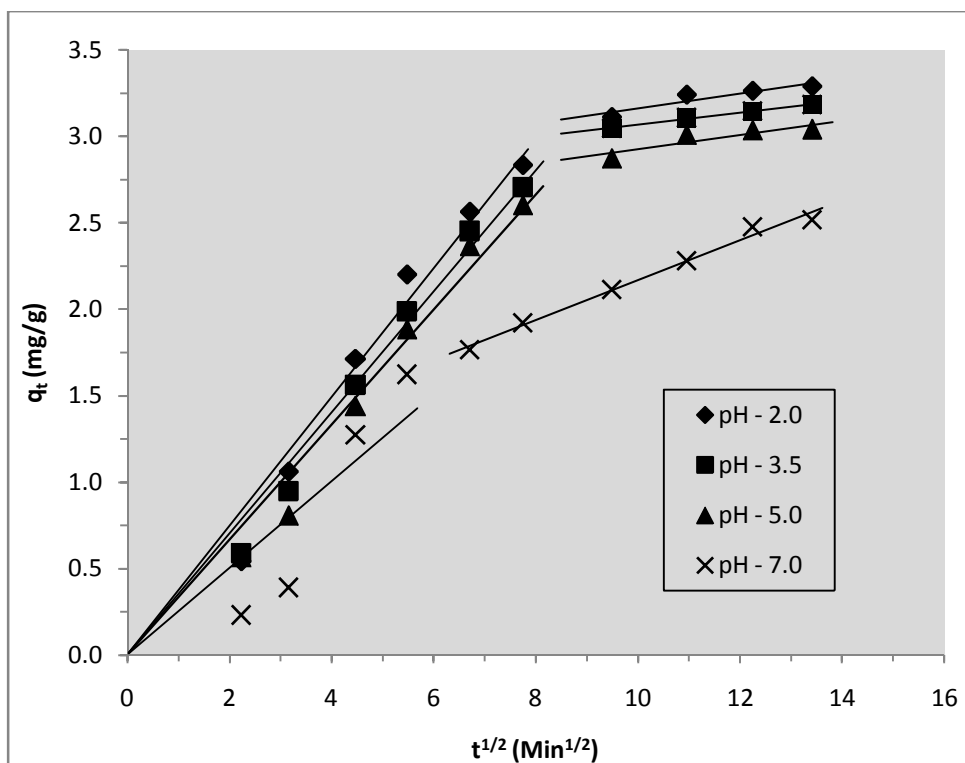


Figure 5.29. Intra-particle diffusion model for the adsorption of Cr(VI) on AC-PA

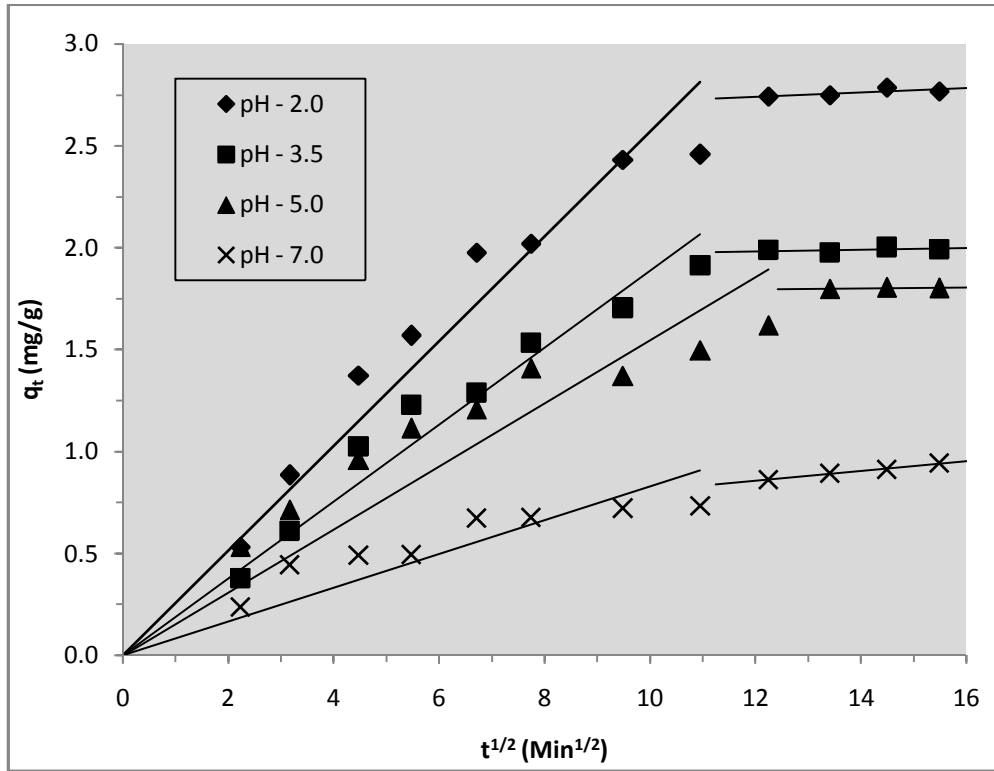


Figure 5.30. Intra-particle diffusion model for the adsorption of Cr(VI) on AC-ZC

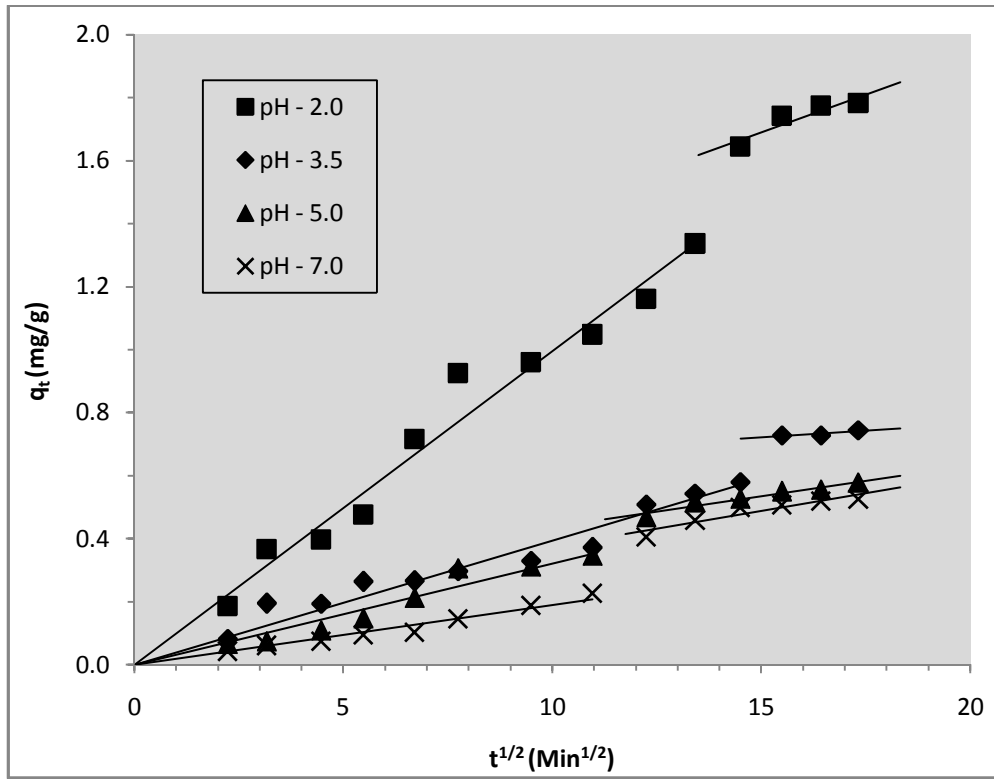


Figure 5.31. Intra-particle diffusion model for the adsorption of Cr(VI) on AC-PH

Table 5.4. Intra-particle diffusion model parameters for adsorption of Cr(VI) on prepared AC samples

pH	AC – PA		AC – ZC		AC – PH	
	K_{id} (mg/g min ^{1/2})	R^2	K_{id} (mg/g min ^{1/2})	R^2	K_{id} (mg/g min ^{1/2})	R^2
2.0	0.373	0.966	0.256	0.919	0.099	0.968
3.5	0.350	0.977	0.188	0.943	0.039	0.943
5.0	0.332	0.965	0.154	0.601	0.032	0.931
6.8	0.251	0.739	0.082	0.515	0.019	0.956

5.4.2. Boyd Model

Due to the double nature of intra-particle diffusion (both film and pore diffusion), and in order to determine the actual rate-controlling step involved in the Cr(VI) adsorption, the kinetic data were further analyzed by using Boyd model. Boyd kinetic equation (Boyd et al., 1947) is represented as

$$F = \frac{6}{\pi^2} \exp(-Bt) \quad (5.11)$$

and

$$F = \frac{q}{q_e} \quad (5.12)$$

where, q_e is the amount of Cr(VI) adsorbed at equilibrium (mg/g) and q represents the amount of Cr(VI) adsorbed at any time t (min), F represents the fraction of solute adsorbed at any time t , and Bt is the mathematical function of F . Equation (XI) can be rearranged by taking as:

$$Bt = -0.4977 - \ln(1 - F) \quad (5.13)$$

The plot of $[-0.4977 - \ln(1 - F)]$ against t was employed to test the linearity of the experimental data. The linearity of these plots is employed to distinguish between external transport and intra-particle transport controlled rates of adsorption of Cr(VI) (Wang et al., 2006). A straight line passing through the origin is an indicative of adsorption processes governed by particle diffusion mechanisms; otherwise they are governed by film diffusion (Mohan and Singh, 2002). The model plots for Cr(VI) adsorption for all the three samples are shown in Figures 5.32, 5.33 and 5.34, respectively.

The diffusion coefficient D_i (m^2/g) is calculated from the B values using the relationship:

$$B = \frac{\pi^2 D_i}{r^2} \quad (5.14)$$

where, D_i is the effective diffusion coefficient of solute in the adsorbent phase and r is the radius of the adsorbent particles.

The Boyd plots of the adsorbents for Cr(VI) adsorption data are neither linear nor passes through the origin. This indicates that, for all the adsorbents film diffusion is the rate-limiting step for the adsorption of Cr(VI). The R^2 and D_i values calculated were presented in Table 5.5. Similar results were obtained by other authors in various studies (El-Kamash et al., 2005; and Wang et al, 2006).

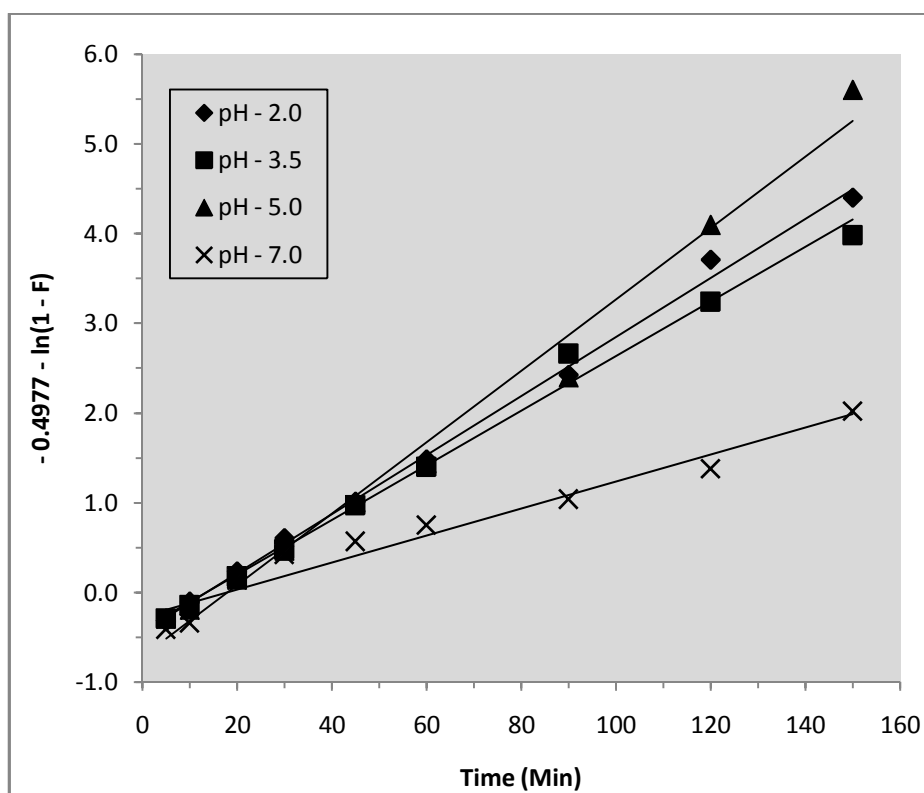


Figure 5.32. Boyd model for the adsorption of Cr(VI) on AC-PA

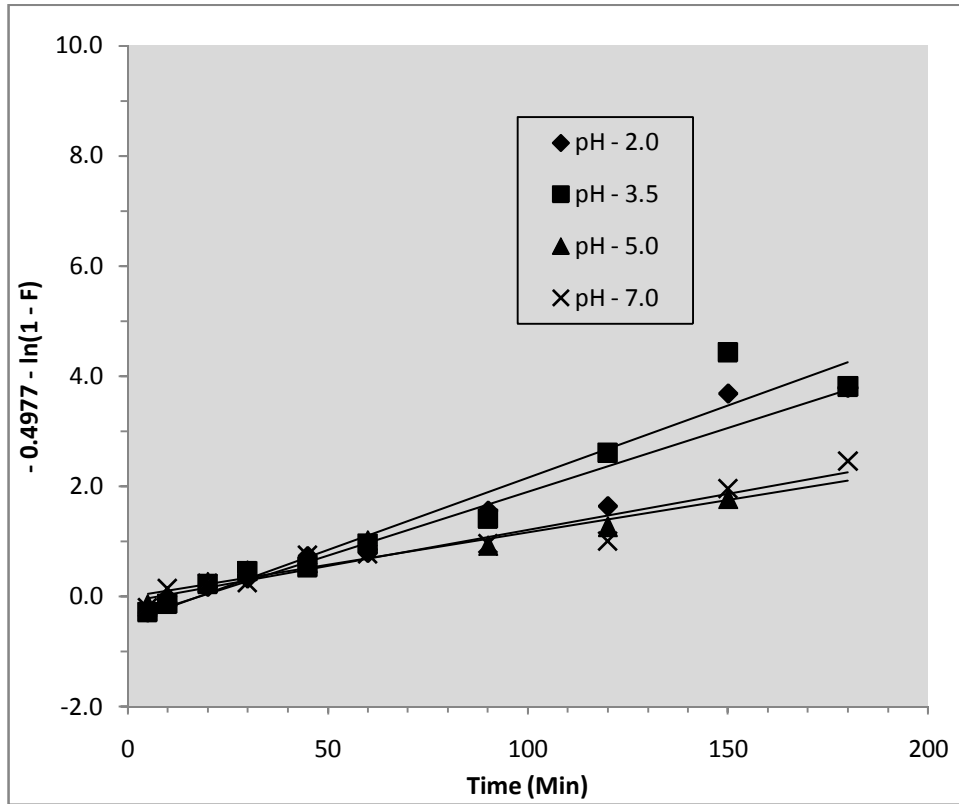


Figure 5.33. Boyd model for the adsorption of Cr(VI) on AC-ZC

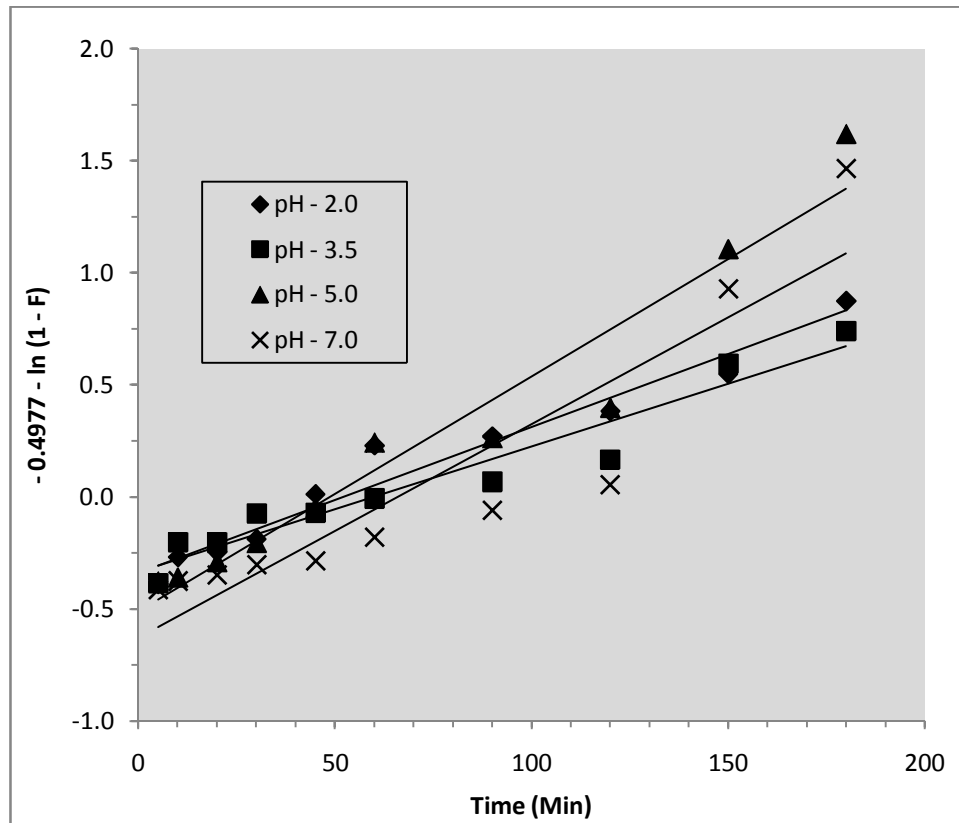


Figure 5.34. Boyd model for the adsorption of Cr(VI) on AC-PH

Table 5.5. Boyd model parameters for the adsorption of Cr(VI) on prepared AC samples

pH	AC-PA			AC-ZC			AC-PH		
	<i>B</i>	<i>D_i X 10⁻⁹</i> (m ² /g)	<i>R</i> ²	<i>B</i>	<i>D_i X 10⁻⁹</i> (m ² /g)	<i>R</i> ²	<i>B</i>	<i>D_i X 10⁻¹⁰</i> (m ² /g)	<i>R</i> ²
2.0	0.028	2.835	0.965	0.019	1.924	0.912	0.006	6.074	0.960
3.5	0.026	2.632	0.962	0.022	2.223	0.905	0.005	5.062	0.936
5.0	0.032	3.240	0.935	0.011	1.114	0.931	0.01	0.101	0.940
7.0	0.012	1.215	0.900	0.012	1.215	0.928	0.009	9.112	0.850

5.5. Adsorption Thermodynamic Study

The nature of the adsorption of Cr(VI) on the prepared ACs was predicted by estimating the thermodynamic parameters. The changes in thermodynamic parameters such as free energy (ΔG°), enthalpy (ΔH°) and entropy (ΔS°) were evaluated from the following equations (Tan et al., 1993; Dwivedi et al., 2008):

$$\Delta G^\circ = -RT \ln K_c \quad (5.15)$$

where, K_c is the equilibrium constant and calculated as

$$K_c = \frac{C_{Ae}}{C_e} \quad (5.16)$$

C_{Ae} (mg/g) and C_e (mg/L) are the equilibrium concentrations for solute on the adsorbent and in the solution, respectively. The K_c values were used to determine the ΔG° , ΔH° and ΔS° . The K_c expressed in terms of the ΔH° (kJ/mol) and ΔS° (kJ/mol) as a function of temperature:

$$\ln K_c = \frac{\Delta H^\circ}{RT} + \frac{\Delta S^\circ}{R} \quad (5.17)$$

ΔH° and ΔS° were obtained from the slopes and intercepts of the plots of $\ln K_c$ against $1/T$ shown in Figure 5.35. The free energy change (ΔG°) indicates the degree of spontaneity of the adsorption process and the higher negative value reflects a more energetically favorable adsorption. The increase in negative value of ΔG° with increase of temperature showed that the adsorption of Cr(VI) on prepared AC samples increased with the rise in temperature. The positive values of ΔH° shown in Table 5.6 confirmed the endothermic nature of the adsorbents

for Cr(VI) adsorption in the studied range 20 – 50 °C. The positive values of ΔS° confirmed the randomness of the adsorption process and it followed the order AC-PA > AC-ZC > AC-PH. Other workers have also been reported similar results for the adsorption of Cr(VI) (Romero-Gonzalez et al., 2005; Oguz, 2005).

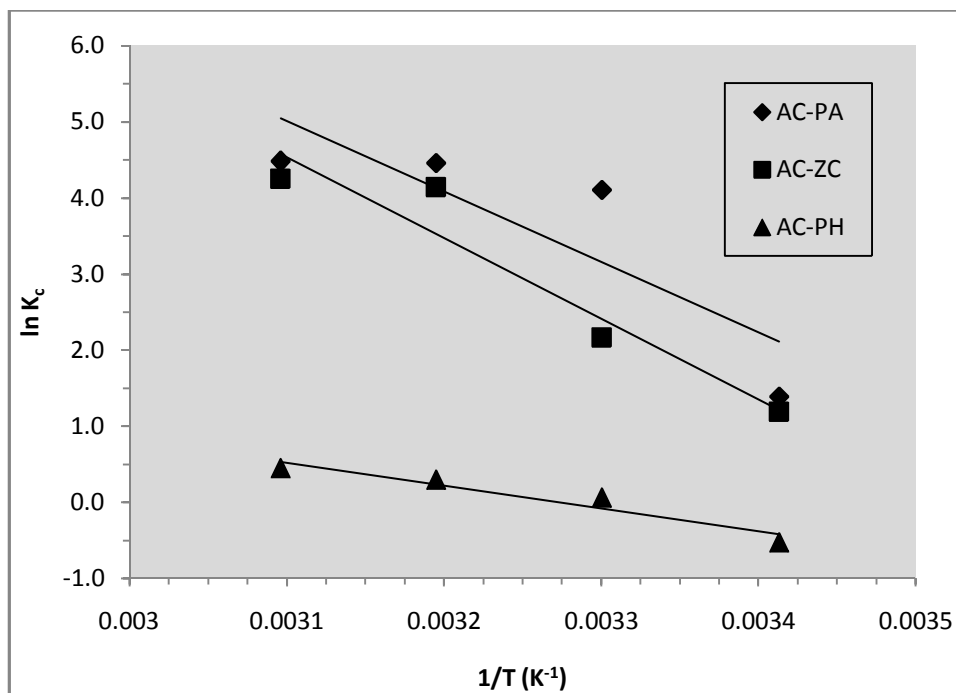


Figure 5.35. Plot of $\ln K_c$ vs. $1/T$ for adsorption of Cr(VI) on prepared AC samples

Table 5.6. Thermodynamic parameters for adsorption of Cr(VI) on AC samples.

AC type	ΔG° (kJ/mol)				ΔH° (kJ/mol)	ΔS° (kJ/mol)
	20 °C	30 °C	40 °C	50 °C		
AC-PA	-3.39	-10.35	-11.61	-12.03	117.99	0.42
AC-ZC	-2.89	-5.45	-10.77	-11.41	112.1	0.39
AC-PH	1.28	-0.15	-0.78	-1.20	31.39	0.10

5.6. Role of Surface Chemistry

The FTIR analysis of H_3PO_4 activated carbon (AC-PA) before and after adsorption of Cr(VI) was carried out to predict the role of surface groups in Cr(VI) adsorption. The spectra of AC-PA was measured within 400 – 4000 cm^{-1} . The functional groups and their respective frequency ranges are summarized in Table 5.7.

The FTIR spectrum of AC-PA before and after adsorption of Cr(VI) was shown in Figure 5.36. The peak observed at $3777 - 3707 \text{ cm}^{-1}$ was due to free hydroxyl groups or surface bonded water (Tangjuank et al., 2009). The bands observed at 3313 cm^{-1} suggest the presence of amine groups. The peaks at $2930 - 2898 \text{ cm}^{-1}$ indicate the presence of C – H stretching vibrations of methyl group (Farinella et al., 2007). The peaks at 1585 cm^{-1} may be attributed to the presence of ketone (C=O) groups. The absorption at 1165 cm^{-1} can be ascribed to –CN stretching and absorption 682 cm^{-1} ($< 1000 \text{ cm}^{-1}$) represents ‘fingerprint’ region which is mainly due to the presence of phosphate groups. These results agree with the surface chemistry of other agricultural by-products such as peach stones (Arriagada et al., 1997), pistachio nut shell (Yang and Lua, 2006) and cashew nut shell (Tangjuank et al., 2009).

After Cr(VI) loading, the band at 3313 cm^{-1} shifted to 3321 cm^{-1} . The shorted peaks at 2930 cm^{-1} and 2898 cm^{-1} disappeared which was attributed to change in nature of binding after interaction with Cr(VI) ions. Besides, the peak corresponding to ketone group was shortened after adsorption of Cr(VI). From the FTIR analysis, it can be confirmed that the surface functional groups such as *N-H* and *C-H* stretchings played very important role in Cr(VI) adsorption. Though, the major percentage of Cr(VI) adsorption was took place by physical adsorption, the surface functional groups have their own importance to drive the Cr(VI) ions to adsorption sites present on the adsorbent.

Table 5.7. Various functional groups found for AC-PA and their frequency ranges

Group frequency (cm^{-1})	Functional group
3770	Free <i>OH</i> groups
3360 - 3310	<i>N-H</i> stretch (Amines)
2935 - 2915	<i>C-H</i> stretch (Methylene)
2900 - 2880	<i>C-H</i> stretch (Methyne)
2360 - 2330	<i>C=N</i> stretch (Nitrile)
1650 - 1550	<i>N-H</i> bend (Amines)
1190 - 1130	<i>C-N</i> stretch (Amines)

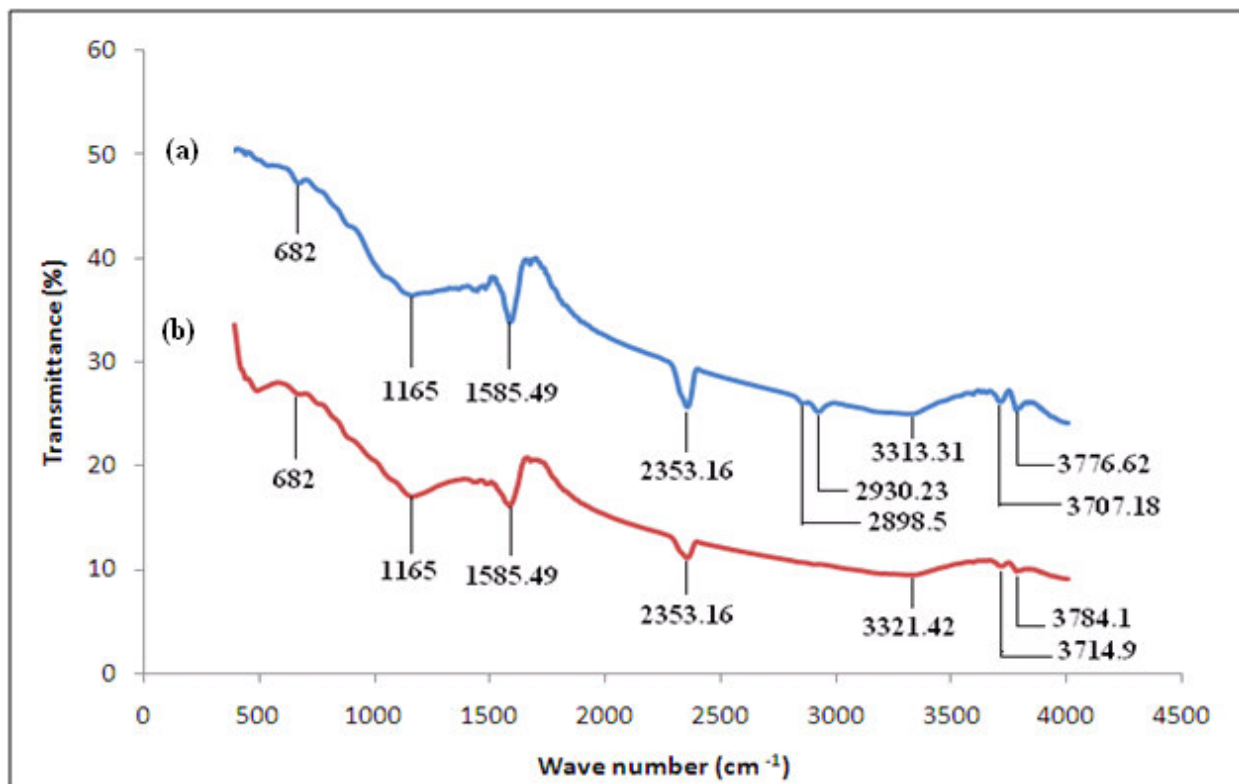


Figure 5.36. Determination of surface functional groups of AC-PA by FTIR (a) before adsorption and (b) after adsorption

5.7. Energy Dispersive X-ray spectroscopy (EDX)

Natural adsorbents bear many oxygen surface groups such as carboxyl, carbonyl, ethers, quinines, lactones and phenols (Serrano et al., 2004).

Energy dispersive X-ray spectroscopy (EDX) data of the three ACs before and after Cr(VI) adsorption was presented in Figure 5.37. In all the three cases, EDX of the ACs before adsorption of Cr(VI) contain the elements P, Zn and K which are incorporated by chemical activation of H_3PO_4 , ZnCl_2 and KOH , respectively. After adsorption, EDX analysis of all samples contains Cr peaks with varying height (percentage). The high adsorption efficiency of AC-PA for Cr(VI) can also be confirmed by observing the EDX profiles of all ACs.

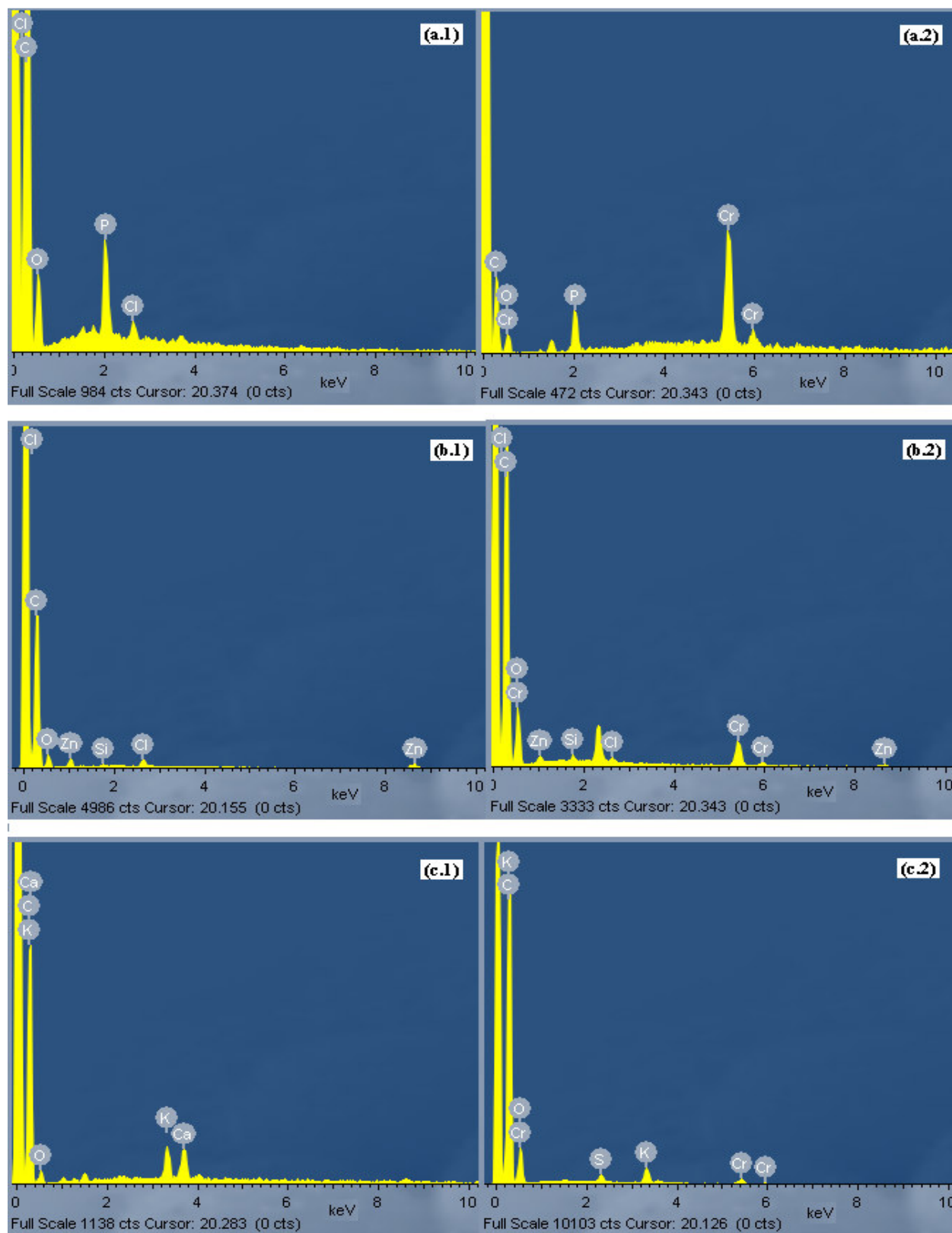


Figure 5.37. EDX analysis of (a) AC-PA, (b) AC-ZC and (c) AC-PH (*a.1* is before adsorption and *a.2* is after adsorption)

5.8. Comparison and Regeneration

Adsorption by activated carbon (AC) is widely used technology for the removal of pollutants in waste water treatment. The economy of the technology greatly depends on the reuse of AC. Various regeneration techniques such as thermal regeneration, chemical regeneration and wet air oxidation are well established (Leng and Pinto, 1996; Torrents et al., 1997; Hu et al., 2003). On the other hand, thermal regeneration process needs to maintain temperature as high as 800 °C, which leads to high energy consumption. It typically involves some loss of carbon and some changes in adsorption characteristics of carbon itself caused due to the enlargement of pores during reactivation process. Regeneration by wet air oxidation requires high pressure oxygen (0.1 – 1.0 MPa) that limits its application. An alternative technique is that of chemical regeneration in which chemical reagents are used for the regeneration of exhausted carbon. The advantages of this process include (1) performance at room temperature (2) requires less energy (3) no additional pressure and (4) the used chemical can be recovered. The prepared activated carbon by H₃PO₄ activation was compared with the commercially available AC for Cr(VI) removal from aqueous phase. In the present study, granular activated carbon exhausted with Cr(VI) was regenerated by using hot water and mild acid (H₂SO₄).

5.8.1. Porous Characteristics

5.8.1.1. N₂ Adsorption – Desorption Isotherms

The N₂ adsorption-desorption isotherms of CAC and AC prepared by H₃PO₄ activation at optimum conditions were shown in Figure 5.38. AC prepared by H₃PO₄ activation shows high adsorption capacity for N₂ gas which indicates the high surface area and pore volume compared to others. The shape of the isotherms clearly indicates that both the samples are rich in micropores including CAC.

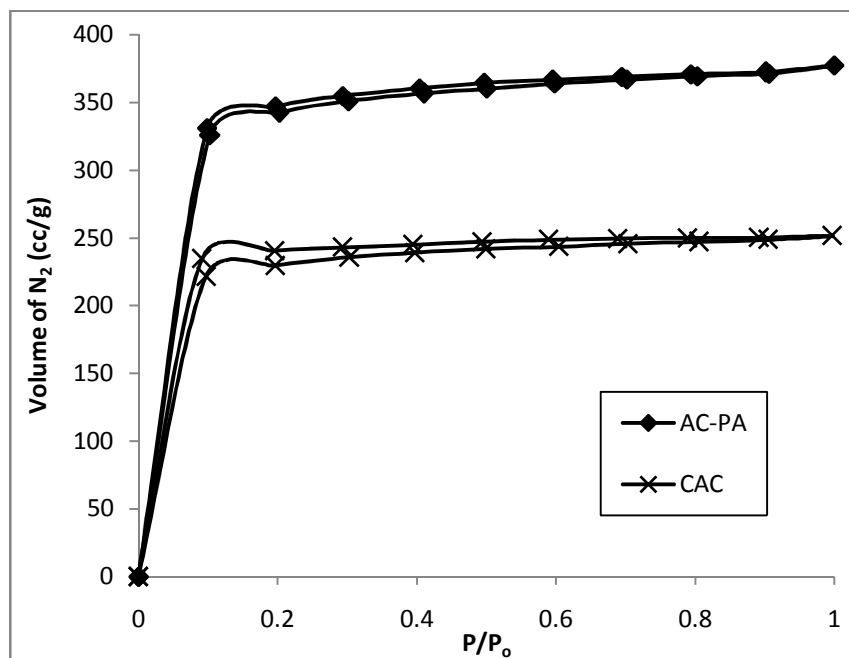


Figure 5.38. N₂ adsorption-desorption isotherms of AC-PA and CAC

The surface area and pore volume of the optimized ACs prepared by different chemical activations and CAC were illustrated in Table 5.8. The surface area and pore volume are high in case of AC prepared by H₃PO₄ activation and are low in case of AC prepared by KOH activation.

The micropore characteristics such as micropore surface area and micropore volume of all the prepared samples at optimum conditions were compared with CAC in Figure 7.3. The contribution of micropores to the total surface area and pore volume is very high and the H₃PO₄ activation results in evolution of more micropores compared to the other activating agents. The surface characteristics of the AC-PA were compared with the CAC and proximate and ultimate analyses were presented in Table 5.9. Different other parameters of ACs were compared in Table 5.10.

Activated carbons, unless preserved in air tight containers, are prone to adsorb moisture from air. The amount of moisture present in prepared ACs depends on various porous characteristics such as surface area and pore volume. Generally, ACs with high surface areas adsorb more moisture when exposed to air. Ash content is the inorganic constituent in carbon that leads to increase in hydrophilic nature and can cause catalytic effects resulting in restructuring during regeneration of AC. Ash content below 2 % is considered to be a superior property of AC. High carbon content in ACs is desirable. The carbon content of AC-PA was

determined as 74.45 % whereas AC-ZC has higher carbon content (83.20 %) than AC-PA. The high oxygen and hydrogen contents in AC-PA were attributed to the H₃PO₄ impregnation. No significant variation was observed in the yield of AC prepared by different chemical activations. Iodine number and methylene blue numbers are approximate methods for estimating the microporosity and mesoporosity in ACs. Iodine number is obviously high in case of AC-PA due to high micropore surface area and micropore volume.

Table 5.8. Comparison of surface characteristics of ACs

Sample	S _T (m ² /g)	V _T (cc/g)	S _{mi} (m ² /g)	V _{mi} (cc/g)	D _{avg} (nm)	(V _{mi} /V _T) X 100
AC-PA	1657	0.58	1625	0.57	1.68	98
AC-ZC	1488	0.53	1339	0.48	1.69	91
AC-PH	937	0.34	924	0.32	1.54	97
CAC	957	0.43	503	0.26	2.47	61

Table 5.9. Proximate and ultimate analyses of prepared ACs and CAC

Sample	Proximate analysis (%)				Ultimate analysis (%)				
	Moisture	Volatiles	Fixed carbon	Ash	C	H	N	S	O
AC-PA	9.35	21.02	72.29	0.85	74.45	4.11	0.44	0.01	20.99
AC-ZC	7.84	15.57	76.13	0.52	83.20	3.26	0.89	0.01	12.64
AC-PH	9.12	15.48	72.51	2.24	76.56	3.94	0.67	0.00	18.83
CAC	6.11	28.73	61.04	0.58	66.21	0.40	2.10	0.00	31.29

Table 5.10. Comparison of other properties of prepared ACs with CAC

Property	AC-PA	AC-ZC	AC-PH	CAC
Yield (%)	76.82	75.14	73.52	-
Bulk density (g/cc)	1.66	1.72	1.77	1.62
Iodine no (mg/g)	1584	1322	857	871
Methylene blue no (mg/g)	480	402	315	333
IEP	4.2	2.0	1.3	1.6

5.8.2. Chromium(VI) Adsorption

Activated carbon prepared at optimum conditions by phosphoric acid (H_3PO_4) activations was compared with the commercial activated carbon (CAC) for removal of Cr(VI) from aqueous phase. Commercial activated carbon was applied for the hexavalent chromium removal from aqueous solution for comparison studies. The batch experimentation was carried out at optimum conditions which are different for different types of activated carbon samples used. Figure 5.39 shows that the removal percentage of Cr(VI) is more in the case of AC-PA. This is due to the high surface area and pore volume of AC-PA than CAC. The experiments were conducted at optimum conditions for AC-PA (pH – 3.5, Cr(VI) concentration – 10.0 mg/L, adsorbent dose – 3.0 g/L and temperature – 30 °C) and for CAC (pH – 2.0, Cr(VI) concentration – 10.0 mg/L, adsorbent dose – 3.0 g/L and temperature – 30 °C).

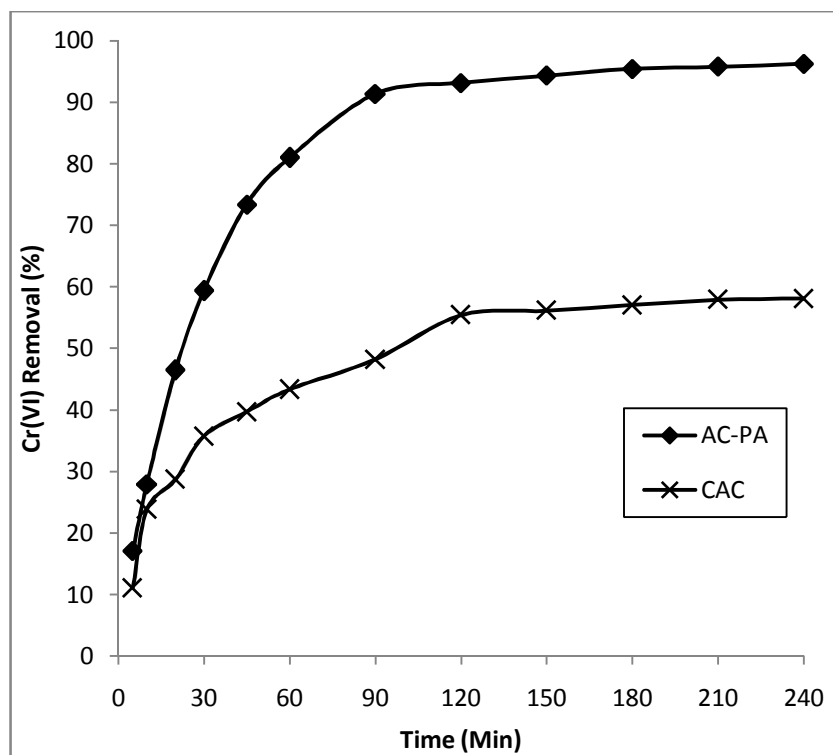


Figure 5.39. Comparison of AC-PA and CAC for Cr(VI) removal efficiency

The adsorption capacities of activated carbons prepared from various precursors were compared in Table 5.11.

Table 5.11. Comparison of Cr(VI) adsorption capacities of activated carbons prepared from different precursors

AC precursor	pH	Initial Cr(VI) concentration (mg/L)	Adsorption capacity (mg/g)	Source
Used Tyres	2.0	60	48.1	Hamadi et al., 2001
Leaf mould	2.0	1000	43.10	Sharma and Forster, 1994
Beech sawdust	1.0	200	16.10	Acar and Malkoc, 2004
Palm shell	3.0 – 4.0	200	12.6	Owlad et al., 2010
Hazelnut shell	2.0	30	17.7	Cimino et al., 2000
Tamarind hull	2.0	25–75	45.95	Verma et al., 2006
Olive cake	2.0	100	33.4	Dakiky et al., 2002
Tarminalia Arjuna nuts	1.0	30	28.4	Mohanty et al., 2005
Hevea brasiliensis sawdust	2.0	-	44.1	Karthikeyan et al., 2005
Peanut shell	2.0	50	8.31	AL-Othman et al., 2012
Tamarind wood	1.0	50	28.02	Acharya et al., 2009
Wheat bran	3.0	15	0.94	Nameni et al., 2008
Sunflower waste	2.0	250	53.76	Jain et al., 2010
Oak wood	2.0	1-100	4.93	Mohan et al., 2011
Oak bark	2.0	1-100	7.51	
Coconut shell	4.0	25	10.88	Babel and Kurniawan, 2000
	2.5	-	20.0	Alaerts et al., 1989
	3.0 – 4.0	120	6.0	Selomulya et al., 1999
	2.0	50	5.95	Tang et al., 2009
Coconut coir	1.5 – 2.0	20–60	38.5	Chaudhuri and Azizan, 2010
Bael Fruit shell	2.0	100	98.6	Present Study
	5.0	100	76.4	Present Study

5.8.3. Regeneration of Spent AC

The spent activated carbon which contains Cr(VI) is unsafe for disposal due to stringent environmental regulations. Hence it is important to propose a methodology to regenerate and reuse the adsorbent so as to reduce the environmental load.

After adsorption of Cr(VI) from aqueous solution, the spent carbon was regenerated by various methods. The regeneration studies explored briefly only for AC-PA as it has more

Cr(VI) removal capacity compared to the other carbons. Thermal regeneration methods were not adopted as the activated carbon used for the adsorption study was prepared at low carbonization temperatures. And the regeneration of AC at high temperatures (700 – 900 °C) may cause the destruction of microporous network developed internally and hence the efficiency of AC might be decreased for Cr(VI) adsorption. In addition to the destruction of porosity, high temperature treatment results in carbon loss due to gasification.

In the present investigation, AC prepared from Bael fruit shell is used for Cr(VI) removal at varying initial concentration (2.0 – 10.0 mg/L). Table 5.12 depicts the comparison for percentage removal of Cr(VI) using fresh and regenerated AC. The regeneration of AC was carried out by simple technique, which is economic. It was observed that there is no significant change in the percentage removal of Cr(VI), but it decreases slightly with each cycle of AC regeneration. Loss of carbon due to the regeneration is very less and about 99.3 % of the spent AC was regenerated successfully for further application after 1st cycle of regeneration. The spent AC was washed with hot water (80 °C) and 0.1 M H₂SO₄ to remove Cr(VI) from AC surface for each cycle of regeneration.

Table 5.12. Regeneration of AC and efficiency of regenerated AC for Cr(VI) adsorption.

Sample stage	Cr(VI) adsorption (%)	Cr(VI) recovered (%)		Total recovery (%)	Cr(VI) retained on AC (%)	AC regeneration (%)
		Step 1	Step 2			
		Hot water (70 °C)	H ₂ SO ₄ (0.1 M)			
1 st cycle	98.74	78.34	16.86	95.20	3.54	99.28
2 nd cycle	92.85	72.23	17.14	89.37	3.48	98.54
3 rd cycle	87.12	69.04	14.73	83.77	3.35	97.13
4 th cycle	82.17	64.00	11.38	75.38	6.79	95.92

Modeling of Chromium(VI) Adsorption

An effective system for any process can be established only after optimization of its process parameters. Conventional and classical methods of studying a process involve studying of one factor at a time by maintaining other factors at unspecified constant levels. This approach does not depict the combined effect of all the parameters involved in the process. This method is not only tedious but also time consuming (Elibol, 2002). These limitations of a classical method can be effectively conquered by optimizing all the parameters collectively by statistical experimental designs such as factorial design (Box et al., 1978; Brasil et al., 2005; Montgomery, 1977). These designs reduce the total number of experiments in order to achieve the best overall optimization of the process.

6.0. Summary

The modeling of Cr(VI) adsorption on prepared ACs (AC-PA, AC-ZC, and AC-PH) was carried out by using Design of Experiments (DoE). A two-level and four-factor Full Factorial Design (FFD) was employed for the process modeling. Different process parameters such as pH, initial concentration of Cr(VI), adsorbent dose and temperature were taken as variables for the designing of experimental matrix. Effects of main factors and their interactions on the response were estimated. Optimization was carried out by using Desirability (D) function to estimate the optimum conditions to achieve better response i.e. percentage of Cr(VI) removal.

6.1. Full Factorial Design

Full Factorial Design (FFD), determines the effect of each factor on response as well as how the effect of each factor varies with the change in level of the other factors (Arenas et al., 2006). Interaction effects of different factors could be attained using design of experiments (DoE) (Brasil et al., 2005, Montgomery 1977). Full factorial design (FFD) comprises the greater

precision in estimating the overall main factor effects and interactions of different factors. In full factorial design every setting of every factor appears with every setting of every other factor. Factorial designs are strong candidates in testing treatment variations. Instead of conducting a series of independent studies we can combine these studies into one. A common experimental design is one with all input factors set at two levels each. These levels are called 'high' and 'low' or '+1' and '-1' respectively. If there are k factors each at 2 levels, a full factorial design have 2^k runs.

A 2^4 full factorial design was employed in this investigation. Thus, a total of 16 experiments were performed for each case. The modeling of the process focused on how Cr(VI) removal efficiency of prepared ACs (AC-PA, AC-ZC and AC-PH) varies with the change in process parameters such as pH, initial Cr(VI) concentration, adsorbent dose and temperature.

6.2. Designing of Experimental Matrix

Different process parameters such as pH, initial concentration of Cr(VI), adsorbent dose and temperature were taken as variables for the designing of experimental matrix. Each factor was studied at two levels 'low' and 'high' level. To analyze the factorial design, the original measurement units for the experimental factors (uncoded units) were transformed into coded units. The factor levels are coded as -1 (low) and +1 (high). The response was expressed as the removal percentage (% R) of Cr(VI).

The experimental runs were carried out with all the prepared AC samples (AC-PA, AC-ZC and AC-PH). The licensed statistical software Design Expert – 7.1.6 was used to design and analyze the experimental matrix, in order to measure the effect of various factors on the removal of Cr(VI) from aqueous phase. The levels and ranges of the studied factors are presented in [Table 6.1](#).

Table 6.1. Experimental ranges and levels of the factors used in the factorial design

Independent variable	Coded symbol	Range and level	
		-1	+1
pH	<i>A</i>	2	7
Initial metal ion concentration (mg/l)	<i>B</i>	2	10
Adsorbent dose (g/l)	<i>C</i>	1	5
Temperature (°C)	<i>D</i>	20	40

The design matrix of all the factors in coded and actual values for all the experimental runs was shown in [Table 6.2](#).

Table 6.2. Factorial design matrix with coded and real values

Run	Coded values				Real values			
	A	B	C	D	pH	Cr(VI) Conc. (mg/L)	Adsorbent dose (g/L)	Temperature (°C)
1	-1	-1	-1	-1	2	2	1	20
2	+1	-1	-1	-1	7	2	1	20
3	-1	+1	-1	-1	2	10	1	20
4	+1	+1	-1	-1	7	10	1	20
5	-1	-1	+1	-1	2	2	5	20
6	+1	-1	+1	-1	7	2	5	20
7	-1	+1	+1	-1	2	10	5	20
8	+1	+1	+1	-1	7	10	5	20
9	-1	-1	-1	+1	2	2	1	40
10	+1	-1	-1	+1	7	2	1	40
11	-1	+1	-1	+1	2	10	1	40
12	+1	+1	-1	+1	7	10	1	40
13	-1	-1	+1	+1	2	2	5	40
14	+1	-1	+1	+1	7	2	5	40
15	-1	+1	+1	+1	2	10	5	40
16	+1	+1	+1	+1	7	10	5	40

The general mathematical model for 2^4 factorial designs in coded values can be given as:

$$\%R = X_0 + X_1A + X_2B + X_3C + X_4D + X_5AB + X_6AC + X_7AD + X_8BC + X_9BD + X_{10}CD + X_{11}ABC + X_{12}ABD + X_{13}ACD + X_{14}BCD + X_{15}ABCD \quad (6.1)$$

where, R is the percentage removal of Cr(VI), X_0 is the global mean, X_i represents the other regression coefficients and A, B, C and D are the coded symbols for the factors under study.

The percentage removal of Cr(VI) by the different activated carbons prepared by activating with chemicals H_3PO_4 (AC-PA), $ZnCl_2$ (AC-ZC) and KOH (AC-PH) was compared with the commercially available activated carbon (CAC). The responses i.e. percentage removal of Cr(VI) (%R) for the design matrix shown in Table 6.2 by different activated carbons were presented in Table 6.3.

Table 6.3. Responses for the Cr(VI) removal by different ACs as per the designed experimental matrix

Run	% R (AC-PA)	% R (AC-ZC)	% R (AC-PH)
1	68.86	23.33	99.62
2	57.11	98.14	78.47
3	94.78	86.57	79.58
4	92.81	85.49	98.78
5	69.44	99.83	95.29
6	60.84	63.64	89.05
7	94.90	81.13	11.02
8	91.41	99.65	4.58
9	69.30	99.71	6.43
10	62.10	82.67	81.64
11	96.80	11.40	28.82
12	92.26	62.10	13.51
13	72.94	49.09	80.97
14	60.53	96.40	99.82
15	96.25	99.38	45.63
16	93.50	54.09	95.46

6.3. Modeling of Chromium(VI) Removal by AC-PA

The individual runs of experimental design shown in Table 6.2 are conducted by using AC-PA and the responses were measured. A linear regression model was fitted for the experimental data using least square technique. The model coefficients, effects and standard error of the factors and interactions are shown in Table 6.4.

Table 6.4. Estimated regression coefficients of model terms and their effects on the response for AC-PA

Factor / Term	Effect	Coefficient	df	Standard error	95% CI Low	95% CI High
Intercept	-	79.61	1	0.19	79.18	80.05
A	-6.59	-3.29	1	0.19	-3.73	-2.86
B	28.95	14.47	1	0.19	14.07	14.91
C	0.72	0.36	1	0.19	-0.076	0.80
D	1.69	0.85	1	0.19	0.41	1.28
AB	3.40	1.70	1	0.19	1.26	2.14
BC	-0.87	-0.44	1	0.19	-0.87	0.001
ABCD	1.46	0.73	1	0.19	0.29	1.17

df – degrees of freedom

The model coefficients are obtained by dividing the effects by two. p-value is the probability value that is used to determine the effects in the model that are statistically significant. Factors having p-value less than 0.05 are considered to be statistically significant for a 95% confidence level. After discarding the insignificant terms the resultant model is represented as:

$$\%R = 79.61 - 3.73A + 14.07B - 0.08C + 0.41D + 1.26AB - 0.87BC + 0.29ABCD \quad (6.2)$$

After estimating the main effects, the effect of interactions were determined by performing the analysis of variance (ANOVA). Sum of squares (SS) of each factor quantifies its importance in the process and as the value of SS increases, the significance of the corresponding factor in the process also increases. The ANOVA results for the Cr(VI) removal by AC-PA were presented in Table 6.5.

Table 6.5. ANOVA results for Cr(VI) removal by AC-PA

Factor	Sum of squares	df	Mean square	F-value	p-value
Model	3596.00	7	513.85	892.72	< 0.0001
A	173.60	1	173.60	301.61	< 0.0001
B	3351.96	1	3351.96	5823.46	< 0.0001
C	2.09	1	2.09	3.63	0.0931
D	11.46	1	11.46	19.91	0.0021
AB	46.25	1	46.25	80.34	0.0001
BC	3.05	1	3.05	5.29	0.0504
ABCD	8.53	1	8.53	14.82	0.0049
Residual	4.60	8	0.58		
Total	3601.54	15			

df – degrees of freedom

6.3.1. Pareto Plot

Pareto plot visually represents the absolute values of the effects of main factors and the effects of interaction of factors. A reference line is drawn to indicate that the factors which extend past this line are potentially important (Antony, 2003). The pareto plot is a useful tool for showing the relative size of effects. The effects of all the factors and their interactions were shown in Figure 6.1. Effects above t-value (2.386) limit are possibly significant terms in the model. The main factors such as pH (A), concentration (B), and temperature (D) and interactions such as AB and ABCD are significantly influenced the response. Other terms like C and BC were added to the model because of their importance.

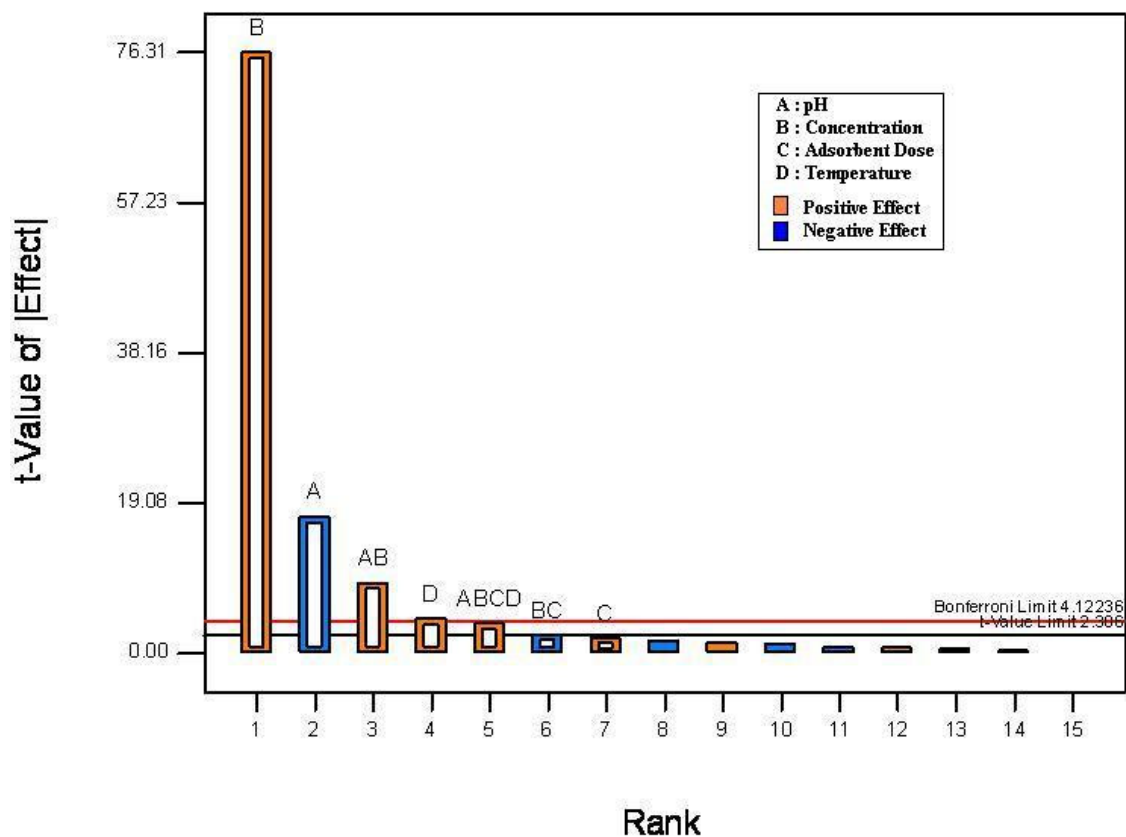


Figure 6.1. Pareto plot for effects of individual factors and interactions for Cr(VI) removal by AC-PA.

6.3.2. Main Effects

The main factors and their effect on the response were shown graphically in Figure 6.2. Among the four main factors, concentration of Cr(VI) in solution greatly influences the response. The sign of the main effect indicates the direction of effect. From the figure, the effect of concentration was characterized by a greater degree of departure from the overall mean having positive effect on the response, whereas pH has a negative effect i.e. with the increase of pH the percentage removal of Cr(VI) decreased. Adsorbent dose and temperature have very little effect comparing to the pH and concentration.

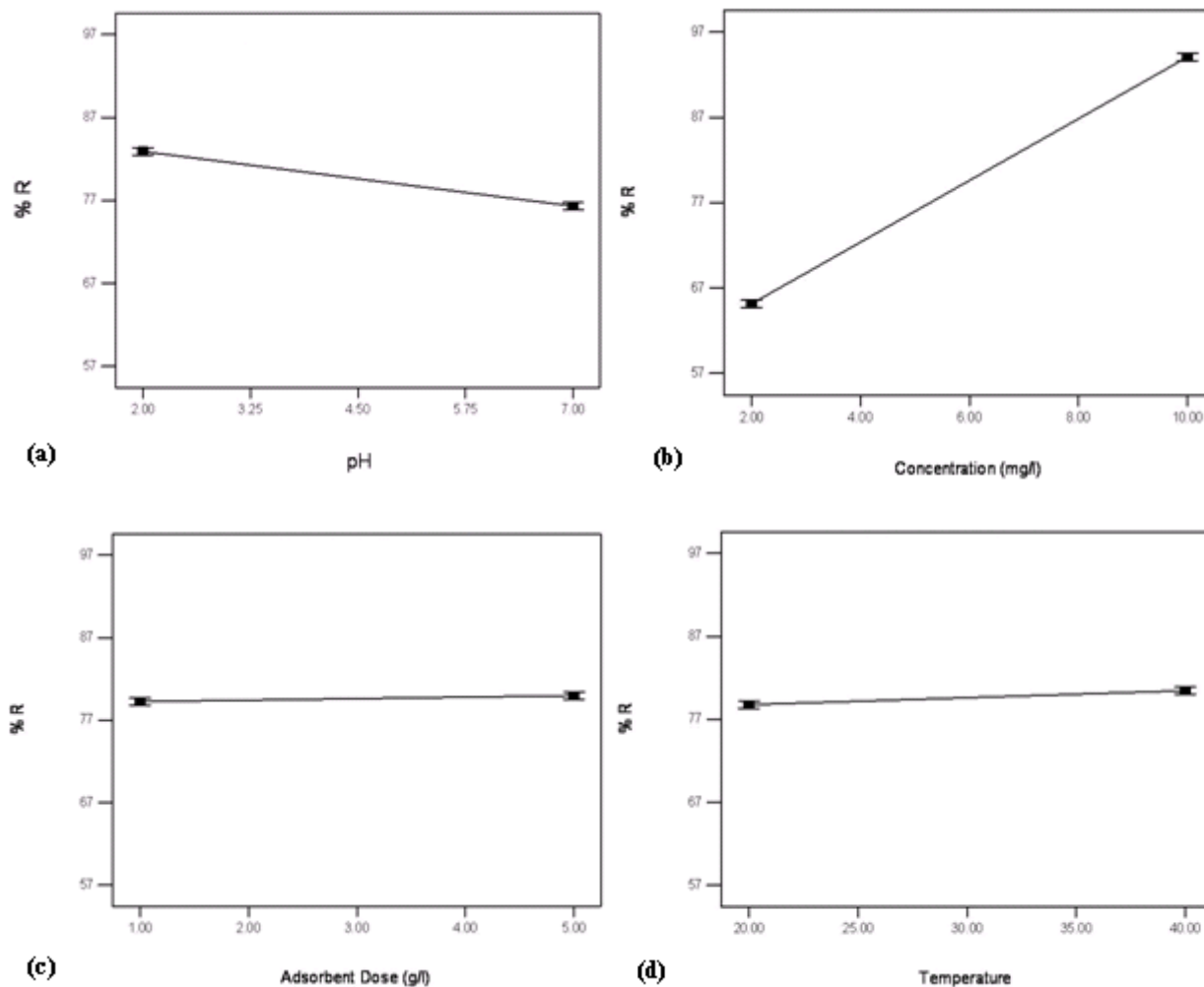


Figure 6.2. Effect of main factors on response for AC-PA (a) pH, (b) concentration, (c) adsorbent dose and (d) temperature.

6.3.3. Interaction Effects

The contour plots of interaction of factors were shown in [Figure 6.3](#). Compared to the effects of main factors, the effect of interaction of factors on the response is very less. From the [Table 6.5](#), the interaction effects pH * concentration (AB) and concentration * adsorbent dose (BC) are considered to be significant in the case of AC-PA for Cr(VI) removal.

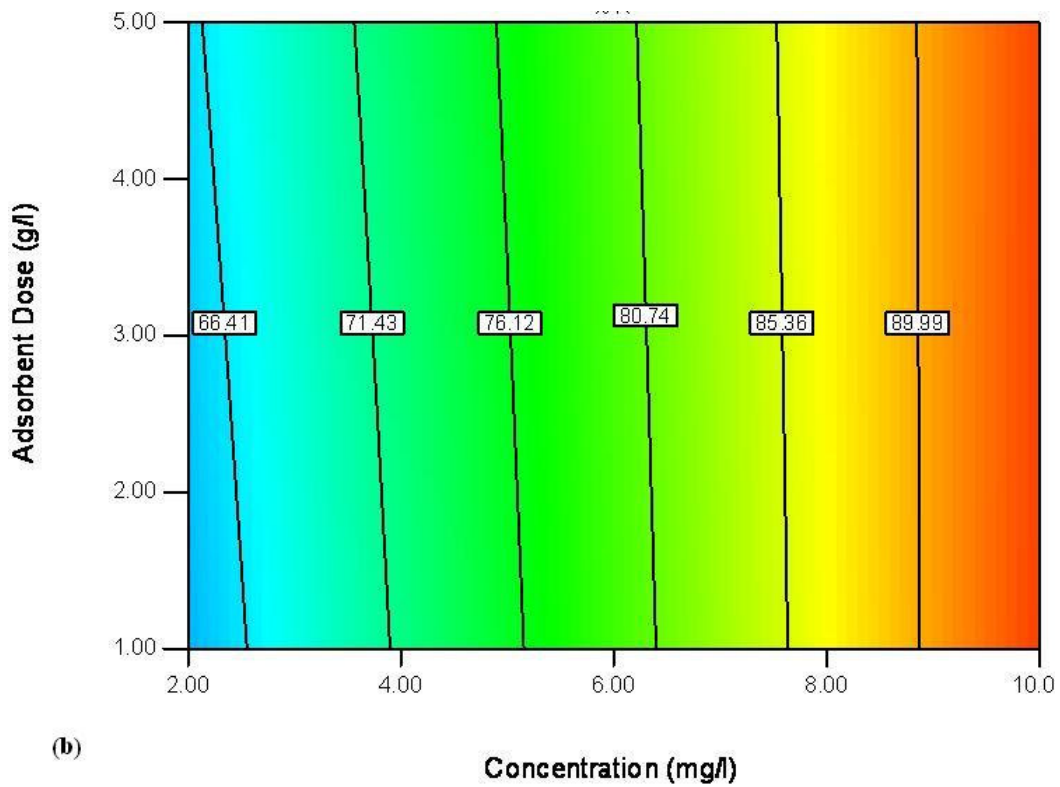
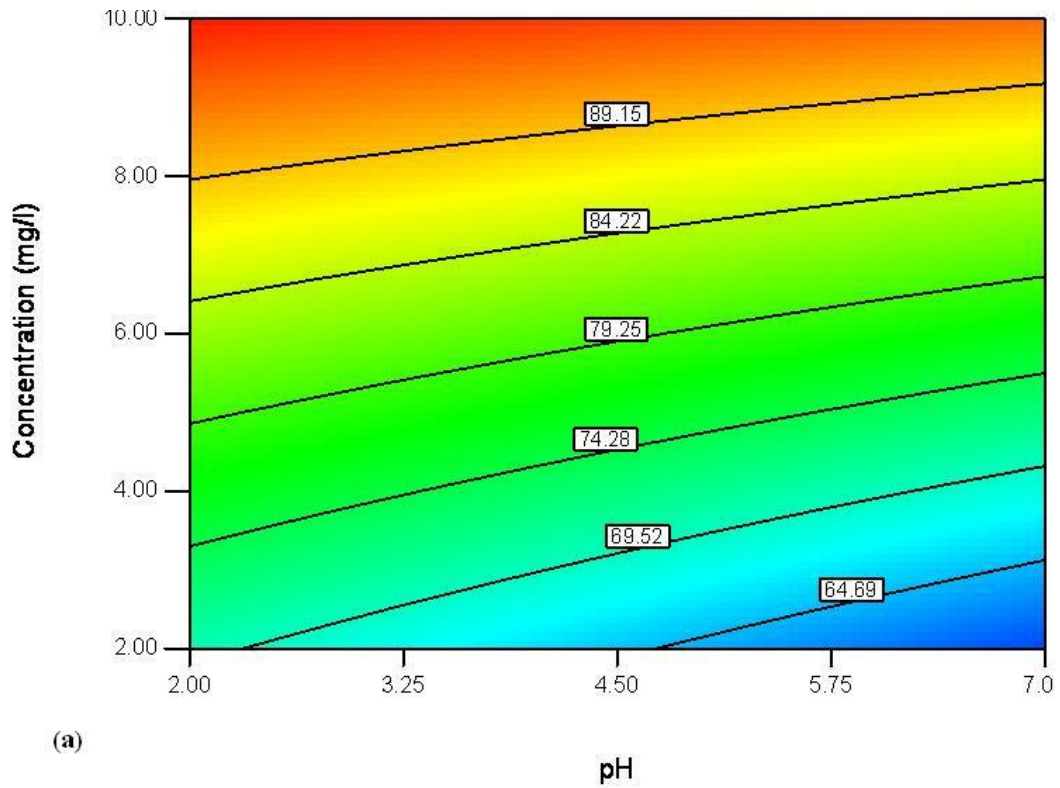


Figure 6.3. Contour plots of interactions for AC-PA (a) pH * Concentration and (b) Concentration * Adsorbent dose

6.3.4. Normal Probability Plot

The normal probability plot indicates whether the residuals follow a normal distribution, in which case the points will follow a straight line. The normality of the data can be checked by plotting a normal probability plot of the residuals. If the data points fall fairly close to the straight line, then the data are normally distributed (Antony, 2003). The statistical analysis of the data in terms of the standardized residual was conducted to verify the normality of the data. The normal probability plot of the residuals of AC-PA for Cr(VI) adsorption was shown in Figure 6.4. The data points fairly close to the straight line indicate that the experiments came from a normally distributed population.

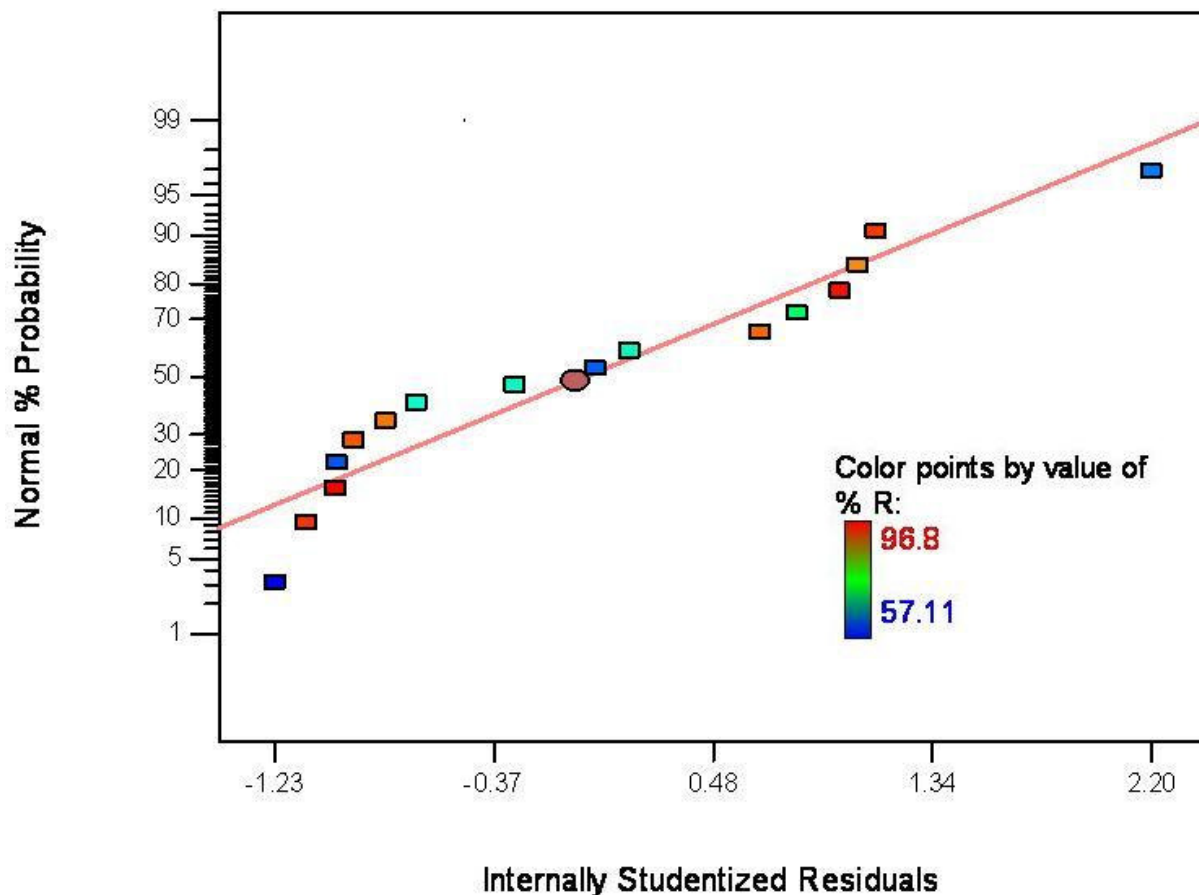


Figure 6.4. Normal probability plot of residuals for Cr(VI) removal by AC-PA.

6.3.5. Optimization

Optimization of Cr(VI) removal was carried out by a multiple response method called desirability (D) function to optimize the process parameters such as pH, initial Cr(VI)

concentration, adsorbent dose and temperature. The goal of optimization was to improve adsorptive removal of Cr(VI) by targeting the process parameters to desired levels. In the present study, pH and temperature were set to be within the studied range, whereas initial concentration was set to maximum and adsorbent dose targeted to minimum within the range. The 3D surface plot of the Cr(VI) removal by AC-PA was shown in Figure 6.5.

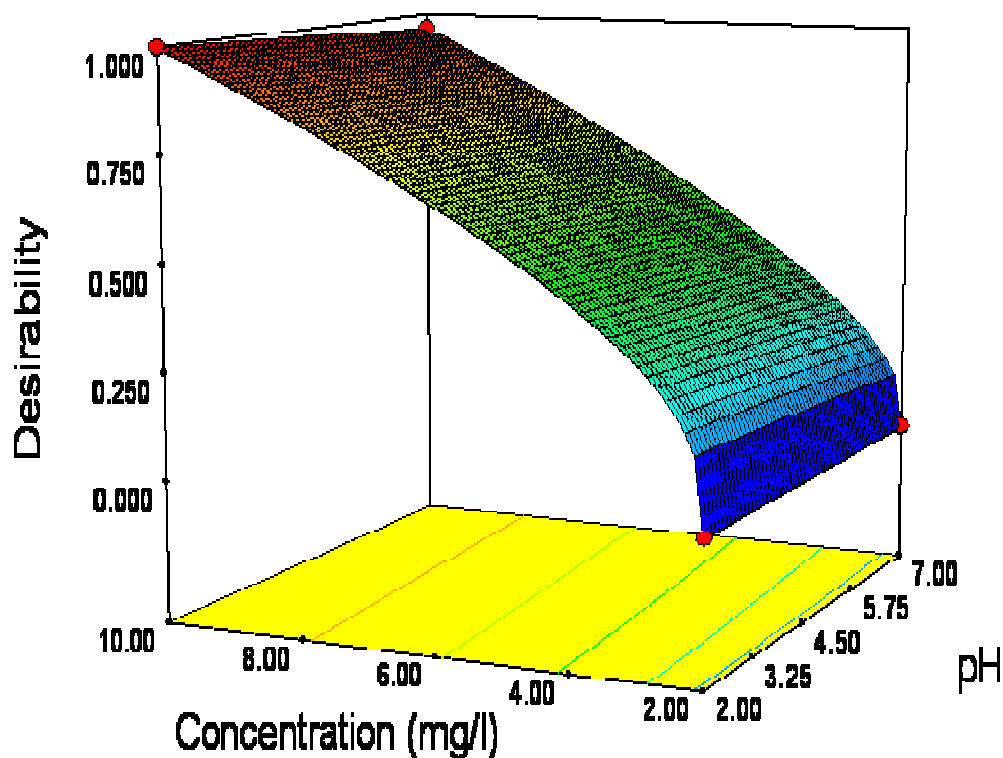


Figure 6.5. Desirability fitted 3D surface plot for Cr(VI) removal by AC-PA (Adsorbent dose – 1 g/L and Temperature – 40 °C).

6.3.6. Validation Experiments

In order to verify the optimization results, an experiment was performed under predicted conditions by the developed model. The model predicted 93.42 % removal of Cr(VI) at pH – 4.26, concentration – 10 mg/L, adsorbent dose – 1.0 g/L and temperature 20 °C. The experimental value obtained at these conditions is 92.71 % and is closely in agreement with the result obtained from the model and hence validated the findings of the optimization.

6.4. Modeling of Chromium(VI) Removal by AC-ZC

The experimental runs shown in Table 6.2 were performed by using activated carbon prepared by zinc chloride activation (AC-ZC). A linear regression model was developed for the experimental data and the coefficients, effects and standard error values are presented in Table 6.6.

Table 6.6. Estimated regression coefficients of model terms and their effects on the response for AC-ZC

Factor / Term	Effect	Coefficient	df	Standard error	95% CI Low	95% CI High
Intercept	–	73.91	1	0.70	72.25	75.57
A	-27.00	-13.50	1	0.70	-15.16	-11.84
B	-33.32	-16.66	1	0.70	-18.32	-15.00
C	23.01	11.51	1	0.70	9.85	13.17
D	1.17	0.58	1	0.70	-1.07	2.24
AB	-12.52	-6.26	1	0.70	-7.92	-4.60
BC	19.78	9.89	1	0.70	8.23	11.55
ACD	4.64	2.32	1	0.70	0.66	3.98
ABCD	3.97	1.99	1	0.70	0.33	3.64

df – degrees of freedom

Depending on the ANOVA results the insignificant terms are discarded from the model and developed model was give as:

$$\%R = 73.91 - 13.50A - 16.66B + 11.51C + 0.58D - 6.26AB + 9.89BC + 2.32ACD + 1.99ABCD \quad (6.3)$$

The value of sum of the squares signifies the importance of the model term. The ANOVA results of the Cr(VI) removal data by AC-ZC was presented in Table 6.7.

Table 6.7. ANOVA results for Cr(VI) removal data by AC-ZC

Factor	Sum of squares	df	Mean square	F-value	p-value
Model	11823.78	8	1477.97	187.64	< 0.0001
A	2915.88	1	2915.88	370.18	< 0.0001
B	4442.19	1	4442.19	563.96	< 0.0001
C	2118.28	1	2118.28	268.93	< 0.0001
D	5.47	1	5.47	0.69	0.4320
AB	627.43	1	627.43	79.65	< 0.0001
BC	1565.45	1	1565.45	198.74	< 0.0001
ACD	85.98	1	85.98	10.92	0.0131
ABCD	63.09	1	63.09	8.01	0.0254
Residual	55.14	7	7.88		
Total	11878.91	15			

df – degrees of freedom

6.4.1. Pareto Plot

The comparison between the relative effects of all the significant factors was shown by pareto chart in [Figure 6.6](#). From the figure, it can be observed that the main factors and some of interactions of different factors play important role. The main factors like concentration of Cr(VI) (B), pH (A) and adsorbent dose (C) and interaction effects such as BC, AB, ACD and ABCD have significant effect on the response. Though the effect of temperature (D) is not significant, it was included in the model considering its importance in the interaction with the other factors.

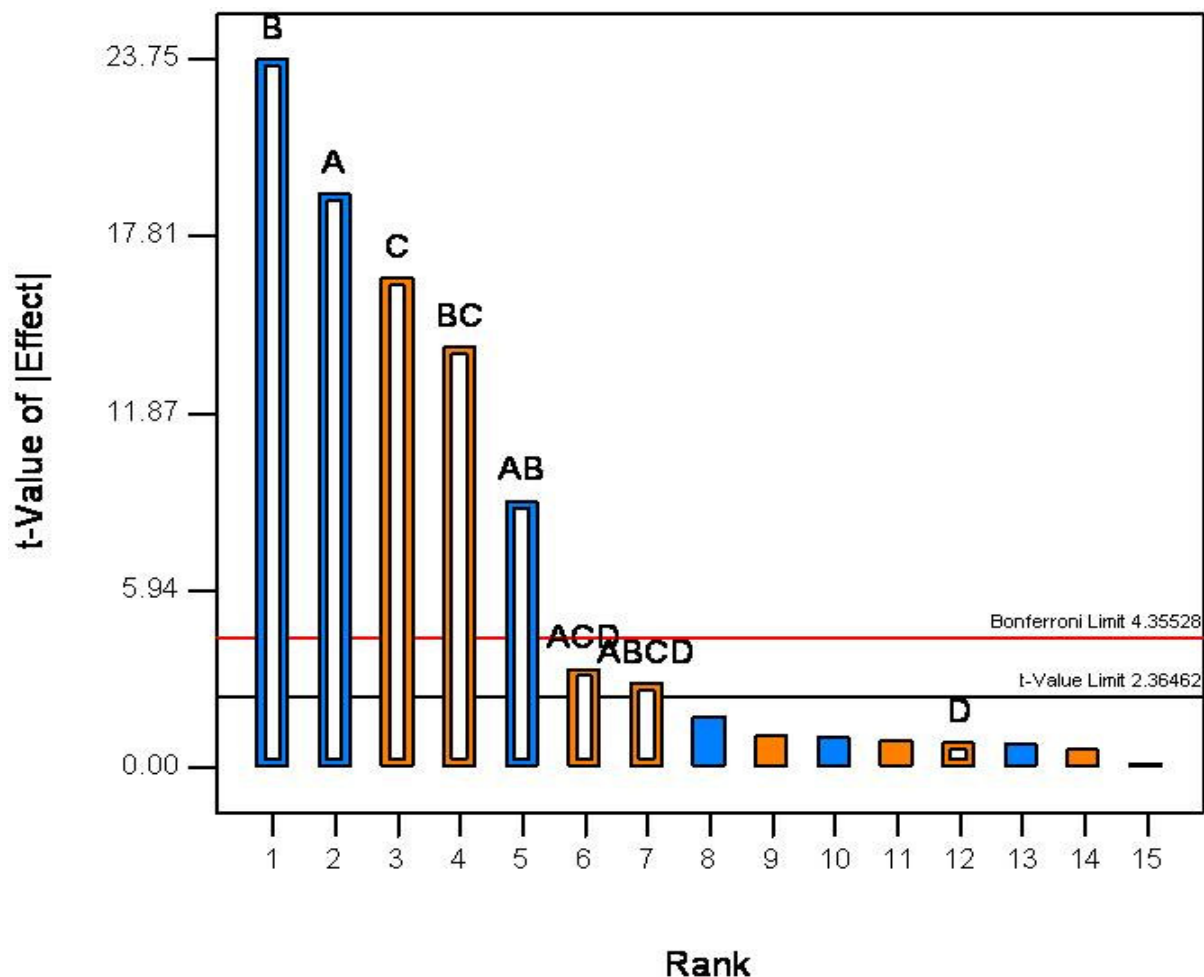


Figure 6.6. Pareto plot for effects of individual factors and interactions for Cr(VI) removal by AC-ZC.

6.4.2. Main Effects

The effect of main factors on the response was shown in Figure 6.7. The main factors like pH and concentration of Cr(VI) have affected negatively i.e. with the increase of pH and concentration the removal percentage decreased to a great extent. The other factors, adsorbent dose and temperature had a positive effect on the response. From the figure it can be clearly observe that the effect of temperature on the response is very less in the studied range when compared to the other factors.

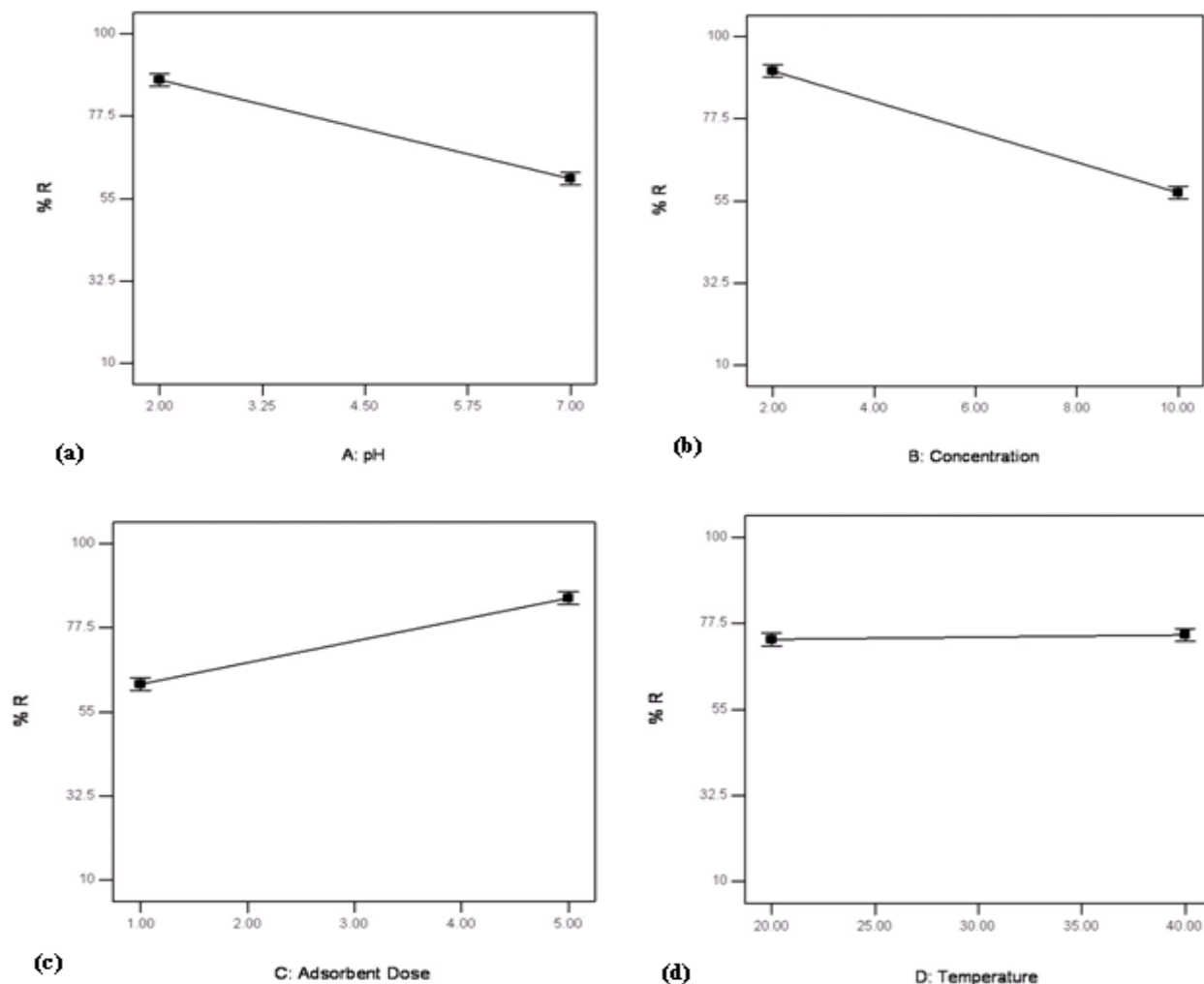
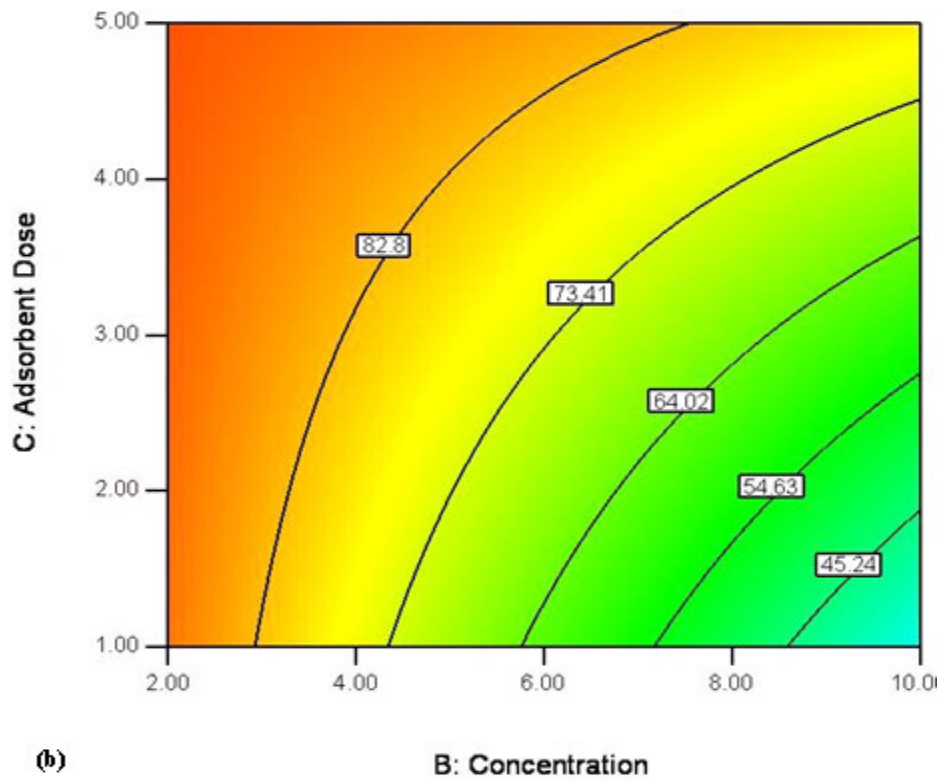
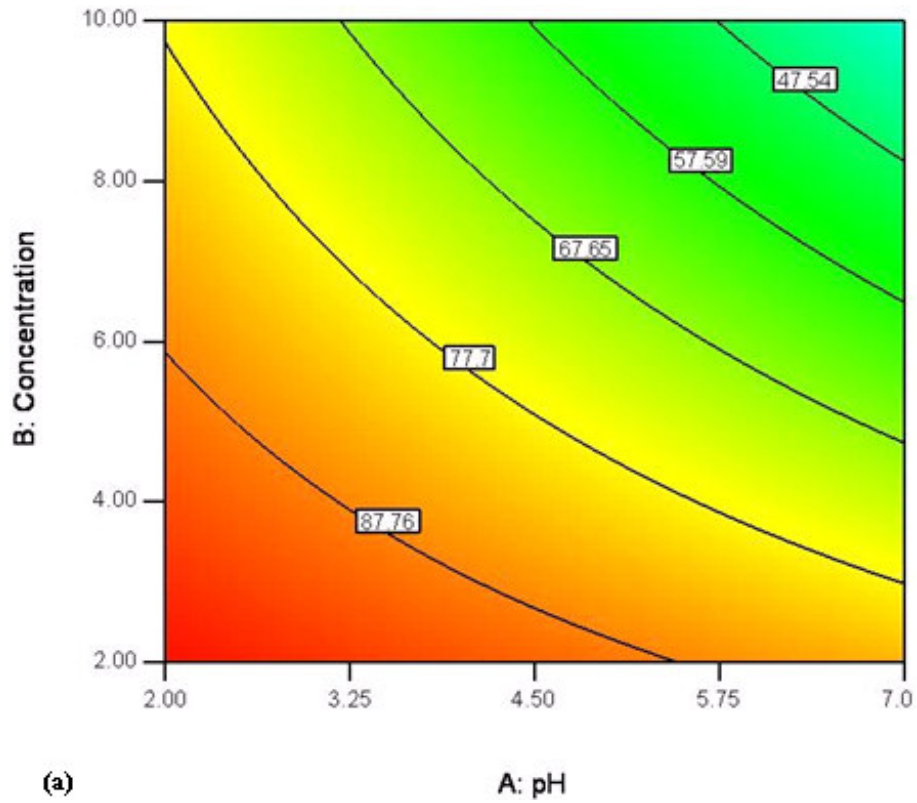


Figure 6.7. Effect of main factors on response for AC-ZC (a) pH, (b) concentration, (c) adsorbent dose and (d) temperature.

6.4.3. Interaction Effects

The effect of interaction of different factors on the response can be observed from the pareto plot (Figure 6.6). The two interactions pH * concentration (AB) and concentration * adsorbent dose (BC) have significant effect comparing to the other interactions. From the Figure 6.8(a), the rapid decrement in the response can be observed with the increase of pH and concentration. From the Figure 6.8(b), if the concentration of Cr(VI) is low then the maximum removal can be achieved by maintaining the adsorbent dose at even low level but with the increase in concentration the adsorbent dose should be increase in order to achieve maximum removal. Figure 6.8(c) represents the cube plot for the interaction of three significant factors pH, adsorbent dose and temperature.



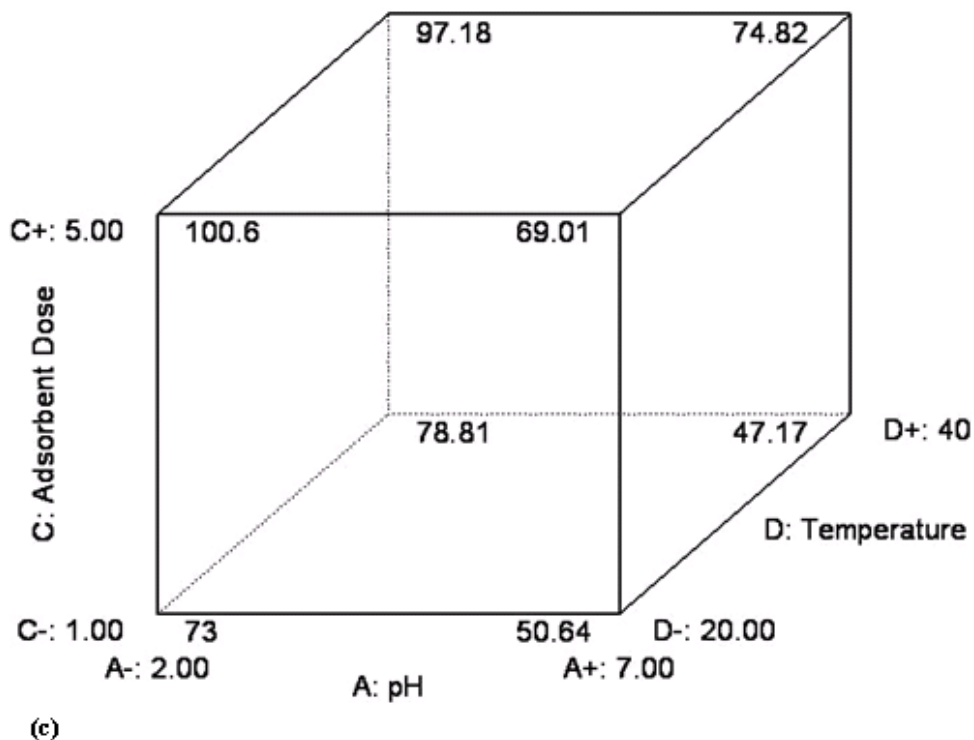


Figure 6.8. Contour and cube plots of interactions for AC-ZC (a) pH * Concentration and (b) Concentration * Adsorbent dose (c) pH*Adsorbent dose*Temperature.

6.4.4. Normal Probability Plot

The normality of the data obtained for the removal of Cr(VI) by AC-ZC was checked by plotting a normal probability plot of the residuals. The data points fell fairly close to the straight line indicate that the data are normally distributed. The normal probability plot of the residuals of AC-ZC for Cr(VI) adsorption was shown in [Figure 6.9](#). The data points fairly close to the straight line indicate that the experiments came from a normally distributed population.

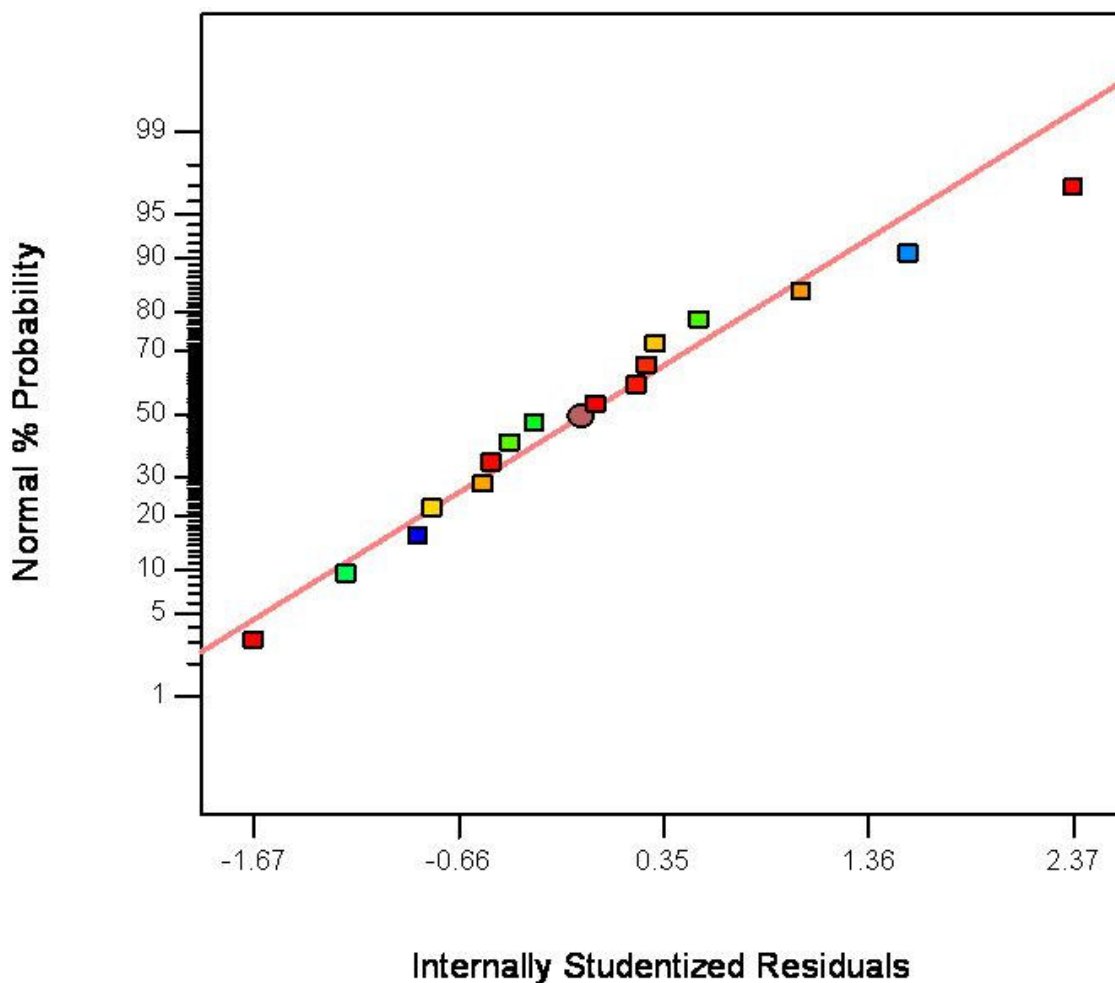


Figure 6.9. Normal probability plot of residuals for Cr(VI) removal by AC-ZC.

6.4.5. Optimization

Optimization of Cr(VI) removal by AC-ZC was performed by using desirability (D) function. The main factors pH, concentration, adsorbent dose and temperature were optimized by targeting maximum removal ($D=1$) of Cr(VI). Total 39 solutions were found with the different combinations of the main factors with the predefined criteria (pH – within the range, concentration – to the maximum, adsorbent dose – minimum and temperature – within the range). Figure 6.10 represents the 3D surface plot of the optimum conditions for two main factors pH and concentration by keeping other two factors constant (adsorbent dose – 1.0 g/L and temperature – 40 °C).

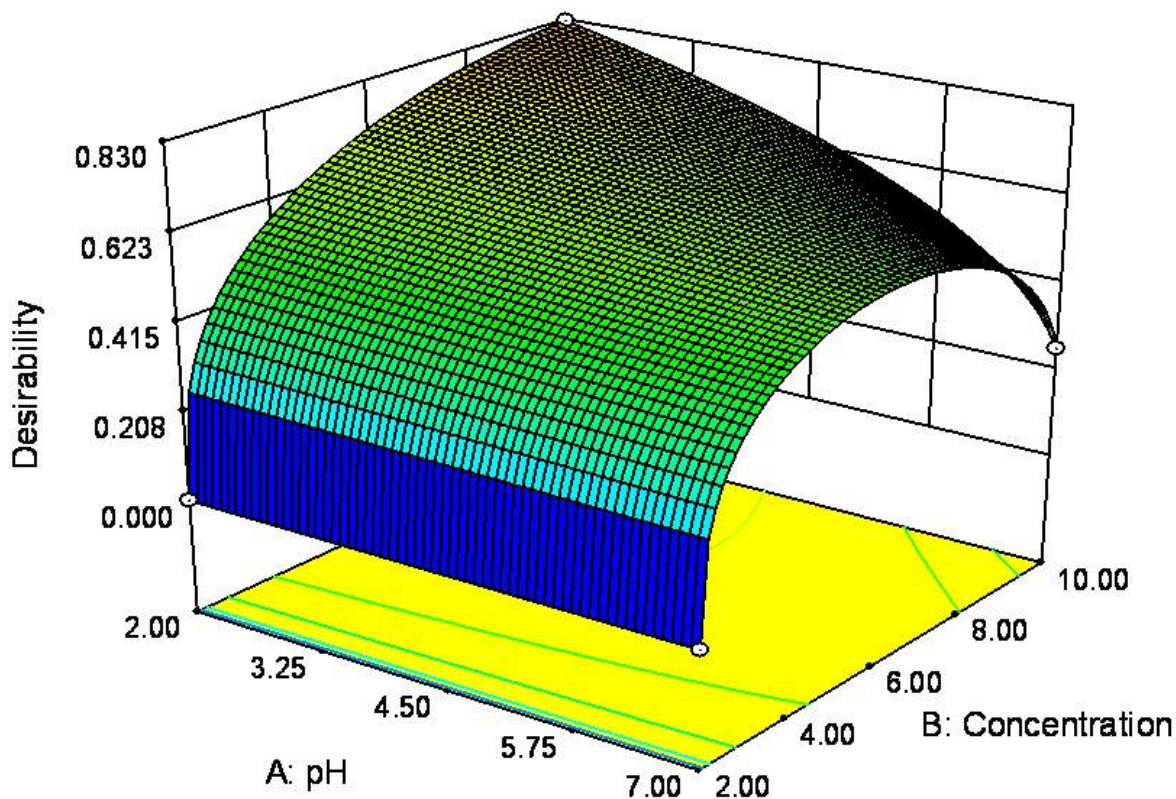


Figure 6.10. Desirability fitted 3D surface plot for Cr(VI) removal by AC-ZC (Adsorbent dose – 1 g/L and Temperature – 40 °C).

6.4.6. Validation Experiments

The model developed was validated by conducting experiments at the predicted conditions. The developed model predicted 51.35 % removal of Cr(VI) at the predicted conditions pH – 6.14, concentration of Cr(VI) – 6.43 mg/L, adsorbent dose – 1.0 g/L and temperature – 20 °C. From the experiment conducted at these conditions, 51.86 % removal was observed which is in good agreement with the predicted result.

6.5. Modeling of Chromium(VI) Removal by AC-PH

Activated carbon (AC) prepared by potassium hydroxide (KOH) activation was applied for the removal of Cr(VI). The combination of values of individual factors in design matrix was shown in Table 6.2. A linear regression model was developed for the adsorption data and the coefficients of each term included in the model and their respective effects were shown in Table 6.8.

Table 6.8. Estimated regression coefficients of model terms and their effects on the response for AC-PH

Factor / Term	Effect	Coefficient	df	Standard error	95% CI Low	95% CI High
Intercept	–	62.41	1	0.42	61.24	63.59
A	-40.70	-20.35	1	0.42	-21.52	-19.18
B	16.37	8.19	1	0.42	7.01	9.36
C	28.40	14.20	1	0.42	13.03	15.37
D	4.96	2.48	1	0.42	1.31	3.65
AC	39.21	19.61	1	0.42	18.43	20.78
AD	-5.35	-2.68	1	0.42	-3.85	-1.50
BC	13.45	6.73	1	0.42	5.55	7.90
CD	10.32	5.16	1	0.42	3.99	6.33
ABD	13.89	6.95	1	0.42	5.78	8.12
ACD	-17.47	-8.74	1	0.42	-9.91	-7.56
ABCD	13.49	6.74	1	0.42	5.57	7.92

Analysis of variance (ANOVA) was done for the obtained data and the terms having p-value less than 0.05 are considered as insignificant. The ANOVA results of Cr(VI) adsorption data for AC-PH was shown in Table 6.9. The developed model after discarding the insignificant terms was given as:

$$\%R = 62.41 - 20.35A + 8.19B + 14.20C + 2.48D + 19.61AC - 2.68AD + 6.73BC + 5.16CD + 6.95ABD - 8.74ACD + 6.74ABCD \quad (6.4)$$

Table 6.9. ANOVA results for Cr(VI) removal data by AC-PH

Factor	Sum of squares	df	Mean square	F-value	p-value
Model	21158.57	11	1923.51	674.74	< 0.0001
A	6625.77	1	6625.77	2324.23	< 0.0001
B	1072.41	1	1072.41	376.19	< 0.0001
C	3225.96	1	3225.96	1131.62	< 0.0001
D	98.28	1	98.28	34.48	0.0042
AC	6150.43	1	6150.43	2157.49	<0.0001
AD	114.50	1	114.50	40.17	0.0032
BC	724.01	1	724.01	253.97	<0.0001
CD	425.93	1	425.93	149.41	0.0003
ABD	772.21	1	772.21	270.88	<0.0001
ACD	1221.22	1	1221.22	428.39	<0.0001
ABCD	727.84	1	727.84	255.32	<0.0001
Residual	11.40	1	2.85		
Total	21169.97	1			

6.5.1. Pareto Plot

All the significant factors and their effects for Cr(VI) removal by AC-PH were shown by pareto plot in [Figure 6.11](#). The main factors such as pH (A), concentration of Cr(VI) (B), adsorbent dose (C) and temperature (D) and various interactions of factors such as AC, BC, CD, AD, ACD, ABD and ABCD have significant effect on the removal of Cr(VI). The main factor temperature (D) had relatively low effect when compared to the other factors. Due to the effect of interactions it involved, the temperature term was included in the model.

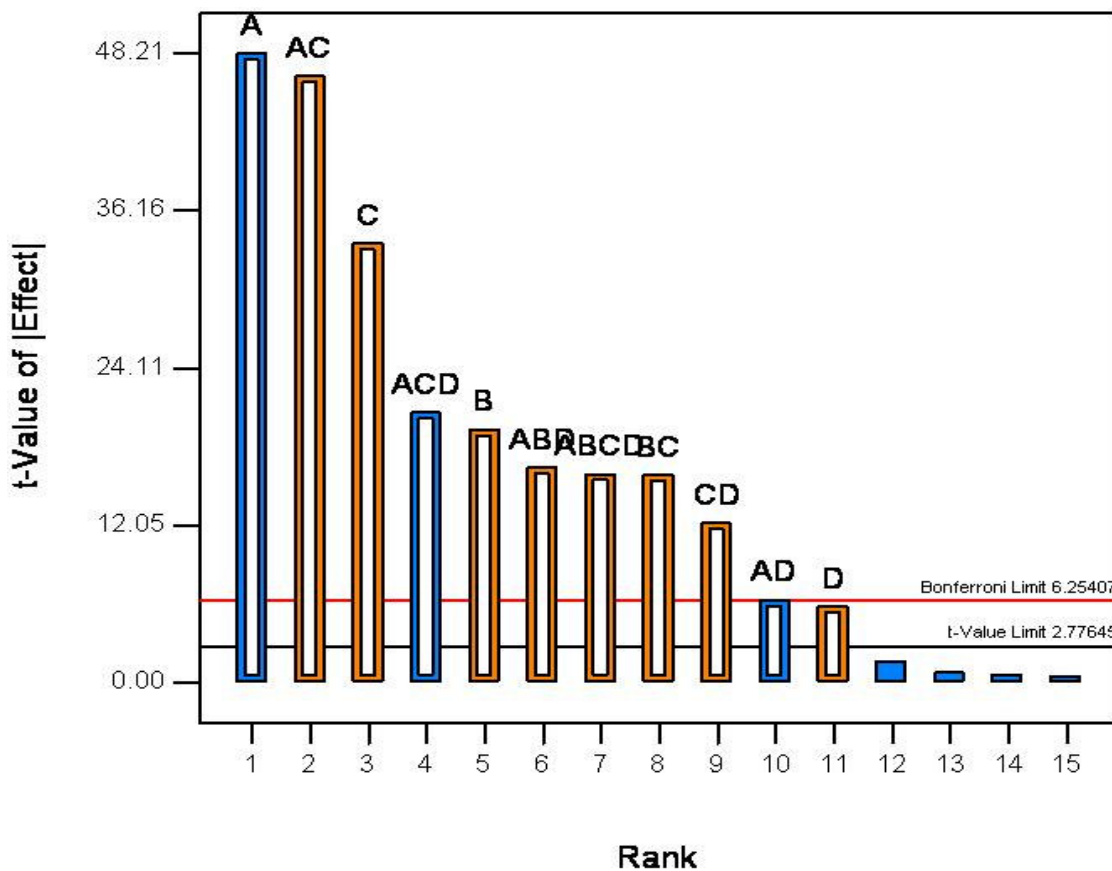


Figure 6.11. Pareto plot for effects of individual factors and interactions for Cr(VI) removal by AC-PH.

6.5.2. Main Effects

The four main factors studied and their individual effect on the percentage removal of Cr(VI) was shown in Figure 6.12. If the deviation of lines is more, the effect is more within the studied range. Solution pH had great influence and with the increase of pH the removal percentage decreased. Other factors concentration of Cr(VI), adsorbent dose and temperature had positive effect on the response i.e. with the increase in the value of parameter, the response also increased. Among all four main factors pH affects the response to a great extent whereas temperature has less effect.

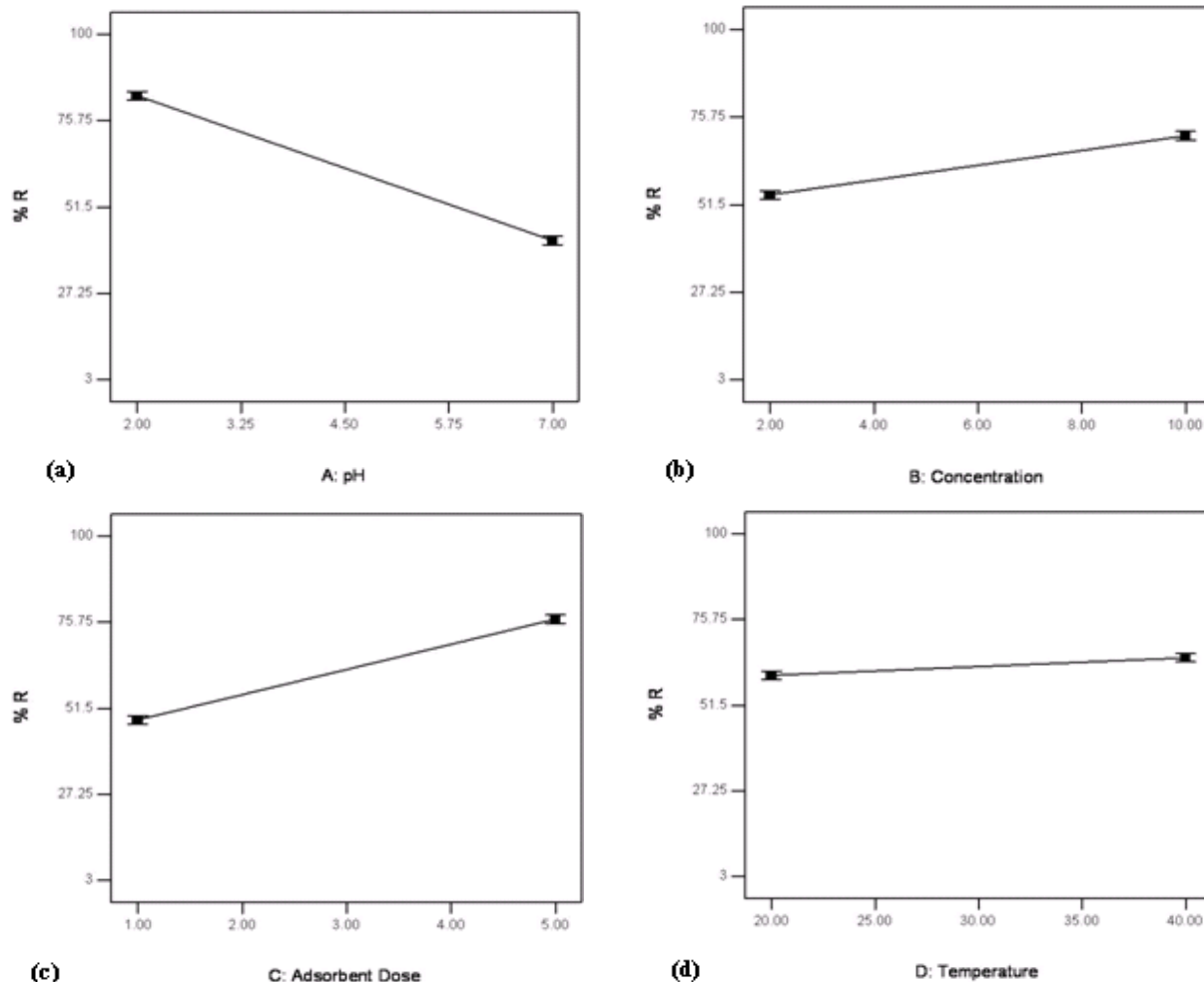
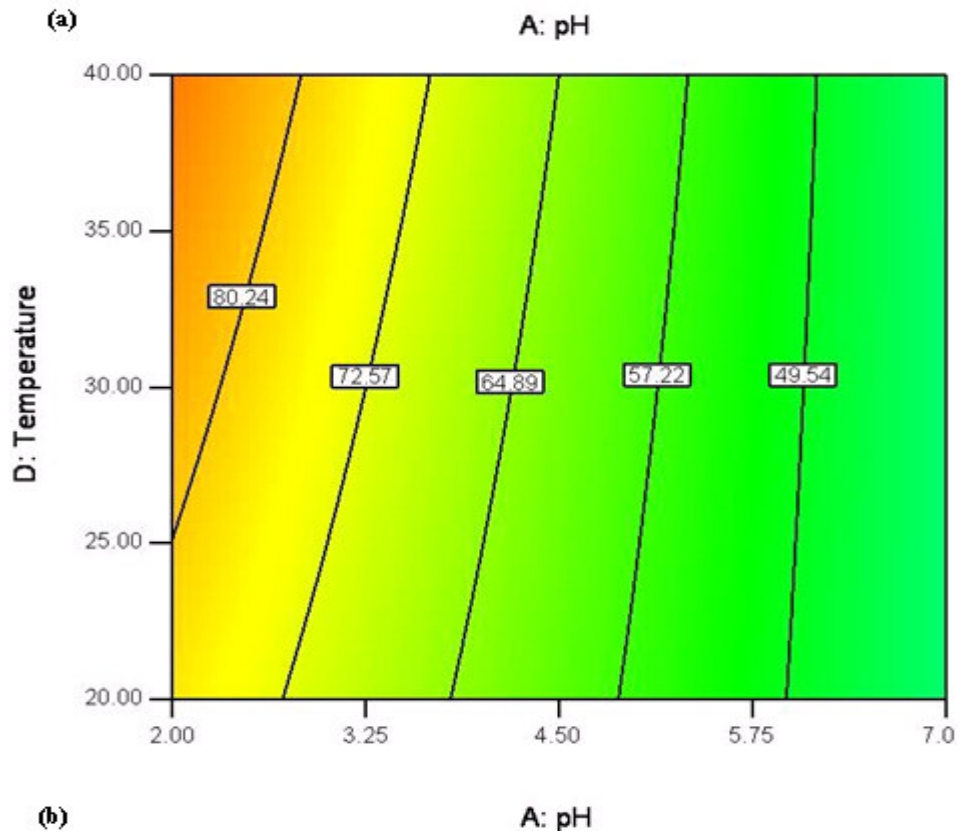
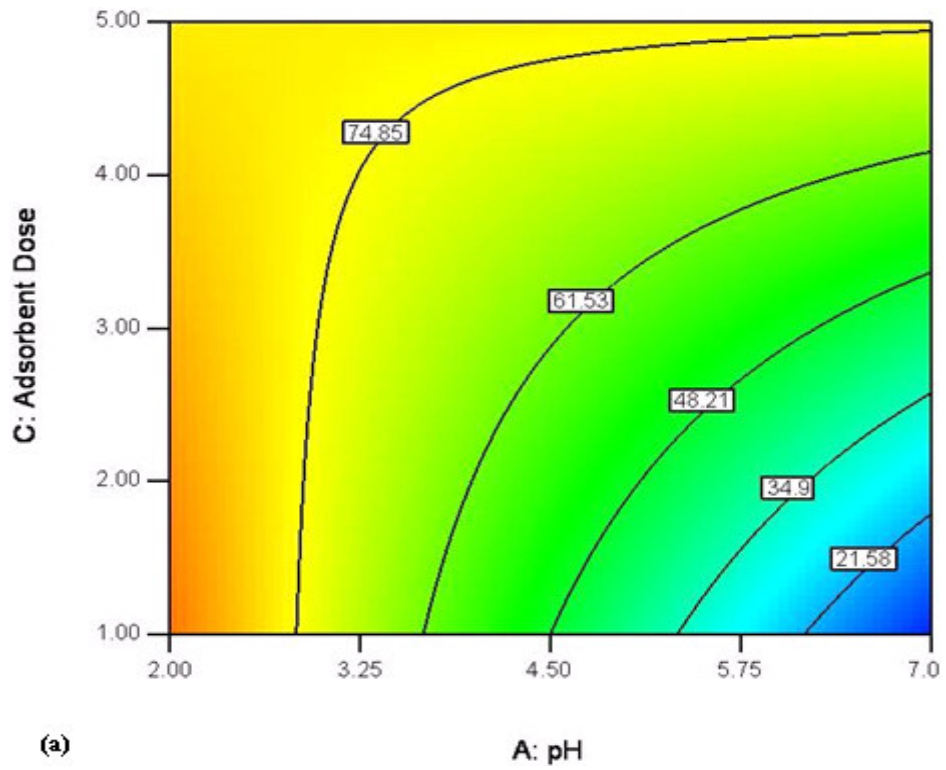
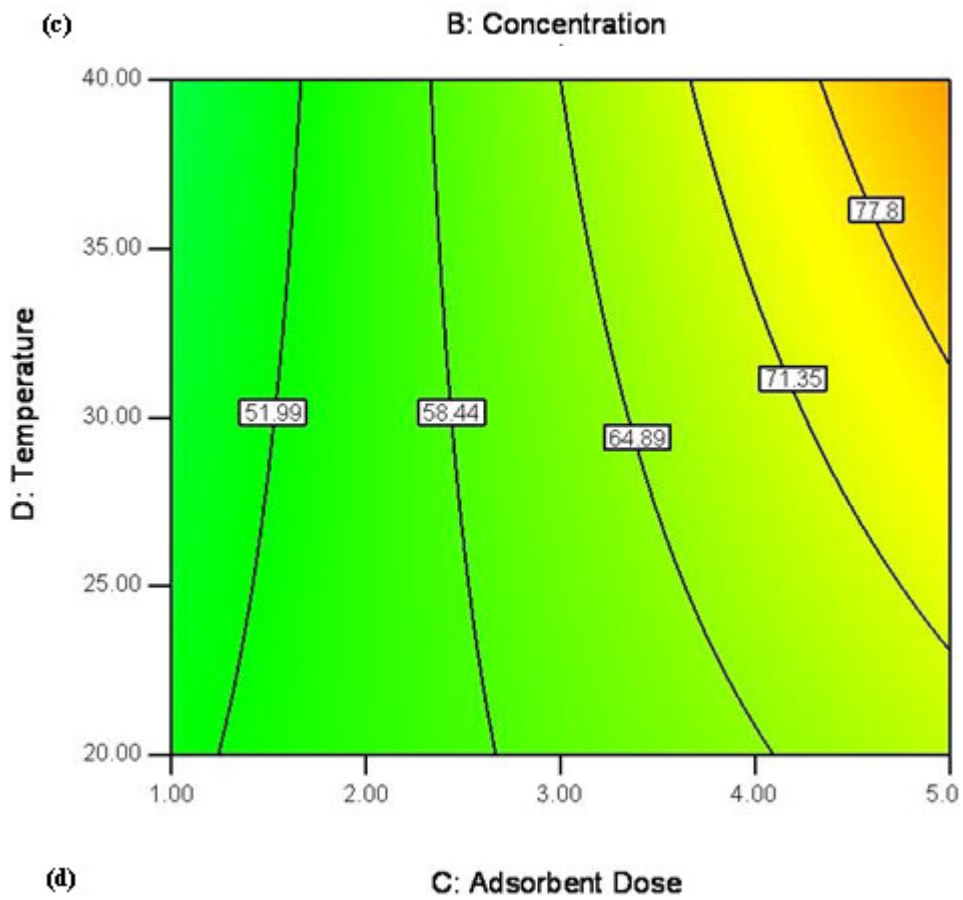
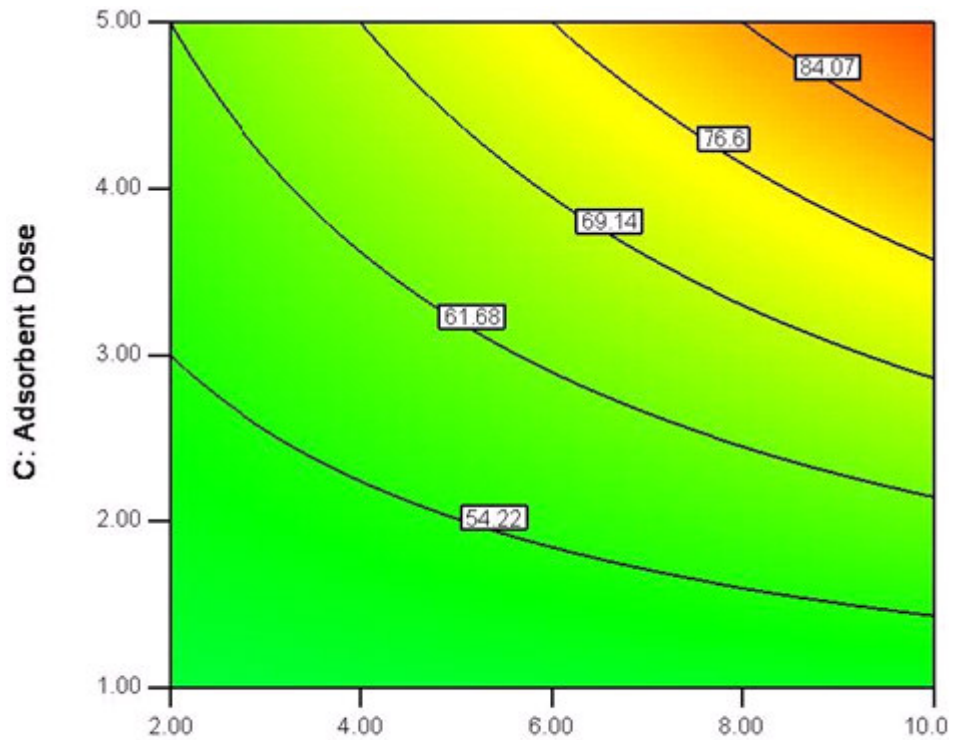


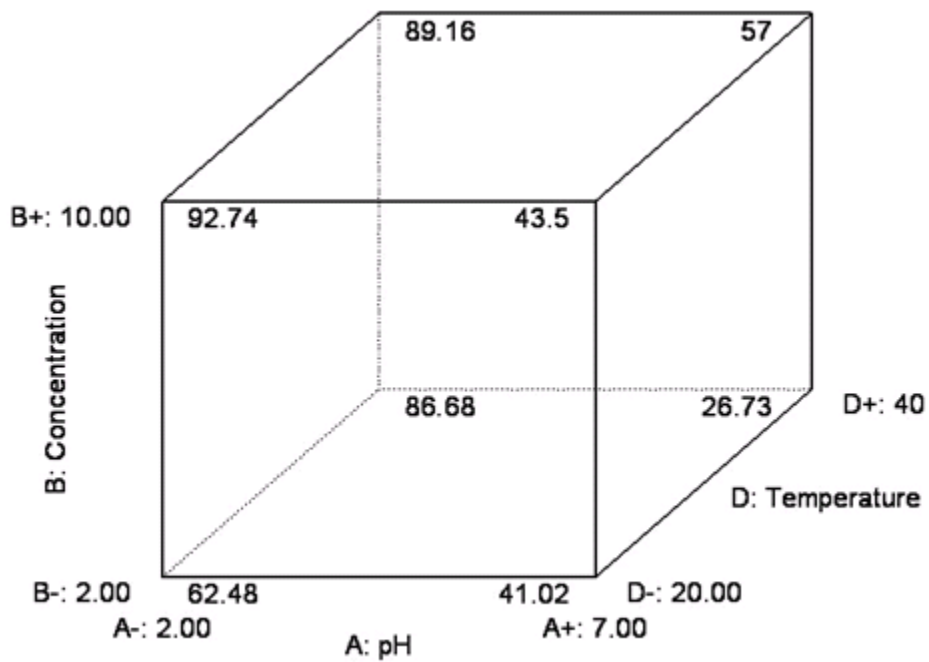
Figure 6.12. Effect of main factors on response for AC-PH (a) pH, (b) concentration, (c) adsorbent dose and (d) temperature.

6.5.3. Interaction Effects

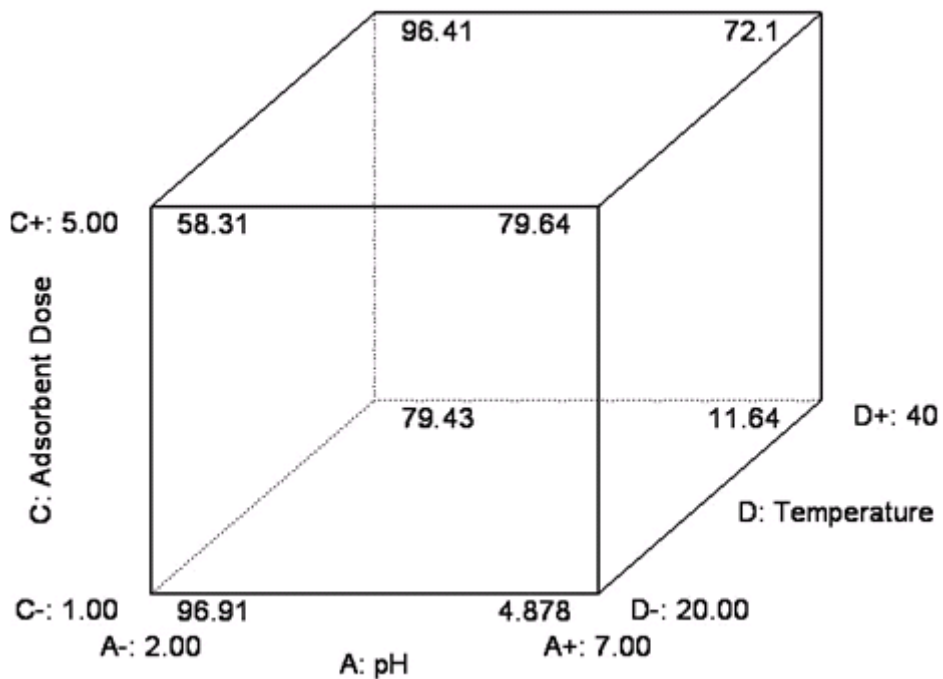
All the main factors are involved in the interaction with the other factors. The interactions of different factors influenced the response significantly can be observed from the pareto chart (Figure 6.11). Various factors involved in the interactions and the relative change in the response with the change in corresponding factors were shown in Figure 6.13. The developed model includes significant two factor (AC, AD, BC, CD), three factor (ABD, ACD) and four factor (ABCD) interactions.







(e)



(f)

Figure 6.13. Contour and cube plots of interactions for AC-ZC (a) pH * Adsorbent dose, (b) pH*Temperature (c) Concentration*Adsorbent dose (d) Adsorbent dose*Temperature (e) pH*Concentration*Temperature and (f) pH*Adsorbent dose*Temperature.

6.5.4. Normal Probability Plot

The normality of the data obtained for the removal of Cr(VI) by AC-PH was checked by plotting the normal probability plot of residuals. The closeness of the data points obtained indicates that the data obtained from a normally distributed population. Figure 6.14 shows the normal probability plot of residuals for the adsorption of Cr(VI) by AC-PH.

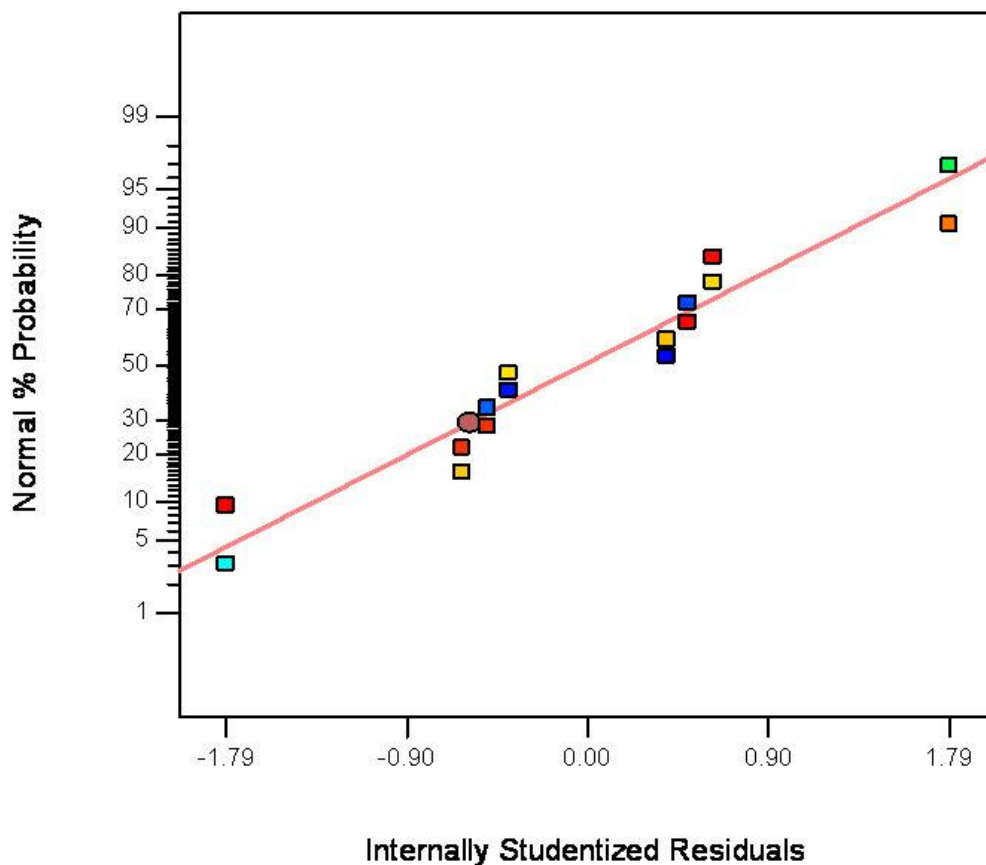


Figure 6.14. Normal probability plot of residuals for Cr(VI) removal by AC-PH.

6.5.5. Optimization

The optimization of Cr(VI) by AC-PH was done by using desirability (D) function. Criteria for determining the optimum conditions were fixed as discussed in previous cases. Figure 6.15 represents the 3D surface plot for Cr(VI) removal by AC-PH. The variation in the desirability can be observed with the change in pH and concentration of Cr(VI).

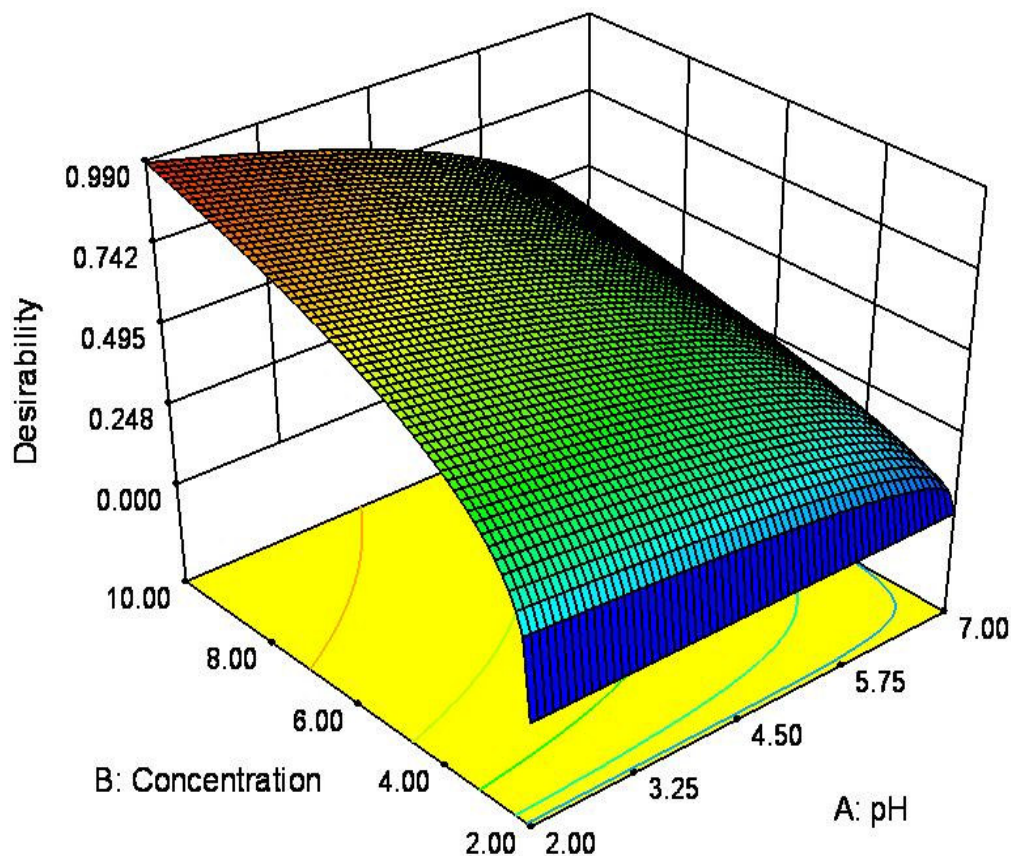


Figure 6.15. Desirability fitted 3D surface plot for Cr(VI) removal by AC-PH (Adsorbent dose – 1.0 g/L and Temperature – 25 °C).

6.5.6. Validation Experiments

The developed model was validated by conducting the experiments at predicted conditions obtained from the model. The predicted values obtained by models were in good agreement with the experimental values obtained by conducting experiments for Cr(VI) removal by AC-PH. The predicted and experimental values of Cr(VI) removal by AC-PH is 76.09 % and 77.23 %, respectively at pH – 3.55, Cr(VI) concentration – 10 mg/L, adsorbent dose – 2.7 g/L and temperature – 32.2 °C. The predicted and experimental values for Cr(VI) removal by prepared ACs and the values of process parameters can be observed in Table 6.10.

Table 6.10. Validation experiments conducted at conditions predicted by models

Sample	pH	Cr(VI) Conc (mg/L)	Ads. Dose (g/L)	Temp (°C)	% R (Pred)	% R (Exp)
AC-PA	2.46	10.0	1.0	20	93.42	92.71
AC-ZC	6.14	6.43	1.0	20	51.35	51.86
AC-PH	3.55	10.0	2.7	32.2	76.09	77.23

Conclusions and Future Perspective

7.0. Summary

The objective of the experimental study was to evaluate the potential of Bael fruit (*Aegle marmelos*) shell as a precursor for activated carbon production. It also aimed to estimate the adsorption capacity of the developed activated carbon for hexavalent chromium present in the water at low concentrations. Activated carbon with high microporosity was developed for this purpose. High percentage of Cr(VI) was adsorbed on the micropores of the carbon structure. Many precursors such as coconut shell, coal, wood have been commercialized for the preparation of activated carbon, but most of them are either limited to availability or found to be expensive. Bael fruit shell is used as precursor for the current investigation being abundantly available as well as is cheap. Full Factorial Design (FFD) was employed for the modeling of adsorption process by studying the effect of main factors and their interactions on removal of Cr(VI).

7.1. Conclusions

Based on the detail experimental investigation the conclusions derived are as follows.

- Bael fruit (*Aegle Marmelos*) shell containing high cellulose (24.35%) and volatile content (72%) proved to be a promising precursor for Activated carbon development.
- Chemical activation of precursor by phosphoric acid, zinc chloride and potassium hydroxide produced ACs of various surface characteristics.
- Development of AC was influenced by various factors such as type of chemical reagent used for impregnation, impregnation ratio, carbonization temperature and holding time etc.
- Maximum yields 74.47 %, 69.33 %, and 85.33 % were obtained at optimum process conditions for AC-PA, AC-ZC, and AC-PH respectively.

- Phosphoric acid treated activated carbon exhibited maximum values for surface area (1657 m²/g) pore volume (0.58 cc/g), micropore surface area (1625 m²/g) and micropore volume (0.56 cc/g) at optimum process conditions (30 % H₃PO₄ impregnation, 400 °C carbonization temperature and 1 h holding time).
- AC-PA could remove 98.7 % Cr(VI) at optimum process conditions (pH – 2.0, Cr(VI) concentration – 10 mg/L, adsorbent dose – 3.0 g/L, temperature – 30 °C and contact time – 3.0 h).
- Adsorption of Cr(VI) on prepared ACs increased with reducing pH from 11.0 to 2.0. AC-PA could remove 76 % Cr(VI) even at neutral pH.
- AC-PA showed adsorption capacities of 3.3 mg/g and 98.6 mg/g at initial Cr(VI) concentrations of 10 mg/L and 100 mg/L, respectively.
- Freundlich model showed best fit to the adsorption data ($R^2 = 0.996$) of AC-PA and the kinetic data followed pseudo-second order model signifying both film and pore diffusion mechanisms during adsorption process.
- Spent AC was regenerated simply by using hot water (80 °C) and mild acid (0.1 M H₂SO₄).
- Modeling of Cr(VI) adsorption on AC-PA by using 2⁴ Full Factorial Design (FFD) revealed that including all the main factors some interactions such as *AB* [pH * concentration of Cr(VI)], *BC* [concentration of Cr(VI) * adsorbent dose] and *ABCD* [pH * concentration of Cr(VI) * adsorbent dose * temperature] significantly influenced the removal of Cr(VI) from aqueous phase.

7.2. Scope of Research

- Extensive investigation should be carried out to produce ACs with even better surface characteristics through different routes such as physical activation, two stage activation and microwave heating etc and can be compared with the results obtained with chemical activation.
- Utilization of AC to treat various other pollutants present in water streams should be undertaken.
- Process economy mainly depends on the selection of raw material and method of preparation of AC. Thus the cost estimation should be carried out to evaluate the potential application of the adsorbent in actual practice.

- Detailed investigation of desorption of Cr(VI) and regeneration of spent AC is essential to evaluate the efficiency of the process which needs an immediate attention.
- The efficiency of AC produced by phosphoric acid activation can be improved further more at neutral pH by modifying the surface functional groups.
- Column studies should be carried out to test the suitability of prepared AC as adsorbent in water purification systems.
- Most of the activated carbon as well as other adsorbents have shown effectiveness in removing chromium species from the waste stream at low pH. However the presence of chromium in the trace amount in drinking water is a major challenge. Hence to combat this problem extensive investigation needs to be carried out to develop an adsorbent and prove its potential to treat the contaminated drinking water at neutral pH.
- Solid waste management is a great environmental concern that is released and disposed by the industries and the agricultural sectors. Hence research activity is needed to utilize the solid waste or convert it to a useful product.

References

- Aber, S., Khataee, A., Sheydaei, M. Optimization of activated carbon fiber preparation from Kenaf using K_2HPO_4 as chemical activator for adsorption of phenolic compounds. *Bioresource Technology*, 100 (24), 2009, 6586-6591.
- Acharya, J., Sahu, J.N., Mohanty, C.R., Meikap, B.C. Removal of lead (II) from wastewater by activated carbon developed from tamarind wood by zinc chloride activation. *Chemical Engineering Journal*, 149, 2009, 249-262.
- Acharya, J., Sahu, J.N., Sahoo, B.K., Mohanty, C.R., Meikap, B.C. Removal of chromium(VI) from wastewater by activated carbon developed from Tamarind wood activated with zinc chloride. *Chemical Engineering Journal*, 150 (1), 2009, 25-39.
- Adhoum, N., Monser, L. Removal of phthalate on modified activated carbon: application to the treatment of industrial wastewater. *Separation and Purification Technology*, 38, 2004, 233-239.
- Adinata, D., Daud, W.M.A.W., Aroua, M.K. Preparation and characterization of activated carbon from palm shell by chemical activation with K_2CO_3 . *Bioresource Technology*, 98, 2007, 145-149.
- Agarwal, G.S., Bhuptawat, H.K., Chaudhari, S. Biosorption of aqueous chromium(VI) by *Tamarindus indica* seeds. *Bioresource Technology* 97, 2006, 949-956.
- Ahmad, M.A., Alrozi, R. Removal of malachite green dye from aqueous solution using rambutan peel-based activated carbon: Equilibrium, kinetic and thermodynamic studies. *Chemical Engineering Journal*, 171 (2), 2011, 510-516.
- Ahmadpour, A., Do, D. The preparation of activated carbon from macadamia nutshell by chemical activation. *Carbon*, 35, 1997, 1723-1732.
- Ahmadpour, A., Do, D.D. The preparation of active carbons from coal by chemical and physical activation. *Carbon*, 34, 1996, 471-479.
- Ahmaruzzaman, Md. Adsorption of phenolic compounds on low-cost adsorbents: A review. *Advances in Colloid and Interface Science*, 143 (1-2), 2008, 48-67.
- AI-Duri, B. Introduction to adsorption. In: McKay, G. (Ed.). *Use of adsorbents for the removal of Pollutants from Wastewaters*. Boca Raton, FL: CRC Press, 1996, 1-6.
- Akgerman, A., Zardkoohi, M. Adsorption of phenolic compounds on fly Ash. *Journal of Chemical and Engineering Data*, 41 (2), 1996, 185-187.
- Aksu, Z., Kutsal, T. A bioseparation process for removing lead(II) ions from waste water by using *C. vulgaris*. *Journal of Chemical Technology and Biotechnology*, 52, 1991, 109-118.

- Alaerts, G.J., Jitjaturant, V., Kelderman, P. Use of coconut shell based activated carbon for Cr(VI) removal. *Water Science and Technology* 21, 1989, 1701-1704.
- Alamansa, C., Molina-Sabio, M., Rodriguez-Reinoso, F. Adsorption of methane into ZnCl₂-activated carbon derived discs. *Microporous and Mesoporous Materials*, 76, 2004, 185-191.
- Allen, S.J., Gan, Q., Matthews, R., Johnson, P.A. Comparison of optimized isotherm models for basic dye adsorption by kudzu. *Bioresource Technology*, 8, 2003, 143-152.
- Amin, N.K. Removal of direct blue-106 dye from aqueous solution using new activated carbons developed from pomegranate peel: adsorption equilibrium and kinetics. *Journal of Hazardous Materials*, 165 (1-3), 2009, 52-62.
- Antony, J. *Design of Experiments for Engineers and Scientists*, Butterworth-Heinemann, New York, 2003.
- Arami-Niya, A., Daud, W.M.A.W., Mjalli, F.S. Comparative study of the textural characteristics of oil palm shell activated carbon produced by chemical and physical activation for methane adsorption. *Chemical Engineering Research and Design*, 89 (6), 2011, 657-664.
- Arenas, L.T., Lima, E.C., Santos, A.A.D., Vaghetti, J.C.P., Coasta, T.M.H., Benvenuti, E.V. Use of statistical design of experiments to evaluate the sorption capacity of 1,4-diazoniabicyclo[2,2,2]octane silica chloride for Cr(VI) adsorption. *Colloids and Surfaces A: Physicochemical and Engineering Aspects*, 297, 2006, 240-248.
- Ariyadejwanich, P., Tanthapanichakoon, W., Nakagawa, K., Mukai, S.R., Tamon, H. Preparation and characterization of mesoporous activated carbon from waste tires. *Carbon*, 41, 2003, 157-164.
- Arriagada, R., Garcia, R., Molina-Sabio, M., Rodriguez-Reinoso, F. Effect of steam activation on the porosity and chemical nature of activated carbons from Eucalyptus globules and peach stones. *Microporous Materials*, 8 (3), 1997, 123-130.
- Aworn, A., Thiravetyan, P., Nakbanpote, W. Preparation and characteristics of agricultural waste activated carbon by physical activation having micro and mesopores. *Journal of Analytical and Applied Pyrolysis*, 82 (2), 2008, 279-285.
- Aworn, A., Thiravetyan, P., Nakbanpote, W. Preparation of CO₂ activated carbon from corncob for methylene glycol adsorption. *Colloids and Surfaces A: Physicochemical Engineering Aspects*, 333, 2009, 19-25.
- Ayranci, E., Hoda, N. Adsorption kinetics and isotherms of pesticides onto activated carbon cloth. *Chemosphere*, 60 (11), 2005, 1600-1607.
- Azevedo, D.C.S., Araujo, J.C.S., Bastos-Neto, M., Torres, A.E.B., Jaguaribe, E.F., Cavalcante, C.L. Microporous activated carbon prepared from coconut shells using chemical activation with zinc chloride. *Microporous and Mesoporous Materials*, 100, 2007, 361-364.

- Babel, S., Kurniawan, T.A. Cr(VI) removal from synthetic wastewater using coconut shell charcoal and commercial activated carbon modified with oxidizing agents and/or chitosan. *Chemosphere*, 54 (7), 2004, 951-967.
- Babu, B.V., Gupta S. Adsorption of Cr(VI) using activated Neem leaves as an adsorbent : kinetic studies. *Adsorption*, 14 (1), 2008, 85-92.
- Bae, J.S., Do, D.D. Study on diffusion and flow of benzene, n-hexane and CCl₄ in activated carbon by a differential permeation method. *Chemical Engineering Science*, 57 (15), 2002, 3013-3024.
- Baek, K., Yang, J., Kwon, T. Cationic starch-enhanced ultrafiltration for Cr(VI) removal. *Desalination*, 206, 2007, 245-250.
- Bagreev, A., Adib, F., Bandosz, T.J. pH of activated carbon surface as an indication of its suitability for H₂S removal from moist air streams. *Carbon*, 39 (12), 2001a, 1897-1905.
- Bagreev, A., Rahman, H., Bandosz, T.J. Thermal regeneration of spent activated carbon previously used as hydrogen sulfide adsorbent. *Carbon*, 39, 2001b, 1319-1326.
- Bandosz, T.J. *Activated Carbon Surfaces in Environmental Remediation*. Academic Press, 2006, The Netherlands.
- Bansal, R.C., Donnet, J.B., Stoeckli, H.F. *Active carbon*. Marcel Dekker, 1988, New York.
- Bansode, R.R., Losso, J.N., Marshall, W.E., Rao, R.M., Portier, R.J. Adsorption of volatile organic compounds by pecan shell and almond shell based granular activated carbons. *Bioresource Technology*, 90, 2003, 175-184.
- Baral, S.S., Das, N., Chaudhury, G.R., Das, S.N. A preliminary study on the adsorptive removal of Cr(VI) using seaweed, *Hydrilla verticillata*. *Journal of Hazardous Materials*, 171, 2009, 358-369.
- Barceloux, D.G. Chromium. *Journal of Toxicology - Clinical Toxicology*, 37, 1999, 173-194.
- Barkat, M., Nibou, D., Chegrouche, S., Mellah, A. Kinetics and thermodynamics studies of chromium (VI) ions adsorption onto activated carbon from aqueous solutions. *Chemical Engineering and Processing: Process Intensification*, 48 (1), 2009, 38-47.
- Basta, A.H., Fierro, V., El-Saied, H., Celzard, A. 2-steps KOH activation of rice straw: An efficient method for preparing high-performance activated carbons. *Bioresource Technology*, 100, 2009, 3941-3947.
- Benjamin, M.M., *Water Chemistry*, McGraw-Hill, New York, 2002.
- Betancur, M., Martinez, J.D., Murillo, R. Production of activated carbon by waste tire thermochemical degradation with CO₂. *Journal of Hazardous Materials*, 168, 2009, 882-887.

- Bhatti, I., Qureshi, K., Kazi, R.A., Ansari, A.K. Preparation and characterization of chemically activated almond shells by optimization of adsorption parameters for removal of chromium VI from aqueous solutions. *World Academy of Science, Engineering and Technology*, 34, 2007, 199-204.
- Blanco-Lopez, M.C., Martinez-Alonso, A., Tascon, J.M.D. Microporous texture of activated carbon fibers prepared from Nomex aramid fibers. *Microporous and Mesoporous Materials*, 34 (2), 2000, 171-179.
- Boehm, H.P. Some aspects of the surface chemistry of carbon blacks and other carbons. *Carbon*, 32 (5), 1994, 759-769.
- Bonelli, P.R., Della Rocca, P.A., Cerrella, E.G., Cukierman, A.L. Effect of pyrolysis temperature on composition, surface properties and thermal degradation rates of Brazil Nut shells. *Bioresource Technology*, 76 (1), 2001, 15-22,
- Boudou, J.P., Chehimi, M., Broniek., E., Siemieniewska, T., Bimer, J. Adsorption of H₂S or SO₂ on an activated carbon cloth modified by ammonia treatment. *Carbon*, 41 (10), 2003, 1999-2007.
- Boudrahem, F. Aissani-Benissad, H. Aït-Amar, Batch sorption dynamics and equilibrium for the removal of lead ions from aqueous phase using activated carbon developed from coffee residue activated with zinc chloride. *Journal of Environmental Management*, 90, 2009, 3031-3039.
- Box, G.E.P., Hunter, W.G., Hunter, J.S. *Statistics for Experimenters-An Introduction to Design, Data Analysis and Model Building*. John Wiley & Sons, New York, 1978.
- Boyd, G.E., Adamson, A.W., Myers Jr, L.S. The exchange adsorption of ions from aqueous solutions by organic zeolites, II: kinetics, *Journal of American Chemical Society*, 69, 1947, 2836-2848.
- Boyd, G.E., Soldano, B.A. Self-diffusion of cations in and through sulfonated polystyrene cation-exchange polymers. *Journal of American Chemical Society*, 75, 1953, 6091-6099.
- Brasil, J.L., Martins, L.C., Ev, R.R., Dupont, J., Dias, S.L.P., Sales, J.A.A., Airoidi, C., Lima, E.C. Factorial design for optimization of flow injection preconcentration procedure for copper(II) determination in natural waters, using 2-aminomethylpyridine grafted silica gel as adsorbent and spectrophotometric detection. *International Journal of Environmental Analytical Chemistry*, 15, 2005, 475-491.
- Brunauer, S., Deming, L.S., Deming, W.S., and Teller, E. On a theory of Van der Waals adsorption of gases. *Journal of American Chemical Society*, 62, 1940, 1723-1732.
- Brunauer, S., Emmet, P.H. The use of van der waals adsorption isotherms in determining the surface area of iron synthetic ammonia catalysts. *Journal of American Chemical Society*, 57 (9), 1935, 1754-1755.
- Brunauer, S., Emmet, P.H., Teller, E. Adsorption of gases in multimolecular layers. *Journal of American Chemical Society*, 60 (2), 1938, 309-319.

- Budinova, T., Ekinci, E., Yardim, F., Grimm, A., Bjornbom, E., Minkova, V., Goranova, M. Characterization and application of activated carbon produced by H_3PO_4 and water vapor activation. *Fuel Process Technology*, 87, 2006, 899-905.
- Burlakova, E.B., Naidich, V.I. *The Effects of Low Dose Radiation: New Aspects of Radiobiological Research Prompted by the Chernobyl Nuclear Disaster*. VSP International Science Publishers, 2005.
- Cabal, B., Budinova, T., Ania, C.O., Tsyntsarski, B., Parra, J.B., Petrova, B. Adsorption of naphthalene from aqueous solution on activated carbons obtained from bean pods. *Journal of Hazardous Materials*, 161 (2-3), 2009, 1150-1156.
- Cagnon, B., Py, X., Guillot, A., Stoeckli, F., Chambat, G. Contributions of hemicellulose, cellulose and lignin to the mass and porous properties of chars and steam activated carbons from various lignocellulosic precursors. *Bioresource Technology*, 100 (1), 2009, 292-298.
- Cal, M.P., Rood, M.J., Larson, S.M. Removal of VOCs from humidified gas streams using activated carbon cloth. *Gas Separation and Purification*, 10 (2), 1996, 117-121.
- Calafat, A., Laine, J., Lopez-Agudo, A., Palacios, J.M. Effect of surface oxidation of the support on the thiophene hydrodesulfurization activity of Mo, Ni, and Ni-Mo catalysts supported on activated carbon. *Journal of Catalysis*, 162 (1), 1996, 20-30.
- Calvo, L., Gilarranz, M.A., Casas, J.A., Mohedano, A.F., Rodriguez, J.J. Hydrodechlorination of diuron in aqueous solution with Pd, Cu, and Ni on activated carbon catalysts. *Chemical Engineering Journal*, 163 (3) 2010, 212-218.
- Cao, D., Wang, W., Shen, Z., Chen, J. Determination of pore size distribution and adsorption of methane and CCl_4 on activated carbon by molecular simulation. *Carbon*, 40 (13), 2002, 2359-2365.
- Carmona, M.E.R., da Silva, M.A.P., Ferreira, S.L.C. Biosorption of chromium using factorial experimental design. *Process Biochemistry*, 40, 2005, 779-788.
- Castro-Muniz, A., Suarez-Garcia, F., Martinez-Alonso, A., Tascon, J.M.D. Activated carbon fibers with a high content of surface functional groups by phosphoric acid activation of PPTA. *Journal of Colloid and Interface Science*, 361, 2011, 307-315.
- Caturla, F., Molina-Sabio, M., Rodriguez-Reinoso, F. Preparation of activated carbon by chemical activation with $ZnCl_2$. *Carbon*, 29, 1991, 999-1007.
- Cerminara, P.J., Sorial, G.A., Papadimas, S.P., Suidan, M.T., Moteleb, M.A., Speth, T.F. Effect of influent oxygen concentration on the GAC adsorption of VOCs in the presence of BOM. *Water Research*, 29 (2), 1995, 409-419.
- Cestari, A.R., Vieira, E.F.S., de Oliveira, I.A., Bruns, R.E. The removal of Cu(II) and Co(II) from aqueous solutions using cross-linked chitosan – Evolution by the factorial design methodology. *Journal of Hazardous Materials*, 143, 2007, 8-16.

- Chen, J.P., Wu, S. Simultaneous adsorption of copper ions and humic acid onto an activated carbon. *Journal of Colloid and Interface Science*, 280, 2004, 334-342.
- Chen, J.P., Wu, S., Chong, K.H. Surface modification of granular activated carbon by citric acid for enhancement of copper adsorption. *Carbon*, 41 (10), 2003, 1979-1986.
- Cheung, W.H., Szeto, Y.S., McKay, G. Intraparticle diffusion processes during acid dye adsorption onto chitosan. *Bioresource Technology*, 98, 2007, 2897-2904.
- Chiang, H.L., Huang, C.P., Chiang, P.C. The surface characteristics of activated carbon as affected by ozone and alkaline treatment. *Chemosphere*, 47 (3), 2002, 257-265.
- Chiang, P.C., Wu, J.S. Evolution of chemical and thermal regeneration of activated carbon. *Water Science and Technology*, 21, 1989, 1697-1702.
- Chingombe, P., Saha, B., Wakeman, R.J. Sorption of atrazine on conventional and surface modified activated carbons. *Journal of Colloid and Interface Science*, 302, 2006, 408-416.
- Choi, H.K., Lee, S.H., Kim, S.S., The effect of activated carbon injection rate on the removal of elemental mercury in a particulate collector with fabric filters. *Fuel Processing Technology*, 90 (1), 2009, 107-112.
- Choy, K.K.H., Porter, J.F., McKay, G. Langmuir isotherm models applied to the multicomponent sorption of acid dyes from effluent onto activated carbon, *Chemical Engineering Journal*, 45, 2000, 575-584.
- Chung, Y.C., Lin, Y.Y., Tseng, C.P. Removal of high concentration of NH₃ and coexistent H₂S by biological activated carbon (BAC) biotrickling filter. *Bioresource Technology*, 96 (16), 2005, 1812-1820.
- Clesceri, L.S., Greenberg, A.E., Eaton, A.D. (Eds.). *Standard Methods for the Examination of Water and Wastewater*, 20th ed., American Public Health Association, 1988. Washington, DC.
- Coates., J. Interpretation of infrared spectra, A practical approach in *Encyclopedia of Analytical Chemistry*, Meyers, R.A (Ed.), John Wiley & Sons Ltd, Chichester, 2000, 10815-10837.
- Cook, D., Newcombe, G., Sztajn bok, P. The application of powdered activated carbon for mib and geosmin removal: predicting pac doses in four raw waters. *Water Research*, 35 (5), 2001, 1325-1333.
- Cronje, K.J., Chetty, K., Carsky, M., Sahu, J.N., Meikap, B.C. Optimization of chromium(VI) sorption potential using developed activated carbon from sugarcane bagasse with chemical activation by zinc chloride. *Desalination*, 275, 2011, 276-284.
- Daifullah, A.A.M., Girgis, B.S. Impact of surface characteristics of activated carbon on adsorption of BTEX. *Colloids and Surfaces A*, 214, 2003, 181-193.
- Daifullah, A.A.M., Girgis, B.S. Removal of some substituted phenols by activated carbon obtained from agricultural waste. *Water Research*, 32 (4), 1998, 1169-1177.

- Das, D., Gaur, V., Verma, N. Removal of volatile organic compound by activated carbon fiber. *Carbon*, 42 (14), 2004, 2949-2962.
- Daud, W.M.A.W., Ali, W.S.W. Comparison on pore development of activated carbon produced from palm shell and coconut shell. *Bioresource Technology*, 93, 2004, 63-69.
- Daud, W.M.A.W., Houshamnd, A.H. Textural characteristics, surface chemistry and oxidation of activated carbon. *Journal of Natural Gas Chemistry*, 19 (3), 2010, 267-279.
- Davis, A.P., Bernstein, C., Gietka, P.M. Waste minimization in electropolishing: process control in : A.K. Sengupta (Ed.), *Proceedings of the twenty seventh mid atlantic industrial waste conference: Hazardous and industrial wastes*. Lancaster, Technomic, 1995, 62-71.
- Delhaes, P. Design and control of structure of activated carbon materials for enhanced performance, Rand, B., Appleyard, S.P., Yardim, M.F. (Eds.), *NATO Science Series, Series E; Applied Sciences*, Kluwer Academic Publishers, 347, 1998, 3-27, The Netherlands.
- Demiral, H., Demiral, I., Tumsek, F., Karabacakoglu, B. Pore structure of activated carbon prepared from hazelnut bagasse by chemical activation. *Surface and Interface Analysis*, 40, 2008, 616-619.
- Demirbas, E., Kobya, M., Oncel, S., Sencan, S. Removal of Ni(II) from aqueous solution by adsorption onto hazelnut shell activated carbon: equilibrium studies. *Bioresource Technology*, 84 (3), 2002, 291-293.
- Demirbas, E., Kobya, M., Senturk, E., Ozkan, T. Adsorption kinetics for the removal of chromium (VI) from aqueous solutions on the activated carbons prepared from agricultural wastes. *Water SA*, 30 (4), 533-539.
- Deng, H., Li, G., Yang, H., Tang, J., Tang, J. Preparation of activated carbons from cotton stalk by microwave assisted KOH and K_2CO_3 activation. *Chemical Engineering Journal*, 163, 2010, 373-381.
- Deng, H., Zhang, G., Xu, X., Tao, G., Dai, J. Optimization of preparation of activated carbon from cotton stalk by microwave assisted phosphoric acid – chemical activation. *Journal of Hazardous Materials*, 182, 2010, 217-224.
- Derbyshire, F., Andrews, R., Jaques, D., Jagtoyen, M., Kimber, G., Rantell, T. Synthesis of isotropic carbon fibers and activated carbon fibers from pitch precursors. *Fuel*, 80 (3), 2001, 345-356.
- Dhungana, T.P., Yadav, P.N. determination of chromium tannery effluent and study of adsorption of Cr(VI) on saw dust and charcoal from sugarcane bagasses. *Journal of Nepal Chemical Society*, 23, 2009, 93-101.
- Di Natale, F., Lancia, A., Molino, A., Musmarra, D. Removal of chromium ions from aqueous solutions by adsorption on activated carbon and char. *Journal of Hazardous Materials*, 145 (3), 2007, 381-390.

- Diao, Y., Walawender, W.P., Fan, L.T. Activated carbons prepared from phosphoric acid activation of grain sorghum. *Bioresource Technology*, 81, 2002, 45-52.
- Doying, E.G., US patent 3256206, 1966.
- Dragan, E.S., Avram, E., Axente, D., and Marcu, C. Ion-exchange resins. III. Functionalization-morphology correlations in the synthesis of some macroporous, strong basic anion exchangers and uranium-sorption properties evaluation. *Journal of Polymer Science Part A: Polymer Chemistry*, 42, 2004, 2451-2461.
- Drain, L.E., Morrison, J.A. Thermodynamic properties of argon adsorbed on rutile. *Transactions of the Faraday Society*, 48, 1952, 840-846.
- Drain, L.E., Morrison, J.A. Thermodynamic properties of nitrogen and oxygen adsorbed on rutile. *Transactions of the Faraday Society*, 49, 1953, 654-672.
- Dubey, S.P., Gopal, K. Adsorption of chromium (VI) on low cost adsorbents derived from agricultural waste material: A comparative study. *Journal of Hazardous Materials*, 145 (3), 2007, 465-470.
- Dubinin, M.M. Fundamentals of the theory of adsorption in micropores of carbon adsorbents: Characteristics of their adsorption properties and microporous structures. *Carbon*, 27 (3), 1989, 457-467.
- Dubinin, M.M., in *Characterization of porous solids*. Gregg, S.J., Sing, K.S.W., Stoeckli, H.F. (Eds.), Society of Chemical Industry, 1979, 1-11, London.
- Dubinin, M.M., Radushkevich, L.V. The equation of the characteristic curve of activated charcoal, *Doklady Akademii Nauk SSSR*, 55, 1947, 327-329.
- Dubinin, M.M., The potential theory of adsorption of gases and vapors for adsorbents with energetically nonuniform surfaces. *Chemical Reviews*, 60 (2), 1960.
- Duman, O., Ayranci, E. Attachment of benzo-crown ethers onto activated carbon cloth to enhance the removal of chromium, cobalt and nickel ions from aqueous solutions by adsorption. *Journal of Hazardous Materials*, 176 (1-3), 2010, 231-238.
- Duran-Valle, C.J., Gomez-Corzo, M., Pastor-Villegas, J., Gomez-Serrano, V. Study of cherry stones as raw material in preparation of carbonaceous adsorbents. *Journal of Analytical and Applied Pyrolysis*, 73 (1), 2005, 59-67.
- Dwivedi, C.P., Sahu, J.N., Mohanty, C.R., Raj Mohan, B., Maikap, B.C. Column performance of granular activated carbon packed bed for Pb(II) removal. *Journal of Hazardous Materials*, 156 (1-3), 2008, 596-603.
- Dwivedi, P., Gaur, V., Sharma, A., Verma, N. Comparative study of removal of volatile organic compounds by cryogenic condensation and adsorption by activated carbon fiber. *Separation and Purification Technology*, 39 (1-2), 2004, 23-37.

- Ebbesen, T.W., Takada, T. Topological and SP³ defect structures in nanotubes. *Carbon*, 33 (7), 1995, 973-978.
- El-Hendawy, A.N.A. Influence of HNO₃ oxidation on the structure and adsorptive properties of corncob-based activated carbon. *Carbon*, 41, 713-722.
- El-Hendawy, A.A., Alexander, A.J., Andrews, R.J., Forrest, G. Effects of activation schemes on porous, surface and thermal properties of activated carbons prepared from cotton stalks. *Journal of Analytical and Applied Pyrolysis*, 82, 2008, 272-278.
- El-Hendawy, A.N.A., Sarma, S.E., Girgis, B.S. Adsorption characteristics of activated carbons obtained from corncobs. *Colloids and Surfaces A: Physicochemical and Engineering Aspects*, 180 (3), 2001, 209-221.
- Elilbol, M., Response surface methodological approach for inclusion of perfluorocarbon in actinorhodin fermentation medium. *Process Biochemistry*, 38, 2002, 667-673.
- El-Kamash, A.M., Zaki, A.A., Abed-El-Geleel, M. Modeling batch kinetics and thermodynamics of zinc and cadmium removal from waste solutions using synthetic zeolite A. *Journal of Hazardous Materials*, 127, 2005, 211-220.
- Emmet, P.H., Brunauer, S. The use of low temperature van der waals adsorption isotherms in determining the surface area of iron synthetic ammonia catalysts. *Journal of American Chemical Society*, 1937, 59 (8), 1553-1564.
- Encinar, J.M., Beltran, F.J., Ramiro, A., Gonzalez, J.F. Pyrolysis/gasification of agricultural residues by carbon dioxide in the presence of different additives: influence of variables. *Fuel Processing Technology*, 55, 1998, 219-233.
- EPA. 1990. Environmental Pollution Control Alternatives. Environmental Protection Agency, Cincinnati, US.
- Erdogan, S., Onal, Y., Akmil-Basar, C., Bilmez-Erdemoglu, S., Sarici-Ozdemir, C., Koseoglu, E., Leduygu, G. Optimization of nickel adsorption from aqueous solution by using activated carbon prepared from waste apricot by chemical activation. *Applied Surface Science*, 252, 2005, 1324-1331.
- Esmaili, A., Ghasemi, S., Rustaiyan, A. Removal of hexavalent chromium using activated carbons derived from marine algae *Gracilaria* and *Sargassum* sp. *Journal of Marine Science and Technology*, 18 (4), 2010, 587-592.
- Faria, P.C.C., Orfao, J.J.M., Pereira, M.F.R. Adsorption of anionic and cationic dyes on activated carbons with different surface chemistries. *Water Research*, 38 (8), 2004, 2043-2052.
- Farinella, N.V., Matos, G.D., Arruda, M.A.Z. Grape bagasse as a potential biosorbent of metals in effluent treatments. *Bioresource Technology*, 98 (10), 2007, 1940-1946.
- Fen, L.T., Rao, A.N. Distribution, morphology, uses and propagation of *Aegle marmelos*. *Journal of Tropical Medicinal Plants*, 8 (1), 2007, 91-96.

- Ferreira, S.L.C., dos Santos, W.N.L., Bezerra, M.A. Use of factorial design and Doehlert matrix for multivariate optimization of an on-line preconcentration system for lead determination by flame atomic adsorption spectroscopy. *Analytical and Bioanalytical Chemistry*, 375, 2003, 443-449.
- Fierro, V., Muniz, G., Basta, A.H., El-Saied, H., Celzard, A. Rice straw as precursor of activated carbons: Activation with ortho-phosphoric acid. *Journal of Hazardous Materials*, 181, 2010, 27-34.
- Finqueneisel, G., Zimny, T., Weber, J.V. On the prediction of adsorption isotherms of methanol/water vapour mixtures on microporous activated carbon. *Carbon*, 43 (5), 2005, 1093-1095.
- Foo, K.Y., Hameed, B.H. Microwave assisted preparation of activated carbon from pomelo skin for the removal of anionic and cationic dyes. *Chemical Engineering Journal*, 173 (2), 2011, 385-390.
- Foo, K.Y., Hameed, B.H. Porous structure and adsorptive properties of pineapple peel based activated carbons prepared via microwave assisted KOH and K_2CO_3 activation. *Microporous and Mesoporous Materials*, 148 (1), 2011, 191-195.
- Foo, K.Y., Hameed, B.H. Preparation and characterization of activated carbon from sunflower seed oil residue via microwave assisted K_2CO_3 activation. *Bioresource Technology*, 2011b (In Press).
- Foo, K.Y., Hameed, B.H. Detoxification of pesticide waste via activated carbon adsorption process. *Journal of Hazardous Materials*, 175 (1-3), 2010, 1-11.
- Fraga, M.A., Mendes, M.J., Jordao, E. Examination of the surface chemistry of activated carbon on enantioselective hydrogenation of methyl pyruvate over Pt/C catalysts. *Journal of Molecular Catalysis A: Chemical*, 179, 2002, 243-251.
- Franklin, R.E. Crystalline growth in graphitizing and non-graphitizing carbons. *Proceedings of The Royal Society A*, 209, 1951, 196-218.
- Freeman, J.J., Tomlinson, J.B., Sing, K.S.W., Theocharis, C.R. Adsorption of nitrogen and water vapour by activated Kelvar chars. *Carbon*, 31 (6), 1993, 865-869.
- Friedel, R.A., Carlson, G.L. Difficult carbonaceous materials and their infra-red and Raman spectra. Reassignments for coal spectra. *Fuel*, 51, 1972, 194-198.
- Friedel, R.A., Hofer, L.J.E. Spectral characterization of activated carbon. *Journal of Physical Chemistry*, 74, 1970, 2921-2922.
- Ganan, J., Gonzalez, J.F., Gonzalez-Garcia, C.M., Ramiro, A., Sabio, E., Roman, S. Air-activated carbons from almond tree pruning: Preparation and characterization. *Applied Surface Science*, 252, 2006, 5988-5992.

- Ganguli, A., Tripathi, A.K. Bioremediation of toxic chromium from electroplating effluent by chromate-reducing *Pseudomonas aeruginosa* A2Chr in two bioreactors. *Applied Microbiology and Biotechnology*, 58, 2002, 416-420.
- Gani, A., Naruse, I. Effect of cellulose and lignin content on pyrolysis and combustion characteristics for several types of biomass. *Renewable Energy*, 32, 2007, 649-661.
- Gao, X., Liu, S., Zhang, Y., Luo, Z., Cen, K. Physicochemical properties of metal-doped activated carbons and relationship with their performance in the removal of SO₂ and NO. *Journal of Hazardous Materials*, 188 (1-3), 2011, 58-66.
- Garcia, T., Murillo, R., Cazorla-Amoros, D., Mastral, A.M., Linares-Solano, A. Role of the activated carbon surface chemistry in the adsorption of phenanthrene. *Carbon*, 42, 2004, 1683-1689.
- Gaur, V., Asthana, R., Nishith, V. Removal of SO₂ by activated carbon fibers in the presence of O₂ and H₂O. *Carbon*, 44 (1), 2006, 46-60.
- Girgis, B.S., EI-Hendawy, A.N.A. Porosity development in activated carbons obtained from date pits under chemical activation with phosphoric acid. *Microporous and Mesoporous Materials*, 52, 2002, 105-117.
- Goel, J., Kadirvelu, K., Rajagopal, C., Kumar Garg, V. Removal of lead(II) by adsorption using treated granular activated carbon: Batch and column studies. *Journal of Hazardous Materials*, 125, 2005, 211-220.
- Gomez, G., Larrechi, M.S., Callao, M.P. Kinetic and adsorption study of acid dye removal using activated carbon. *Chemosphere*, 69 (7), 2007, 1151-1158.
- Gomez-Sarrano, V., Cuerda-Correa, E.M., Fernandez-Gonzalez, M.C., Alexandre-Franco, M.F., Macias-Garcia, A. Preparation of activated carbons from chestnut wood by phosphoric acid-chemical activation. Study of microporosity and fractal dimension. *Materials Letters*, 59, 2005, 846-853.
- Gonzalez-Serrano, E., Cordero, T., Rodriguez-Mirasol, J., Cotoruelo, L., Rodriguez, J.J. Removal of water pollutants with activated carbons prepared from H₃PO₄ activation of lignin from kraft black liquors. *Water Research*, 38 (13), 2004, 3043-3050.
- Goswami, S., Ghosh, U.C. Studies on adsorption behavior of Cr(VI) onto synthetic hydrous stannic oxide. *Water SA*, 31 (4), 2005, 579-602.
- Gregg, S.J., Sing, K.S.W. *Adsorption, Surface Area and Porosity*, Academic Press, 1982, London.
- Guo, J., Lua, A.C. Textural characterization of activated carbon prepared from oil-palm stones with various impregnating agents. *Journal of Porous Materials*, 7 (4), 2000, 491-497.
- Guo, S., Peng, J., Li, W., Yang, K., Zhang, L., Zhang, S., Xia, H. Effects of CO₂ activation on porous structures of coconut shell-based activated carbons. *Applied Surface Science*, 255, 2009, 8443-8449.

- Guo, Y., Qi, J., Yang, S., Yu, K., Wang, Z., Xu, H. Adsorption of Cr(VI) on micro- and mesoporous rice husk-based active carbon. *Materials Chemistry and Physics*, 78, 2002, 132-137.
- Guo, Y., Rockstraw, D.A., Activated carbons prepared from rice hull by one-step phosphoric acid activation. *Microporous and Mesoporous Materials*, 100, 2007, 12-19.
- Gupta, V.K., Gupta, B., Rastogi, A., Agarwal, S., Nayak., A. Pesticides removal from waste water by activated carbon prepared from waste rubber tire. *Water Research*, 45 (13), 2011, 4047-4055.
- Gupta, V.K., Mittal, A., Jain, R., Mathur, M., Sikarwar, S. Adsorption of safranin-T from wastewater using waste materials – activated carbon and activated rice husks. *Journal of Colloid and Interface Science*, 303, 2006, 80-86.
- Hagstam., K.E., Larsson, L.E., Thysell., H. Experimental studies on charcoal haemoperfusion in phenobarbital intoxication and uraemia, including histopathologic findings. *Acta Med Scand*, 180 (5), 1966, 593-603.
- Hai, F.I., Yamamoto, K., Nakajima, F., Fukushi, K. Bioaugmented membrane bioreactor (MBR) with a GAC – packed zone for high rate textile wastewater treatment. *Water Research*, 45 (6), 2011, 2199-2206.
- Haimour, N.M., Emeish, S., Utilization of date stones for production of activated carbon using phosphoric acid. *Waste Management*, 26 (6), 2006, 651-660.
- Hamadi, N.K., Chen, X.D., Farid, M.M., Lu, M.G.Q. Adsorption kinetics for the removal of chromium(VI) from aqueous solution by adsorbents derived from used tyres and sawdust. *Chemical Engineering Journal*, 84, 2001, 95-105.
- Hao, G.P., Li, W.C., Wang, S., Wang, G.H., Qi, L., Lu, A.H. Lysine-assisted rapid synthesis of crack free hierarchical carbon monoliths with a hexagonal array of mesopores. *Carbon*, 49, 2011, 3762-3772.
- Hayashi, J., Horikawa, T., Takeda, I., Muroyama, K., Ani, F.N. Preparing activated carbon from various nutshells by chemical activation with K_2CO_3 . *Carbon*, 40, 2002, 2381-2386.
- Helfferich., F. Ion exchange. New York: McGraw-Hill; 1962.
- Hijnen, W.A.M., Suylen, G.M.H., Bahlman, J.A., Brouwer-Hanzens, A., Medema, G.J. GAC adsorption filters as barriers for viruses, bacteria and protozoan (oo)cysts in water treatment. *Water Research*, 44 (4), 2010, 1224-1234.
- Ho, Y.S. Citation review of Lagergren kinetic rate equation on adsorption reactions. *Scientometrics*, 59, 2004, 171-177.
- Ho, Y.S. Review of second-order models for adsorption systems. *Journal of Hazardous Materials*, 136, 2006, 681-689.

- Ho, Y.S. Second-order kinetic model for the biosorption of cadmium onto tree fern: a comparison of linear and non-linear methods. *Water Research*, 40, 2006, 119-125.
- Ho, Y.S., McKay G. The kinetics of biosorption of divalent metal ions onto sphagnum moss peat. *Water Research*, 34, 2000, 735-742.
- Ho, Y.S., McKay, G. Biosorption of dye from aqueous solution by peat. *Chemical Engineering Journal*, 70, 1998, 115-124.
- Ho, Y.S., McKay, G. Pseudo-second order model for biosorption processes. *Process Biochemistry*, 34, 1999, 451-465.
- Ho, Y.S., Ofomaja, A.E. Kinetics and thermodynamics of lead ion biosorption on palm kernel fibre from aqueous solution. *Process Biochemistry*, 40, 2005, 3455-3461.
- Horikawa, T., Kitakaze, Y., Sekida, T., Hayashi, J., Katoh, M. Characteristics and humidity control capacity of activated carbon from bamboo. *Bioresource Technology*, 101, 2010, 3964-3969.
- Horshall, M. Jnr., Spiff, A.I., Abia, A.A. Studies on the influence of mercaptoacetic acid (MAA) modification of cassava (*Manihot sculenta* Cranz) waste biomass on the adsorption of Cu^{2+} and Cd^{2+} from aqueous solution. *Bulletin of Korean Chemical Society*, 25 (7), 2004, 969-976.
- Hosseini-Bandegharai, A., Hosseini, M.S., Sarw-Ghadi, M., Zowghi, S., Hosseini, E., Hosseini-Bandegharai, H. Kinetics, equilibrium and thermodynamic study of Cr(VI) sorption into toluidine blue o-impregnated XAD-7 resin beads and its application for the treatment of wastewaters containing Cr(VI). *Chemical Engineering Journal*, 160, 2010, 190-198.
- Hsu, L.Y., Teng, H., Influence of different chemical reagents on the preparation of activated carbons from bituminous coal. *Fuel Processing Technology* 64 (1-3), 2000, 155-166.
- Hsu, N.H., Wang, S.L., Liao, Y.H., Huang, S.T., Tzou, Y.M., Huang, Y.M. Removal of hexavalent chromium from acidic aqueous solutions using rice straw-derived carbon. *Journal of Hazardous Materials*, 171 (1-3), 2009, 1066-1070.
- Hu, Z., Lei, L., Li, Y., Ni, Y. Chromium adsorption on high-performance activated carbons from aqueous solution. *Separation and Purification Technology*, 31, 2003, 13-18.
- Hu, Z., Srinivasan, M.P. Mesoporous high-surface-area activated carbon. *Microporous and Mesoporous Materials*, 43, 2001, 267-275.
- Hu, Z., Srinivasan, M.P., Preparation of high-surface-area activated carbons from coconut shell. *Microporous and Mesoporous Materials*, 27 (1), 1999, 11-18.

- Huang, C.C., Chen, C.H., Chu, S.M. Effect of moisture on H₂S adsorption by copper impregnated activated carbon. *Journal of Hazardous Materials*, 136 (3), 2006, 866-873.
- Huang, H.H., Lu, M.C., Chen, J.N., Lee, C.T. Catalytic decomposition of hydrogen peroxide and 4-chlorophenol in the presence of modified activated carbons. *Chemosphere*, 51 (9), 2003, 935-943.
- Huang, Z.H., Kang, F., Liang, K.-M., Hao, J. Breakthrough of methylethylketone and benzene vapors in activated carbon fiber beds. *Journal of Hazardous Materials B*, 98, 2003, 107-115.
- Humbert, H., Gallard, H., Suty, H., Croue, J.-P. Natural organic matter (NOM) and pesticides removal using a combination of ion exchange resin and powdered activated carbon (PAC). *Water Research*, 42 (6-7), 2008, 1635-1643.
- Iang, X., Ju, X., Huang, M. Preparation and characterization of porous carbon spheres with controlled micropores and mesopores. *Journal of Alloys and Compounds*, 509, 2011, S864-S867.
- Igwe, J.C., Abia, A.A. Equilibrium sorption isotherm studies of Cd(II), Pb(II) and Zn(II) ions detoxification from waste water using unmodified and EDTA-modified maize husk. *Electronic Journal of Biotechnology*, 10 (4), 2007, 536-548.
- Ioannidou, O., Zabaniotou, A. Agricultural residues as precursors for activated carbon production – A review. *Renewable and Sustainable Energy Reviews*, 11, 2007, 1966-2005.
- Ioannidou, O.A., Zabaniotou, A.A., Stavropoulos, G.G., Islam, A., Albanis, T.A. Preparation of activated carbons from agricultural residues for pesticide adsorption. *Chemosphere*, 80 (11), 2010, 1328-1336.
- Ip, A.W.M., Barford, J.P., McKay, G. Production and comparison of high surface area bamboo derived activated carbons. *Bioresource Technology*, 99, 2008, 8909-8916.
- Ishazaki, C., Marti, I. Surface oxide structures on a commercial activated carbon. *Carbon*, 19, 1981, 409-412.
- Ishizaki, C., Ishizaki, K., Ogura, M., An analytical electron microscopy study of a commercial activated carbon. *Carbon*, 26 (3), 1988, 317-326.
- Issabayeva, G., Aroua, M.K., Sulaiman, N.M.N. Removal of lead from aqueous solutions on palm shell activated carbon. *Bioresource Technology*, 97, 2006, 2350-2355.
- IUPAC Manual of Symbols and Terminology, Appendix 2, Pt.1, Colloid and Surface Chemistry. *Pure and Applied Chemistry*, 31, 1972, 578.
- Jagiello, J., Thommes, M. Comparison of DFT characterization methods based on N₂, Ar, CO₂, and H₂ adsorption applied to carbons with various pore size distributions. *Carbon*, 42 (7), 2004, 1227-1232.
- Jagtøyen M, Derbyshire F. Activated carbons from yellow poplar and white oak by H₃PO₄ activation. *Carbon*, 36, 1998, 1085-97.

- Jagtoyen M, Derbyshire F. Activated carbons from yellow poplar and white oak by H₃PO₄ activation. *Carbon*, 36, 1998, 1085-1097.
- Jagtoyen, M., Derbyshire, F. Activated carbon from yellow poplar and white oak by H₃PO₄ activation. *Carbon*, 36, 1998, 1085-1097.
- Janick, J., Paull, R.E. *The encyclopedia of fruit and nuts*. CABI, 2008, 768-769.
- Jankowska, H., Swiatkowski, A., Choma, J. in *Active Carbon*. Ellis Harwood, 1991, 50-52, New York.
- Jaramillo, J., Alvarez, P.M., Gomez-Serrano, V. Oxidation of activated carbon by dry and wet methods: Surface chemistry and textural modifications. *Fuel Processing Technology*, 91 (11), 2010, 1768-1775.
- Jarvie, M.E., Hand, D.W., Bhuvendralingam, S., Crittenden, J.C., Hokanson, D.R. Simulating the performance of fixed-bed granular activated carbon adsorbers: Removal of synthetic organic chemicals in the presence of background organic matter. *Water Research*, 39 (11), 2005, 2407-2421.
- Jenkins, G.M., Kawamura, K. *Polymeric carbons*. Cambridge University Press, 1976, Cambridge.
- Jia, Y.F., Thomas, K.M. Adsorption of cadmium ions on oxygen surface sites in activated carbon. *Langmuir*, 16, 2000, 1114-1122.
- Jia, Y.F., Xiao, B., Thomas, K.M. Adsorption of Metal ions on nitrogen surface functional groups in activated carbons. *Langmuir*, 18, 2002, 470-478.
- Jusoh, A., Hartini, W.J.H., Ali, N., Endut, A. Study on the removal of pesticide in agricultural runoff by granular activated carbon. *Bioresource Technology*, 102 (9), 2011, 5312-5318.
- Kadirvelu, K., Kavipriya, M., Karthika, C., Radhika, M., Vennilamani, N., Pattabhi, S. Utilization of various agricultural wastes for activated carbon preparation and application for the removal of dyes and metal ions from aqueous solutions. *Bioresource Technology*, 87, 2003, 129-132.
- Kadirvelu, K., Namasivayam, C. Activated carbon from coconut coir pith as metal adsorbent: adsorption of Cd(II) from aqueous solution. *Advances in Environmental Research*, 7 (2), 2003, 471-478.
- Kadirvelu, K., Senthilkumar, P., Thamaraiselvi, K., Subburam, V. Activated carbon prepared from biomass as adsorbent: elimination of Ni(II) from aqueous solution. *Bioresource Technology*, 81 (1), 2002, 87-90.
- Kalavathy, H., Karthik, B., Miranda, L.R. Removal and recovery of Ni and Zn from aqueous solution using activated carbon from *Hevea Brasiliensis*: Batch and column studies. *Colloids and Surfaces B: Biointerfaces*, 78 (2), 2010, 291-302.

- Kalderis, D., Bethanis, S., Paraskeva, P., Diamadopoulos, E. Production of activated carbon from bagasse and rice husk by a single-stage chemical activation method at low retention time. *Bioresource Technology*, 99, 2008, 6809-6816.
- Kante, K., Deliyanni, E., Bandosz, T.J. Interactions of NO₂ with activated carbons modified with cerium, lanthanum and sodium chlorides. *Journal of Hazardous Materials*, 165, 2009, 704-713.
- Karthikeyan, S., Balasubramanian, R., Iyer, C.S.P. Evaluation of the marine algae *Ulva fasciata* and *Sargassum* sp. For the biosorption of Cu(II) from aqueous solutions. *Bioresource Technology*, 98 (2), 2007, 452-455.
- Karthikeyan, T., Rajagopal, S., Miranda, L.R. Chromium (VI) adsorption from aqueous solution by *Hevea Brasilinesis* sawdust activated carbon. *Journal of Hazardous Materials B*, 124, 2005, 192-199.
- Kawano, T., Kubota, M., Onyango, M.S., Watanabe, F., Matsuda, H. Preparation of activated carbon from petroleum coke by KOH chemical activation for adsorption heat pump. *Applied Thermal Engineering*, 28, 2008, 865-871.
- Kennedy, L.J., Vijaya, J.J., Kayalvizhi, K., Sekaran, G. Adsorption of phenol from aqueous solutions using mesoporous carbon prepared by two-stage process. *Chemical Engineering Journal*, 132, 2007, 279-287.
- Kennedy, L.J., Vijaya, J.J., Sekaran, G. Effect of two-stage process on the preparation and characterization of porous carbon composite from rice husk by phosphoric acid activation. *Industrial Engineering and Chemistry Research*, 43, 2004, 1832-1838.
- Khalili, N.R., Campbell, M., Sandi, G., Golas, J. Production of micro- and mesoporous activated carbon from paper mill sludge I. Effect of zinc chloride activation. *Carbon*, 38, 2000, 1905-1915.
- Khezami, L., Capart, R. Removal of chromium (VI) from aqueous solution by activated carbons: Kinetics and equilibrium studies. *Journal of Hazardous Materials B*, 123, 2005, 223-231.
- Kim, D., Cai, Z., Sorial, G.A. Determination of gas phase adsorption isotherms – a simple constant volume method. *Chemosphere*, 64 (8), 2006, 1362-1368.
- Klijanienko, A., Lorenc-Grabowska, E., Gryglewicz, G. Development of mesoporosity during phosphoric acid activation of wood in steam atmosphere. *Bioresource Technology*, 99 (15), 2008, 7208-7214.
- Ko, Y.N., Choi, U.S., Kim, J.S., Park, Y.S. Novel synthesis and characterization of activated carbon fiber and dye adsorption modeling. *Carbon*, 40 (14), 2002, 2661-2672.
- Kohl, S., Drochner, A., Vogel, H. Quantification of oxygen surface groups on carbon materials via diffuse reflectance FT-IR spectroscopy and temperature programmed desorption. *Catalysis Today*, 150 (1-2), 2010, 67-70.
- Kuzin, A.M. *Foundations of Radiation Biology* (in Russian) Atomizdat Publ., 1964, Moscow.

- Kyzas, G.Z., Kostoglou, M., and Lazaridis, N.K. Copper and chromium(VI) removal by chitosan derivatives-equilibrium and kinetic studies. *Chemical Engineering Journal*, 152, 2009, 440-448.
- Lai, K.C., Lo, I.M. Removal of chromium (VI) by acid-washed zero-valent iron under various ground water geochemistry conditions. *Environmental Science & Technology*, 42, 2008, 1238-1244.
- Langmuir, I. The adsorption of gases on plane surfaces of glass, mica, and platinum. *Journal of American Chemical Society*, 40 (9), 1918, 1361-1403.
- Laszlo, K., Szucs, A. Surface characterization of polyethyleneterephthalate(PET) based activated carbon and the effect of pH on its adsorption capacity from aqueous phenol and 2,3,4-trichlorophenolsolutions. *Carbon*, 39, 2001, 1945-1953.
- Laszlo, K. Adsorption from aqueous phenol and anilinesolutions on activated carbons with different surface chemistry. *Colloids and Surfaces A: Physicochemical and Engineering Aspects*, 265, 2005, 32-39.
- Lazaro, M.J., Galvez, M.E., Artal, S., Palacios, J.M., Moliner, R. Preparation of steam-activated carbons as catalyst supports. *Journal of Analytical and Applied Pyrolysis*, 78 (2), 2007, 301-315.
- Lee, Y.W., Choi, D.K., Park, J.W. Performance of fixed-bed KOH impregnated activated carbon adsorber for NO and NO₂ removal in the presence of oxygen. *Carbon*, 40 (9), 2002, 1409-1417.
- Lei, S., Miyamoto, J., Kanoh, H., Nakahigashi, Y., Kaneko, K. Enhancement of the methylene blue adsorption rate for ultra-microporous carbon by addition of mesopores. *Carbon*, 44 (10), 2006, 1884-1890.
- Li, K., Ling, L., Lu, C., Liu, Z., Liu, L., Mochida, I. Influence of CO-evolving groups on the activity of activated carbon fiber for SO₂ removal. *Fuel Processing Technology*, 70 (3), 2001, 151-158.
- Li, K., Ling, L., Lu, C., Qiao, W., Liu, Z., Liu, L., Mochida, I. Catalytic removal of SO₂ over ammonia activated carbon fibers. *Carbon*, 39 (12), 2001, 1803-1808.
- Li, L., Liu, S., Liu, J. Surface modification of coconut shell based activated carbon for the improvement of hydrophobic VOC removal. *Journal of Hazardous Materials*, 192 (2), 2011, 683-690.
- Li, Y., Du, Q., Wang, X., Zhang, P., Wang, D., Wang, Z., Xia, Y. Removal of lead from aqueous solution by activated carbon prepared from *Enteromorpha prolifera* by zinc chloride activation. *Journal of Hazardous Materials*, 183, 2010, 583-589.
- Li, Y.H., Wang, S., Cao, A., Zhao, D., Zhang, X., Xu, C., Luan, Z., Ruan, Liang, J., Wu, D., Wei, B. Adsorption of fluoride from water by amorphous alumina supported on carbon nanotubes. *Chemical Physics Letters*, 350, 2001, 412-416.

- Lillo-Rodenas, M.A., Juan-Juan, J., Cazorla-Amoros, D., Linares-Solano, A. About reactions occurring during chemical activation with hydroxides. *Carbon*, 42 (7), 2004, 1371-1375.
- Ling, L., Li, K., Liu, L., Miyamoto, S., Korai, Y., Kawano, S., Mochida, I. Removal of SO₂ over ethylene tar pitch and cellulose based activated carbon fibers. *Carbon*, 37 (3), 1999, 499-504.
- Liou, T.H. Development of mesoporous structure and high adsorption capacity of biomass-based activated carbon by phosphoric acid and zinc chloride activation. *Chemical Engineering Journal*, 158, 2010, 129-142.
- Lithoxoos, G.P., Labropoulos, A., Peristeras, L.D., Kanellopoulos, N., Samios, J., Economou, I.G. Adsorption of N₂, CH₄, CO and CO₂ in single walled carbon nanotubes: A combined experimental and Monte Carlo molecular simulation study. *The Journal of Supercritical Fluids*, 55 (2), 2010, 510-523.
- Liu, C., Liang, X., Liu, X., Wang, Q., Teng, N., Zhan, L., Zhang, R., Qiao, W., Ling, L. Wettability modification of pitch-based spherical activated carbon by air oxidation and its effects on phenol adsorption. *Applied Surface Science*, 254, 2008, 2659-2665.
- Liu, Z.S. Adsorption of SO₂ and NO from incineration flue gas onto activated carbon fibers. *Waste Management*, 28 (11), 2008, 2329-2335.
- Liu, Q., Liu, Z. Carbon supported vanadia for multi-pollutants removal from flue gas. *Fuel*, 2011 (In press).
- Liyan, S., Youcai, Z., Weimin, S., Ziyang, L. Hydrophobic organic chemicals (HOCs) removal from biologically treated landfill leachate by powder-activated carbon (PAC), granular-activated carbon (GAC) and biomimetic fat cell (BFC). *Journal of Hazardous Materials*, 163 (2-3), 2009, 1084-1089.
- Lodewyckx, P. The effect of water uptake in ultramicropores on the adsorption of water vapour in activated carbon. *Carbon*, 48 (9), 2010, 2549-2553.
- Long, X.L., Xin, Z.L., Wang, H.X., Xiao, W.D., Yuan, W.K. Simultaneous removal of NO and SO₂ with hexamminecobalt(II) solution coupled with the hexamminecobalt(II) regeneration catalyzed by activated carbon. *Applied Catalysis B: Environmental*, 54 (1), 2004, 25-32.
- Lopez de Letona Sanchez, M., Macias-Garcia, A., Diaz-Diez, M.A., Cuerda-Correa, E.M., Ganan-Gomez, J., Nadal-Gisbert, A. Preparation of activated carbons previously treated with hydrogen peroxide: Study of their porous texture. *Applied Surface Science*, 252 (17), 2006, 5984-5987.
- Lopez M, Labady M, Laine J. Preparation of activated carbon from wood monolith. *Carbon*, 34, 1996, 825-827.
- Lopez, D., Buitrago, R., Sepnveda-Escribano, A., Rodriguez-Reinoso, F., Mondragon, F. Low temperature catalytic adsorption of SO₂ on activated carbon. *Journal of Physical Chemistry C*, 112, 2008, 15335-15340.

- Lopez, D., Buitrago, R., Sepulveda-Escribano, A., Rodriguez-Reinoso, F., Mondragon, F. Surface complexes formed during simultaneous catalytic adsorption of NO and SO₂ on activated carbons at low temperatures. *Journal of Physical Chemistry C*, 111, 2007, 1417-1423.
- Lu, C., Liu, C., Purnachandra Rao, G. Comparisons of sorbent cost for the removal of Ni²⁺ from aqueous solution by carbon nanotubes and granular activated carbon. *Journal of Hazardous Materials*, 151 (1), 2008, 239-246.
- Lu, C.Y., Wey, M.Y. Simultaneous removal of VOC and NO by activated carbon impregnated with transition metal catalysts in combustion flue gas. *Fuel Processing Technology*, 88 (6), 2007, 557-567.
- Lu, Z., Mercedes Maroto-Valer, M., Schobert, H.H. Catalytic effects of inorganic compounds on the development of surface areas of fly ash carbon during steam activation. *Fuel*, 89, 2010, 3436-3441.
- Lua, A.C., Yang, T. Characteristics of activated carbon prepared from pistachio-nut shell by zinc chloride activation under nitrogen and vacuum conditions. *Journal of Colloid and Interface Science*, 290, 2005, 505-513.
- Madhava Rao, M., Kumar Reddy, D.H.K., Venkateswarlu, P., Seshaiiah, K. Removal of mercury from aqueous solutions using activated carbon prepared from agricultural by-product/waste. *Journal of Environmental Management*, 90 (1), 2009, 634-643.
- Madhava Rao, M., Ramesh, A., Purna Chandra Rao, G., Seshaiiah, K. Removal of copper and cadmium from the aqueous solutions by activated carbon derived from *Ceiba pentandra* hulls. *Journal of Hazardous Materials*, 129, 2006, 123-129.
- Madhava Rao, M., Chandra Rao, G.P., Seshaiiah, K., Choudary, N.V., Wang, M.C. Activated carbon from *Ceiba pentandra* hulls, an agricultural waste, as an adsorbent in the removal of lead and zinc from aqueous solutions. *Waste Management*, 28 (5), 2008, 849-858.
- Maji, S.K., Pal, A., Pal, T., Adak, A. Adsorption thermodynamics of arsenic on Laterite soil. *Journal of Surface Science and Technology*, 2007, 22 (3-4), 161-176.
- Mamcilovic, M., Purenovic, M., Bojic, A., Zarubica, A., Randelovic, M. Removal of lead (II) ions from aqueous solutions by adsorption onto pine cone activated carbon. *Desalination*, 276 (1-3), 2011, 53-59.
- Marsh, H., Rodriguez-Reinoso, F., *Activated Carbon*, Elsevier, 2006.
- Martin-Gullon, I., Font, R. Dynamic pesticide removal with activated carbon fibers. *Water Research*, 35 (2), 2001, 516-520.
- Masuda, J., Fukuyama, J., Fujii, S. Influence of concurrent substances on removal of hydrogen sulfide by activated carbon. *Chemosphere*, 39 (10), 1999, 1611-1616.
- McEnaney B. Estimation of the dimensions of micropores in active carbons using the Dubinin-Radushkevich equation. *Carbon*, 25, 1987, 69-75.

- Meena, A.K., Mishra, G.K., Rai, P.K., Rajagopal, C., & Nagar, P.N. Removal of heavy metal ions from aqueous solutions using carbon aerogel as an adsorbent. *Journal of Hazardous Materials*, 150, 2008, 604-611.
- Menendez-Diaz, J.A., Martin-Gullon, I. Types of carbon adsorbents and their production. *Interface Science and Technology*, 7, 2006, 1-47.
- Mishra, S. Report on Design of a cheap water filter for chromium contaminated water. Water initiative technology, DST, India.
- Miyawaki, J., Shimohara, T., Shirahama, N., Yasutake, A., Yoshikawa, M., Mochida, I., Yoon, S.H. Removal of NO_x from air through cooperation of the TiO₂ photocatalyst and urea on activated carbon fiber at room temperature. *Applied Catalysis B: Environmental*, 110, 2011, 273-278.
- Mochida, I., Korai, Y., Shirahama, M., Kawano, S., Hada, T., Seo, Y., Yoshikawa, M., Yasutake, A. Removal of Sox and NO_x over activated carbon fibers. *Carbon*, 38 (2), 2000, 227-239.
- Mohamed, M.M. Acid dye removal: comparison of surfactant modified mesoporous FSM-16 with activated carbon derived from ricehusk. *Journal of Colloid and Interface Science*, 272, 2004, 28-34.
- Mohammadi, S.Z., Karimi, M.A., Afzali, D., Mansouri, F. Removal of Pb(II) from aqueous solutions using activated carbon from sea-buckthorn stones by chemical activation. *Desalination*, 262 (1-3), 2010, 86-93.
- Mohan ,D., Singh, K.P., Singh, V.K. Trivalent chromium removal from waste water using low cost activated carbon derived from agricultural waste material and activated carbon fabric cloth. *Journal of Hazardous Materials*, 135 (1-3), 2006, 280-295.
- Mohan, D., Singh, K.P. Single and multi-component adsorption of cadmium and zinc using activated carbon derived from bagasse – an agricultural waste. *Water Research*, 36, 2002, 2304-2318.
- Mohan, D., Singh, K.P., Singh, V.K. Removal of hexavalent chromium from aqueous solution using low-cost activated carbons derived from agricultural waste materials and activated carbon fabric cloth. *Industrial and Engineering Chemistry Research*, 44, 2005, 1027-1042.
- Mohanty, K., Jha, M., Meikap, B.C., Biswas, M.N. Removal of Cr(VI) from dilute aqueous solutions by activated carbon developed from Terminalia arjuna nuts activated with zinc chloride. *Chemical Engineering Science*, 60, 2005, 3049-3059.
- Molina-Sabio, M., Rodriguez-Reinoso, F. Role of chemical activation in the development of carbon porosity. *Colloids and Surfaces A: Physicochem and Engineering Aspects*, 241, 2004, 15-25.
- Monser, L., Adhoum, N. Modified activated carbon for the removal of copper, zinc, chromium and cyanide from wastewater. *Separation and Purification Technology*, 26, 2002, 137-146.

- Monser, L., Adhoum, N. Tatrazine modified activated carbon for the removal of Pb(II), Cd(II) and Cr(III). *Journal of Hazardous Materials*, 161 (1), 2009, 263-269.
- Montane, D., Torne-Fernandez, V., Fierro, V. Activated carbons from lignin: kinetic modeling of the pyrolysis of Kraft lignin activated with phosphoric acid. *Chemical Engineering Journal*, 106, 2005, 1-12.
- Monteleone, G., De Francesco, M., Galli, S., Marchetti, M., Naticchioni, V. Deep H₂S removal from biogas for molten carbonate fuel cell (MCFC) systems. *Chemical Engineering Journal*, 173 (2), 2011, 407-414.
- Montgomery, D.C. *Design and Analysis of Experiments*, fourth ed., John Wiley and Sons, New York, 1997.
- Mor, S., Ravindra K., Bishnoi, N.R. Adsorption of Chromium from aqueous solution by activated alumina and activated charcoal. *Bioresource Technology*, 98, 2007, 954-957.
- Moreno-Castilla, C. Adsorption of organic molecules from aqueous solutions on carbon materials. *Carbon*, 42 (1), 2004, 83-94.
- Moreno-Castilla, C., Rivera-Utrilla, J. Carbon materials as adsorbents for the removal of pollutants from the aqueous phase. *Materials Research Society Bulletin*, 26, 2001, 890-894.
- Mozammel, H.M., Masahiro, O., Bhattacharya, S.C. Activated charcoal from coconut shell using ZnCl₂ activation. *Biomass and Bioenergy*, 22, 2002, 397-400.
- Munoz-Gonzalez, Y., Arriagada-Acuna, R., Soto-Garrido, G., Garcia-Lovera, R. Activated carbons from peach tones and pine sawdust by phosphoric acid activation used in clarification and decolorization processes. *Journal of Chemical Technology & Biotechnology*, 84, 2009, 39-47.
- Muthukrishnan, M., and Guha, B.K. Effect of pH on rejection of hexavalent chromium by nanofiltration. *Desalination*, 219, 2008, 171-178.
- Muthukumar, K., Beulah, S. Removal of Chromium (VI) from wastewater using chemically activated *Syzygium jambolanum* nut carbon by batch studies. *Procedia Environmental Sciences*, 4, 2011, 266-280.
- Nabais, J.V., Carrott, P., Carrott, M.M.L.R., Luz, V., Ortiz, A.L. Influence of preparation conditions in the textural and chemical properties of activated carbons from a novel biomass precursor: the coffee endocarp. *Bioresource Technology*, 99, 2008, 7224-7231.
- Nabais, J.M.V., Nunes, P., Carrot, P.J.M., Carrot, M.M.L.R., Garcia, A.M., Diaz-Diaz, M.A. Production of activated carbons from coffee endocarp by CO₂ and steam activation. *Fuel Processing Technology*, 89, 2008, 262-268.
- Nadeem, M., Mahmood, A., Shahid, S.A., Shah, S.S., Khalid, A.M., McKay, G. Sorption of lead from aqueous solution by chemically modified carbon adsorbents. *Journal of Hazardous Materials*, 138, 2006, 604-613.

- Nahil, M.A., Williams, P.T. Recycling of carbon fiber reinforced polymeric waste for the production of activated carbon fibers. *Journal of Analytical and Applied Pyrolysis*, 91 (1), 2011, 67-75.
- Namasivayam, C., Sangeetha D., Gunasekaran, R. Removal of anions, heavy metals, organics and dyes from water by adsorption onto a new activated carbon from *Jatropha* husk, an agro-industrial solid waste. *Process Safety and Environmental Protection*, 85 (2), 2007, 181-184.
- Namasivayam, C., Yamuna, R.T. Adsorption of chromium(VI) by a low-cost adsorbent: biogas residual slurry. *Chemosphere*, 30, 1995, 561-578.
- Navarri, P., Marchal, D., Ginestet, A. Activated carbon fiber materials for VOC removal. *Filtration and Separation*, 38 (1), 2001, 33-40.
- Norma Espanola UNE 32001-81. Hulla y antracita: determinacion de la humedad total. Noviembre 1981.
- Norma Espanola UNE 32004-844. Combustibles minerales solidos: determinación de cenizas. Diciembre 1984.
- Nowicki, P., Pietrzak, R., Wachowska, H. Siberian anthracite as a precursor material for microporous activated carbons. *Fuel*, 87, 2008, 2037-2040.
- Nunes, C.A., Guerreiro, M.C. Estimation of surface area and pore volume of activated carbons by methylene blue and iodine numbers. *Quimica Nova*, 34 (3), 2011, 472-476.
- Oguz, E. Adsorption characteristics and kinetics of the Cr(VI) on the *Thuja orientalis*. *Colloids and Surfaces A: Physicochemical and Engineering Aspects*, 252, 2005, 121-128.
- Oh, G.H., Park, C.R. Preparation and characteristics of rice-straw-based porous carbons with high adsorption capacity. *Fuel*, 81 (3), 2002, 327-336.
- Oh, W.C., Jang, W.C. Physical properties and biological effects of activated carbon fibers treated with the herbs. *Carbon*, 41 (9), 2003, 1737-1742.
- Okada, K., Yamamoto, N., Kameshima, Y., Yasumori, A. Porous properties of activated carbons from waste newspaper prepared by chemical and physical activation. *Journal of Colloid and Interface Science*, 262 (1), 2003, 179-193.
- Olivares-Marin M, Fernandez-Gonzalez C, Macias-Garcia A, Gomez-Serrano V. Preparation of activated carbons from cherry stones by activation with potassium hydroxide. *Applied Surface Science*, 252 (17), 2006, 5980-5983.
- Olivares-Marin, M., Fernandez-Gonzalez, C., Macias-Garcia, A., Gomez-Serrano, V. Preparation of activated carbon from cherry stones by chemical activation with $ZnCl_2$. *Applied Surface Science*, 252 (17), 2006, 5967-5971.
- Opperman, D.J., van Heerden, E. Aerobic Cr(VI) reduction by *Thermus scotoeductus* strain SA-01. *Journal of Applied Microbiology*, 103, 2007, 1907-1913.

- Ormad, M.P., Miguel, N., Claver, A., Matesanz, J.M., Ovelleiro, J.L. Pesticides removal in the process of drinking water production. *Chemosphere*, 71 (1), 2008, 97-106.
- Ould-Idriss, A., Stitou, M., Cuerda-Correa, E.M., Fernandez-Gonzalez, C., Marcias-Garcia, A., Alexandre-Franco, M.F., Gomez-Serrano, V. Preparation of activated carbons from olive-tree wood revisited. II. Physical activation with air. *Fuel Processing Technology*, 92, 2011, 266-270.
- Oya, A., Wakahara, T., Yoshida, S. Preparation of pitch-based antibacterial activated carbon fiber. *Carbon*, 31 (8), 1993, 1243-1247.
- Palmer C.D., Puls, R.W. Natural Attenuation of Hexavalent Chromium in Ground Water and Soils, U.S. EPA Ground Water Issue Paper, EPA/540/5-94/505 (U.S. EPA, Office of Research and Development, Washington, 1994).
- Palmer, C.D., Wittbrodt, P.R. Processes affecting the remediation of chromium contaminated sites. *Environmental Health Perspectives*, 92, 1991, 25-40.
- Pandey, K.K., Prasad, G., Singh, V.N. Use of wollastonite for the treatment of Cu(II) rich effluent. *Water Air and Soil Pollution* 27, 1986, 287-296.
- Park, S.J., Park, B.J., Ryu, S.K. Electrochemical treatment on activated carbon fibers for increasing the amount and rate of Cr(VI) adsorption. *Carbon*, 37, 1999, 1223-1226.
- Passow, H., Clarkson, T.W. Rothstein, A. General pharmacology of heavy metals, *Pharmacological Reviews* 13, 1961, 185-224.
- Pastor-Villegas, J., Valanzuela-Calahorro, C., Bernalte-Garcia, A., Gomez-Serrano, V. Characterization study of char and activated carbon prepared from raw and extracted rockrose. *Carbon*, 31 (7), 1993, 1061-1069.
- Patnukao, P., Pavasant, P. Activated carbon from *Eucalyptus camaldulensis* Dehn bark using phosphoric acid activation. *Bioresource Technology*, 99, 2008, 8540-8543.
- Petkovic, L.M., Ginosar, D.M., Rollins, H.W., Burch, K.C., Deiana, C., Silva, H.S., Sardella, M.F., Granados, D. Activated carbon catalysts for the production of hydrogen via the sulfur-iodine thermochemical water splitting cycle. *International Journal of Hydrogen Energy*, 34 (9), 2009, 4057-4064.
- Petrov, N., Budinova, T., Razvigorova, M., Parra, J., Galiatsatou, P. Conversion of olive wastes to volatiles and carbon adsorbents. *Biomass & Bioenergy*, 32 (12), 2008, 1303-1310.
- Petrova, B., Budinova, T., Tsyntsarski, B., Kochkodan, V., Shkavro, Z., Petrov, N. Removal of aromatic hydrocarbons from water by activated carbon from apricot stones. *Chemical Engineering Journal*, 165, 2010, 258-264.
- Phan, N.H., Rio, S., Faur, C., Le Cog, L., Le Cloirec, P., Nguyen, T.H. Production of fibrous activated carbons from natural cellulose (jute, coconut) fibers for water treatment applications. *Carbon*, 44, 2006, 2569-2577.

- Pipatmanomai, S., Kaewluan, S., Vitidsant, T. Economic assessment of biogas-to-electricity generation system with H₂S removal by activated carbon in small pig farm. *Applied Energy*, 86 (5), 2009, 669-674.
- Polshina, A.E., Puziy, A.M., Polshin, E.V., Faragher, R.G.A., Mikhailovsky, S.V. A Mossbauer study of iron adsorption on active carbons. *Fundamentals of adsorption*, LeVan, M.D. (ed.), Kluwer Academic Publishers, Boston, MA, 1996, 741-748.
- Prahas, D., Kartika, Y., Indraswati, N., Ismadji, S. Activated carbon from jackfruit peel waste by H₃PO₄ chemical activation: Pore structure and surface chemistry characterization. *Chemical Engineering Journal*, 140, 2008, 32-42.
- Prakash Kumar, B.G., Shivakamy, K., Miranda, L.R., Velan, M. Preparation of steam activated carbon from rubberwood sawdust (*Hevea brasiliensis*) and its adsorption kinetics. *Journal of Hazardous Materials B*, 136, 2006, 922-929.
- Qian, Q., Machida, M., Tatsumoto, H. Preparation of activated carbons from cattle-manure compost by zinc chloride activation. *Bioresource Technology*, 98, 2007, 353-360.
- Quintanilla, A., Casas, J.A., Rodriguez, J.J. Catalytic wet air oxidation of phenol with modified activated carbons and Fe/activated carbon catalysts. *Applied Catalysis B: Environmental* 76 (1-2), 2007, 135-145.
- Rahman, I.A., Saad, B., Shaidan, S., Sya Rizal, E.S. Adsorption characteristics of malachite green on activated carbon derived from rice husks produced by chemical-thermal process. *Bioresource Technology*, 96, 2005, 1578–1583.
- Ranganathan, K. Chromium removal by activated carbons prepared from *Casurina Equisetifolia* leaves. *Bioresource Technology*, 73, 2000, 99-103.
- Ren, L., Zhang, J., Li, Y., Zhang, C. Preparation and evaluation of cattail fiber-based activated carbon for 2,4-dichlorophenol and 2,4,6-trichlorophenol removal. *Chemical Engineering Journal*, 168 (2), 2011, 553-561.
- Rodriguez-Reinoso, F. The role of carbon materials in heterogeneous catalysis. *Carbon*, 36 (3), 1998, 159-175.
- Rodriguez-Reinoso, F., Molina-Sabio, M. Activated carbons from lignocellulosic materials by chemical and/or physical activation: an overview. *Carbon*, 30 (7), 1992, 1111-1118.
- Rodriguez-Reinoso, F., Molina-Sabio, M., Munecas, M.A. Effect of microporosity and oxygen surface groups of activated carbon in the adsorption of molecules of different polarity. 96, 1992, 2707-2713.
- Romero-Gonzalez, J., Peralta-Videa, J.R., Rodriguez, E., Ramirez, S.L.J.L. Determination of thermodynamic parameters of Cr(VI) adsorption from aqueous solution onto *Agave lechuguilla* biomass. *Journal of Chemical Thermodynamics*, 37, 2005, 343-347.
- Rosas, J.M., Bedia, J., Rodriguez-Mirasol, J., Cordero, T. HEMP – derived activated carbon fibers by chemical activation with phosphoric acid. *Fuel*, 88, 2009, 19-26.

- Rozada, F., Calvo, L.F., Garcia, A.I., Martin-Villacorta, J., Otero, M. Dye adsorption by sewage sludge-based activated carbons in batch and fixed-bed systems. *Bioresource Technology*, 87, 2003, 221-230.
- Sag, Y., Aktay, Y. Kinetic studies on sorption of Cr(VI) and Cu(II) ions by chitin, chitosan and *Rhizopus arrhizus*. *Biochemical Engineering Journal*, 12 (2), 2002, 143-153.
- Sahu, J.N., Acharya, J., Meikap, B.C. Optimization of production conditions for activated carbons from Tamarind wood by zinc chloride using response surface methodology. *Bioresource Technology*, 101, 2010, 1974-1982.
- Sakanishi, K., Wu, Z., Matsumura, A., Saito, I., Hanaoka, T., Minowa, T., Tada, M., Iwasaki, T. Simultaneous removal of H₂S and COS using activated carbons and their supported catalysts. *Catalysis Today*, 104 (1), 2005, 94-100.
- Salvador, F., Sanchez-Montero, M.J., Montero, J., Izquierdo, C. Hydrogen storage in carbon fibers activated with supercritical CO₂: Models and the importance of porosity. *Journal of Power Sources*, 190, 2009, 331-335.
- Sarin, V., Pant, K.K. Removal of chromium from industrial waste by using eucalyptus bark. *Bioresource Technology*, 97, 2006, 15-20.
- Satyawali, Y., Balakrishnan, M. Performance enhancement with powdered activated carbon (PAC) addition in a membrane bioreactor (MBR) treating distillery effluent. *Journal of Hazardous Materials*, 170 (1), 2009, 457-465.
- Scala, F., Chirone, R., Lancia, A. Elemental mercury vapor capture by powdered activated carbon in a fluidized bed reactor. *Fuel*, 90 (6), 2011, 2077-2082.
- Scharf, R.G., Johnston, R.W., Semmens, M.J., Hozalski, R.M. Comparison of batch sorption tests, pilot studies, and modeling for estimating GAC bed life. *Water Research*, 44 (3), 2010, 769-780.
- Sekaran, G., Shanmugasundaram, K.A., Mariappan, M. Characterization and utilisation of buffing dust generated by the leather industry. *Journal of Hazardous Materials*, 63, 1998, 53-68.
- Selomulya, C., Meeyoo, V., Amal, R. Mechanisms of Cr(VI) removal from water by various types of activated carbons. *Journal of Chemical Technology and Biotechnology*, 74, 1999, 111-122.
- Selvaraj, K., Manonmani, S., Pattabhi, S. Removal of hexavalent chromium using distillery sludge. *Bioresource Technology*, 89, 2003, 207-211.
- Serrano, E.G., Cordero, T., Mirasol, J.R., Cotoruelo, L., Rodriguez, J.J. Removal of water pollutants with activated carbons prepared from H₃PO₄ activation of lignin from Kraft black liquors. *Water Research*, 38, 2004, 3043-3050.

- Shafeeyan, M.S., Daud, W.M.A.W., Houshmand, A., Shamiri, A.A. review on surface modification of activated carbon for carbon dioxide adsorption. *Journal of Analytical and Applied Pyrolysis*, 89 (2), 2010, 143-151.
- Sharma, D.C., Forster, C.F. The treatment of chromium wastewaters using the adsorptive potential of leaf mould. *Bioresource Technology*, 49, 1994, 31-40.
- Shen, Z., Ma, J., Mei, Z., Zhang, J. Metal chlorides loaded on activated carbon to capture elemental mercury. *Journal of Environmental Sciences*, 22 (11), 2010, 1814-1819.
- Shi, Q., Zhang, J., Zhang, C., Li, C., Zhang, B., Hu, W., Xu, J., Zhao, R. Preparation of activated carbon from cattail and its application for dyes removal. *Journal of Environmental Sciences*, 22 (1), 2010, 91-97.
- Shin, S., Jang, J., Yoon, S.H., Mochida, I. A study on the effect of heat treatment on functional groups of pitch based activated carbon fiber using FTIR. *Carbon*, 35(12), 1997, 1739-43.
- Sidheswaran, M.A., Destailats, H., Sullivan, D.P., Cohn, S., Fisk, W.J. Energy efficient indoor VOC air cleaning with activated carbon fiber (ACF) filters. *Building and Environment*, 47, 2012, 357-367.
- Sing, K.S.W., Everett, D.H., Haul, R.A.W., Moscou, L., Pierotti, R.A., Rouquerol, J., Siemieniewska, T. Reporting Physisorption data for gas/solid interface with special reference to the determination of surface area and porosity, *Pure and Applied Chemistry*, 57, 1985, 603-619.
- Skubiszewska-Zieba, J. VPO catalysts synthesized on substrates with modified activated carbons. *Applied Surface Science*, 256, 2010, 5520-5527.
- Smisek, M., Cerney, S. *Active carbon*. Elsevier, New York, 1970, 10-48.
- Soleimani, M., Kaghazchi, T. Activated hard shell of apricot stones: a promising adsorbent in gold recovery. *Chinese Journal of Chemical Engineering*, 16, 2008, 112-118.
- Solum, M.S., Pugmire, R.J., Jagtoyen, M., Derbyshire, F. Evolution of carbon structure in chemically activated wood. *Carbon*, 33, 1995, 1247-1254.
- Song, X., Liu, H., Cheng, L., Qu, Y. Surface modification of coconut-based activated carbon by liquid-phase oxidation and its effects on lead ion adsorption, *Desalination*, 255, 2010, 78-83.
- Soto, M.L., Moure, A., Dominguez, H., Parajo, J.C. Recovery, concentration and purification of phenolic compounds by adsorption: A review. *Journal of Food Engineering*, 105 (1), 2011, 1-27.
- Sricharoenchaikul, V., Chiravoot, P., Duangdao, A., Duangduen, A.T. Preparation and characterization of activated carbon from the pyrolysis of physic nut (*Jatropha curcas L.*) waste, *Energy Fuels* 22 (2008) 31-37.
- Srinivasakannan, C., Abu Bakar, M.Z., Production of activated carbon from rubber wood sawdust. *Biomass & Bioenergy*, 27 (1), 2004, 89-96.

- Srinivasan, A., Viraraghavan, T. Oil removal from water by fungal biomass: A factorial design analysis. *Journal of Hazardous Materials*, 175, 2010, 695-702.
- Stavropoulos, G.G., Zabaniotou, A.A. Production and characterization of activated carbons from olive-seed waste residue. *Microporous and Mesoporous Materials*, 82, 2005, 79-85.
- Stumm, W., Morgan, J.J., *Aquatic Chemistry*, 3rd ed., Wiley & Sons, 1996.
- Suarez-Garcia, F., Martinez-Alonso, A., Tascon, J.M.D. Beneficial effects of phosphoric acid as an additive in the preparation of activated carbon fibers from Nomex aramid fibers by physical activation. *Fuel Processing Technology*, 2002, 77-78, 237-244.
- Sumathi, S., Bhatia, S., Lee, K.T., Mohamed, A.R. Adsorption isotherm models and properties of SO₂ and NO removal by palm shell activated carbon supported with cerium (Ce/PSAC). *Chemical Engineering Journal*, 162 (1), 2010, 194-200.
- Sumathi, S., Bhatia, S., Lee, K.T., Mohamed, A.R. Cerium impregnated palm shell activated carbon (Ce/PSAC) sorbent for simultaneous removal of SO₂ and NO – Process study. *Chemical Engineering Journal*, 162, 2010, 51-57.
- Sumathi, S., Bhatia, S., Lee, K.T., Mohamed, A.R. Selection of best impregnated palm shell activated carbon (PSAC) for simultaneous removal of SO₂ and NO_x. *Journal of Hazardous Materials*, 176, 2010, 1093-1096.
- Suzuki, M. *Adsorption Engineering*. Elsevier, Tokyo, 1990.
- Swami., N, Dreisinger., D.B. Kinetics of zinc removal from cobalt electrolytes by ion exchange. *Solvent Extraction and Ion Exchange*, 13, 1995, 1037-1062.
- Tajar, A.F., Kaghazchi, T., Soleimani, M. Adsorption of cadmium from aqueous solutions on sulfurized activated carbon prepared from nut shells. *Journal of Hazardous Materials*, 165 (1-3), 2009, 1159-1164.
- Tan, W.T., Ooi, S.T., Lee, C.K. Removal of Chromium(VI) from solution by coconut husk and palm pressed fibers. *Environmental Technology*, 14, 1993, 277-282.
- Tancredi, N., Medero, N., Moller, F., Piriz, J., Plada, C., Cordero, T. Phenol adsorption onto powdered and granular activated carbon, prepared from Eucalyptus wood. *Journal of Colloid and Interface Science*, 279, 2004, 357-363.
- Tang, C., Zhang, R., Wen, S., Li, K., Zheng, X., Zhu, M. Adsorption of hexavalent chromium from aqueous solution on raw and modified activated carbon. *Water Environment research*, 81 (7), 2009, 728-734.
- Tang, Q., Tang, X., Hu, M., Li, Z., Chen, Y., Lou, P. Removal of Cd(II) from aqueous solution with activated Firmiana Simplex Leaf: Behaviors and affecting factors. *Journal of Hazardous Materials*, 179 (1-3), 2010, 95-103.

- Tangjuank, S., Insuk, N., Udeye, V., Tontrakoon, J. Chromium (III) sorption from aqueous solutions using activated carbon prepared from cashew nut shells. *International Journal of Physical Sciences*, 4 (8), 2009, 412-417.
- TAPPI Standard T 264 om-97. Preparation of wood for chemical analysis, 1997.
- TAPPI Standard T 222 om-98. Acid insoluble lignin in wood and pulp, 1998.
- TAPPI Standard T 203 om-93. Alpha-, beta- and gamma-cellulose in pulp and wood, 1998.
- Temkin, M.J., Pyzhev, V. Kinetics of ammonia synthesis on promoted iron catalysts. *Acta Physicochimica URSS*, 12, 1940, 217-222.
- Tham, Y.J., Latif, P.A., Abdullah, A.M., Shamala-Devi, A., Taufiq-Yap, Y.H. Performances of toluene removal by activated carbon derived from durian shell. *Bioresource Technology*, 102, 2011, 724-728.
- Thimmaiah, S.K. *Standard Methods of Biochemical Analysis*. Kalyani Publishers, 1999, New Delhi.
- Tongpoothorn, W., Sriuttha, M., Homchan, P., Chanthai, S., Ruangviriyachai, C. Preparation of activated carbon derived from *Jatropha curcas* fruit shell by simple thermo-chemical activation and characterization of their physic-chemical properties. *Chemical Engineering Research and Design*, 89, 2011, 335-340.
- Torrents, A., Damera, R., Hao, O.J. Low-temperature thermal desorption of aromatic compounds from activated carbon. *Journal of Hazardous Materials*, 54, 1997, 141-153.
- Tseng, R.L., Tseng, S.K., Wu, F.C., Hu, C.C., Wang, C.C. Effects of micropore development on the physicochemical properties of KOH-activated carbons. *Journal of Chinese Institute of Chemical Engineers*, 39, 2008, 37-47.
- Ustinov, E.A., Do, D.D., Fenelonov, V.B. Pore size distribution analysis of activated carbons : Application of density functional theory using non-graphitized carbon black as a reference system. *Carbon*, 44 (4), 2006, 653-663.
- Ubago-Perez, R., Carrasco-Marin, F., Fairen-Jimenez, D., Moreno-Castilla, C. Granular and monolithic activated carbons from KOH-activation of olive stones. *Microporous and Mesoporous Materials*, 92, 2006, 64-70.
- Valderrama, C., Gamisans, X., de las Heras, X., Farran, A., Cortina, J.L. Sorption kinetics of polycyclic aromatic hydrocarbons removal using granular activated carbon: Intra-particle diffusion coefficients. *Journal of Hazardous Materials*, 157, 2008, 386-396.
- Valdes, H., Sanchez, M., Rivera, J. Effect of ozone treatment on surface properties of activated carbon. *Langmuir*, 18, 2002, 2111-2116.
- Valix, M., Cheung, W.H., McKay, G. Preparation of activated carbon using low temperature carbonization and physical activation of high ash raw bagasse for acid dye adsorption. *Chemosphere*, 56, 2004, 493-501.

- Valix, M., Cheung, W.H., Zhang, K. Role of heteroatoms in activated carbon for removal of hexavalent chromium from wastewaters. *Journal of Hazardous Materials B*, 135, 2006, 395-405.
- Vitolo, S., Seggiani, M. Mercury removal from geothermal exhaust gas by sulfur-impregnated and virgin activated carbons. *Geothermics*, 31 (4), 2002, 431-442.
- Von Kienle, H., Kunze, N., Mertens, D.H. The use of activated carbon in the removal of VOC's. *Studies in Environmental Science*, 61, 1994, 321-329.
- Wang, J., Zhao, F., Hu, Y., Zhao, R., Liu, R. Modification of activated carbon fiber by loading metals and their performance on SO₂ removal. *Chinese Journal of Chemical Engineering*, 14 (4), 2006, 478-485.
- Wang, L., Zhang, J., Zhao, R., Li, Y., Li, C., Zhang, C. Adsorption of Pb(II) on activated carbon prepared from *Polygonum orientale* Linn: kinetics, isotherms, pH, and ionic strength studies. *Bioresource Technology*, 101, 2010, 5808-5814.
- Wang, X., Liang, X., Wang, Y., Wang, X., Liu, M., Yin, D., Xia, S., Zhao, J., Zhang, Y. Adsorption of copper (II) onto activated carbons from sewage sludge by microwave-induced phosphoric acid and zinc chloride activation. *Desalination*, 278 (1-3), 2011, 231-237.
- Wang, X.S., Qin, Y., Li, Z.F. Biosorption of zinc from aqueous solutions by rice bran: kinetics and equilibrium studies. *Separation Science and Technology*, 41, 2006, 747-756.
- Wang, Z.-M., Yamashita, N., Wang, Z.-X., Hoshinoo, K., Kanoh, H. Air oxidation effects on microporosity, surface property, and CH₄ adsorptivity of pitch-based activated carbon fibers. *Journal of Colloid and Interface Science*, 276 (1), 2004, 143-150.
- Weber, W.J., Morris, J.C. Kinetics of adsorption on carbon from solution, *Journal Sanitary Engineering Division- American Society of Civil Engineering*, 89, 1963, 31-60.
- Williams, P.T., Reed, A.R. Development of activated carbon pore structure via physical and chemical activation of biomass fibre waste. *Biomass & Bioenergy*, 30, 2006, 144-152.
- Wu, F.C., Tseng, R.L. Preparation of highly porous carbon from fir wood by KOH etching and CO₂ gasification for adsorption of dyes and phenols from water. *Journal of Colloid and Interface Science*, 294, 2006, 21-30.
- Wu, F.C., Tseng, R.L., Juang, R.S. Comparisons of porous and adsorption properties of carbons activated by steam and KOH. *Journal of Colloid and Interface Science*, 283, 2005, 49-56.
- Wu, F.C., Wu, P.H., Tseng, R.L., Juang, R.S. Preparation of activated carbons from unburnt coal in bottom ash with KOH activation for liquid-phase adsorption. *Journal of Environmental Management*, 91, 2010, 1097-1102.
- Wu, F.C., Wu, P.H., Tseng, R.L., Juang, R.S. Preparation of novel activated carbons from H₂SO₄-pretreated corncob hulls with KOH activation for quick adsorption of dye and 4-chlorophenol. *Journal of Environmental Management*, 92, 2011, 708-713.

- Xiao, Y., Wang, S., Wu, D., Yuan, Q. Experimental and simulation study of hydrogen sulfide adsorption on impregnated activated carbon under anaerobic conditions. *Journal of Hazardous Materials*, 153, 2008, 1193-2000.
- Yan, R., Liang, D.T., Tsen, L., Tay, J.H. Influence of surface properties on the mechanism of H₂S removal by alkaline activated carbons. *Environmental Science and Technology*, 38, 2004, 316-323.
- Yan, R., Liang, D.T., Tsen, L., Tay, J.H. Kinetics and mechanisms of H₂S adsorption by alkaline activated carbon. *Environmental Science and Technology*, 36, 2002, 4460-4466.
- Yang, J.K., Park, H.J., Lee, H.D., Lee, S.M. Removal of Cu(II) by activated carbon impregnated with iron(III). *Colloids and Surfaces A: Physicochemical and Engineering Aspects*, 337 (1-3), 2009, 154-158.
- Yang, T., Lua, A.C. Textural and chemical properties of zinc chloride activated carbons prepared from pistachio-nut shells. *Materials Chemistry and Physics*, 100, 2006, 438-444.
- Yao, M., Zhang, Q., Hand, D.W., Perram, D.L., Taylor, R. Adsorption and regeneration on activated carbon fiber cloth for volatile organic compounds at indoor concentration levels. *Journal of Air and Waste Management Association*, 59 (1), 2009, 31-36.
- Yavuz, R., Orbak, I., Karatepe, N. Factors affecting the adsorption of chromium (VI) on activated carbon. *Journal of Environmental Science and Health Part A*, 41, 2006, 1967-1980.
- Yilmaz, A., Kaya, A., Alpoguz, H., Ersoz, M, and Yilmaz, M. Kinetic analysis of chromium(VI) ions transport through a bulk liquid membrane containing p-tert-butylcalix[4]arene dioxaoctylamide derivative. *Separation and Purification Technology*, 59, 2008, 1-8.
- Youssef, A., Radwan, N., Abdel-Gawad, I., Singer, G. Textural properties of activated carbons from apricot stones. *Colloids and Surfaces A*, 252, 2005, 143-51.
- Youssef, A.M., El-Nabarawy, T., Samra, S.E. Sorption properties of chemically-activated carbons: 1. Sorption of cadmium (II) ions. *Colloids and Surfaces A: Physicochemical and Engineering Aspects*, 235, 2004, 153-163.
- Youssef, A.M., Radwan, N.R.E., Abdel-Gawad, I., Singer, G.A.A. Textural properties of activated carbons from apricot stones. *Colloid and Surfaces A: Physicochemical and Engineering Aspects*, 252, 2005, 143-151.
- Yue, Z., Bender, S.E., Wang, J., Economy, J. Removal of chromium Cr(VI) by low-cost chemically activated carbon materials from water. *Journal of Hazardous Materials*, 166 (1), 2009, 74-78.
- Yusup, S., Aminudin, A., Azizan, M.T., Abdullah, S.S., Sabil., K.M. Improvement of rice husk and coconut shell properties for enhancement of gasification process. *Proceedings of Third International Symposium on Energy from Biomass and Waste*, Venice, Italy, 2010.
- Zabaniotou, A., Stavropoulos, G., Skoulou, V. Activated carbon from olive kernels in a two-stage process: Industrial improvement. *Bioresource Technology*, 99, 2008, 320-326.

- Zhang, F.S., Nriagu, J.O., Itoh, H. Mercury removal from water using activated carbons derived from organic sewage sludge. *Water Research*, 39 (2-3), 2005, 389-395.
- Zhang, H., Tang, Y., Cai, D., Liu, X., Wang, X., Huang, Q., Yu, Z. Hexavalent chromium removal from aqueous solution by algal bloom residue derived activated carbon: Equilibrium and kinetic studies. *Journal of Hazardous Materials*, 181 (1-3), 2010, 801-808.
- Zhang, J., Fu, H., Lu, X., Tang, J., Xu, X. Removal of Cu(II) from aqueous solution using the rice husk carbons prepared by the physical activation process. *Biomass and Bioenergy*, 35, 2011, 464-472.
- Zhang, J., Giorno, L., Drioli, E. Study of a hybrid process combining PACs and membrane operations for antibiotic wastewater treatment. *Desalination*, 2006, 194 (1-3), 101-107.
- Zhang, N., Lin, L.S., Gang, D. Adsorptive selenite removal from water using iron-coated GAC adsorbents. *Water Research*, 42 (14), 2008, 3809-3816.
- Zhang, T., Walawender, W., Fan, L. Preparation of carbon molecular sieves by carbon deposition from methane. *Bioresource Technology*, 96, 2005, 1929-35.
- Zhao, J., Yang, L., Li, F., Yu, R., Jin, C. Structural evolution in the graphitization process of activated carbon by high-pressure sintering. *Carbon*, 47, 2009, 744-751.
- Zhao, Y., Wang, J., Luan, Z., Peng, X., Liang, Z., Shi, L. Removal of phosphate from aqueous solution by red mud using a factorial design. *Journal of Hazardous Materials*, 165, 2009, 1193-1199.
- Zhu, Y., Gao, J., Li, Y., Sun, F., Gao, J., Wu, S., Qin, Y. Preparation of activated carbons for SO₂ adsorption by CO₂ and steam activation. *Journal of the Taiwan Institute of Chemical Engineers*, 43 (1), 2012, 112-119.
- Zhu, Z., Li, A., Yan, L., Liu, F., Zhang, Q. Preparation and characterization of highly mesoporous spherical activated carbons from divinyl benzene-derived polymer by ZnCl₂ activation, *Journal of Colloid and Interface Science*, 316, 2007, 628-634.
- Zuo, S., Yang, J., Liu, J., Cai, X. Significance of the carbonization of volatile pyrolytic products on the properties of activated carbons from phosphoric acid activation of lignocellulosic material. *Fuel Processing Technology*, 90, 2009, 994-1001.

Ramakrishna Gottipati

Ph.D Scholar,
National Institute of Technology, Rourkela,
Orissa, India – 769008.

Phone - +91-9238532935

E-mail: ramakrishnagottipati@gmail.com

Qualification

- Ph.D
N.I.T., Rourkela, Odisha, India
- B – Tech (Biotechnology)
Jawaharlal Nehru Technological University, Hyderabad [First Class with Distinction]
- Intermediate (Mathematics, Physics and Chemistry)
Board of Intermediate Education, Andhra Pradesh [First Class]
- SSC
Board of Secondary School Education, Andhra Pradesh [First Class]

Permanent Address

At/Po – Uppalapadu, Via – Pedakakani,
Dist – Guntur, Andhra Pradesh – 522509, India.

Date of Birth

10th November, 1984

Publications

Journal Papers Published/Accepted

1. **Ramakrishna Gottipati**, Susmita Mishra. Process optimization of adsorption of Cr(VI) on activated carbons prepared from plant precursors by a two-level full factorial design, *Chemical Engineering Journal*, 160 (1), 2010, 99-107.
2. **Ramakrishna Gottipati**, Susmita Mishra. A kinetic study on pyrolysis and combustion characteristics of oil cakes: Effect of cellulose and lignin content, *Journal of Fuel Chemistry and Technology*, 39 (4), 2011, 265-270.
3. **Ramakrishna Gottipati**, Susmita Mishra. application of biowaste (waste generated in biodiesel plant) as an adsorbent for the removal of hazardous dye – methylene blue – from aqueous phase, *Brazilian Journal of Chemical Engineering*, 27 (2), 2010, 357-367.
4. Mishra.S, Prakash. D.J., **Ramakrishna. G.** Characterization and utilization of *Mahua oil Cake* – a new adsorbent for removal of congo red dye from aqueous phase, *Electronic Journal of Environmental, Agriculture and Food chemistry*, 8 (6), 2009, 425-436.
5. **Ramakrishna Gottipati**, Susmita Mishra. Application of response surface methodology for optimization of Cr(III) and Cr(VI) adsorption on commercial activated carbons, *Research Journal of Chemical Sciences*, 2(2), 2012, 40-48.
6. **Ramakrishna Gottipati**, Bharadwaj Adiraju, Susmita Mishra. Application of granular activated carbon developed from agricultural waste as a natural gas storage vehicle, *IACSIT International Journal of Engineering and Technology*, 4(4), 2012, 468-470.
7. **Ramakrishna Gottipati**, Susmita Mishra. Simultaneous removal of trivalent and hexavalent chromium by commercial activated carbons: Effect of solution pH and PSD of adsorbent. *Environmental Progress & Sustainable Energy* (**Accepted**)
8. **Ramakrishna Gottipati**, Susmita Mishra. Preparation of microporous activated carbon from Aegle Marmelos fruit shell by KOH activation. *Canadian Journal of Chemical Engineering* (**Accepted**)

Communicated

Ramakrishna Gottipati, Susmita Mishra. Kinetic and equilibrium modeling of Cr(VI) adsorption on AC prepared from Aegle marmelos fruit shell by H₃PO₄ activation. *Journal of Hazardous Materials*.

Conference Presentations

1. *Ramakrishna Gottipati*, Abhishankar Kumar, Bharadwaj Adiraju, Susmita Mishra. Application of granular activated carbon developed from agricultural waste as a natural gas storage vehicle. *International Conference on Product Development and Renewable Energy resources (ICPDRE-2011)*, Chennai, India.
2. *Ramakrishna Gottipati*, Susmita Mishra. Treatment of Cr(VI) in the Sukinda Mine Water Discharges. *Conference on Emerging Trends in Mining and Allied Industries*, N.I.T., Rourkela, India, 266-270.